University of Bath

UNIVERSITY OF BATH

PHD

Orthogonal multicarrier modulation for high-rates mobile and wireless communications

Al-Susa, Emad Adnan

Award date:
2000

Awarding institution:
University of Bath

[Link to publication](#)

ORTHOGONAL MULTICARRIER MODULATION FOR HIGH-RATES MOBILE AND WIRELESS COMMUNICATIONS

Submitted By
Emad Adnan Al-Susa
For the degree of Ph.D.
Of the University of Bath
2000

COPYRIGHT

I

UMI Number: U601662

UMI

Dissertation Publishing

ProQuest

Acknowledgement

Many thanks are owed to my supervisors Prof. Richard Ormondroyd and Dr. Steve Pennock for their continuing encouragement and support throughout the duration of my postgraduate studies.

I also wish to thank the University of Bath and the ORS committee for sponsoring me.

Finally, I would like to express my heartfelt gratitude to my family and friends for their support and encouragement throughout my years of research.

List of Publications

➢ E. Al-Susa and R.F. Ormondroyd, "*An Improved Channel Inversion Based OFDM System In the Presence of Channel Errors and Rapid Time variations*", to be published in the proceedings of the IEEE VTC'00, Boston-USA, Sept. 2000.

➢ E. Al-Susa and R.F. Ormondroyd, "*A Predictor-Based Decision Feedback Channel Estimation Method for COFDM with High Resilience to Rapid Time-Variations*", Proceedings of the IEEE VTC'99 falls, pp. 273-278, Amsterdam, Sept. 1999.

➢ E. Al-Susa and R. F. Ormondroyd, "*Improved Equalisation for a Broadband COFDM System in a Time-Varying Frequency Selective Fading Channel Using Predictor Based Channel Estimation*", Submitted to the IEEE Transactions of Vehicular Technology.

➢ R.F. Ormondroyd and E. Al-Susa, "*A High Efficiency Channel Estimation and Equalisation Strategy for a broadband COFDM System*", Proceedings of the ISSSE'98, pp.471-475, Peza Italy, Sept. 1998.

➢ R. F. Ormondroyd and E. Al-Susa, "*Impact of Multipath Fading and Partial Band Interference on the Performance of a COFDM/CDMA Modulation Scheme for Robust Wireless Communications*", Proceedings of the IEEE MILCOM'98, Boston USA, Oct.1998.

➢ R.F. Ormondroyd, J. Maxey and E. Al-Susa "*COFDM-An Alternative Multiple Access Strategy for next-Generation Mobile Communications*", Proceedings of the IEE colloquium on Mobile Communications Towards the Next Millennium and Beyond, vol. 1996/115, pp. 8/1-8/6, Savoy Place London, May 1996.

➢ E. Al-Susa and R.F. Ormondroyd, " *A High Efficiency Channel Estimation Technique for Broadband OFDM Systems*", Proceedings of the IEE colloquium on The Challenge of the Channel, IEE Centre Birmingham, May 1997.

Summary

Supremacy of the digital technology to the analogue in terms of performance, flexibility of design and robustness, accompanied with the technological advances in the solid state micro-electronics have played a major role for the present evolution of wireless and mobile communication systems.

The work in this thesis has been motivated by the challenges of the third-generation mobile communication systems using high data rates, in particular the challenges of the mobile radio channel. One of the major advantages of orthogonal frequency division multiplexing (OFDM) is its robustness to multipath dispersion.

This thesis has focussed on two major issues associated with the OFDM technique. These were, channel estimation/equalisation and adaptive modulation.

Several channel estimation techniques have been investigated. These included the decision directed feedback and pilot symbol assisted channel estimation techniques. By modifying such a technique to include a time-domain based predictor, a significant reduction in the irreducible BER floor was achieved especially in the presence of high Doppler. A new channel estimation technique which is based on the simultaneous transmission of two spreading sequences, one for the data symbols and the other for the channel estimation, have been proposed as an alternative technique. A comparison between the three techniques has shown that the decision feedback channel estimator provided the best overall performance under slowly time varying channels. On the other hand, the pilot assisted technique was found to be robust against Doppler spreading, at the expense of system capacity. In channels with large coherence bandwidth and moderate Doppler spreading, the new technique was found to provide a good trade-off between performance and system capacity.

Chapter seven of this thesis concentrated on studying three adaptive OFDM techniques. A fast converging algorithm for adaptive constellation was proposed. An improvement in excess of 7 dB in terms of signal to noise ratio was achieved compared to an OFDM system which uses a fixed modulation technique. It was also found that by careful arrangement between the transmitter and the receiver such degradation due to channel errors could be kept to a minimum of 1dB. A comparison between the three adaptive techniques shows that power adaptation using channel inversion provides the best compromise between complexity and BER performance.

Table of Contents

List of Abbreviations

3G	Third Generation
ACI	Adjacent Channel Interference
ACTS	Advanced Communications Technologies and Services
AD	Analogue to Digital Conversion
ADSL	Asymmetric Digital Subscriber Line
AE	Automatic Equaliser
AFC	Automatic Frequency Control
AM	Amplitude Modulation
AMPS	Advanced Mobile Phone Services
AWGN	Additive White Gaussian Noise
BER	Bit Error Rate
BPSK	Binary Phase Shift Keying
B-ISDN	Broadband Integrated Services Digital Networks
BS	Base Station
CDMA	Code Division Multiple Access
COFDM	Coded Orthogonal Frequency Division Multiplexing
CCI	Co-channel Interference
CCETT	Centre Commun. d'Etudes de Telediffusion et Telecommunications
CSI	Channel State Information
COST	Co-operation in the Field of Scientific and Technical Research
CC	Convolutional Coding
CE	Controlled Equalisation
CP	Cyclic Prefix
DAB	Digital Audio Broadcasting
DTTB	Digital Terrestrial Television Broadcasting
D-AMPS	Digital Advanced Mobile Phone Services
DCS 1800	Digital Communication System
DS-CDMA	Direct Sequence Code Division Multiple Access
DBPSK	Differential Binary Phase Shift Keying
DQPSK	Differential Quadrature Phase Shift Keying
DAPSK	Differential Amplitude and Phase Shift Keying
DMC	Discrete Memoryless Channel
DWT	Discrete Wavelet Transform
DFT	Discrete Fourier Transform
DS	Discrete Sequence
EDGE	Enhanced Data rates for GSM Evolution
EGC	Equal Gain Combining
ETSI	European Telecommunication Standards Institute
FBE	FeedBack Equalisation
FFE	FeedForward Equalisation
FDMA	Frequency Division Multiple Access
FEC	Forward Error Correction
FFT	Fast Fourier Transform
FM	Frequency Modulation
FSFC	Frequency Selective Fading Channel
FTD	Fourier Transform Domain
FPLMTS	Future Public Land Mobile Telecommunication Systems
FRAMES	Future Radio Wideband Multiple Access Systems
GRAN	Generic Radio Access Networks
GPRS	general packet radio service
GWSSUS	Gaussian Wide-Sense Stationary Uncorrelated Scattering
GSM	Global System for Mobile or Group Special Mobile
GB	Guard Band

GI	Guard Interval
HDSL	High bit rate Digital Subscriber Line
HPA	High Power Amplifier
IMT-2000	International Mobile Telecommunication program 2000
ISDN	Integrated Services Digital Networks
ISI	Intersymbol Interference
ICI	Interchannel Interference
IDFT	Inverse Discrete Fourier Transform
IC	Interference Cancellation
IFFT	Inverse Fast Fourier Transform
ITU	International Telecommunication Union
Kbps	Kilo bits per second
LAN	Local Area Network
LE	Linear Equaliser
LMS	Linear Mean Square
LPF	Low-Pass Filter
LOS	Line of Sight
MBS	Mobile Broadcasting Services
Mbps	Mega bits per second
MMSE	Minimum Mean Square Error
MC	MultiCarrier
MC-CDMA	MultiCarrier Code Division Multiple Access
MCM	MultiCarrier Modulation
MC-SS	MultiCarrier Spread Spectrum
MT-CDMA	Multi-Tone Code Division Multiple Access
MRC	Maximum Ratio Combining
MLD	Maximum Likelihood Detection
NMT	Nordic Mobile Telephone
MSE	Mean Square Error
MU	Mobile User
OFDM	Orthogonal Frequency Division Multiplexing
OFDMA	Orthogonal Frequency Division Multiple Access
PDC	Personal Digital Communications
PMR	Private Mobile Radio
PDA	Personal Digital Assistant
PN	Pseudo-Random Noise Sequence
PRMA	Packet Reservation Multiple Access
PS	Parallel to Serial Conversion
PC	Personal Computer
QPSK	Quadrature Phase Shift Keying
QAM	Quadrature Amplitude Modulation
QoS	Quality of Service
RF	Radio Frequency
SS	Spread Spectrum
SSMA	Spread Spectrum Multiple Access
SNR	Signal to Noise Ratio
SP	Serial to Parallel Conversion
TACS	Total Access Communication Systems
TDMA	Time Division Multiple Access
UMTS	Universal Mobile Telecommunication System
VA	Viterbi Algorithm
WSS	Wide Sense Stationary
WER	Word Error Rate
ZF	Zero-Forcing

List of Symbols

τ_m	Maximum delay spread
B_c	Coherence Bandwidth
T_c	Coherence time
$c(\tau, t)$	Channel Impulse Response
$\alpha_i(t)$	Amplitude of the ith received signal ray
$\tau_i(t)$	Time of arrival of the ith received signal ray
$\varphi_i(t)$	Phase of the ith received signal ray
$n(t)$	Additive noise
N	Number of Subcarriers
N_o	Noise power spectral density
f_c	Carrier Frequency
$x(t)$	Transmitted time domain signal
$y(t)$	Received time domain signal
η	Noise power
v	Speed of the vehicle
f_D	Doppler Frequency
f_m	Maximum Doppler Frequency
c	Speed of light
σ^2	Variance
σ	Standard deviation
λ	Wavelength
W	Bandwidth
$P_{Rice}(x)$	Ricean Distribution of x
$P(x)$	Log-normal distribution of x
$H(s)$	s-domain approximation of a filter
A	Attenuation
$\varphi_{j,k}$	Continuous OFDM signal
$g_k(t)$	Rectangular pulse
T	OFDM symbol duration
Ts	Serial symbol duration
$s(t)$	Continuous OFDM baseband time-domain OFDM signal
$r(t)$	Continuous received time-domain OFDM signal
E_s	Transmitted energy per subcarrier
T_{cyc}	Time-domain duration of the cyclic prefix
T'	Total symbol duration
d_n	Complex symbols sequence
ΔF	Subcarrier spacing
f_{offset}	Frequency offset
X	Discrete frequency domain signal
SNR_{loss}	Signal to noise ratio loss due to CP
h	Discrete impulse response
ζ	Spectral Efficency
L	Length of the cyclic prefix
β	Shaping filter roll-off factor
R	Data rate
M	Length of the channel's impulse response

Symbol	Description
$H(f)$	Channel transfer function
$CDFT$	Complex discrete Fourier Transform
R	Received frequency domain signal
σ_{ICI}^2	Variance of the ICI component
$\hat{\sigma}_{ICI}^2$	Estimated variance of the ICI component
σ_{ISI}^2	Variance of the ISI component
$\hat{\sigma}_{ISI}^2$	Estimated variance of the ISI component
σ_H^2	Variance of the channel response
$\bar{\gamma}$	Average SNR
BER_{AWGN}	BER in AWGN Channel
BER_{Ray}	BER in Rayleigh fading channel
E_b/N_o	Energy per bit to noise power ratio
$\hat{r}$	ISI free time-domain received symbol
$\tilde{R}$	ISI contaminated frequency-domain signal
$\hat{R}^{CYC}$	Cyclic prefixed frequency domain signal
$E_{i,n}$	Error signal of the nth subcarrier at the ith symbol
$W_{i,n}$	Filter coefficient of the ith tap at the nth iteration
μ	Control tuning factor
N_{OFS}	Number of interleaved OFDM blocks
mod	Modulo
N_T	Number of interleaved bits
ID	Interleaving depth
W^T	Transpose of filter coefficients
P	Cross-correlation vector
R	Auto-correlation vector
Δ	Gradient of the performance
$\overset{n}{H}$	Noisy estimate of the channel response
Z	Decision vector
$\dot{H}$	Smoothed estimate of the channel
ΔSNR	SNR loss due to channel mismatch
P_{BER}	Probability of BER using feedback
μc	Cross-correlation coefficient
ρ	Percentage of pilot tones to data symbols
$\hat{h}$	Estimated impulse response
a	Predictor coefficients
ϕ	Autocorrelation vector
$\hat{\pi}$	Reflection coefficients
e^f	Forward error
e^b	Backward error
Hp	Channel response at the pilot positions
Xp	Pilot symbols
Yp	Received pilot tones
Hp^{ZF}	Zero-forcing estimate of channel response at pilots position
C_0, C_1, C_2	Interpolator coefficients
Hp_{lmmse}	LMMSE estimate of the channel response at the pilots position
R_{HH}	Autocorrelation matrix
N_t	Pilot spacing in the time direction
N_f	Pilot spacing in the frequency direction
T_s	Symbol duration

PSR	Pilot to signal power ratio
ϕ^p	The change in phase caused by the frame error
E_m^{Hp}	The estimation error.
CP	Data spreading orthogonal code
Cp	Pilots spreading orthogonal code
S_x	Energy per signal
S_n	Energy per noise sample
C	Channel capacity
$\tilde{C}$	Aggregate capacity across a frequency selective fading channel
$S(f)$	optimum transmit spectrum
Γ	SNR gap representing how far the system is from achieving capacity
γ_m	System performance margin
K_n	The number of nearest neighbours
d_n	The minimum distance between constellation points
TBR	Total number of bits per frame
$AFRD$	Average fade rate duration
lcr	Level crossing rate
π_j	The steady state distribution corresponding to the jth region of a Markov channel model
$p_{j,j+1}$	The transition probabilities between regions of a Markov channel model
α_{thrsh}	Threshold level

List of Figures

Chapter One

Introduction

1. Chapter One

1.1. Overview of Current Advances in Mobile Communications

With well over 100 million public mobile users today, and more new mobile systems being rapidly installed all over the world, there is very little doubt that wireless will be the main access of choice for the future.

The rapid progress in digital and RF technology making available highly compact and integrated terminal devices, and the introduction of sophisticated wireless data software, are providing more value and making wireless access more user friendly.

At present, wireless networks support the first-generation analogue systems such as AMPS, TACS and NMT as well as the second-generation digital systems, which include D-AMPS, GSM, PDC, CDMA and DCS 1800, [1]-[4]. While the first generation systems are limited in terms of services and freedom of mobility, the second-generation systems such as the pan European GSM system allow users to roam through most countries in Europe, with the same handset in addition to providing services such as paging, fax and data facilities.

The phenomenal growth of the Internet, however, and the ever increasing reliance on personal computers and timely availability of information has demanded an expansion in the current wireless networks in order to accommodate many of the new requirements of today's modern world. Although many new services have been supported by the second generation systems, current mobile users are served by a wide range of different technical standards in many different parts of the radio frequency spectrum, (e.g. cellular, paging, cordless phones, mobile data and wireless LAN). In addition, numerous planned or operational satellite services further complicate the equipment choice for mobile users despite the availability of ways to link some of these services via, for instance, multimode and multiband mobile terminal products. In other words, the present situation cannot be described as providing seamless mobile service "*anywhere- anytime*".

The most extensive efforts to provide an integrated system which provides compatibility as well as supporting high bit rates can be found among the third generation, 3G, projects around the world, [1]. The International Telecommunication Union, ITU, programme IMT-2000, formally called FPLMTS, was initiated in 1986 with a goal of producing a global standard for third generation wireless access, using the frequency bands 1885-2025 MHz and

2110-2200 MHz. In Europe, the concepts of UMTS, [4][5][6], and MBS [7], have been the subjects of extensive research carried out within the European community research program RACE and ACTS, [8]. The main design objective for the 3G systems is to extend the services provided by current second-generation systems with high rate data capabilities. In particular, the goals are to provide 144 Kbps (preferably 344 Kbps) for high mobility users with wide area coverage and 2 Mbps for low mobility users with local coverage. The main application will initially be wireless packet transfer, particularly for wireless Internet access. However, supported services include circuit voice, circuit video, e-mail, short messages, multimedia, simultaneous voice and data and the broadband integrated service digital network (B-ISDN) access. In the search for the most appropriate multiple access technology for third generation wireless systems, a wide range of new multiple access schemes have been proposed for the ITU, [9]. These efforts have resulted in proposals based on wideband code division multiple access (WCDMA) and CDMA2000 using 5 MHz channels and EDGE using 200 kHz channels. Current efforts and consensus among GSM carriers and IS-136 carriers to converge GSM and IS-136 onto a common platform of EDGE general packet radio service (GPRS) creates the most backward compatibility among the 3G proposals with 600-800 million subscribers expected to be using GSM or time division multiple access services by 2003. Moreover, the EDGE/GPRS 3G proposal requires the minimum spectrum for 3G services. Because of these advantages of EDGE/GPRS, IS-136 carriers such as AT & T Wireless Services and many GSM carriers have committed to and planned to deploy such systems to provide their customers with 3G specified services.

By 1997, the proposals for UTRA have been narrowed down to only two candidates. These were W-CDMA and W-TD/CDMA, [10]. WCDMA being used for paired spectrum bands and TD/CDMA for the unpaired bands. Because there is more paired than unpaired spectrum, in effect, WCDMA will be the dominant air interface within UMTS. WCDMA will utilise a chip rate of 4.096 Mbps enabling each carrier to fit within a 5 MHz bandwidth. With the current expectation that most operators will be awarded either 2 X 15 MHz or 2 X 20 MHz, this will enable operators to deploy three to four carriers in total. As with existing CDMA technologies, the same frequency will be re-used in each section of each cell. However, in the case of microcells, separate carrier frequencies will normally need to be used with one being used for the microcells and a separate frequency used for the macrocells due to the very different levels of power that will be used in these two environments.

Among the proposals of FRAMES for the next generation air interface technique was the OFDMA technique examined by group *Gamma* of ETSI. This however, had not been selected for the final round for the reason that there was not a test bed for such technique to

2

hard-prove its potentials. Furthermore, it lacked the support of strong manufacturers because of its lack of compatibility with the present systems.

The changes that wireless communications is undergoing has been likened with that which personal computers have undergone [11]. In the early 1980's, personal computers supported a large number of features and a high degree of functionality, but the level of knowledge required to exploit these features to the full prohibited their use by the layman. With the advent of applications such as MS Windows, PCs suddenly became far more accessible and personal computing was revolutionised. In wireless communications many of the services that a user might wish for exist at the current time, but it will take a unifying concept, such as UMTS, to make them accessible to everyone. Ultimately, this world-wide digital telecommunications system will offer wireless telephone and other digital services, such as data transmission, paging facsimile and position location. The phrase "personal digital assistant", PDA, has been given to describe the portable device that will integrate all of these communications services.

1.2. Common Multiple Access Techniques

The terms multiple access and multiplexing are usually used in the contents of multi-user systems. The subtle difference between these two terms is the fact that multiplexing is normally used when the communication resource allocations are known a priori and are fixed. Whereas, the term multiple access usually involves the remote sharing of a communication resource, such as, a satellite or a base-station. Because in a multiple access system the users needs are dynamically changing, the system controller must always be aware of these changes and quickly adapt. The amount of time required for adaptation constitutes an overhead and sets an upper limit on the efficiency of the utilisation of the communication resource.

The most desirable way of increasing the efficiency of a multi-user communication system is the use of an efficient multiple access technique that optimises the available communication resource. There are at least five major multiple access techniques in use today. These include:

- Frequency division multiple access, FDMA. Each user is allocated a particular frequency [12]
- Time division multiple access, TDMA. Each user is given a time slot [13].

- Code division multiple access, CDMA. Each user is given a specific code having a low cross correlation with other codes [14].

- Space division multiple access, SDMA. Uses spot beams antennas pointing in different directions.

- Polarisation division multiple access, PDMA. Orthogonal polarisation is used to separate different users.

The common factor for all such techniques is that various users share the same communication resource without creating unmanageable interference to each other in the detection process. While the FDMA, TDMA and CDMA techniques are the most common for many users-to-one station link and *vice-versa*, SDMA and PDMA are more commonly used for satellite-to-ground station up-downlink. Each of these techniques has its proponents and antagonists, and the debate over which technique offers the greatest bandwidths efficiency that can support the largest number of simultaneous users with the lowest complexity will continue for some time.

While broadcasting is a one-to-many channel, with one transmitter serving many users, multiple access is a many-to-one channel, with one serving base station or satellite hub station receiving from or transmitting to multiple users. Until the advent of cellular wireless telephony, multiple access systems were limited to one cell. The implementation of cellular services have made frequency reuse central to realising multiple access for a much larger user population scattered over a large area.

FDMA, TDMA and CDMA differ in the way in which they apportion time and frequency to users. In FDMA users are allocated differing frequencies in the available bandwidth and transmit simultaneously. Usually this entails the use of guard intervals in the frequency domain between users to avoid cross talk between adjacent channels. In TDMA, users occupy the entire available bandwidth but transmit sequentially in time, which requires accurate synchronisation of all users in the network. In CDMA, the signal may be multiplied by a high rate PN code, (direct sequence CDMA), or pseudo-randomly hopped in frequency. In both techniques the effect is to spread the information across the entire available bandwidth. Multiple users can be supported in the same bandwidth as the average power for each user is low. Interference between users is minimised by using different spreading codes with very low cross-correlation for each user.

While in FDMA and TDMA systems, the performance is independent of the number of users, in CDMA it gradually degrades as the number of users is increased. On the other hand, while CDMA systems can theoretically accommodate an infinite number of users, TDMA and FDMA systems can only support a fixed number of users determined by the available time slots or frequency bands.

The requirements of the future generation systems of continually higher data rates and greater freedom of mobility will always demand more research into advanced and robust new strategies. The harshness of the channel and increased levels of intersymbol interference are the main limiting factors on the data rates that can be accomplished. With second generation mobile systems, in particular, this requires more complex equalisation, coding and modulation strategies, and therefore this thesis pays particular attention to these issues. For the next generation digital radio services, it will be necessary to suggest simpler alternative solutions that will accomplish these tasks, and current research is focussing on systems that will be simpler to implement in practice and at the same time provide adequate data throughput.

Multicarrier orthogonal frequency division multiplexing systems are one alternative solution that has received considerable attention with regard to these issues. These systems solve the problem of increased equaliser complexity by shifting the problem of ISI from the time domain into the frequency domain. The problem of the channel frequency selectivity thus presents a smaller problem for multicarrier systems than their conventional single carrier counterparts. A number of articles have shown that the use of multicarrier based designs provide better performance in frequency selective fading channels, e.g. [11]-[22].

1.3. Thesis Outline

This thesis is concerned with the theory, design and implementation of broadband multicarrier based systems employing forward error correction techniques, frequency equalisation and adaptive modulation. The proposed schemes are intended to provide an alternative solution to conventional single carrier techniques using time domain equalisers.

Chapter two serves as an introduction to the mobile radio environment. The statistics of Rayleigh and Ricean fading are presented together with some more fundamental work on the properties of time and frequency selective fading. The categorisation of the different channel properties through the time-delay spread, Doppler spread, *rms* delay spread, number of taps and the different COST channel models is presented with an outline on how to simulate a

continuous power delay profile in the discrete time domain. A brief description of channel countermeasures including, diversity techniques, equalisation, channel coding and high order modulation techniques is also presented.

Chapter three gives a concise mathematical description of the generation and reception of OFDM signals and provides an analysis into the theoretical performance of such systems in multipath Rayleigh fading channels in the presence of ICI, ISI and AWGN.

Chapter four is concerned with the performance of OFDM systems under a variety of different channel conditions. This includes the effect of varying the number of sub-carriers and Doppler frequency on the average bit error rate of the system. Also the impact of forward error correction coding and different types of interleaving is examined. The importance of using the cyclic prefix to combat ISI is assessed and compared to an alternative technique based on decision feedback. The use of different forms of differential modulation was also discussed and its performance relative to coherent modulation was assessed.

In chapter five, the use of decision directed adaptive feedback based channel estimation and tracking technique is investigated. The structure of the system that uses such technique is firstly presented and described. Then, a mathematical model of the mean square error (*MSE*) of the channel estimate and the bit error rate (*BER*) performance for QPSK is derived. The performance of the system is then more comprehensively analysed using computer simulations. This included the effect of increasing the time variation of the channel through increasing the Doppler frequency or increasing the block duration. An estimate of the best compromise between the bandwidth efficiency and training sequence channel estimation is also given. It is shown that filtering the channel estimate is essential and hence some sub-optimal filtering techniques will be analysed in terms of the mean square error. The analysis is based on a transmission rate of 25Mbps in an AWGN and time varying frequency selective fading channel using QPSK and DQPSK. Finally the impact of using a time domain based predictor on the estimators performance was investigated.

In chapter six, the basic principle of the scattered pilots based channel estimation method for OFDM transmission is presented. The use of different estimation criteria, such as, zero forcing, ZF, minimum mean square error, MMSE, and Fourier transform domain, FTD, are discussed and a comparison on the basis of BER performance is given in both urban and hilly channels. The impact of increasing the pilot tones power level on the system's overall BER performance was evaluated. The sensitivity of such channel estimation technique to

frame misalignment and its impact on the system performance are analysed using computer simulation. Finally, a new alternative method that is based on orthogonal code spreading for simultaneous channel estimation and data transmission is presented. Such method allows the transmission of 100% pilot tones without altering the data throughput. Thus alleviating some of the problems associated with the scattered pilot tone technique.

The aim of chapter seven is to provide an insight into fixed-throughput adaptive modulation schemes for OFDM based systems. Mainly, we concentrate on variable constellation adaptive modulation and compare it to fixed modulation, channel inversion and adaptive subcarrier allocation schemes. A comparison between three sub-optimal bit-loading algorithms in terms of performance and speed of convergence will be provided. The sensitivity of such system to channel estimation errors and high Doppler frequency is also evaluated. Finally a comparison between three adaptive techniques in terms of performance and complexity is given.

Conclusions and recommendations are finally given in chapter eight.

1.4.References

[1] J. E. Padgett, C. G. Gunther and T. Hattori, *"Overview of Wireless Personal Communications"*, IEEE Communications Magazine, Vol. 33, pp. 28-41, January 1995.

[2] K. Kinoshita, M. Kuramoto, and N. Nakajima, *"Development of a TDMA Digital Cellular System Based on a Japanese Standard "*, Proceedings of the IEEE VTC'91 Conference, pp. 642-645, 1991.

[3] G. Calhoum, *"Digital Cellular Radio"*, Norwood, MA, Artech House, 1998.

[4] R. Prasad, "Universal Wireless Personal Communications", Boston-London, Artech House, 1998.

[5] R. Prasad and T. Ojanpera, *" Development of UMTS in Europe"*, Proceedings of the IEEE Fourth Symposium on Communications and Vehicular Technology in the Benelux, Gent, Belgium, pp. 6-11, Oct. 1996.

[6] T. Ojanpera and R. Prasad, *"An Overview of Third-generation Wireless Personal Communications: A European perspective"*, IEEE Personal Communications, Vol. 5. No. 5, pp. 59-65, Dec. 1998.

[7] L. M. Correia and R. Prasad, *"An Overview of Wireless Broadband Communications"*, IEEE Communications Magazine, Vol. 45, pp. 28-33, January 1997.

[8] J. S. Da silva, D. Arroyo-Fernandez, B. Barani, J Pereira and D Ikonomou, *"Mobile and Personal Communications: Acts and beyond"*, Proceedings of the IEEE PIMRC'97, Helsinki, Finland, Sept. 1997.

[9] http://www.itu/imt/2-radio-dev/index.html

[10] M. Gallagher and W. Web, *"UMTS: The Next Generation of Mobile Radio "*, IEE Review, pp. 59-63, March 99.

[11] P. Radley, *"The Time to Change is Now"*, MTN, p. 22, September 1993.

[12] I. Rubin"*Message Delay in FDMA and TDMA Communication Channels"*, IEEE Transactions on Communications, Vol. COM27, no. 5, pp. 769-777, May 1979.

[13] S. Campanella and D. Schaefer, *"Time Division Multiple Access Systems (TDMA)"*, Prentice-Hall, Inc,. Englewood Cliffs, N. J., 1983.

[14] R. Prasad, *"CDMA for Wireless Personal Communications"*, Norwood, MA, Artech House, 1996.

[15] N. Yee, J-P. Linnartz and G. Fettweis, " *Multicarrier CDMA in Indoor Wireless Radio Networks"*, IEEE PIMRC'93, Conference Proceedings, pp. 109-113, Yokohama, Japan, Sept. 1993.

[16] K. Fazel and L. Papake, *"On the Performance of Convolutionally Coded CDMA/OFDM For Mobile Communications Systems"*, IEEE PIMRC'93, Conference Proceedings, pp. 468-472, Yokohama, Japan, Sept. 1993.

[17] V. M. DaSilva and E. S. Sousa, *"Performance of Orthogonal CDMA Codes for Quasi-synchronous Communication Systems"*, IEEE ICUPC'93, Conference Proceedings pp. 995-999, Ottawa, Canada, Oct. 1993.

[18] S. Kondo and L. B. Milstein, *" Performance of Multicarrier DS CDMA Systems"*, IEEE Transactions on Communications, Vol. 44, No. 2, pp. 238-246, February 1996.

[19] E. Sourour and M. Nakagawa, *"Performance of Multicarrier CDMA in Multipath Fading Channel"*, IEEE Transactions on Communications, Vol. 44, No. 3, pp. 356-67, March 1996.

[20] L. Vandendorpe, "Multitone Direct Sequence CDMA in an Indoor Wireless Environment ",IEEE Proceedings of the First Symposium of Communications and Vehicular Technology in the Benelux, pp. 4.1-1.4.1.8, Delft, The Netherlands, Oct. 1993.

[21] R. Prasad and S. Hara, *"An Overview of Multicarrier CDMA"*, IEEE ISSSTA'96 Conference Proceedings, pp. 107-113, 1996.

[22] S. Hara, *"Transmission Performance Analysis of Multicarrier Modulation in Frequency Selective Fast Rayleigh Fading Channel"*, Wireless Personal Communications, Vol. 2, No. 4, pp. 335-356, 1995/1996

Chapter Two

The Mobile Radio Channel

2 Chapter Two

2.1 Introduction

The mobile radio propagation channel is the physical medium that supports the electromagnetic wave propagation between a transmitter and a receiver. When transmitting a signal in such channel, a number of factors indirectly contribute to changing the nature of the signal. These include the geometry of the surrounding environment, the movement of the receiver and the carrier frequency of the signal. The geometry of the environment is dictated by obstacles, such as, buildings, mountains, cars, etc. present in the vicinity of the receiver giving rise to effects such as reflection, diffraction, shadowing and scattering. These effects force the transmitted signal to follow a number of different propagation paths before arriving at the receiver as depicted in Figure 2.1.1. The impact of these effects on the received signal is to impose a range of attenuations, delays and phase and frequency shifts.

A: Direct Line of Sight
B: Diffraction,
C: Reflection,
D: Double reflection
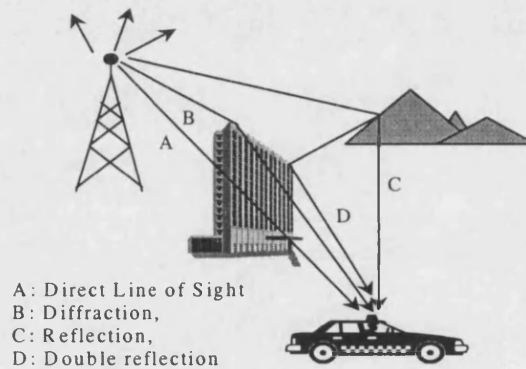
Figure 2.1.1: A Typical Urban Environment

At the receiving antenna a voltage is produced that represents a vector summation of these amplitude-scaled and phase-shifted signals. This will lead to either, constructive additions, in which case the signal is amplified, or destructive cancellations in which case the signal is attenuated and is considered to be in fade. When this occurs, a multipath situation is said to exist. If the mobile user is in motion a situation known as "dynamic multipath" arises. In such situations a continuous change in the electrical length of every propagation path will be inflicted and the relative phase shifts between the different paths will be changing as a function of the spatial location. The resulting signal's envelope is one in which some positions have constructive additions whilst at others there might be complete cancellation. An example of such signal envelope and phase variations is shown in Figure 2.1.2 and Figure 2.1.3.

While the geometry of the environment and movement of the mobile receiver together determine the nature of the channel to transmit through, the carrier frequency of the transmitted signal dictates the propagation characteristics as well as how fast the signal changes.

When using the same carrier frequency for both the uplink and downlink, it can always be assumed that the mobile radio propagation channel is both linear and reciprocal [5]. The linearity property of the channel implies that the output of the channel for a signal made from the sum of two separate signals is the same as the sum of the outputs of the two signals transmitted separately. The reciprocity of the channel implies that the impact of the channel on the transmitted signal is the same regardless of its direction of flow.
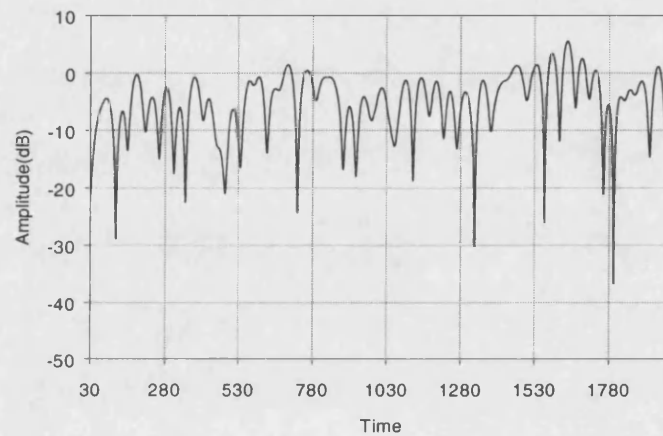
Figure 2.1.2: Received Signal's Envelope Due to Multipath
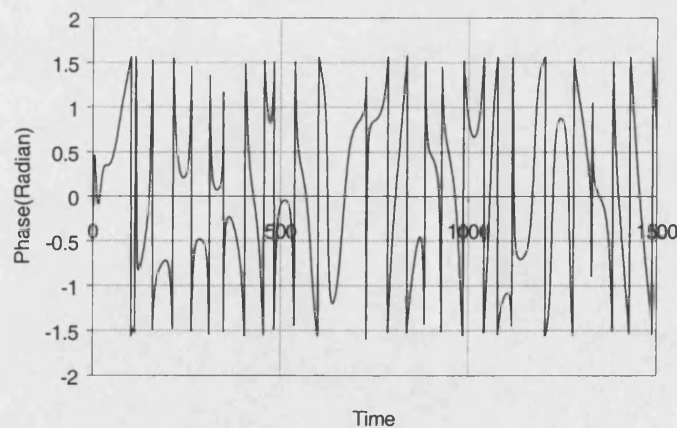
Figure 2.1.3: Received Signal's Phase Variations Due to Multipath

This chapter introduces concepts in understanding, modelling and utilising mobile radio channels.

2.2 Multipath Channels

The multipath phenomenon arises as mentioned earlier due to obstacles in the vicinity of the mobile station causing several copies (*echoes*) of the same signal to arrive at the receiver within relatively short intervals of time. The difference between the arrival times of the first and the last of these echoes is termed the maximum delay spread of the channel, τ_m. This, together with the transmission rate of the data determine whether the channel is narrowband or wideband. If the data rate is narrower than the coherence bandwidth of the channel, $B_c=1/(\tau_m)$, then all the frequency components of the transmitted signal encounter nearly identical propagation delays and the channel is termed narrowband [1]. If on the other hand, the transmission rate is sufficiently high such that some of the echoes of one symbol arrive at the same time as those of other consecutive symbols, the channel is termed wideband and inter-symbol interference (*ISI*) is said to exist. When such a situation is present, the signal can be recovered by removing the *ISI*, a process that requires the estimation of the impulse response of the channel. The wideband channel can be fully characterised by its impulse response, which is defined as the received power versus excess time delay for a transmitted impulse. Mathematically, the impulse response of a time variant multipath channel can be written as:

$$c(\tau;t) = \sum_i \alpha_i(t)e^{-j\theta_i(t)} \qquad\qquad 2.2.1$$

Where $\qquad \theta_i(t) = 2\pi f_c \tau_i(t)$

Where $\alpha_i(t)$, $\tau_i(t)$ and $\varphi_i(t)$ are the amplitude, arrival time and phase of the received signal from the ith path, respectively. Assuming that there is a finite number of propagation paths, the received signal is given as the convolution of the transmitted signal with the impulse response of the channel as shown in equation 2.2.2.

$$y(t) = x(t) * c(\tau,t) + n(t) = \Re\left\{\left[\sum_{i=0}^{N-1}\alpha_i(t)e^{-j2\pi f_c \tau_i(t)}x_l(t-\tau_i(t))\right]e^{j2\pi f_c t} + n(t)\right\} \quad 2.2.2$$

Where * stands for convolution, $n(t)$ is the additive white Gaussian noise (AWGN), $\Re$ stands for the real part only and $x(t) = \Re[x_l(t)e^{j2\pi f_c t}]$. The rate at which both $\alpha_i(t)$ and $\varphi_i(t)$ will be varying is dependent on the Doppler frequency which is a function of the carrier frequency, f_c, vehicle speed, v, and the angle of incidence, φ, as given by equation 2.2.3.

$$f_D = \frac{v \cdot f_c}{c} \cdot \cos\varphi_i \qquad\qquad 2.2.3$$

Where c is the speed of light.

2.3 Fast Fading

Fast fading refers to the instantaneous variations in the envelope of the transmitted signal. These variations can be as much as a few tens of decibels below the local mean of the signal's level. The presence of fast fading is a direct result of the arrival of a number of copies of the same signal each with a different phase shift, amplitude and time of arrival. The complex baseband signal's amplitude and phase can be given by:

$$a(t) = \sqrt{a_i^2(t) + a_q^2(t)}$$

$$\varphi(t) = \tan^{-1}\left(\frac{a_q(t)}{a_i(t)}\right)$$

         2.3.1

Where $a_i(t)$ and $a_q(t)$ are the inphase and quadrature components of the signal. Assuming there are many independent echoes arriving at the receiver via different paths results in making the distribution of $a_i(t)$ and $a_q(t)$ become Gaussian [2]. Depending on whether a line of sight exists or not, the distribution of the amplitude can therefore be either Ricean or Rayleigh [4], while the distribution of the phase will be uniform over the range $-\pi$ to π. In urban areas, the possibility of having a direct line of sight is small and therefore the distribution of the amplitude is always assumed to be Rayleigh. Whereas, in rural not hilly areas, the chance of having a strong line of sight is high and thus the amplitude distribution is approximated to be Ricean. The Ricean and Rayleigh distribution may be given by a single formula as shown in equation 2.3.2:

$$P_{Rice}(a) = \frac{a}{\sigma^2} \cdot e^{-\frac{a^2}{2\sigma^2}} \cdot e^{-K} \cdot I_0\left(\frac{a}{\sigma} \cdot \sqrt{2K}\right)$$

$$I_0(x) = \sum_{i=0}^{\infty} \frac{x^{2i}}{2^{2i}(i!)^2}$$

$$K = s^2 / 2\sigma^2$$

$$s^2 = \sum_{i=1}^{n} \overline{a}_i^2$$

         2.3.2

Where $\overline{a}_i$ and σ^2 is the corresponding means and variance of the different paths, respectively. The factor K gives a measure of the ratio of the power received in the direct line of sight to the total power received via other indirect paths. Thus, when there is no line of sight, ie. $K=0$, and the distribution of the received signal's amplitude becomes Rayleigh. On the other hand if there is only one line of sight and no indirect paths then the received signal will have a constant amplitude and the channel is then termed Gaussian for the simple reason that it will mainly be corrupted by the additive white Gaussian noise (AWGN).

P(Amplitude)
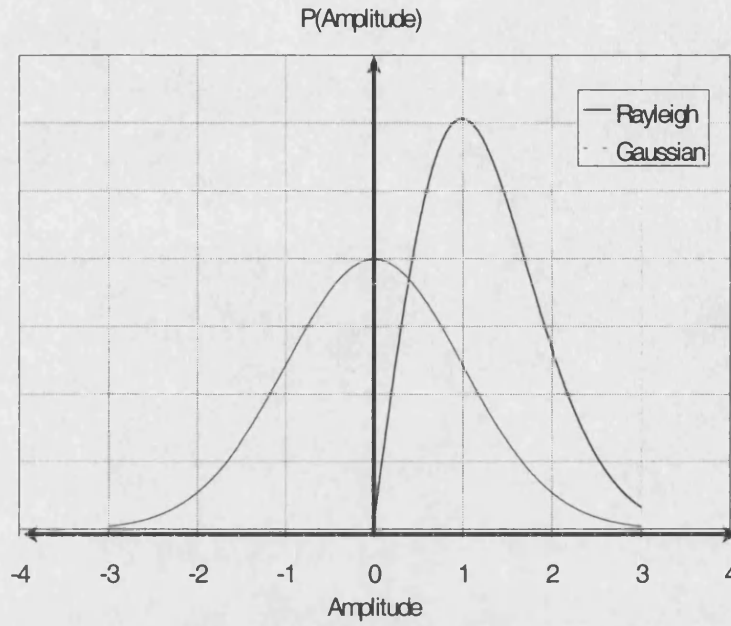
Figure 2.3.1: Probability Density Function of a Rayleigh and Gaussian Distributions

2.4   Slow fading

Slow fading is defined as the variation in the average field strength of the transmitted signal. Such fading is mainly caused by the configurations of the terrain and the built environment between the base station and the mobile unit. Unlike the fast fading phenomenon, slow fading is not affected by the speed of the mobile unit, instead it is only sensitive to the nature of the location of the mobile unit with respect to the base station. It was shown by a number of people [4]-[9] that slow fading could be, in most, cases modelled as a log-normal distribution with a standard deviation of 5 to 12dB. The log-normal distribution is given by equation 2.4.1 which is plotted on Figure 2.4.1.

$$P(x) = \frac{1}{\sqrt{2\pi} \cdot \sigma \cdot x} \cdot \exp\left(\frac{-1}{2\sigma^2} \cdot \left(\ln(x) - \mu\right)^2 \right)$$
         2.4.1
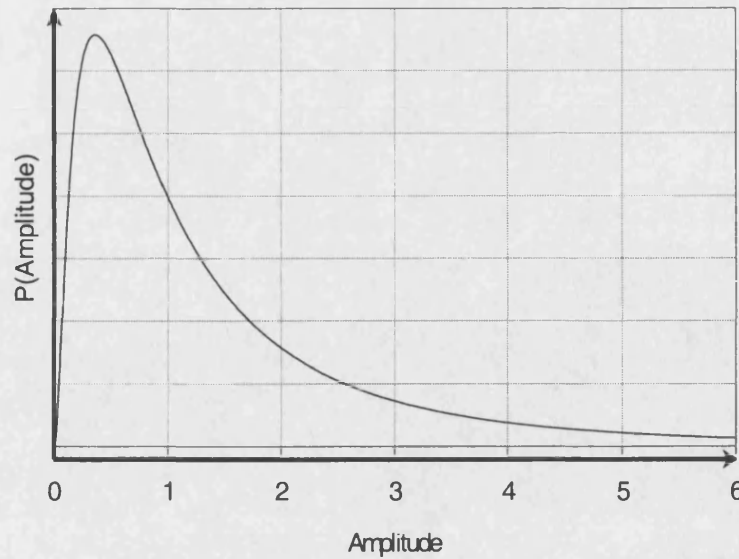
Figure 2.4.1: Log-Normal Distribution, $\mu = 0$, $\sigma = 1$

2.5 Channel Characterisation

In mobile radio multipath channels, there are two main kinds of spread. These are, the Doppler frequency spread caused by the movement of the mobile unit and other moving objects in its vicinity, and the time delay spread caused by the multiple arrival of many signal echoes. The Doppler spreading gives rise to both time selective fading and frequency dispersion. Whereas the time delay spread results in time dispersion and hence frequency selective fading. Although all of the above mentioned channel effects are almost always present, the classification of the channel is based upon the transmitted signal's nature and the most dominant of these effects.

2.5.1 Time dispersive/Frequency selective

This kind of channels results from the presence of significant multipath delay spread which leads to stretching the signal in time so that the duration of the received signal is greater than that of the transmitted one. Time dispersive channels are also called frequency selective fading channels for the reason that the frequencies that constitute the signal could be faded by significantly different amounts. The impact of the time dispersion and frequency selective fading increases as the bandwidth of the transmitted signal is increased.

The minimum transmission bandwidth at which time dispersion is observable is inversely proportional to the maximum excess delay of the channel, τ_m, where the excess delay is the actual delay minus the delay of the first arrival path. Similarly, the transmission bandwidth at which frequency selective fading becomes significant is often based on the channels

15

coherence bandwidth, B_c, which may be defined as the frequency separation at which the correlation coefficient between the attenuations of two signal frequency components becomes less than 0.5 [4]. The sensitivity of the system to the correlation coefficient is mainly dependent on the order of modulation used. For example, a certain QAM constellation may perform perfectly satisfactorily at a correlation coefficient value of 0.5 whereas the performance of a higher order QAM system may be severely degraded at that value. The main impact of such channel on the transmitted signal is the intersymbol interference effect which imposes a limit on the maximum allowable transmission rate.

2.5.2 *Frequency dispersive/Time selective*

Frequency dispersion is a direct result of the Doppler spread phenomenon that is created due to the relative movement of the transmitter and receiver. On the contrary of the time spreading, the Doppler effect changes the bandwidth of the transmitted signal to greater or less than that of the original one. The presence of the Doppler effect gives rise to time selective fading due to the fact that the channel changes characteristics while the signal is still in flight and hence different parts of the signal may be subjected to different levels of fading. To illustrate the Doppler effect, consider a simple case in which an un-modulated carrier frequency f_c is transmitted from a base station. When this carrier arrives at a mobile station at an angle of φ_i, where the subscript i stands for the ith path, it introduces a relative carrier phase shift. This phase shift is proportional to the amount by which the wavelength of the carrier is changed. This is depicted in Figure 2.5.2.1.
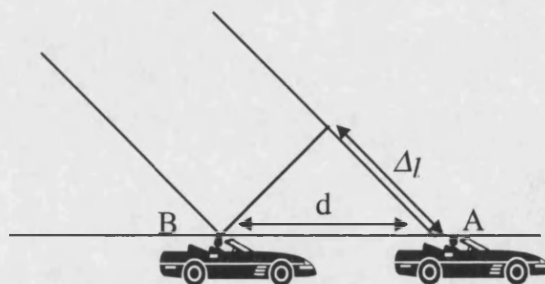
Figure 2.5.2.1: Doppler Effect

If the wavelength is shortened by $\Delta l = \lambda$, where $\lambda = c/f_c$ with c being the speed of light, this corresponds to a phase change of 2π. In the general case when Δl is arbitrary, the phase change is given by

$$\Delta\theta = \pm 2\pi \cdot \frac{\Delta l}{\lambda}$$
<div align="right">2.5.2.1</div>

Where the minus and plus signs correspond to the cases in which the mobile station is travelling in the direction of the base station or away from the base station respectively. Using Figure 2.5.2.1 it is evident that $\Delta l = d \cdot \cos\varphi_i$, where $d = v\Delta t$, v is the speed of the mobile station and Δt is the time taken by the mobile station to cross from point A to point B. Thus, The Doppler frequency is defined as the phase change due to the movement of the mobile station during the time interval Δt. That is

$$f_D = \pm \frac{1}{2\pi} \frac{\Delta\theta}{\Delta t} = \frac{v}{\lambda} \cdot \cos\varphi_i \qquad\qquad 2.5.2.2$$

In general, the received RF Doppler spectrum, $S(f_D)$, can be expressed as:

$$S(f_D) = \frac{-1}{2\pi f_m \sqrt{1 - (f_D / f_m)^2}}, \qquad\qquad 2.5.2.3$$

which when plotted results in the well-known Jake's [9] U shaped spectrum as shown in Figure 2.5.2.2.

The minimum signal duration at which frequency dispersion becomes noticeable is inversely proportional to the magnitude of the maximum Doppler shift f_m experienced by the signal. Similarly, the minimum signal duration at which time selective fading becomes apparent is related to the channel's coherence time $T_c(t)$, which is defined as [5]:

$$T_c(t) = \frac{9}{16\pi f_m} \qquad\qquad 2.5.2.4$$

The presence of the Doppler spread makes carrier recovery difficult in coherent systems and may also give errors in non-coherent systems.

$S(f_D)$

Doppler Frequency, *Hz*
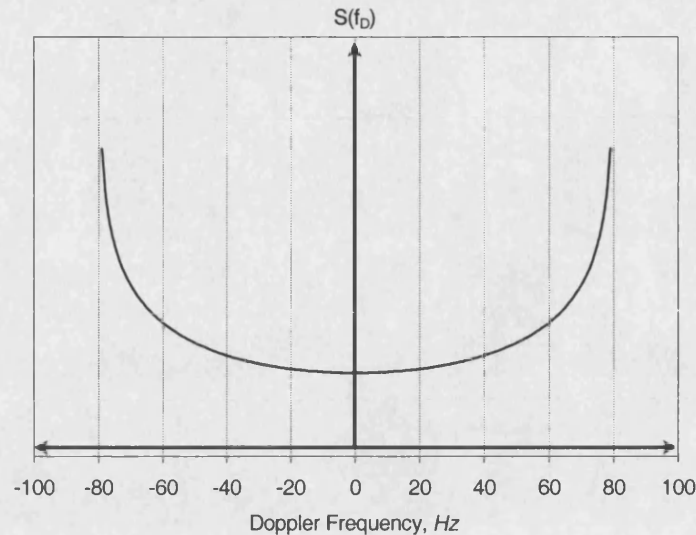
Figure 2.5.2.2: Doppler Spectrum

2.5.3   Non-dispersive

Another name for this type of channels is flat-flat or doubly-flat channels. In such channels the signal does not fade with either time or frequency. For a signal to be subjected to doubly-flat channel its bandwidth and duration must be less than the coherence bandwidth and the coherence time of the mobile channel, respectively. This type of channels might arise when the data transmission rate does not exceed a few kilobits per second and a very strong line of sight path exists.

2.5.4   Doubly dispersive

This kind of channels exhibits both frequency selective fading and time selective fading due to long propagation delays and high mobile unit speed, respectively. An example of such channels is the communication link between an aircraft and a satellite, where the high Doppler frequencies arise due to the high aircraft speed and the long delays are due to strong reflections from the surface of the earth.

2.6   Channel modelling

The models presented here are based on the assumption that the echoes of the signal are uncorrelated and have Gaussian distributions. This model is better known as the Gaussian wide-sense stationary uncorrelated scatters (GWSSUS) model [3]. In this section we start by developing a model for the narrowband channel where the received signal echoes all arrive within short intervals of each other such that the impulse response of the channel may be modelled as a single multiplicative complex Gaussian random time variant variable. Then a

model of the multipath (wideband) channel based on that of the narrowband channel is developed.

2.6.1   *Narrowband Channel*

The generation of the real and imaginary parts of the multiplicative narrowband coefficient can be achieved by using two uncorrelated Gaussian distributed random numbers. In order to account for the Doppler effect, the real and imaginary parts are passed through a lowpass filter with a frequency response defined by the Doppler spectrum. The inclusion of the filter does not affect the statistical distribution of the random numbers [4], but may affect their variances. This, however, can be corrected for by inserting an appropriate scaling factor [12]. The cutoff frequency of the lowpass filter is the maximum Doppler frequency to be used. Filtering inserts some correlation between the output samples and the amount of correlation changes according to the cutoff frequency. The cutoff frequency is inversely proportional to the correlation factor. The generation of the Gaussian random numbers can be achieved using the Box-Muller algorithm [4] described in appendix 2. The filtering of the random numbers may be done in either the frequency domain or the time domain as discussed below.

2.6.1.1   Time domain implementation

In this type of simulation, the time domain Gaussian numbers are convolved with the impulse response of the Doppler filter of equation 2.5.2.3. A time domain based filter having the Doppler spectrum can be implemented using two cascaded second order Butterworth filters. Using one filter to ring at the wanted cutoff frequency and another to act as a normal lowpass filter was found to give a very good approximation. The s-domain approximation of this two-stage filter is given by [14]:

$$H(s) = \frac{1}{s^2 + \sqrt{2}s + 1} \cdot \frac{1}{s^2 + 0.02s + 1}$$
$$\text{2.6.1.1.1}$$

The steps involved in the design of this filter are fully explained in appendix 2B at the end of this chapter. The theoretical and resulting simulated filter's spectral characteristics at a maximum Doppler frequency of 50Hz and sampling frequency of 2KHz are shown in Figure 2.6.1.1.1 below.

One major drawback of this type of method is the need to use possibly, thousands of tap values when the Doppler bandwidth is much smaller than that of the sampling frequency in

order to accommodate for the slowly decaying impulse response of the filter. This drawback, however, can be overcome by using a relatively small sampling frequency combined with an interpolation algorithm to increase the sampling frequency to the wanted value without inflicting a significant change on the statistics of the coefficient.
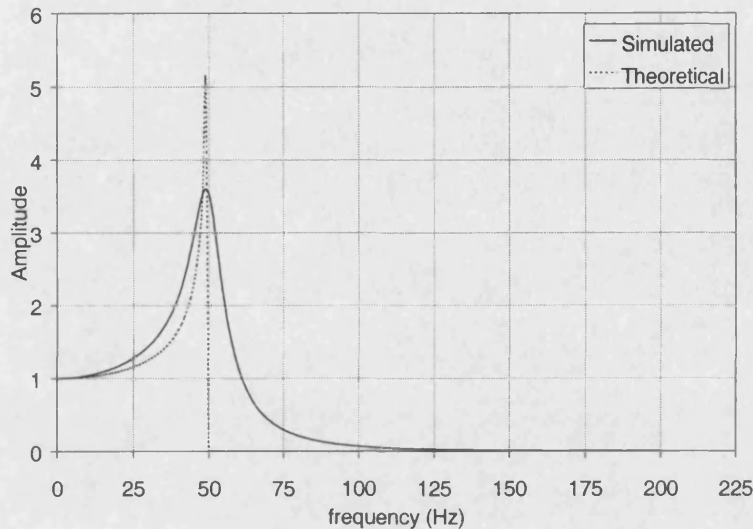
Figure 2.6.1.1.1: Simulated and Theoretical Response of the Doppler Lowpass Filter

2.6.1.2 Frequency domain Implementation

This method is based on the discrete Fourier transform, in which the real and imaginary parts of the complex multiplicative coefficient are multiplied by the Doppler transfer function of equation 2.5.2.3. Exploiting the fact that the Fourier transform of a Gaussian process is another Gaussian process, transformation is only need once. Similar to the time domain method, when the Doppler bandwidth is much smaller than that of the sampling frequency, a very large Fourier transform size is needed in order to ensure that a significant proportion of the input samples would fall in the Doppler's bandwidth[4]. At the output of the Fourier transform, a scaling factor is used to ensure that the variance of the output samples is not changed.

2.6.2 Wideband Channel

This type of channels arises when the path delay differences are longer than the symbol duration resulting in the arrival of one symbol's echoes at the time of arrival of other consecutive symbols. The impulse response of such channel may be represented in discrete form as consisting of a number of delta functions whose amplitude have Rayleigh/Ricean distribution. A typical wideband channel impulse response is shown in Figure 2.6.2.1 below.

Although various impulse response models have been used in the past, the best known ones are those of the COST 207 specified by the Group Special Mobile committee (GSM) for different environments, such as, typical urban, bad urban, rural and hilly terrain. The sets of six tap GSM impulse responses for the two most common channel models are summarised in the table 2.6.2.1.

Since the response of the channel outside the signal's bandwidth is of little importance, the channel can be sampled at the symbol rate leading to the tapped delay line model [3] as shown in Figure 2.6.2.2. When the baseband signal is applied to the series of delays, the output from each tap is multiplied by a time varying coefficient, R, that characterises the fast fading and by a further gain, A, in order to keep the average power of that path at a certain wanted level. The outputs from all the taps are then added together using a complex summer and combined with some additive Gaussian noise before being passed to the output.
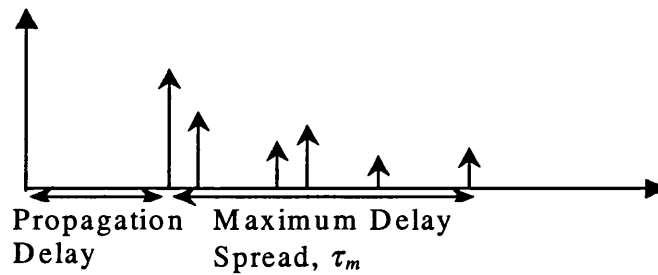
Figure 2.6.2.1: Typical Wideband Impulse Response

Path	1	2	3	4	5	6
Spectrum	Rayleigh	Rayleigh	Rayleigh	Rayleigh	Rayleigh	Rayleigh
Delay μsec	0.0	0.2	0.4	0.6	15.0	17.2
Attenuation	0	2.0	4.0	7.0	6.0	12.0
Correlation	0	0	0	0	0	0

(a)

Path	1	2	3	4	5	6
Spectrum	Rayleigh	Rayleigh	Rayleigh	Rayleigh	Rayleigh	Rayleigh
Delay μsec	0.0	0.2	0.6	1.6	2.4	5.0
Attenuation	3.0	0.0	2.0	6.0	8.0	10.0
Correlation	0	0	0	0	0	0

(b)

Table 2.6.2.1: Table of Channel Parameters, (a) Hilly Terrain, (b) Typical Urban
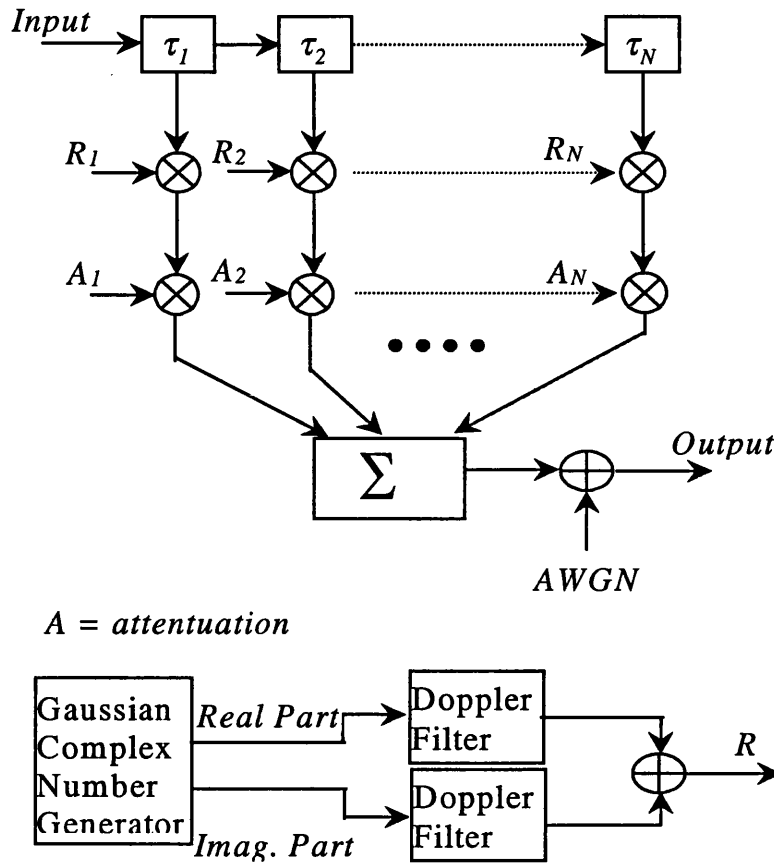
Figure 2.6.2.2: Schematic of the Channel Simulator

2.7 Additive White Gaussian Channel (AWGN)

As is the case with all forms of signal transmission, additive noise is always present to contribute in the corruption of the signal. The sources of such noise are many, some of which are human made impulsive noise, galactic noise and noise generated at the receiver due to temperature. It is almost universally agreed that such impairments have the characteristics of additive white Gaussian noise. The probability distribution of such noise is derived from the zero mean Gaussian distribution function as shown below:

$$p(x) = \frac{1}{\sqrt{2\pi\eta}} \exp\left(\frac{-x^2}{2\eta}\right) \qquad\qquad 2.7.1$$

Where η, is the noise power. For a system bandwidth of W, the noise power is related to the two sided channel noise power spectral density, $N_0/2$, by:

$$\eta = W \cdot N_0 \qquad\qquad 2.7.2$$

Where N_0 is given in units of *Watts/Hz*. The Gaussian channel is usually used to provide an upper bound on the system's BER performance.

2.8 Channel's Countermeasures

A number of techniques for combating many of the challenges dictated by the communication channels have been and still are the subject of intense research to produce better and more efficient communication systems. These techniques vary in complexity, BER performance, bandwidth efficiency and type of channel designed for. The choice of which technique to use is based on the type of the dominant channel characteristics present as well as the type of application intended. In this section, the principles and drawbacks of some of these techniques are briefly reviewed.

2.8.1   Diversity [1]

Diversity is one of the ways to achieve a lower BER at some cost. The idea of diversity is to transmit a signal simultaneously via more than one way so the composite signal received at the other end has gone through independent channels. It is then very likely that the fades imposed by one channel will be at different locations from those of the other channels and hence satisfactory error ratio may be maintained. There are three main different techniques of diversity, namely, frequency, space and time diversity. The most commonly used diversity technique is space diversity in which a few antennas separated apart are used [23]. Since the channel imposed fading is mainly due to phase difference between the received echoes, it is most likely to find the fading on different antennas separated a few wavelength apart completely uncorrelated. This type of diversity technique is usually used at base stations but not at mobile hand portable phones. In the case of frequency and time diversity, the information signal is transmitted simultaneously at different frequencies, or in different time slots, respectively. To achieve best performance when using these two techniques it is important to transmit at frequencies separated by at least the coherence bandwidth of the channel or in the case of time diversity on time slots separated by at least the coherence time of the channel. Below is a brief description of these techniques.

2.8.1.1   Time Diversity [15]

Time diversity is mainly suitable for rapidly changing channels. If such condition is satisfied it is easy to spread an information symbol over more than one data symbol separated in time. The success of such technique is however not only dependent on the speed of the mobile receiver, but also the carrier frequency used and the data transmission rate. If for instance the carrier frequency used was 100 MHz and the mobile receiver is travelling at 70 miles per hour, the maximum Doppler frequency is about 10 Hz. To get two independent fading, the two symbols must be separated by at least half the coherence time of the channel (0.1 second), or alternatively half a wavelength of the carrier frequency, (1.5 meters). For a data

rate of 10ksps, this corresponds to 500 symbols. For a carrier frequency of 1 GHz, the maximum Doppler frequency is 100 Hz, therefore the symbols need to be separated by at least 50 symbols. It is clear from the above example that the practicality of such diversity technique depends on systems parameters used as well as the maximum tolerable delay. The point to stress here is that time diversity depends on a number of factors, some of which are beyond the designers control, such as the speed of the mobile receiver, and therefore may be very difficult to optimally utilise.

2.8.1.2 Frequency Diversity [18]

In a wideband system, the mobile radio channel becomes frequency selective. The presence of such phenomenon makes frequency diversity highly desirable since one can use more than one carrier to deliver the same signal to the receiver. In order to fully utilise such diversity technique, the carriers have to be separated in frequency such that they are subjected to independent fading. This is related to the coherence bandwidth of the channel, which is governed by the type of environment present. For example, in urban or hilly environments, the coherence bandwidth can be on the average about, 200kHz and 50kHz, respectively. Therefore the frequency diversity will lower the average probability of error. In sub-urban environments however, the coherence bandwidths can be in excess of 1 MHz, which requires a set of very widely separated carriers to fully exploit such diversity technique. This may prove to be spectrum in efficient.

2.8.1.3 Space Diversity [16][17]

Space diversity, unlike the previous forms of diversity techniques, does not depend on the coherence time or bandwidth of the channel. This technique uses an array of antennas spaced by a half wavelength or more apart. Although such diversity technique is independent of the channel conditions present, it has one major drawback. This is the need to have enough receiver area to accommodate all the antennas spaced by half a wavelength. The practicality of such technique is largely governed by the carrier frequency used, which in turn determines the minimum size of the receiver. For instance, if the carrier frequency is 1 GHz, the receiver's size cannot be smaller than 0.3 meter if space diversity is to be used. If on the other hand, the carrier frequency used is 100 MHz, the minimum receiver's area required is 3 meters. Although, such diversity technique is independent of the channel coherence time and bandwidths, it relies on the reception different multipath rays by the different antennas.

2.8.1.4 Diversity Combining Techniques

There are two basic ways of exploiting diversity. These are diversity combining, which include maximum ratio combing, (MRC), and equal gain combing, (EGC), and selection diversity combing, (SDC) [1]. The most common of these is the MRC technique in which the diversity branches are weighted proportionately to the signal's amplitude before being summed. In the case of EGC, the diversity branches are all given equal weights whereas the SDC technique chooses only one branch at a time depending on which has the strongest signal. Assuming F independent signals, in a flat-fading environment, $y_0, y_1, \cdots y_{F-1}$, where:

$$y_i = h_i x_i + n_i$$
$$i = 0,1 \cdots F - 1$$

2.8.1.4.1

and x is the transmitted signal, h is a complex Gaussian random variable and n is AWGN. Using maximum ratio combining on the received signals in the same fashion as in [1]:

$$z = \sum_{i=0}^{F-1} h_i^* y_i$$
$$= \sum_{i=0}^{F-1} |h_i|^2 + \sum_{i=0}^{F-1} h_i^* n_i$$

2.8.1.4.2

Therefore the received SNR of the received signal becomes:

$$SNR = \frac{\left|\sum_{i=0}^{F-1} |h_i|^2\right|^2}{\sigma^2 \sum_{i=0}^{F-1} |h_i|^2} = \frac{\left|\sum_{i=0}^{F-1} |h_i|^2\right|}{\sigma^2}$$

2.8.1.4.3

Where σ^2 is the variance of the AWGN

It is clear from 2.8.1.4.3 that the received SNR, γ, is governed by the distribution of the random variable h. Proakis, [1], has derived, the probability distribution of such parameter, which was:

$$p(\gamma) = \frac{1}{(L-1)! \cdot SNR^F} \cdot \gamma^{F-1} \cdot e^{-\gamma / SNR}$$

2.8.1.4.4

Using selection diversity combining, the received signal would be:

$$z = h_{max} x + n$$

2.8.1.4.5

where $|h_{max}|^2 > |h_i|^2$, $0 \le i < F$. Therefore, the SNR of the received signal is [1]:

$$SNR = \frac{\max_{i=0}^{F-1}\left|h_i\right|^2}{\sigma^2}$$

and the probability distribution of the instantaneous value of the selected branch's SNR is given by:

$$p(\gamma) = \frac{F}{SNR}\left(1 - e^{\left(-\gamma/SNR\right)}\right)^{F-1} \cdot e^{\left(-\gamma/SNR\right)}$$

                                                                             2.8.1.4.6

2.8.2   Equalisation [19]

While diversity techniques are for combating channel fading, equalisation is responsible for compensating for the linear distortions caused by the filtering processes at the transmitter and receiver, and the dispersion of the channel. The presence of the combined effect of this chain of distortions gives rise to ISI, which unless compensated for can cause serious degradation in the system's performance. This is the task of the equaliser, which is usually in the form of a filter with a frequency response equal to the inverse of the combined frequency response of the channel, transmitter filter and receiver filter. The most common types of equalisers are the linear, feedback and the Viterbi equaliser, a brief description of which is given below.

2.8.2.1 Linear Equaliser

The principle of this type of equaliser is to linearly combine the received signal's samples in such a way that ISI is minimised. It is usually in the form of a finite impulse response filter whose coefficients are updated using a suitable adaptive algorithm that takes account of the channel's time variations. This type of equalisers is mainly used in the case of static channels such as telephone lines [21]. In channels with rapid time variations and deep nulls due to the absence of the line of sight, this type of equalisers is disadvantageous. This is because the equaliser may not be able to keep up with the time variations of the channel and also the presence of deep nulls in the channel's response gives rise to compensatory peaks in the equaliser's response resulting in noise enhancement.

2.8.2.2 Feedback Equaliser

This type of equalisers is made up of two sections whose combined operation results in minimising the ISI effect. The first section is used to condition the received signal, then the ISI term due to previous symbols, fed back from the feedback section, is subtracted from the conditioned signal to produce the equalised symbol. A copy of the equalised signal is then fed to the output as well as the feedback section to calculate the ISI term of this symbol on

the new received one, and so on. The main disadvantage of this type of equalisers is the feedback error propagation resulting from an erroneous detection of a few symbols. This type of equalisers was studied by [22]-[24] and found to be more appropriate than the linear equaliser for mobile radio channels.

2.8.2.3 Maximum Likelihood Sequence Estimator (MLSE)

This type of equalisers is based on the Viterbi algorithm in which the channel is treated as a finite state machine where the different states represent the different combinations of input data. The Viterbi algorithm is used to trace all the possible data sequences and select the one that was most likely to have been transmitted. Although the MLSE method is considered to be the optimum estimator, its application is limited as its complexity increases exponentially with the channel memory length. This type of equalisation has been investigated by a number of researchers, some of whom are Omura and Forney [25][26], respectively.

2.8.3   Channel Coding [30]

The idea behind channel coding is to create a relationship between the transmitted information symbols such that when some of these symbols are received in error, the FEC relationship may be used to detect or correct those errors. The basic principle of this relationship is to increase the separation between possible sequences of symbols in a bandwidth efficient manner. While, in static channels, increasing the distance between the sequences may be sufficient it is not the case in time variant channels which require one to also increase the diversity factor of the received signal. One way to do this is by using well-designed interleavers.

There are two main families of codes that have been developed for the AWGN channels. These are the block codes and the convolutional codes, which also includes Trellis coded modulation. Both types take k-input bits and output n coded bits giving a rate k/n code. A decoder can either use the sliced bit values, 0 or 1, or the received noisy symbol values. If the sliced bits are used, this is called *hard decoding*, because the demodulator takes a hard decision before sending the bits to the decoder. If on the other hand the noisy symbols are fed straight in the decoder, this is called *soft decoding*, because no hard decision was made on the symbols. In the hard decoding system some information is usually lost by the receiver, which may consequently impact on the decoder's performance. In general, a soft-decoder outperforms a hard-decoder, but at the expense of extra receiver complexity. While block codes and convolutional codes require an increase in bandwidth or alternatively a reduction in throughput, trellis coded modulation requires neither but uses an expanded constellation to

transmit the coded symbols. The field of coding is a subject of its own rights and has been intensively investigated by many authors [30][31][32].

2.8.4 Interleaving [27]

Diversity to the received signal can be added by combining coding with interleaving. Such diversity is a key to improving the performance of the coding scheme in a fading channel. When interleaving is used, one ensures that all the symbols in a given codeword are not transmitted at the same time. In a system without interleaving, given a code word with the codeword symbols, y_1, y_2, $...y_m$, the system could transmit each element of the codeword in order and receive them in order. If all codewords are transmitted together one codeword may be subjected to many errors. Error correction codes can only correct a limited number of errors. The presence of error bursts can cause the code to fail.

Interleaving the symbols of a given codeword with the symbols of other codewords can distribute these bursts more evenly, so that fewer errors occur in more codewords. If the number of errors per codeword is reduced sufficiently, then the code has a better chance of correcting the errors. This is one way interleaving can help reduce bursty errors.

A parameter for describing interleaving in a given coded system is the interleaving depth, D. For a convolutional code, to interleave at a depth D, one replaces the delays in the encoding circuit by delays of length D. That is if the convolutional encoder is $C(X) = (1 + X, 1+X + X^2)$, the interleaving encoder is $C(X) = (1 + X^D, 1 + X^D + X^{2D})$. Rather than implement D independent encoders, this is implemented with the original encoder and an interleaver in front of the encoder. For a block code of length n, with an interleaver depth of D, the effective length of the code is nD. Rather than transmit each successive code symbol, one would transmit first y_1, y_{D+1}, $... y_{(n-1)D+1}$, y_2, $...$, y_{nD}.

For a fading channel, if fading is changing rapidly enough, interleaving can ensure that the SNRs of the codeword symbols in a given code are independent. If the SNR of each codeword symbol entering the decoder is uncorrelated with the SNRs of the rest of the codeword symbols, we say that the system has perfect interleaving. Unfortunately, not all wireless channels are rapidly changing, and therefore one cannot rely on such parameter for design the optimum interleaver. This is one of the design trade-offs of wireless systems.

2.8.5 High Level Modulation [4]

The use of high level modulation, such as MQAM and MPSK, allows the transmission of more data bits per symbol and hence a much reduced transmission bandwidth. For example,

instead of transmitting 1kbps on a bandwidth of 1kHz using BPSK, the same amount of data can be transmitted using 64QAM at just 200Hz resulting in a five time more bandwidth efficient scheme. Such reduction in the transmission bandwidth is translated into a reduction into the ISI effect.

There are three main drawbacks of using high-level modulation techniques. The first is that high level modulation techniques are more sensitive to additive noise and therefore the bandwidth efficiency provided is merely at the expense of higher SNR. Secondly, the fact that high-level modulation techniques are non-constant envelope makes them more susceptible to severe distortions when used with high power non-linear amplifiers. Finally, the use of high level modulation techniques imposes a restriction on exploiting the inherent diversity in wideband transmission as it uses narrowband signals.

Extensive studies have been carried out to examine the feasibility of using of QAM modulation for audio and TV broadcasting [33][34].

2.8.6   Spread Spectrum SS [28]

Spread spectrum systems are characterised by two major features. The first is the fact that their transmission bandwidth is much greater than that of the information rate. Although, such bandwidth expansion may make the system arguably spectrum inefficient, it is what makes the system able to overcome many of the different levels of interference that are encountered in the transmission of digital signals over the mobile radio channel. The other distinctive feature of such system is its pseudo-randomness, which makes the signals appear similar to random noise and difficult to demodulate by receivers other than the intended ones. Such feature is intimately related to the application or purpose of such signals. While for non-civilian applications, SS is employed to achieve privacy and protection against jamming, for the commercial applications it is mainly used to achieve multi-user multiple access systems. The sub-class of SS systems used for this purpose is called Code Division Multiple Access, CDMA.

In general, the most popular spread spectrum techniques are categorised into three groups, these are direct sequence, DS, frequency hopping, FH, and a hybrid, DS/FH. In the DS type, the data stream first modulates the carrier and then the resultant carrier is combined with a pseudo-noise, PN, sequence. The elements of the PN sequence are normally chosen such that the cross-correlation between different PN sequences is kept very small. Only the intended receiver has a replica of the PN sequence, which is used to extract the transmitted information using a correlator. In FH, the modulated carrier is shifted periodically according

to some predetermined pattern. There are two sub-classes of such system, slow frequency hopping, SFH, and fast frequency hopping, FFH. While for the SFH, the hopping rate is of the order of one hop every many symbols, the FFH system completes many hops per symbol. Similar to the DS case, the intended receiver knows the exact hopping pattern and therefore hops in synchronism with the transmitter to extract the data.

Finally, the DS/FH hybrid technique utilises both of the former two techniques to achieve both time and frequency diversity, but of course at the expense of extra system complexity. In this system, first DS spreading is employed followed by FH.

A typical DS-CDMA transmitter spreads the individual symbols of the serial data stream using a given spreading code in the time domain. The capability of the receiver suppressing the multi-user interference effect is determined by the cross-correlation characteristic of the used spreading codes. In the presence of multipath channels, the auto-correlation property of the individual spreading codes plays a very important role in distinguishing the different components of the composite received signal. Figure 2.8.6.1 shows the DS-CDMA transceiver structure of the jth user for a coherent BPSK based system, where G_{DS} represents the processing gain and $C^j(t)=[C^j{}_1, C^j{}_2, \dots C^j{}_{GDS}]$ is the spreading code for the jth user.
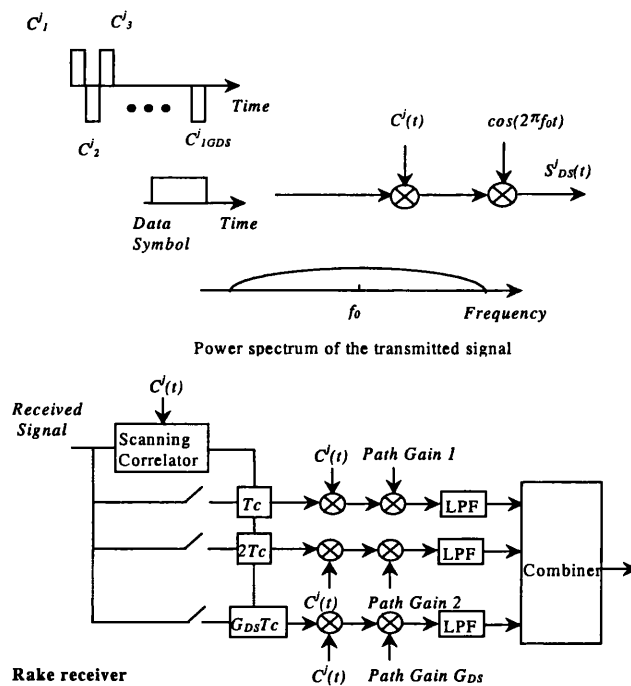
Figure 2.8.6.1: DS-CDMA Transceiver

In general, spread spectrum techniques are usually used in conjunction with the rake receiver to combat ISI and at the same time exploit the inherent diversity of wideband transmission [38][39]. The idea of the rake receiver is to correlate the signal with delayed replicas of the

user's signature, where the delays correspond to the channel delays and thus each synchronises with a different multipath component. The outputs are then corrected in phase and amplitude before being combined together.

2.8.7 Multicarrier Modulation [55][56]

Multicarrier modulation, MC, also known as Orthogonal Frequency Division Multiplexing, OFDM, is a modulation technique that is known for its spectrum efficiency. In such techniques a given spectrum is divided into several overlapping sub-bands in the aim to convert a highly frequency selective channel into many flat fading sub-channels. Thus, a high rate bit stream may be transmitted simultaneously on narrowband subchannels at much lower rate. Because the data is transmitted in parallel over the individual sub-bands, the symbol duration is now stretched in time and therefore the signal is much more robust against the dispersive behaviour of the channel [40][41]. An OFDM signal may be easily generated and demodulated using the fast Fourier transform and its inverse, which has shown to be a more practical alternative to using a bank of filters [42][43].

In order to preserve the orthogonality of the sub-carriers and ensure that the received symbols are ISI free, a cyclic prefix of the same length as the maximum delay spread of the channel may be added at the beginning of every symbol. Although the addition of the cyclic prefix reduces the spectrum efficiency of the system, its advantages outweighs the drawbacks since it can be used for more than just ISI elimination, such as, channel estimation and synchronisation.

MCM combined with differential demodulation eliminates the need for equalisation completely. Although, in the case of coherent modulation, it is necessary to equalise, the kind of equalisation required is much simpler than that required for high data rate transmission. In addition, in the case of slowly time varying channel, it is possible to use decision directed adaptive feedback techniques with high bandwidth efficient and very good BER performance.

There are two main special forms of OFDM that have attracted a lot of attention in practice. These are the coded OFDM and the code division multiple access OFDM, CDMA/OFDM. Below is a brief description of each.

2.8.8 Coded OFDM, COFDM

The presence of frequency selective fading in mobile radio channels implies that some of the OFDM signal's subcarriers would be attenuated much more than others and therefore the data carried on those subcarriers might be completely destroyed. In order to avoid such situations, the diversity inherent in the OFDM system can be fully exploited by using coding and interleaving across the subcarriers. This introduces a relationship between the information carried on the different subcarriers such that at the receiver this relationship can be used to recover the data affected by deep nulls in the channel's frequency response. This issue was mentioned by sari *et al* in [48], who warned against over enthusiastic pursuit of OFDM. Techniques than coding and interleaving can also be used to counteract this problem. These include the use of adaptive bit-loading, [35][36], in which different signal constellations are used on different subcarriers depending on the positions of the deep nulls in the frequency response of the channel. In contrary to adaptive bit-loading, pre-equalisation using the channel inversion technique, [37], can also be used in the aim to keep the power spectral density of the received composite signal, almost, uniformly distributed. Signal spreading across the subcarriers can also be used, for example according to a linear matrix operation as proposed in orthogonal multicarrier code division multiplexing.

2.8.9 Multicarrier Code division Multiple access, MCDMA [50]-[56]

The use of OFDM in conjunction with other schemes for establishing reliable multiple access communication links has attracted a lot of attention in the 1990s, [43]. Three main schemes based on the combination of CDMA and OFDM have been proposed and analysed by different researchers. These were, multicarrier-code-division multiple access, MC-CDMA, by [49] and [50], multicarrier direct sequence code division multiple access, MC-DS-CDMA, by [51] [52] and multitone code division multiple access, MT-CDMA, by [53][54]. A brief description of each of these techniques along with the original DS-CDMA technique is given below.

2.8.9.1 MC-CDMA Scheme

This scheme is based on the first category described above in which the spreading code is assumed to be in the frequency domain [49][50]. The use of orthogonal codes, such as Walsh-Hadamard codes for such a system guarantees the absence of multiple access interference (MAI) in an ISI-free channel [50][55]. Because this scheme uses all the received signal's energy scattered in the frequency domain, it has an additional degree of freedom compared to the single carrier DS-CDMA scheme.

Figure 2.8.9.1.1 shows the MC-CDMA transmitter of the jth user for a coherent BPSK based system along with the power spectrum of the transmitted signal. G_{MC} is the processing gain, N_c is the number of subcarriers and $C^j(t)$ is the spreading code of the jth user.

Although the system described in [49] assumes that the spreading code length is equal to the number of subcarriers, this is not a condition that has to be satisfied [55]. A modified version of this technique was proposed by [55], in which the number of subcarriers is P times the spreading code length. Figure 2.8.9.1.2 shows the modification needed to cope when the number of subcarriers exceeds the code length.
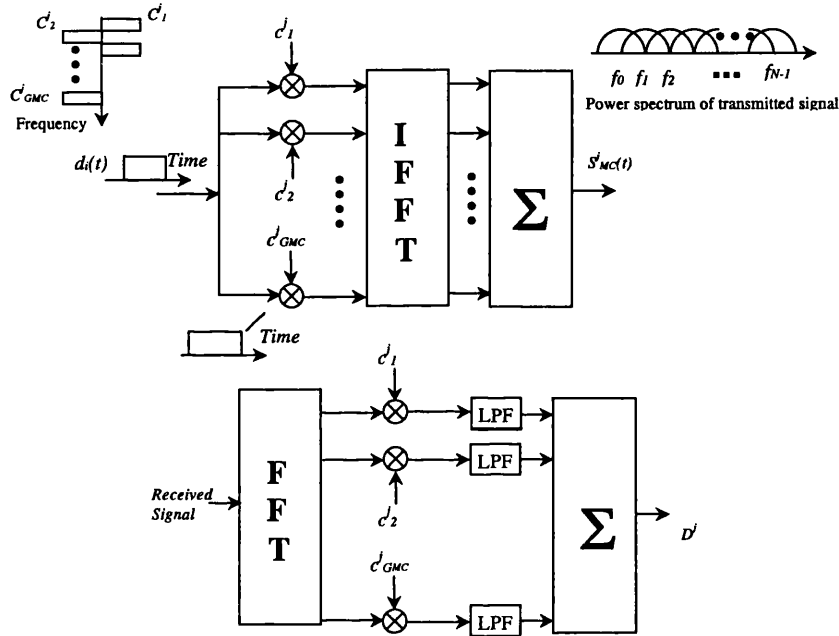
Figure 2.8.9.1.1: MC-DS-CDMA Transmitter

Proper choice of the number of subcarriers and guard interval is important in order to increase the robustness of the system to frequency selective fading and possible ISI. Given the characteristic of the radio channel, [56] proposes an 'optimal' way of minimising the BER as a function of the number of subcarriers and guard interval duration.
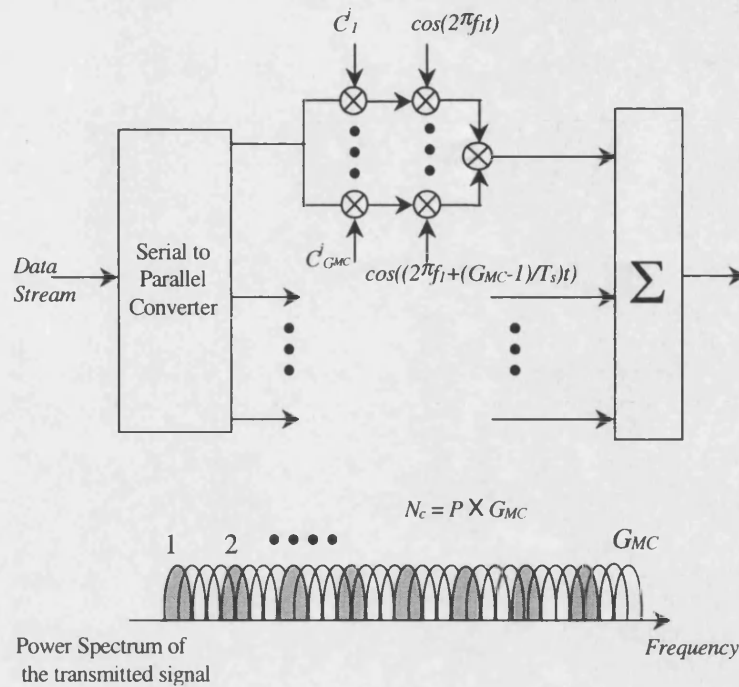
Figure 2.8.9.1.2: Modified MC-CDMA Transceiver

2.8.9.2   MC-DS-CDMA Scheme

This type of multicarrier scheme spreads the serial to parallel converted symbols in the time domain using a given spreading code such that the resulting spectrum of the individual carriers satisfies the orthogonality condition [51]. This scheme was proposed as a candidate technique for the uplink communication channel. Although this scheme benefits from time diversity, the frequency diversity option can only be utilised if coding and interleaving is employed. Alternatively, frequency interleaving can be exploited by using subcarrier hopping techniques or transmitting the same information simultaneously on more than one subcarrier.

Figure 2.8.9.2.1 shows the structure of the transceiver of such system and the power spectral density of the resulting signal. In [52] a multicarrier based DS-CDMA system with a larger subcarrier separation was proposed in order to yield both frequency diversity improvement and narrowband interference suppression. In order to provide frequency diversity a MC-DS-CDMA system was examined by Sourour et al, [53], in which the data symbol was sent on more than one subcarrier.
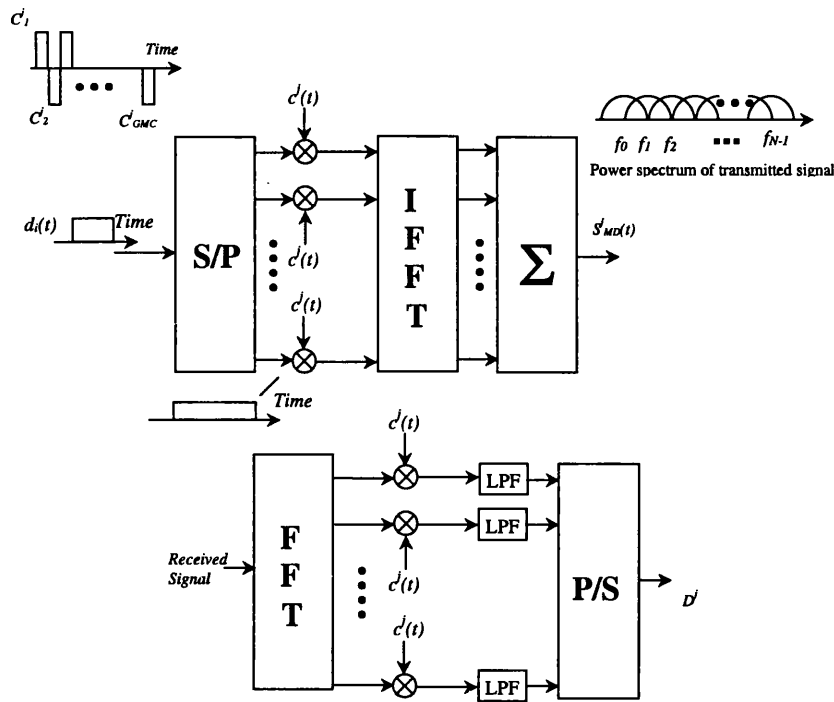
Figure 2.8.9.2.1: MC-DS-CDMA Transceiver

2.8.9.3 MT-CDMA Scheme

The multitone CDMA, MT-CDMA, technique is based on spreading the serial to parallel converted symbols using a spreading code in the time domain so that the spectrum of the subcarriers prior to spreading satisfies the orthogonality condition [54]. Thus, the spectrum of the individual subcarriers after spreading no longer satisfies the orthogonality condition. Normally, MT-CDMA systems use longer spreading codes in proportion to the number of subcarriers as compared to single carrier DS-CDMA systems and therefore can accommodate more users. In Figure 2.8.9.3.1 a block diagram of an MT-CDMA based system is presented where G_{MT} is the processing gain of the spreading code used. The fact that the spectrum of the transmitted signal consists of more densely spaced subcarriers than that of the other techniques gives rise to ICI. On the other hand, the use of longer codes helps to reduce self-interference as well as multiple access interference that are normally associated with CDMA transmission. Since this type of transmission is more likely to experience frequency selective fading, rake receivers are normally used for proper signal detection.
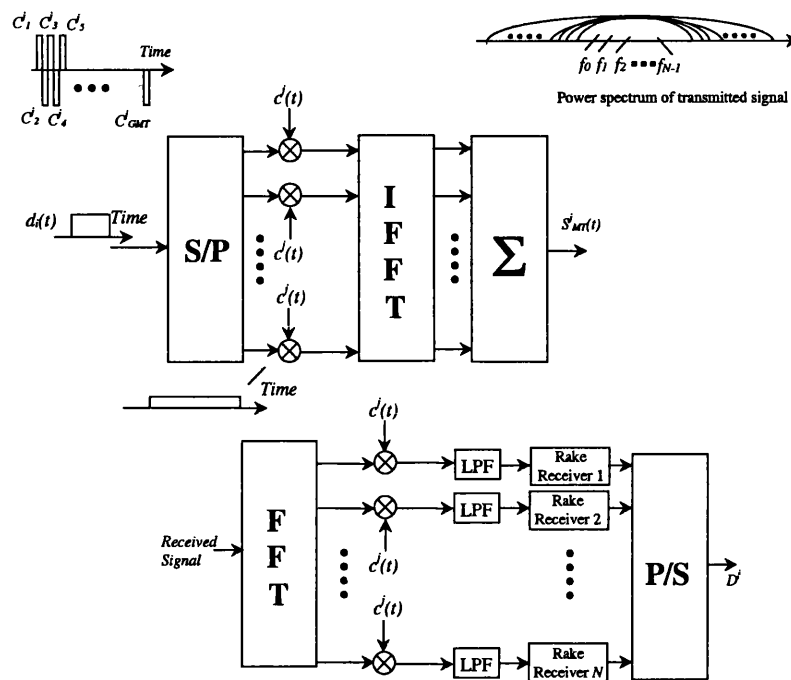
Figure 2.8.9.3.1: MT-CDMA Transceiver

2.9 Summary

In this section the mechanism of signal transmission through the mobile radio channel has been described. It was shown how the impact of the multipath phenomenon could severely degrade the quality of the transmitted signal. The worst scenario of a mobile radio channel is when there no line of sight in which case the channel is termed Rayleigh. The impact of the multipath effect is worsened when the mobile user is in motion due to the Doppler spreading which makes it difficult for the receiver to track the carrier frequency of the transmitted signal. In wideband systems, the phenomenon of multipath gives rise to intersymbol interference and imposes a constraint on the maximum transmission rate. Intersymbol interference can be reduced by the use of channel equalisation, which requires an up to date estimate of the channel frequency response. A channel is termed narrowband when the transmission bandwidth is less than the coherence bandwidth of the channel, otherwise it is referred to as wideband. The signal fading resulting from the distance travelled by the signal and the multipath effect may be split into two categories, namely, fast fading and slow fading. Fast fading refers to the instantaneous changes in the signal's amplitude and may be approximated to be Ricean or Rayleigh distributed depending on whether a line of exists or not, respectively. Slow fading, on the other hand, refers to the variations in the average signal's field strength and may be approximated to have a Log normal distribution.

The COST 207 channels delay profiles for typical urban and hilly terrain environments have been outlined for a discrete GWSSUS tapped delay line channel model. The time varying properties of the channel is modelled by generating time varying complex multiplicative coefficients. These are produced by using pairs of uncorrelated AWGN generators, where each pair represents the real and imaginary part of one coefficient. The Doppler effect is simulated by passing the coefficients though a lowpass filter with a frequency response defined by the Doppler spectrum.

A number of techniques for combating the channel's imposed limitations have been briefly reviewed. These included techniques such as diversity, equalisation, forward error correcting coding, spread spectrum and multicarrier modulation.

2.10 References

[1] J. G. Proakis, *"Digital Communications"*, 3ed, McGraw Hill, 1995.

[2] R. C. V. Macario, *"Modern Personal Radio Systems "*, IEE, 1996.

[3] P. A. Bello, *"Characterisation of Randomly Time Variant Linear Channels"*, IEEE Transactions on Communications systems, Vol. CS-11, pp. 36-393, Dec 1963.

[4] W. T. Webb and L. Hanzo, *"Modern Quadrature Amplitude Modulation"*, IEEE Press, 1995.

[5] R. Steele. *"Mobile Radio Communications"*, 3ed edition, IEEE Press, 1992.

[6] M. Schwartz and W. R. Bennet, *"Communications Systems and Techniques"*, McGraw-Hill, Inc., 1996

[7] H. Suzuki, *"A Statistical Model for Urban Radio Propagation"* IEEE Transactions on Communications, Vol. 25, pp. 673-680, July 1977.

[8] W. C. Lee, *"Mobile Communications, Design and Fundamentals"*, John Wiley and Sons, 2ed 1993.

[9] W. C. Jakes, *"Microwave Mobile Communications"* John Wiley and Sons, 1974.

[10] D. C. Cox and R. P. Leck, *"Correlation Bandwidth and Multipath Delay Spread Multipath Propagation Statistics for 910Mhz Urban Mobile Radio Channels"*, IEEE Transactions, Vol.COM-23, No. 11, pp. 1271-1280, Nov. 1975.

[11] P. A. Bello and B. D. Nelin, *"The Effect of Frequency Selective Fading on the Binary Error Probabilities of Incoherent and Differentially Coherent Matched Filter Receivers"*, IEEE Transactions, Vol.CS-11, No. 2, pp. 170-186, June 1963.

[12] E. C. Ifeature and B. W. Jervis, *"Digital Signal Processing, A Practical approach"*, Addison Wesley publishers ltd, 1993.

[13] W. H. Press, S. A. Teukolsky, W. T. Vetterling and B. P. Flannery, *"Numerical recipes in C"*, 2nd edition, Cambridge.

[14] D. I. Laurenson, D. G. M. Gruickshank and G. J. Povey, *"A computationally Efficient Multipath Channel Simulator for the Cost 207 Models"*, IEEE conference proceedings 1996.

[15] W. C. Wong, R. Steele, B. Glance and D. Horn, *"Time Diversity With Adaptive Error-Detection to Combat Rayleigh Fading in Digital Mobile Radio"*, IEEE Transactions On Communications, vol. 31 no 3 pp. 378-387, 1983.

[16] E. S. Golovin, *"Space-Time Diversity Reception in Mobile Radio Systems"*, Telecommunications and Radio Engineering, vol. 39-4, no. 2, pp. 78-80, 1985.

[17] Y. G. Li, J. C.Chuang and N. R. Sollenberger, *"Transmitter diversity for OFDM systems and its impact on high-rate data wireless networks"*, IEEE Journal on Selected Areas in Communications, vol. 17, no. 7, pp. 1233-1243, 1999.

[18] T. Kumagai , T. Sakata, and M. Morikura ,*"A maximal ratio combining frequency diversity ARQ scheme for high- speed OFDM systems"*, IEICE Transactions on Communications, vol. E82B, no. 12, pp. 1914-1922 , 1999.

[19] S. Qureshi, *"Adaptive Equalisation"*, IEEE Communications Magazine, pp. 9-16, 1982.

[20] A. D. Whalen, *"Detection of Signals in Noise"*, Academic Press, New York and London, 1971.

[21] R. W. Lucky, J. Salz and E. J. Weldon, *"Automatic Equalisation for Digital Communication"*, Bell System Technology Journal, Vol. 45, pp. 547-588, Apr. 1965.

[22] P. Monsen, *"Feedback Equalisation for Fading Dispersive Channels"*, IEEE Transactions on Information Theory, Vol. IT-17, pp. 56-64, Jan. 1971.

[23] P. Monsen, *"Digital Transmission Performance on Fading Dispersive Diversity Channels"*, IEEE Transactions on Communications, Vol. COM-21, pp. 33-39, Jan. 1973.

[24] P. Monsen, *"Adaptive Equalisation of The Slow Fading Dispersive Channels"*, IEEE Transactions on Communications, Vol. COM-22, pp. 1064-1075, Aug. 1974.

[25] J. Omura, *"Optimal Receiver Design for Convolutional Codes and Channels with Memory via Control Theoretical Concepts"*, Inform. Sci., Vol. 3, pp. 490-497, July 1974.

[26] G. D. Forney, *"Maximum Likelihood Sequence Estimation of Digital Sequences in the Presence of Intersymbol Interference"*, IEEE Transactions on Infromation Theory, Vol. IT-18, pp. 363-378, May 1972.

[27] B. Sklar, *"Digital Communications: Fundamentals and applications"*, Prentice-Hall, International Edition, 1988.

[28] M. K. Simon, J. K. Omura, R. A. Scholtz and B. K. Levitt, *"Spread Spectrum Communications"*, vol. 1, Computer Science Press, Inc. Rockville, Md., 1985.

[29] J. D. Parsons and J. G. Gardiner, *"Mobile Communications Systems"*, Blackei, 1989.

[30] S. Lin and D. Costello, *"Error Control Coding Fundamentals and Applications"*, Prentice Hall, 1983.

[31] J. L. Massey, *"Threshold Decoding"*, MIT Press, Cambridge Mass., 1963.

[32] E. R. Berlekamp, *"Algebric Coding Theory"*, McGraw-Hill, New York, 1968.

[33] P. Dupuis, *"16QAM Modulation for High Capacity Digital Radio System"*, IEEE Transactions on Communications, Vol. COM-27, pp. 1771-1782, Dec. 1979.

[34] I. Horikawa, *"Design and Performance of a 200Mbps 16QAM Digital Radio System, IEEE Transactions on Communications"*, Vol. COM-27, pp. 1953-1958, Dec. 1979.

[35] J.K Cavers, *"Variable Rate Transmission for Rayleigh Fading Channels"*, ", IEEE Transactions on Communications Technology, vol. COM-20, pp. 15-22, Feb. 1972.

[36] W. T. Webb, and R. Steele, *"Variable Rate QAM for Mobile Radio"*, IEEE Transactions on Communications Technology, Vol. 43, pp. 2223-2230, July 1995.

[37] T. Keller and L Hanzo, *"Sub-Band Adaptive Pre-Equalised OFDM Transmission"*, Proceedings of VTC'99 falls, pp. 334-338, Sept. 1999.

[38] R. Price, *"A Communication Technique for Multipath Channels "*, Proc. IRE, Vol. 46, pp. 555-570, March 1958.

[39] M. L. Doelz, E. T. Heald, and D. L. Martin, *"Binary Data Transmission Techniques for Linear systems"*, Proc. IRE, Vol. 45, pp. 656-661, May 1957.

[40] R. W. Chang, *"Synthesis of Bandlimited Orthogonal Signals for Multichannel Data Transmission"*, The Bell System Technology Journal, pp. 1775-1796, Dec. 1966.

[41] B. R. Saltzberg, *"Performance of an Efficient Parallel Data Transmission System"*, IEEE Transactions on Communications Technology, Vol. COM-15, No. 6, pp. 805-811, Dec. 1967.

[42] S. B. Weinstein and P. M. Ebert, *"Data Transmission by Frequency Division Multiplexing using the Discrete Fourier Transform"*, IEEE Transactions on Communications, Vol. COM-19, pp. 628-634, Oct. 1971.

[43] M. Alard and R. Lassal, *"Principles of Modulation and Channel Coding for Digital Broadcasting for Mobile Receivers"*, EBU Review-Technical, No. 224, pp. 168-190, Aug. 1987.

[44] E. Feig and A. Nadas, *"The Performance of Fourier Transform Division Multiplexing Schemes on Peak Limited Channels "*, GLOBCOM'88, pp. 1141-1144, Dec. 1988.

[45] C. Rapp, *"Effect of HPA-Nonlinearity on 4-DPS/OFDM Signal for a Digital Sound Broadcasting System"*, Proc. Second European Conference on Satellite Communication, Belgium, ESA SP-332, pp. 178-184, 22-24, Oct. 1991.

[46] R. G. Gallager, *"Information Theory and Reliable Communication"*, John Wiley, 1968.

[47] N. Seshadri, Personal communications, 1993.

[48] H. Sari, G. Karam and I. Jeanclaude, *"Transmission Technique for Digital Terrestrial TV Broadcasting "*, IEEE Communications Magazine, Vol. 33, No. 2, pp. 100-109, Feb. 1995.

[49] N. Yee, J-P. Linnartz and G. Fettweis, *" Multicarrier CDMA in Indoor Wireless Radio Networks"*, IEEE PIMRC'93, Conference Proceedings, pp. 109-113, Yokohama, Japan, Sept. 1993.

[50] K. Fazel and L. Papake, "*On the Performance of Convolutionally Coded CDMA/OFDM For Mobile Communication Systems*", IEEE PIMRC'93, Conference Proceedings, pp. 468-472, Yokohama, Japan, Sept. 1993.

[51] V. M. DaSilva and E. S. Sousa, "*Performance of Orthogonal CDMA Codes for Quasi-synchronous Communication Systems*", IEEE ICUPC'93, Conference Proceedings pp. 995-999, Ottawa, Canada, Oct. 1993.

[52] S. Kondo and L. B. Milstein, " *Performance of Multicarrier DS CDMA Systems*", IEEE Transactions on Communications, Vol. 44, No. 2, pp. 238-246, Feb.1996.

[53] E. Sourour and M. Nakagawa, "*Performance of Multicarrier CDMA in Multipath Fading Channel*", IEEE Transactions on Communications, Vol. 44, No. 3 , pp. 356-67, March 1996

[54] L. Vandendorpe, "Multitone Direct Sequence CDMA in an Indoor Wireless Environment ",IEEE Proceedings of the First Symposium of Communications and Vehicular Technology in the Benelux, pp. 4.1-1.4.1.8, Delft, The Netherlands, Oct. 1993.

[55] R. Parsad and S. Hara, "*An Overview of Multicarrier CDMA*", IEEE ISSSTA'96 Conference Proceedings, pp. 107-113, 1996.

[56] S. Hara, "*Transmission Performance Analysis of Multicarrier Modulation in Frequency Selective Fast Rayleigh Fading Channel*", Wireless Personal Communications, Vol. 2, No. 4, pp. 335-356, 1995/1996

Chapter Three

General Description of OFDM Systems

3 Chapter Three

3.1 Introduction

The mobile radio channel is a hostile transmission environment that simultaneously contains multiple paths, interference and impulsive noise. As described in the previous chapter, the impulse response of the channel can be represented as the sum of Dirac pulses each with a Rayleigh/Rican distributed amplitude and different delay. As the impulse response of the mobile channel may extend over many microseconds it makes the transmission of data at high rates (several Mbps) a difficult task. Several techniques have been investigated in order to make the transmission of data at high rates successful. These are mainly based on extending the duration of the transmitted symbol (in the time domain or frequency domain) by increasing the dimension of the symbol alphabet. Among these techniques is spread spectrum. The principle of this technique is to stretch the spectrum of the transmitted symbols and maintain the autocorrelation function of these symbols narrow so that the different paths that compose the signal are separable at the receiver. The principle is to define an alphabet of M pseudo-random orthogonal sequences and to transmit one of these sequences, which is equivalent to $\log_2 M$ bits. However, the constraint of intercorrelation between different sequences leads to an important increase in the bandwidth which is far from being compensated by increasing the number of bits per symbol, hence this technique is considered to be relatively spectrally inefficient [23].

Another approach that has found considerable attention stretches the signal in the time domain by transmitting a high bit rate stream of data simultaneously on many parallel low rate subchannels [3], thus, transforming a highly selective wideband channel into a large number of parallel non-selective narrowband channels. Furthermore, the use of coding and interleaving techniques that are adapted to the fading nature of the channel improves the performance of such a system considerably.

The advantages and principles of this technique will be the theme of this chapter. In the next section, a brief description of the up to date history of this technique, which is known as Orthogonal Frequency Division Multiplexing, OFDM will be presented. This will be followed by a review of the implementation issues of OFDM as well as a mathematical analysis. Finally, the theoretical performance of OFDM in both time and frequency selective fading channels will be presented.

3.2 History of OFDM

The history of OFDM can be dated back as far as the 1950s when it was considered for bandwidth efficient data transmission over telephone and HF radio channels [1][2]. The concept of parallel transmission attracted more attention in the 1960s when Chang followed by Saltzberg, [3][4], published their work on the synthesis of bandlimited signals for multichannel transmission and on the performance of such system, respectively. The contribution of Weinstein et al [5] was a turning point in the history of OFDM when it was shown that the modulation and demodulation of the baseband OFDM signals can be performed using the discrete Fourier transform. This contribution mainly focussed on the processing efficiency of generating the OFDM signals eliminating the need to use a bank of oscillators and filters as initially proposed. In addition, a completely digital implementation could be built around special purpose hardware performing the Fast Fourier Transform (FFT). Although Weinstein *et al* proposed the use of a time guard interval to combat ISI over dispersive channels, their system did not have perfect orthogonality between the subcarriers and it was Peled et al [6] who solved this problem by proposing the use of a cyclic prefix, CP. Because now the time guard interval is filled with a cyclic extension of the OFDM symbol, this method effectively simulates a channel performing cyclic convolution with the transmitted symbol, in which case when the CP is longer than the maximum delay spread, the subcarriers remain orthogonal.

The use of different pulse shaping techniques for the purpose of reducing the impact ICI have been investigated by a number of authors e.g. [7][8].

Although OFDM suffers from high peak to average power ratios, a number of techniques such as the use of special block codes, [9], and selective scrambling, [10], have been investigated and shown to be potential solutions.

A number of researchers have proposed the use of OFDM for various applications. Hirosaki, [12], has designed and tested a 19.2 Kbps voiceband data modem using orthogonally multiplexed QAM. A number of other OFDM based modems for telephone lines have also been investigated, e.g. [13][14].

OFDM, under the name of discrete multitone transmission, DMT, has attracted a lot of attention as a potential technique for high-speed transmission on the existing telephone network [15][16].

In the non-transmission applications, Feig et al explored the use of discrete multitone technique using DFT for applications in the linearised magnetic storage channel [17][18].

In the 1990s, OFDM has been investigated for wideband data communications over the mobile radio channels, high bit rate digital subscriber lines (HDSL), asymmetric digital subscriber lines (ADSL), very high-speed digital subscriber lines, (VHDSL), digital audio broadcasting, (DAB), digital television and HDTV terrestrial broadcasting, [20].

Casas et al [19], proposed OFDM/FM for data communication over mobile radio channels. It was claimed that OFDM/FM systems could be implemented simply and inexpensively by retrofitting existing FM radio systems.

Chow et al [20], analysed the multitone modulation with discrete Fourier transform in transceiver design and showed that it is an excellent method for delivering high speed data to customers, both in terms of performance and cost for ADSL (1.536Mbps), HDSL (1.6Mbps) and VHDSL (100Mbps).

In response to the intensive research into practical high-speed data OFDM based systems for wireless applications [21]-[25], the use of OFDM modulation for two digital terrestrial broadcasting services has been standardised in Europe. These systems are the digital audio broadcasting, DAB, and digital terrestrial video broadcasting, DTVB. Both are pure broadcasting services that transmit data over broadband radio channels. DAB is suited for mobile receivers and the total data rate is 1.7 Mbps. DTVB has a net data rate of more than 20Mbps and is designed for stationary reception only. Furthermore, it is now being discussed for extending DAB in order to enable high data rates for multimedia services [21]. Recently, OFDM was also standardised in Japan for digital TV broadcasting [26].

At present, the application of OFDM modulation is discussed for various broadband communication systems and services. OFDM is now considered the physical layer modulation scheme for the wireless ATM/LAN [28]. In 1998, the IEEE 802.11 standardisation group decided to select OFDM as the basis for a new physical layer standard extension to the existing 802.11 MAC standard. The new standard is targeting a range of data rates from 6 up to 54 Mbps in the 5 GHz band. Following this, ETSI-BRAN in Europe and MMAC in Japan also based their new standards on OFDM with the aim of creating a single international standard for wireless LAN. J.J Van de Beek et al [30], have proposed OFDM for the universal mobile telecommunication systems, UMTS. This however has not

been selected for the final round on standardising the 3G air-interface technique due to lack of support from manufacturers amongst other reasons.

The application of adaptive OFDM systems has been the subject of intense interest for the past few years until present. The use of adaptive constellation, coding, power allocation, subcarrier allocation or any combination of such parameters has shown to greatly improve the performance of such system, see for example [31]-[38].

The use of OFDM in environments containing intentional interference as well as Rayleigh fading has been investigated by a number of researchers [39]-[43]. While multicarrier systems proposed in [39][40] consider receivers with sub-optimal combining techniques, the receivers considered in [41]-[43] are designed to selectively root out the effects of the intentional interference.

3.3 Basic Principle Of OFDM

In conventional serial data transmission systems the symbols are transmitted sequentially such that the frequency spectrum of each symbol is allowed to occupy the entire available bandwidth.

The OFDM technique is one in which several sequential streams of data are transmitted simultaneously, so that at any instant in time many data symbols are being transmitted. In such a system, the bandwidth of every individual stream, which is known as the subchannel, occupies a small fraction of the available bandwidth. By transmitting the data simultaneously over many low rate subchannels, the wideband transmission system is now converted into many narrowband systems, which individually experience mainly flat fading. To obtain high spectral efficiency, the frequency response of the subchannels are allowed to partially overlap with specific orthogonality constraints to facilitate the separation of the carriers at the receiver. The orthogonality between the subchannels can be maintained, even if the signal is passed through a time-dispersive channel, by appending a cyclic prefix at the front of every OFDM symbol. The cyclic prefix is a copy of the last part of the OFDM symbol of length equal to or greater than the maximum delay spread of the channel. Although the insertion of a cyclic prefix imposes a penalty in terms of transmitted power and available bandwidth, it is well agreed that it's the best compromise between performance and efficiency in the presence of ISI. A more detailed discussion of this topic will be presented later. An OFDM signal can be generated as shown in Figure 3.3.1 below.

The *M*-bit groupings at the output of the serial to parallel converter are applied to a signal mapper to set the amplitude and phase of each subchannel in the form of complex values according to some predetermined constellation. The IFFT is then used to convert the frequency-domain phase and amplitude data for each subchannel into a block of *N* time domain samples. The samples are then parallel to serial converted before being appended a cyclic prefix. The resulting time domain samples are then appropriately converted to an analogue modulating signal, which is then input to the RF modulator. At the receiver the reverse process is implemented. The FFT is used to extract the phase and amplitude of each received subchannel from the block of received samples. The larger *N* is made the longer the symbol period becomes and the less susceptible the system is to burst errors and delay spread. The number of subcarriers *N*, however, is in practice limited by the limitations in the filtering process, computational time, the available transmission bandwidth of the mobile channel and the Doppler frequency which imposes limits on the separation band as will be explained later in this report.

The Fast Fourier Transform (FFT) and the Inverse FFT (IFFT) are in practice used instead of the IDFT/DFT due to their computational efficiency.

Input	*Output*
Serial To Parallel Converter	FEC Decoder & De-Interleaver
... M bits	
FEC Encoder & Interleaver	Demapper e.g. QAM
Mapper e.g. QAM	Parallel To Serial Converter
IFFT	FFT
Parallel To Serial Converter	Serial To Parallel Converter
Cyclic Prefix Insertion	Cyclic Prefix Extraction
DAC	ADC
RF	Channel	RF
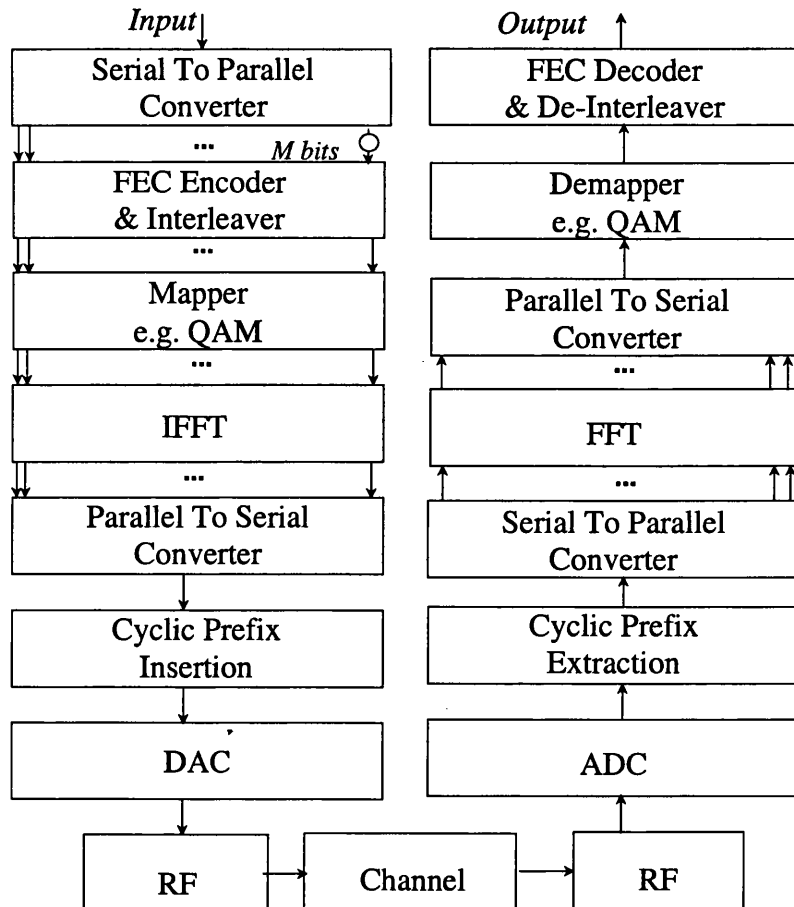
Figure 3.3.1 : Schematic of the OFDM Transceiver

3.4 Mathematical Modelling of OFDM

The difficulties associated with a complete analysis of this system make it rather awkward for theoretical studies. Thus, it is common practice to use simplified models resulting in tractable analysis. These are classified as the continuous time and discrete time models.

3.4.1 Continuous Time Model

Since the first OFDM system was not implemented in a digital form, the continuous time model presented here is considered the ideal OFDM system. For simplicity, it is initially assumed that no ISI is present and hence no cyclic prefix is needed.

The continuous OFDM signal can be formed using the following set of elementary orthogonal signals:

$$\varphi_{m,k} = g_k(t - mT),$$

3.4.1.1

where

$$-\infty < m < \infty$$

$$0 \le k < N$$

N = number of carriers to be considered,

T is the duration of the symbol,

$g_k(t)$ is a rectangular pulse modulated onto N subcarriers and defined as:

$$g_k(t) = \begin{cases} \dfrac{e^{j2\pi f_k t}}{\sqrt{T}} & for\, 0 \le t < T \\ 0 & Otherwise \end{cases},$$

3.4.1.2

where $f_k = \dfrac{k}{T}$ or $f_k = \dfrac{k}{NT_s}$,

And T_s is the serial symbol duration.

Therefore, the transmitted OFDM baseband signal of the mth symbol is represented as

$$s_m(t) = \sum_{k=0}^{N-1} x_{k,m} \varphi_k(t - mT),$$

3.4.1.3

where $x_{k,m}$ are a set of complex numbers having values taken from a finite alphabet and representing the emitted data signal.

The OFDM signal can therefore be in general written as

$$s(t) = \sum_{m=-\infty}^{\infty} s_m(t)$$
$$= \sum_{m=-\infty}^{\infty} \sum_{k=0}^{N-1} x_{k,m} \varphi_{m,k}(t)$$

$$\text{,} \qquad\qquad 3.4.1.4$$

The demodulation of the OFDM signals is achieved using a bank of filters matched to $\varphi_k(t)$, that is

$$y_{k,m} = \int_{-\infty}^{\infty} r(t)\varphi_{k,m}^*(t)d(t) , \qquad\qquad 3.4.1.5$$

The generation of a continuous time OFDM signal can be represented in a block diagram as shown in Figure 3.4.1.1 below.
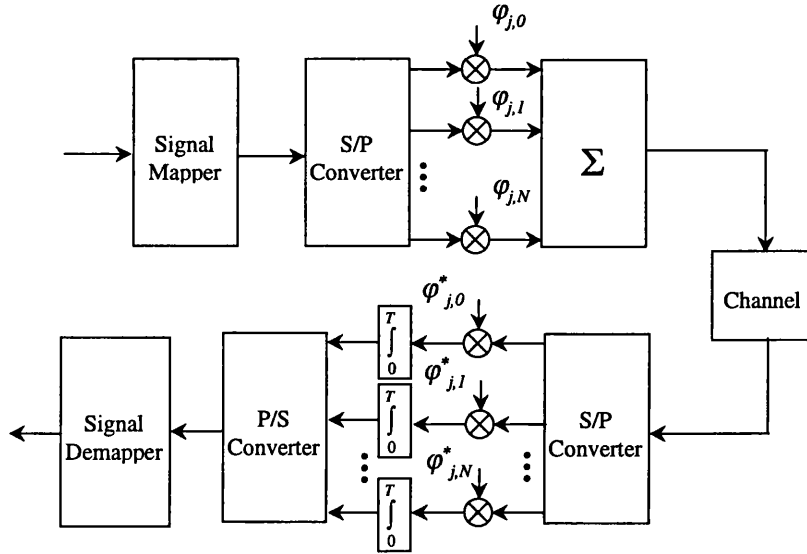
Figure 3.4.1.1: Baseband Continuous OFDM System Model

The transmitted energy per subcarrier, E_s, can be given by:

$$E_s = \int_{-\infty}^{\infty} |\varphi_k(t)|^2 dt , \qquad\qquad 3.4.1.6$$

In the presence of ISI, the duration of the OFDM symbols is usually extended by appending a cyclic prefix of length equal to the maximum significant delay spread of the channel. Taking this into account, the new OFDM duration, T', is given as:

$$T' = T + T_{cyc}$$
     3.4.1.7

where T_{cyc} is the duration of the cyclic prefix.

Thus, the elementary signals, $\varphi_{m,k}(t)$, are modified as follows:

$$\varphi'_{m,k} = g'(t - mT'),$$
     3.4.1.8

And

$$g'_k(t) = \begin{cases} \dfrac{e^{j2\pi f_k t}}{\sqrt{T + T_{cyc}}} & for - T_{cyc} \le t < T \\ 0 & Otherwise \end{cases},$$
     3.4.1.9

3.4.2   Discrete Time Model

A discrete time model of the OFDM system is shown in Figure 3.3.1. Assuming that the data to be transmitted is encoded into complex symbols, d_n, such that $d_n = a_n + jb_n$, then the signal at the output of the OFDM transmitter can represented mathematically as:

$$\begin{aligned} X(t) &= \sum_{n=0}^{N-1} a_n \cos(\omega_n t) + b_n \sin(\omega_n t) \\ &= \Re\left\{ \sum_{n=0}^{N-1} (a_n + jb_n) e^{(j\omega_n t)} \right\} \\ &= \Re\left\{ \sum_{n=0}^{N-1} d_n e^{(j\omega_n t)} \right\} \end{aligned}$$
     3.4.2.1

where a_n and b_n are the inphase and quadrature components of the signal and $\omega_n = 2\pi f_n$ is the subcarrier frequency. It can be shown mathematically that taking the DFT of the parallel data input symbols, d_n, and transmitting the output in series is equivalent to the operation done at the OFDM transmitter of Figure 3.4.1.1 [54].

Using the complex conjugate equality equation 3.4.2.1 can be rewritten as

$$X(t) = \sum_{n=0}^{N-1} \frac{1}{2} \left\{ d_n e^{(j2\pi f_n t)} + d_n^* e^{(-j2\pi f_n t)} \right\},$$
     3.4.2.2

Which is equivalent to

$$X(t) = \frac{1}{2} \sum_{n=(-N+1)}^{N-1} d_n e^{(j2\pi f_n t)} \, ,$$

         3.4.2.3

where $n = 0,1,....,N-1$

     Δf = subcarrier spacing

     $f_n = n\Delta f$

     $d_{-n} = d_n^*, d_0 = 0, f_{(-n)} = -f_n, f_0 = 0$

In order to simplify the above, a new coefficient, F_n, can be included which is defined as [54]:

$$F_n = \begin{cases} \frac{1}{2}d_n & if & 1 < n \le (N-1) \\ \frac{1}{2}d_n^* & if & (-N+1) \le n \le -1 \\ 0 & if & n = 0 \end{cases},$$

Using this new coefficient and substituting the discrete equivalent of t, $i\Delta t$, and $n\Delta f$ for f_n, equation 3.4.2.3 can be rearranged in a form that very closely resembles the DFT as shown below.

$$X(i\Delta t) = \sum_{n=0}^{M-1} F_n e^{(\frac{j2\pi ni}{M})} \, ,$$

         3.4.2.4

Where $M = 2(N-1)$ and $i = 0,1,...M-1$

By exploiting the conjugate complex symmetry of the spectrum for the Fourier coefficients F_n, we get

$$F_n = \begin{cases} F_{n-M} = F_{M-n}^* & if & (\frac{M}{2}+1) \le n \le M-1 \\ 0 & if & N-1 < n \le \frac{M}{2} \end{cases},$$

3.5 The Cyclic Prefix Implementation

The transient response of the channel gives rise to ISI, which results in the loss of orthogonality between the subcarriers and hence a higher bit error rate. One way of eliminating this channel impairment is by increasing the duration of the OFDM symbol until the duration of the delay spread is comparatively much shorter. This method, however, cannot be enough on its own in practice since the maximum possible duration of the OFDM symbol is limited by a number of factors such as, the Doppler frequency, the coherence bandwidth of the channel and some technical limitation such as phase offsets and time delay. A more practical approach to solve this problem is by sacrificing some of the emitted energy

by preceding each signal by a time guard interval, which is used to absorb any intersymbol interference present and hence make the OFDM symbols completely independent of each other. During the guard interval a copy from the rear end of the signal is transmitted to allow cyclic convolution with the channel impulse response. At the receiver, the guard interval is discarded and only the useful symbol is considered. This method is more commonly known as the *cyclic prefix* method [6].

The cyclic prefix can be implemented as follows, let x be an OFDM symbol of N samples and $h(n)$ be the channel impulse response of length M, where $N < M$. In order to eliminate ISI, x has to be cyclically extended by M-1 samples. This is done by taking a copy from the back of the same OFDM symbol of length M-1 and inserting it at the front in the guard interval to form the new extended symbol $\overset{\backprime}{x}$ as shown below

$$\overset{\backprime}{x} = \{x(N\text{-}M\text{+}1)\,x(N\text{-}M\text{+}2)\,x(N\text{-}M\text{+}3)\,...\,x(N\text{-}1)\,x(0)\,x(1)\,...\,x(N\text{-}1)\}$$

where $x = \{x(0)\,x(1)\,x(2)\,...\,x(N\text{-}1)\}$,

For example if $M = 3$ (ie a channel is of the form $1 + D^2$) and $N = 6$, then the new cyclically extended symbol is of length 8 and has the following form: $\overset{\backprime}{x}(0) = x(4)$, $\overset{\backprime}{x}(1) = x(5)$, $\overset{\backprime}{x}(2) = x(0)$, $\overset{\backprime}{x}(3) = x(1)$, $\overset{\backprime}{x}(4) = x(2)$, $\overset{\backprime}{x}(5) = x(3)$, $\overset{\backprime}{x}(6) = x(4)$, $\overset{\backprime}{x}(7) = x(5)$. Thus the cyclically extended OFDM symbol looks as if it is periodical and hence cyclic convolution with the channel impulse response is achieved. In other words, the following DFT transform pair holds:

$$h(n) * x \Leftrightarrow H(k) \cdot X$$

where $*$ denotes convolution, X and $H(k)$ are the DFT of x and $h(n)$ respectively.

For the previous example, after discarding the cyclic extension, at the receiver the following subset of six samples is obtained:

$$y = x \begin{bmatrix} h(0) & h(1) & h(2) & 0 & 0 & 0 \\ 0 & h(0) & h(1) & h(2) & 0 & 0 \\ 0 & 0 & h(0) & h(1) & h(2) & 0 \\ 0 & 0 & 0 & h(0) & h(1) & h(2) \\ h(2) & 0 & 0 & 0 & h(0) & h(1) \\ h(1) & h(2) & 0 & 0 & 0 & h(0) \end{bmatrix},$$

It has to be said here that the cyclic extension only removes the intersymbol interference between the OFDM symbols, whereas interbin interference within each symbol will still exist due to the channel transient response and still has to be compensated for.

The main disadvantages of using a cyclic prefix in combating ISI is the resulting wastes in channel capacity as well as transmitted power. The signal to noise ratio loss due to the insertion of the cyclic extension is given by:

$$SNR_{loss} = 10\log\left(\frac{N + M - 1}{N}\right)$$

The interchannel interference may be eliminated if the frequency response of the channel, *H(k)*, at each bin was known. There are a number of ways to estimate *H(k)*. Two of the most common ones are the use of a pseudo random training sequences that are known both at the receiver and transmitter, and the other one is the use of pilot tones which act as reference signals within the OFDM symbol, which are then used by the receiver to estimate *H(k)*. These two methods and others will be discussed in a subsequent chapter.

3.6 System's Waveforms

In this section we intend to provide a description of the OFDM signal's time and frequency domain waveforms in order to give a better understanding of its physical meaning.

The time domain waveform of an OFDM signal contains random variations and its amplitude has a Gaussian distribution. Figure 3.6.1 and Figure 3.6.2 show an example of the time domain structure of an OFDM signal and its power, respectively. It can be seen from these two figures that the OFDM signal can exhibit a high peak to mean power ratio (PMEPR) which imposes a limit on using non-linear amplifiers and requires the use of the less power efficient linear ones. This issue has attracted a lot of attention and several methods have been investigated, which included the use of special block codes, scrambling techniques, amplitude limiting and *m*-sequences [9][10][44][53]. As this is an important issue for OFDM systems, it will be revisited and discussed more in a subsequent chapter.
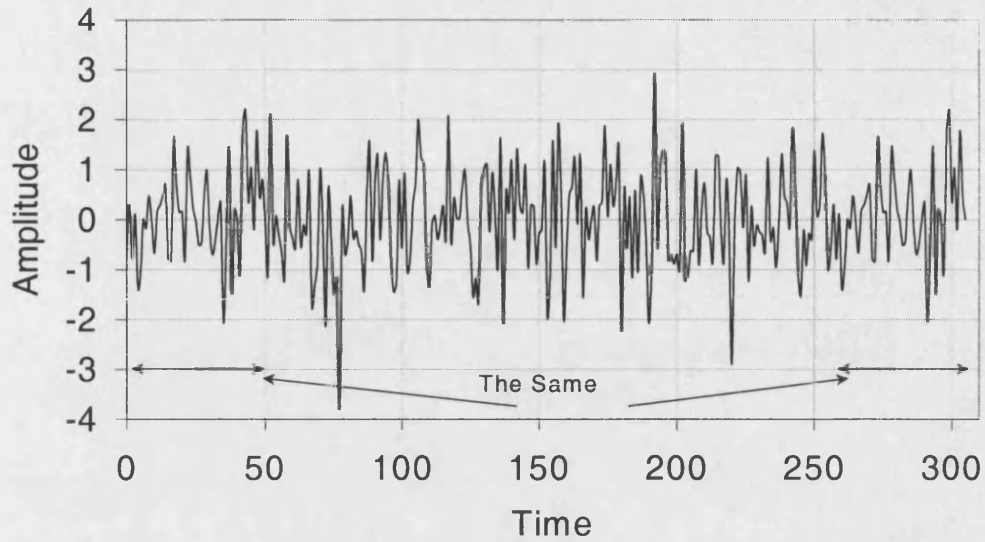
Figure 3.6.1 : Time Domain OFDM Signal, FFT = 256
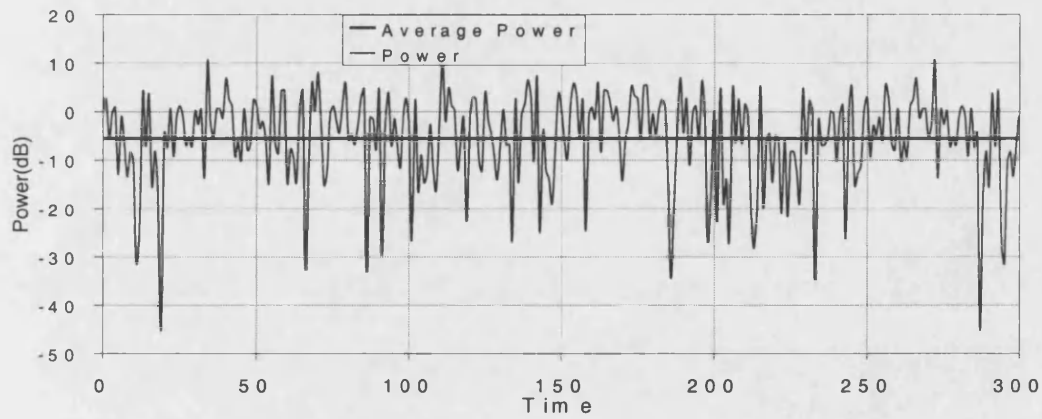
Figure 3.6.2 : OFDM Signal's Power (dB), FFT = 256

The envelope distribution of the OFDM signal is shown in Figure 3.6.3. It can be seen that as the number of subcarriers is increased, the distribution converges to Gaussian.

(a)   (b)
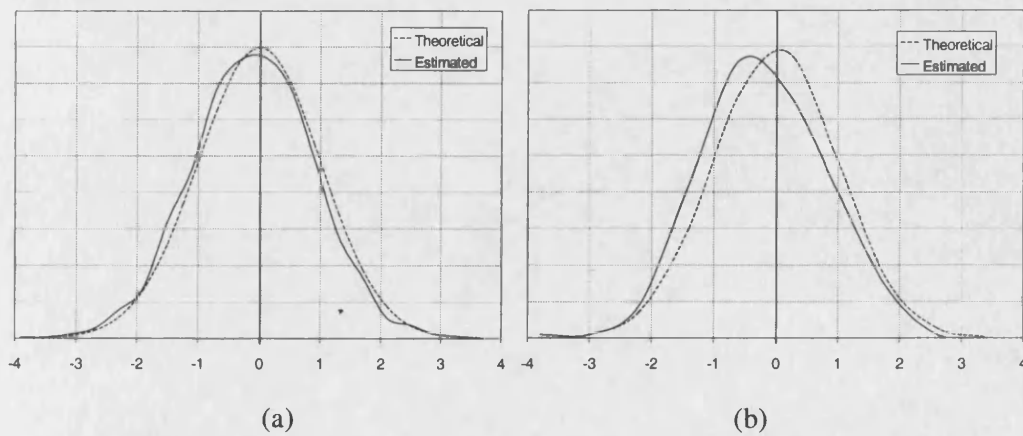
Figure 3.6.3 : OFDM Signal Distribution, (a) FFT = 4096, (b) FFT = 256

Figure 3.6.4 displays a picture of the frequency response of the individual subchannels of an OFDM signal. It can be seen that due to the rectangular windowing of the transmitted sinusoids the spectra of each subchannel is in the form of a sinc function.
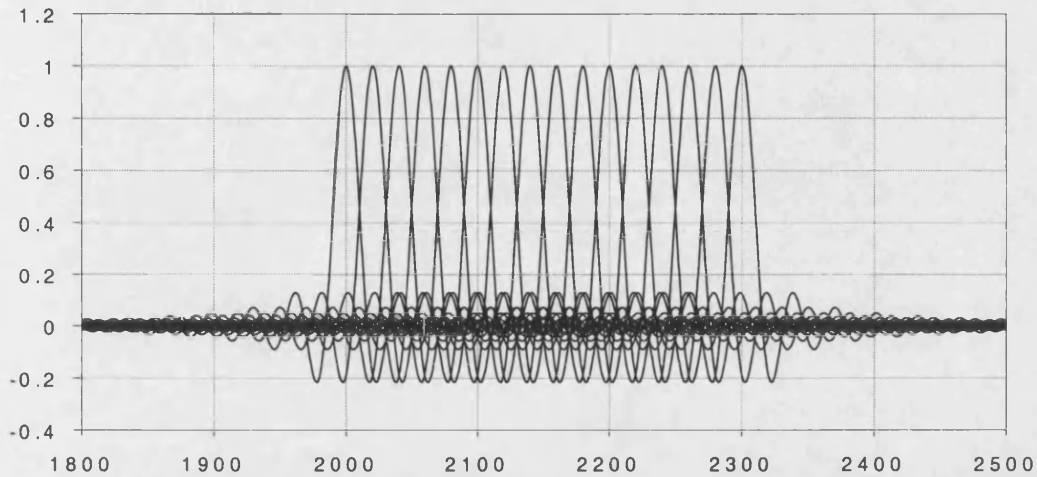
Figure 3.6.4 : Spectrum of Individual Subchannels, FFT = 16

In Figure 3.6.5 it can be seen that the spectrum of an OFDM signal tends asymptotically towards a rectangular shape. In some cases, it is required that the edges of the OFDM signal's spectrum fall much quicker than this, therefore other pulse shaping techniques may be used. These include raised cosine and well localised pulses [5][55].
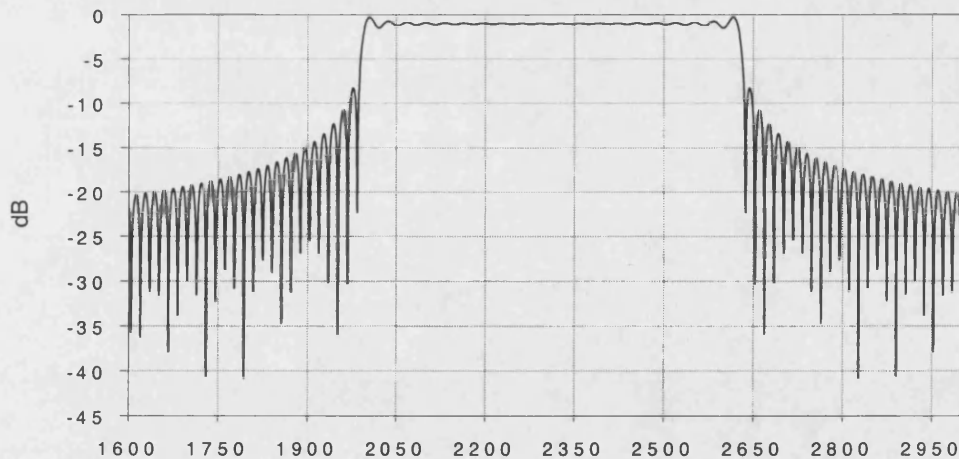
Figure 3.6.5 : Power Spectral Density of an OFDM Signal, FFT = 32

It can also be noted from Figure 3.6.5 that the secondary lobes can have high amplitude. Nevertheless, their widths depend on the OFDM symbol duration and therefore their relative value decreases as the FFT size is increased.

3.7 OFDM Bandwidth Efficiency

The spectral efficiency of an OFDM system may be given by:

$$\zeta = \varepsilon_1 \cdot \varepsilon_2 ,$$ 3.7.1

where

$$\varepsilon_1 = \frac{N}{N+L} \, and \quad \varepsilon_2 = \frac{1}{1+\beta} ,$$ 3.7.2

and N, L and β are the Number of subcarriers, cyclic prefix length and the shaping filter roll off factor, respectively.

The bandwidth efficiency approaches the Nyquist rate as ratio of L/N and β approaches zero. If R_s is the symbol rate of the serial stream at the input of the S/P converter and it is aimed to keep the rate of the actual data the same, then the transmission rate at the input of the channel has to be increased in order to accommodate of the cyclic prefix. Thus the new data rate, R_p, is given by:

$$R_p = \frac{N+L}{N} \cdot R_s ,$$ 3.7.3

Using equation 3.7.2 and 3.7.3 it is easy to show that the corresponding length of the cyclic prefix, L_{new}, is given by:

$$L_{new} = \frac{R_s \tau_m}{\varepsilon_1} ,$$ 3.7.4

Where τ_m is the maximum delay spread of the channel.

When assuming an ideal OFDM system, the maximum achievable bandwidth efficiency is given by:

$$Log_2 M \quad bits/s/Hz ,$$ 3.7.5

where M refers to the number of bits used in an M-ary digital modulation scheme.

3.8 OFDM Received Signals

In this section, an expression of the received OFDM signal in two types of channels, namely time selective and frequency selective channels, is presented.

3.8.1 Time Selective Channel

As the name implies, this type of channel results in producing variations in the transmitted signal's amplitude and phase but does not result in any ISI.

The impulse response of such channel is given by:

$$\hbar_i = h_i \cdot e^{j\varphi_i} \qquad i = 0,1\cdots,N-1,$$ 3.8.1.1

Where, as discussed in chapter 2, the amplitude, h_i and phase, φ_i, have Gaussian and uniform distributions, respectively. The index, i, is a time index and it is inserted here to emphasise on the time domain correlation of the channel. Assuming that the OFDM symbol's duration is less than the coherence time of the channel, then the subcarriers will undergo almost identical attenuation and phase shift. Therefore, The transfer function of this cannel, $H(f)$, may be approximated by

$$H(f) = h_{average} \cdot e^{j\varphi_{average}},$$ 3.8.1.2

Assuming that X is a vector of complex coefficients representing the symbols to be transmitted, the samples of the jth OFDM symbol at the input of the channel is given by:

$$x_{i,k,} = \frac{1}{\sqrt{N}} \cdot \sum_{m=0}^{N-1} X_m \cdot e^{j2\pi mk/N},$$

3.8.1.3

The received samples at the input of the receiver's FFT are thus then given by:

$$r_{i,k} = \frac{1}{\sqrt{N}} \cdot \sum_{m=0}^{N-1} X_m \cdot h_m \cdot e^{j\left(\frac{2\pi km}{N} + \varphi_k\right)},$$ 3.8.1.4

Where for simplicity the additive noise term has been omitted here. When these samples are applied to the FFT, the resulting decision variable samples, Z, are given by:

$$Z_{i,l} = \frac{1}{\sqrt{N}} \sum_{k=0}^{N-1} r_{i,k} \cdot e^{-j2\pi lk/N} = \frac{1}{N} \sum_{k=0}^{N-1} \left(\sum_{m=0}^{N-1} X_m \cdot h_m \cdot e^{j\left(\frac{2\pi km}{N} + \varphi_k\right)} \right) \cdot e^{-j2\pi lk/N}$$

$$= \frac{1}{N} \cdot \sum_{k=0}^{N-1} \sum_{m=0}^{N-1} X_m \cdot h_m \cdot e^{j\varphi_m} \cdot e^{\frac{j2\pi k}{N}(m-l)}$$ 3.8.1.5

$$= X_l \cdot h_l \cdot e^{j\varphi_l} + n_l^{'}$$

And therefore, an estimate of the transmitted samples, $\hat{X}$, may be constructed as shown below:

$$\hat{X}_{i,k} = \frac{Z_{i,k}}{h_i} \cdot e^{-j\varphi_i},$$
          3.8.1.6

3.8.2   Frequency Selective Channel

In a frequency selective fading channel, the situation is more complicated as the finite impulse response duration of the channel results in ISI and much less correlated channel frequency response than that of the time selective. Since the OFDM technique stretches the duration of the transmitted symbols in time, the analysis presented here assumes that the ISI occurs between pairs of OFDM symbols only. In other words, the impulse response dispersion does not exceed more than one consecutive symbol at a time. In this type of channels, the impulse response, *h(t)*, may be represented as a vector of samples as shown below:

$$h(t) = [h_0, h_1, \cdots, h_{N-1}],$$

where it is assumed that the *h(t)* is causal and sampled at a Nyquist sampling rate over a period equal to the OFDM symbol duration. In addition, the individual samples of the channel impulse response are assumed to be uncorrelated Gaussian random variables. Using this definition of the impulse response, the received signal at the input of the FFT may be given as:

$$r_{i,k} = \sum_{m=0}^{k} x_{i,m} \cdot h_{i,k-m} + \sum_{m=k+1}^{N-1} x_{i-1,m} \cdot h_{i,N+k-m} + n_{i,k}$$
          3.8.2.1

$$k = 0,1 \cdots, N-1, \quad m = 0,1, \cdots, L-1, \quad i = 0,1, \cdots, \infty$$

The above equation may be broken further into the following form:

$$r_{i,k} = h_{i,0} \cdot CDFT^{-1}(X_{i,k}) + \sum_{m=0}^{i-1} h_{i,k-m} \cdot CDFT^{-1}(X_{i,m}) +$$

$$r_{i,k} = h_{i,0} \cdot CDFT^{-1}(X_{i,k}) + \sum h_{i,k-m} \cdot CDFT^{-1}(X_{i,m}) +$$
$$\sum_{m=k+1} h_{i,N=k-m} \cdot CDFT^{-1}(X_{i-1,m}) + n_{i,k}$$
          3.8.2.2

If we substitute for *x* and *h* using equation 3.8.1.1, 3.8.1.3 and 3.8.1.4 the resulting expression at the output of the receiver's FFT will look very complicated and difficult to follow therefore we use a different strategy here to represent the signal at he the output of the receiver's FFT. Since the transmitted signal vector, *x*, can be represented in a matrix form as *x = CDFT⁻¹ · X* where *CDFT⁻¹* is an *NXN* matrix representing the complex inverse Fourier transform and *X* is a vector of the complex symbols to be transmitted, equation 3.8.2.1 can be rewritten as:

$$r_{i,k} = \underbrace{x_{i,k} \cdot h_{i,0}}_{\substack{desired \\ sample}} + \underbrace{\sum_{m=0}^{k-1} x_{i,m} \cdot h_{i,k-m}}_{} + \underbrace{\sum_{m=k+1}^{N-1} x_{i-1,m} \cdot h_{i,N+k-m}}_{ISI} + \underbrace{n_{i,k}}_{\substack{additive \\ noise}} , \qquad 3.8.2.3$$

Therefore, the received vector at the input of the receiver's FFT is given by:

$$r_i = \overset{m1}{h_i} \cdot CDFT^{-1} \cdot X_i + \overset{m2}{h_i} \cdot CDFT^{-1} \cdot X_{i-1} + n_i , \qquad 3.8.2.4$$

Where, $\overset{m1}{h}, \overset{m2}{h}$ and $CDTF^{-1}$ are three $N X N$ matrices defined as given below:

$$\overset{m1}{h} = \begin{bmatrix} h_0 & 0 & 0 & \cdots \\ h_1 & h_0 & 0 & \cdots \\ \cdot & \cdot & \cdot & \cdot \\ h_{n-1} & h_{N-2} & \cdots & h_0 \end{bmatrix}, \qquad \overset{m2}{h} = \begin{bmatrix} 0 & h_{N-1} & h_{N-2} & \cdots & h_1 \\ 0 & 0 & h_{N-1} & \cdots & h_2 \\ \cdot & \cdot & \cdot & \cdot & \cdot \\ 0 & 0 & 0 & \cdots & 0 \end{bmatrix},$$

and

$$CDFT^{-1} = \begin{bmatrix} D_N^{0 \cdot 0} & D_N^{1 \cdot 0} & D_N^{2 \cdot 0} & \cdots & D_N^{(N-1) \cdot 0} \\ D_N^{0 \cdot 1} & D_N^{1 \cdot 1} & D_N^{2 \cdot 1} & \cdots & D_N^{(N-1) \cdot 1} \\ D_N^{0 \cdot 2} & D_N^{1 \cdot 2} & D_N^{2 \cdot 2} & \cdots & D_N^{(N-1) \cdot 2} \\ \vdots & \vdots & \vdots & \vdots & \vdots \\ D_N^{0 \cdot (N-1)} & D_N^{1 \cdot (N-1)} & D_N^{2 \cdot (N-1)} & \cdots & D_N^{(N-1) \cdot (N-1)} \end{bmatrix}, \quad D_N = \frac{1}{\sqrt{N}} \cdot e^{2 j \pi / N} ,$$

At the output of the receiver's FFT, the signal is given by:

$$R_i = CDFT(r_i) = CDFT \left(\overset{m1}{h_i} \cdot CDFT^{-1} \cdot X_i + \overset{m2}{h_i} \cdot CDFT^{-1} \cdot X_{i-1} + n_i \right)$$

$$= (CDFT \cdot \overset{m1}{h_i} \cdot CDFT^{-1}) \cdot X_i + (CDFT \cdot \overset{m2}{h_i} \cdot CDFT^{-1}) \cdot X_{i-1} + CDFT \cdot n_i \quad 3.8.2.5$$

$$= \underbrace{W_i \cdot X_i}_{\substack{desired \\ samples \\ + \\ ICI}} + \underbrace{V_i \cdot X_{i-1}}_{ISI} + \underbrace{N_i}_{AWGN}$$

where $\qquad W_i = CDFT \cdot \overset{m1}{h_i} \cdot CDFT^{-1} \qquad (N X N \text{ matrix})$

$$V_i = CDFT \cdot \overset{m2}{h_i} \cdot CDFT^{-1} \qquad (N X N \text{ matrix})$$

and $\qquad N_i = CDFT \cdot n_i \qquad (N X N \text{ matrix}),$

The matrices W and V are both triangular and may be written in an iterative form as:

$$W_{k,m} = \frac{1}{N} \cdot \sum_{n=0}^{N-1} \left(e^{-j 2 \pi k n / N} \cdot \sum_{p=0}^{n} h_{N+n-p} e^{j 2 \pi m p / N} \right)$$

$$V_{k,m} = \frac{1}{N} \cdot \sum_{n=0}^{N-1} \left(e^{-j 2 \pi k n / N} \cdot \sum_{p=n+1}^{N} h_{n-p} e^{j 2 \pi m p / N} \right) ,$$

Therefore an estimate of the transmitted signal can be obtained provided a good estimate of W and V is available. This may be given in a matrix form as:

$$\hat{X}_i = V^{-1} \cdot R_i - V^{-1} \cdot W \cdot X_{i-1},$$ 3.8.2.6

3.9 Theoretical BER Performance

The approach followed here to establish a bound for the BER of an OFDM system is based on finding the average signal to noise plus interference ratio, SNIR. The individual components making up the received signal are given by expanding equation 3.8.2.5:

$$R_{i,l} = \frac{1}{N} \left[\sum_{n=0}^{N-1} X_{j,n} \left(\sum_{k=0}^{M-L-1} \sum_{m=0}^{k+L} h_{i,k,m} \cdot e^{-j2\pi m/N} \cdot e^{j2\pi k(n-1)/N} + \sum_{k=M-L}^{N-1} \sum_{m=0}^{M-1} h_{i,k,m} \cdot e^{-j2\pi mn/N} \cdot e^{j2\pi k(n-1)/N} \right) + \sum_{n=0}^{N-1} X_{i-1,n} \cdot \sum_{k=0}^{M-L-1} \sum_{m=k+L+1}^{M-1} h_{i,k,m} \cdot e^{-j2\pi n(L-m)/N} \cdot e^{j2\pi k(n-1)/N} \right] +$$

$$\frac{1}{\sqrt{N}} \cdot \sum_{k=0}^{N-1} n_{i,k} \cdot e^{-j2\pi kl/N}$$ 3.9.1

where $R_{i,l}$ represents the transmitted signal through the lth subcarrier during the block i^{th} interval

and $\quad x_{i,k} = \frac{1}{\sqrt{N}} \cdot \sum_{m=0}^{N-1} X_{i,k,m} \cdot e^{j2\pi mk/N} \quad -L \leq k < N,$

and the four distinct components equation are:

$$R_{i,l} = H_{i,l} \cdot X_{i,l} + ICI_{i,l} + ISI_{i,l} + N_{i,l},$$

where

$$H_{i,l} = \frac{1}{N} \cdot \left(\sum_{k=M-L}^{N-1} \sum_{m=0}^{M-1} h_{i,k,m} \cdot e^{-j2\pi dm/N} + \sum_{k=0}^{M-L-1} \sum_{m=0}^{k+L} h_{i,k,m} \cdot e^{-j2\pi dm/N} \right),$$

$$ICI_{i,l} = \frac{1}{N} \cdot \sum_{n \neq l} X_{i,n} ; \left(\sum_{k=M-L}^{N-1} \sum_{m=0}^{M-1} h_{i,k,m} \cdot e^{-j2\pi dm/N} \cdot e^{-j2\pi d(n-1)/N} + \sum_{k=0}^{M-L-1} \sum_{m=0}^{k+L} h_{i,k,m} \cdot e^{-j2\pi dm/N} \cdot e^{-j2\pi d(n-1)/N} \right),$$

$$ISI_{i,l} = \frac{1}{N} \cdot \sum_{n=0}^{N-1} X_{i-1,n} \cdot \sum_{k=0}^{M-L-1} \sum_{m=k+L+1}^{M-1} h_{i,m,k} \cdot e^{-j2\pi n(L-m)/N} \cdot e^{j2\pi k(n-1)/N},$$

and

$$N_{i,l} = \frac{1}{\sqrt{N}} \cdot \sum_{k=0}^{N-1} n_{i,k} \cdot e^{-j2\pi kl/N},$$

Because the tap coefficients, $h_{i,k,m}$ are samples from an independent zero-mean complex Gaussian process, the fading term $H_{i,k,m}$ can be considered a zero-mean Gaussian complex process. The underlying assumption here is that each subchannel is a Rayleigh fading channel. Also, since the Fourier transform of a Gaussian noise process is another Gaussian noise process, the noise term, $N_{i,k,m}$ is Gaussian. Although, the *ICI* and *ISI* terms are made of correlated components, it is widely acceptable to model them as Gaussian variables when the input data symbols are i.i.d and have a mean of zero and variance of E_s [56][57]. To calculate the average BER, it is first required to find the average SNIR of the system in the presence of all the aforementioned interference terms.

Under the isotropic scattering assumption, the autocorrelation of the tap coefficients is [58]:

$$E\{h_{i,k,p} \cdot h_{i,k,q}^*\} = \sigma_k^2 \cdot J_0\left(2\pi f_D T_{p-q}\right), \qquad\qquad 3.9.2$$

where σ_k^2 and $J_0(\cdot)$ are the power of the kth channel tap and the zeroth-order Bessel function.

Therefore, the variance of the *ICI* term is [57]:

$$\sigma_{ICI}^2 = E\{ICI_{i,l} \cdot ICI_{i,l}^*\}$$

$$= \frac{E_s'}{N^2} \cdot \sum_{n \neq l} \left[\begin{array}{l} \sum_{k=M-L}^{N-1} \sum_{u=M-L}^{N-1} \sum_{m=0}^{M-1} \sigma_m^2 J_0\left(2\pi f_D T_{k-u}\right) \cdot e^{j2\pi(k-u)(n-1)/N} + \\[2mm] \sum_{u=M-L}^{N-1} \sum_{k=0-L}^{M-L-1} \sum_{m=0}^{k+L1} \sigma_m^2 J_0\left(2\pi f_D T_{k-u}\right) \cdot e^{j2\pi(k-u)(n-1)/N} + e^{-j2\pi(k-u)(n-1)/N} + \\[2mm] \sum_{k=0}^{M-L-1} \sum_{u=0}^{M-L-1} \sum_{m=0}^{\min(u,k)+L} \sigma_m^2 J_0\left(2\pi f_D T_{k-u}\right) \cdot e^{j2\pi(k-u)(n-1)/N} \end{array} \right]$$

$$= \frac{E_s'}{N^2} \left[\begin{array}{l} (N-M-L) \cdot \sum_{m=0}^{M-1} \sigma_m^2 - \sum_{k=M-L}^{N-1} \sum_{u=M-L}^{N-1} \sum_{m=0}^{M-1} \sigma_m^2 J_0\left(2\pi f_D T_{k-u}\right) - \\[2mm] 2 \cdot \sum_{u=M-L}^{N-1} \sum_{k=0}^{M-L-1} \sum_{m=0}^{k+L} \sigma_m^2 J_0\left(2\pi f_D T_{k-u}\right) + \\[2mm] N \cdot \sum_{k=0}^{M-L-1} \sum_{m=0}^{M+L} \sigma_m^2 - \\[2mm] \sum_{k=0}^{M-L-1} \sum_{u=0}^{M-L-1} \sum_{m=0}^{\min(u,k)+L} \sigma_m^2 J_0\left(2\pi f_D T_{k-u}\right) \end{array} \right]$$

$$\cong E_s' \hat{\sigma}_{ICI}^2$$

where

$$E_s' = \frac{E_s}{1 + L/N},$$

Similarly the variance of *ISI* and *H* is given by:

$$\sigma^2_{ISI} = \frac{E'_s}{N} \cdot \sum_{k=0}^{M-L-1} \sum_{m=k+L+1}^{M-1} \sigma^2_m \cong E'_s \cdot \hat{\sigma}^2_{ISI} \; ,$$

and

$$\sigma^2_H = \frac{1}{N^2} \cdot \left[\begin{array}{l} \displaystyle\sum_{k=M-L}^{N-1} \sum_{u=M-L}^{N-1} \sum_{m=0}^{M-1} \sigma^2_m J_0 \left(2\pi f_D T_{k,u}\right) + 2 \cdot \sum_{k=0}^{M-L-1} \sum_{u=M-L}^{N-1} \sum_{m=0}^{k+L} \sigma^2_m J_0 \left(2\pi f_D T_{k,u}\right) + \\[2ex] \displaystyle\sum_{k=0}^{M-L-1} \sum_{u=0}^{M-L-1} \sum_{m=0}^{\min(k,u)+L} \sigma^2_m J_0 \left(2\pi f_D T_{k,u}\right) \end{array} \right] \qquad 3.9.3$$

Assuming that the channel transfer function was estimated perfectly, the BER performance can be estimated using the following average SNIR,

$$\begin{aligned} \bar{\gamma} &= \frac{E'_s \cdot \sigma^2_H}{\sigma^2_{ICI} + \sigma^2_{ISI} + N_0} \\[2ex] &= \frac{\sigma^2_H}{\hat{\sigma}^2_{ICI} + \hat{\sigma}^2_{ISI} + \dfrac{N_0}{E_s} \cdot (1 + L/N)} \; , \end{aligned} \qquad 3.9.4$$

In [59] the BER for an AWGN channel with MQAM modulation and ideal coherent phase detection is tight bounded to within 1dB for $0 \le SNR \le 30$ dB by:

$$BER_{AWGN} \approx \frac{1}{5} \cdot \exp\left(\frac{-3 \cdot SNR}{2 \cdot (M-1)} \right), \qquad 3.9.5$$

In fact this serves as a lower bound for $M = 2$ and an upper bound for $M \ge 4$.

Assuming that the SNIR is Rayleigh distributed, then the probability density function of the instantaneous SNIR, γ, is given by:

$$p(\gamma) = \frac{1}{\bar{\gamma}} \cdot e^{-\gamma/\bar{\gamma}} \qquad \gamma > 0, \qquad 3.9.6$$

Therefore, using 3.9.5, the average BER can be calculated as:

$$\begin{aligned} BER_{Ray} &\approx \int_0^\infty \frac{1}{5} \cdot e^{[-3\cdot\gamma/2\cdot(M-1)]} \cdot \frac{1}{\bar{\gamma}} \cdot e^{-\gamma/\bar{\gamma}} d\gamma \\[2ex] &\cong \frac{1/5}{\left(1 + \dfrac{3\cdot\bar{\gamma}}{2\cdot(M-1)}\right)} \; , \end{aligned} \qquad 3.9.7$$

where $\bar{\gamma}$ is defined in 3.9.4.

3.10 Conclusion

In this chapter an up to date history of the OFDM technique and its related recent applications was provided. A brief description of the principle of this modulation scheme has then been presented. It was shown how the use of such technique could make wideband transmission over frequency selective fading channel achievable. The fact that OFDM can be implemented using the fast Fourier transform and its inverse makes the implementation of this technique a reality and avoids the need to use a bank of oscillators and filters. Since the subcarriers are allowed to partially overlap in an OFDM system, the available bandwidth is more efficiently utilised. Although the performance and bandwidth efficiency of such system improves as the number of subcarriers used increases, there is a limit on the maximum number of subcarriers that can be used. This is determined by the Doppler spread and the computational time required. It has been shown that in order to preserve the orthogonality between the subcarriers and prevent significant ISI, the use of a cyclic prefix is indispensable. A simplified description of the mathematical representation of an OFDM signal in the presence of time and frequency selective fading channel has been given. In addition, a theoretical analysis of the BER performance of MQAM/OFDM has been provided, which could be used to show the trade off between the system BER performance, number of subcarriers and duration of the cyclic prefix.

3.11 References

[1] M. L. Doelz, E. T. Heald and D. L. Martin, *"Binary Data Transmission Techniques for Linear systems"*, Proc. IRE, Vol. 45, pp. 656-661, May, 1957.

[2] R. R. Mosier and R. G. Clabaugh, *"Kineplex, a Bandwidth Efficient Transmission System "*, AIEE Transactions, Vol. 76, pp. 723-728, Jan. 1958.

[3] R. W. Chang, *"Synthesis of Bandlimited Orthogonal Signals for Multichannel Data Transmission "*, Bell Systems Technology Journal, Vol. 45, pp. 1775-1796, Dec. 1966.

[4] B. R. Saltzberg, *"Performance of an Efficient Parallel Data Transmission System"*, IEEE Transactions on Communications Technology, Vol. COM-15, pp. 805-813,Dec. 1967.

[5] S. B. Weinstein and P. M. Ebert, *" Data Transmission by Frequency Division Multiplexing Using the Fourier Transform"*, IEEE Transactions on Communications Technology, Vol. COM-19, No. 15, pp. 628-634, Oct. 1971.

[6] A. Peled and A. Ruiz, *"Frequency Domain Data Transmission Using Reduced Computational Complexity Algorithms"*, IEEE International Conference on Acoustics, Speech and Signal Processing, pp. 964-967, Denver, CO, 1980.

[7] B. Le Floch, M. Alard and C. Berrou, "Coded Frequency Division Multiplexing", proceedings of the IEEE, Vol. 83, No. 6, pp.982-996, June 1995.

[8] A. Vahlin and N. Holte, *"Optimal Finite Duration Pulses for OFDM"*, IEEE Transactions on Communications, Vol. 44, No. 1, pp. 10-14, Jan. 1996.

[9] A. E. Jones, T. A. Wilkinson and S. K. Barton, *"Block Coding Scheme for Reduction of Peak to Mean Average Envelope Power Ratio of Multicarrier Transmission Schemes "*, Electronic letters, Vol. 30, No. 25, pp. 2098-2099, Dec. 1994.

[10] P. Van Eetvelt, G. Wade and M. Tomlinson, "Peak to Average Power Reduction for OFDM Schemes By selective scrambling", Electronic Letters, Vol. 32, No. 21, pp. 1963-1964, Oct. 1996.

[11] B. Hirosaki, *"An Orthogonally Multiplexed QAM System Using the Discrete Fourier Transform "*, IEEE Transactions on Communications, Vol. COM-29, pp. 982-989, July 1981.

[12] B. Hirosaki, *"A 19.2 kbps Voiceband Data Modem Based on Orthogonaly Multiplexed QAM Techniques "*,Proceedings of the IEEE ICC'85, pp. 21.1.1-5, 1985.

[13] W. E. Keasler and D. L. Bitzer, *"High Speed Modem Suitable for Operating with a Switched Network"*, U. S. Patent, No. 4,206,320, June 1980.

[14] T. Kelly, *"Digital Modem Packs Data onto 40 Bauds for 9600 bps Data Comms. Over Voice Lines"*, Canadian Data system, Vol. 11, Apr. 1979.

[15] J. A. C. Bingham, *"Multicarrier Modulation for Data Transmission: An Idea Whose Time has Come"*, IEEE Communications Magazine, Vol. 28, No. 5, pp. 5-14, May 1990.

[16] G. Young, K. T. Foster and J. W. Cook, *"Broadband Multimedia Delivery Over Copper "*,BT Technology Journal, Vol. 13, No. 4, pp. 78-96, Oct. 1995.

[17] E. Feig and Mintzer, *"Sequence Transmission: Coding in Frequency Domain "*, IBM Res. Rep. RC 13701, IBM T.J. Watson, Res. Cen., March. 1988.

[18] E. Feig and A. Nada, *"The performance of Fourier Transform Division Multiplexing Schemes on Peak Limited Channels "*, IBM Res. Rep. RC13828, IBM T. J. Watson Res. Cen., June 1988.

[19] E. F. Casas and C. Leung, *"OFDM for Data Communications Over-Mobile Radio FM Channels-part-1: Analysis and Experimental Results"*, IEEE Transactions on Communications, Vol. COM-39, No. 5, pp.680-683, May 1991.

[20] P. S. Chow, J. C. Tu and J. M. Cioffi, *"Performance Evaluation of a Multichannel Transceiver System for ADSL and VHDSL services"*, IEEE Journal on Selected Areas in Communications, Vol. SAC-9, pp.909-919, Aug. 1991.

[21] T. Lauterbach and M. Unbehauen, *"Multimedia Environments for Mobiles (MEMO) Interactive Multimedia Services To Portable and Mobile Terminals "*,In the Proceedings of ACTS Mobile Communications Summit. Aalborg, Denmark, Oct. 7-10, 1997.

[22] Radio Broadcasting systems, *"Digital audio Broadcasting (DAB) to Mobile , Portable, and Fixed Receivers"*, ETS 300 401, ETSI- European Telecommunication Standards Institute, Valbonne, France, Feb. 1995.

[23] B. Le Floch, R. Lassalle and D. Castelain, *"Digital Sound Broadcasting to Mobile Receivers"*, IEEE Transactions on Consumer Electronics, pp.493-503, Aug. 1989.

[24] J. F. Helard and B. Le Floch, *"Trellis-Coded Orthogonal Frequency Division Multiplexing for Digital Video Transmission "*, Proc. GLOBCOM'91, pp.785-791, Dec. 1991.

[25] B. Marti, N. Lodge, P. bernard and R. Schafer, *"European activities on Digital Television Broadcasting: from Company to Comparative Projects"*, Proc. Of HDTV World'93, Las Vegas, Apr. 1993

[26] R. Van Nee, *"A New OFDM Standard for High Rtaes Wireless Lan in the 5 GHz Band"*, Proceedings of the IEEE VTC'99 Falls , pp. 258-261, The Netherlands, Sept. 1999.

[27] EN, 300 744 V1.1.2 European Telecommunications Standards Institute, 1997-08.

[28] H. Cheon, B. Park and Daesik Hong, *"Adaptive Multicarrier System With Reduced Feedback Information in Wideband Radio Channels"*, VTC'99 Fall, pp. 2880-2884, 1999.

[29] H. Sari, G. Karam and I. Jeanclaude, *"Transmission Technique for Digital Terrestrial TV Broadcasting "*, IEEE Communications Magazine, Vol. 33, No. 2, pp. 100-109, Feb. 1995.

[30] J. J. Van de Beek, P. O. Borjesson, M. L. Boucheret, D. Landstrom, J. M. Arenas, P. Odling, S. K. Wilson, C. Ostberg and M. Wahlqvist, " *Synchronisation of a TDMA-OFDM Frequency Hopping System*", In the Proceedings of the IEEE VTC'98, vol. 5, Ottawa, Canada, pp. 18-21, 1998.

[31] B. S. Krongold, K. Ramchandran and D. L. Jones, "*Computationally Efficient Optimal Power Allocation Algorithms for Multicarrier Communication Systems*", IEEE Transactions on Communications, vol. 48, no. 1, pp. 23-27, 2000.

[32] C. Y. Wong, R. S. Cheng, K. Ben Letaief and R. D. Murch, "*Multiuser OFDM with Adaptive Subcarrier, Bit, and Power Allocation*", IEEE Transactions on Selected Areas in Communications, vol. 17, no. 10, pp. 1747-1758, Oct. 1999.

[33] M. C. Aguayo-Torres, J. T. Entrambasaguas, F. Ruiz and J. Banos, "*Variable Rate DFE-QAM and OFDM Systems for Maximum Capacity in Multipath Frequency Selective Fading Channels*", Proceedings of the IEEE VTC'99, pp. 263-267, The Netherlands, Sept. 1999.

[34] H. Cheon, B. Park and D. Hong, "*Adaptive Multicarrier System with Reduced Feedback Information in Wideband radio Channels*", Proceedings of the IEEE VTC'99, pp. 2880-2884, The Netherlands, Sept. 1999.

[35] K. Hamaguchi and E. Moriyama, "*Performance of Multicarrier /QAM-Level-Controlled Adaptive Modulation for Land Mobile Communication Systems*", IEICE Transactions on Communications, vol. E81-B, no. 4, pp. 770-776, Apr. 1998.

[36] T. Keller and L Hanzo, "*Sub-Band Adaptive Pre-Equalised OFDM Transmission*", Proceedings of VTC'99 falls, pp. 334-338, Sept. 1999

[37] P. S. Chow, J. M. Cioffi and J. A. C. Bingham, "*A Practical Discrete Multitone Transceiver Loading Algorithm for Data Transmission Over Spectrally Shaped Channels*", IEEE Trans. on Comm., 43(2/3/4), pp. 773-775, Feb./March/Apr. 1995.

[38] R. F. H. Fischer and J. B. Huber, "*A New Loading Algorithm for Discrete Multitone Transmission*", Proceedings of IEEE Globcom'96, pp. 724-728, London, Nov. 1996.

[39] D. N. Rowitch and L. B. Milstein, "*Convolutionally Coded Multicarrier DS-CDMA Systems in a Multipath Fading Channel-Part I: Performance Analysis*", IEEE Transactions on Communications, vol. 47, pp. 1570-1592, Oct. 1999.

[40] D. N. Rowitch and L. B. Milstein, "*Convolutionally Coded Multicarrier DS-CDMA Systems in a Multipath Fading Channel-Part II: Narrow Band Interference Suppression*", IEEE Transactions on Communications, vol. 47, no. 11, pp. 1729-1736, Oct. 1999.

[41] S. Kondo and L. B. Milstein, "*On the Performance of Multicarrier DS-CDMA Systems*", IEEE Transactions on Communications, vol. 44, pp. 238-246, Feb. 1996.

[42] R.F.Ormondroyd and E.Al-Susa, 'Impact of Multipath Fading and Partial Band Interference on the Performance of a COFDM/CDMA Modulation Scheme for Robust Wireless Communications', Proceedings IEEE Military Communications Conference, MILCOM'98, Boston, pp.673-678, Oct. 1998.

[43] G. J. Saulnier, Z. ye and M. J. Medley, "*Performance of a Spread spectrum OFDM System in a Dispersive Fading Channel with Interference*", Proceedings IEEE Military Communications Conference, MILCOM'98, Boston, pp.679-683, Oct.1998.

[44] P. W. J. Van Eetvelt, S. J. Shepherd and S. K. Barton, "*The Distribution of Peak Factor in QPSK Multicarrier Modulation*", Wireless personal Communications, Vol. 2, No. 1-2, pp. 87-96, 1995.

[45] N. Yee, J-P. Linnartz and G. Fettweis, " *Multicarrier CDMA in Indoor Wireless Radio Networks*", IEEE PIMRC'93, Conference Proceedings, pp. 109-113, Yokohama, Japan, Sept. 1993.

[46] K. Fazel and L. Papake, "*On the Performance of Convolutionally Coded CDMA/OFDM For Mobile Communication Systems*", IEEE PIMRC'93, Conference Proceedings, pp. 468-472, Yokohama, Japan, Sept. 1993.

[47] V. M. DaSilva and E. S. Sousa, "*Performance of Orthogonal CDMA Codes for Quasi-synchronous Communication Systems*", IEEE ICUPC'93, Conference Proceedings pp. 995-999, Ottawa, Canada, Oct. 1993.

[48] S. Kondo and L. B. Milstein, " *Performance of Multicarrier DS CDMA Systems*", IEEE Transactions on Communications, Vol. 44, No. 2, pp. 238-246, Feb 1996.

[49] E. Sourour and M. Nakagawa, "*Performance of Multicarrier CDMA in Multipath Fading Channel*", IEEE Transactions on Communications, Vol. 44, No. 3, pp. 356-67, March 1996.

[50] L. Vandendorpe, "Multitone Direct Sequence CDMA in an Indoor Wireless Environment ", IEEE Proceedings of the First Symposium of Communications and vehicular Technology in the Benelux, pp. 4.1-1.4.1.8, Delft, The Netherlands, Oct. 1993.

[51] R. Parsad and S. Hara, "*An Overview of Multicarrier CDMA*", IEEE ISSSTA'96 Conference Proceedings, pp. 107-113, 1996.

[52] S. Hara, "*Transmission Performance Analysis of Multicarrier Modulation in Frequency Selective Fast Rayleigh Fading Channel*", Wireless Personal Communications, Vol. 2, No. 4, pp. 335-356, 1995/1996.

[53] X. Li and J. A. Ritcey, "*M-sequencies for OFDM Peak to Average Power Ratio Reduction and Error Correction* ", Electronic Letters, Vol. 33, No. 7, pp. 554-555, March 1997.

[54] W. Webb and L. Hanzo, "*Modern Quadrature Amplitude Modulation, Principles and Applications for Fixed and Wireless Channels*", IEEE press, 1994.

[55] D. Bhatoolaul, "*Spectrum Shaping in N-Channel QPSK-OFDM Systems*", IEE Proceedings on Image and signal Processing, Vol. 142, No. 5, pp.333-338, Oct. 1995.

[56] M. Okada, S. Hara and N. Morinaga, "*Bit error Rate Performance of Orthogonal Multicarrier Modulation Radio Transmission Systems*", IEICE Transactions on Communications, Vol. E76-B, No. 2, pp.113-119, 1610-1615, Feb. 1993.

[57] Y. Hee Kim, I. Song, H. G. Kim, T. Chang and H. M. Kim, *"Performance Analysis for Coded OFDM System in Time-Varying Multipath Rayleigh Fading Channels"*, IEEE Transactions on Vehicular Technology, vol. 48, No. 5, Sept.1999.

[58] J. G. Proakis, *"Digital Communications"*, Appendix C, McGraw-Hill, 3^{ed} 1995.

[59] A. J. Goldsmith and S-G. Chua, *"Variable Rate Variable Power MQAM For Fading Channels"*, IEEE Transactions on Communications, Vol. 45, pp. 1218-1230, Oct. 1997.

[60] H. Nikookar, *"Wireless Channel Modelling and Code Division Multiple Access for Indoor Communications"*, Ph. D. Thesis, Delft University, The Netherlands, 1996.

[61] M. Schwartz, W. R. Bennet and S. Stein, *"Communication Systems and Techniques"*, McGraw-Hill, 1996.

[62] W. C. Lee, *"Mobile Communication Engineering"*, McGraw-Hill, 1982.

Chapter Four

OFDM Performance Evaluation

4. Chapter Four

4.1. Introduction

In the previous chapters the characteristics of the mobile radio channel and the theoretical description of the OFDM system were given. In this chapter, the aim is to study the behaviour of this modulation technique in the presence of various channels and receiver impairments. In particular this chapter will show the impact of channel time variation and frequency selectivity on the system performance and how these factors influences the system parameters. The advantages and disadvantages of using the cyclic prefix in the aim to reduce ISI are then discussed and an alternative technique that is based on feedback compensation is presented. The sensitivity of OFDM systems to some synchronisation errors, such as frequency, phase and timing are also discussed and a number of estimation algorithms are presented. The influence of time and frequency interleaving combined with convolutional coding is also analysed under different channel conditions. Finally a comparison between two OFDM based differential detector structures, namely, serial OFDM-DPSK and parallel OFDM-DPSK, is presented along with the relative advantages and disadvantages of each technique.

In conventional serial data transmission schemes, the symbols are transmitted sequentially, with the frequency spectrum of each symbol allowed to occupy the entire available transmission bandwidth. Since the duration of each transmitted symbol is inversely proportional to the symbol transmission rate, this scheme imposes a limit on the maximum allowable transmission bandwidth, *BW*. This is because the system's susceptibility to channel dispersion increases in proportion to the transmission rate. In addition, in the presence of dispersive channels, serial transmission schemes require the use of complicated equalisers when transmitting at high data rates in order to ensure a successful recovery of the transmitted data.

Unlike the serial transmission scheme, parallel transmission increases the duration of each transmitted symbol to *N* times longer than the reciprocal of the total transmission bandwidth without altering the total data throughput of the system. Therefore, a parallel approach has the advantage of spreading out a fade or a burst of errors over many symbols so that instead of several adjacent symbols becoming completely destroyed, many symbols are only slightly affected and thus may be successfully reconstructed. In addition, because of dividing the channel bandwidth into many narrow sub-bands, the channel frequency response over each

of these sub-bands becomes relatively flat. This makes equalisation potentially simpler than in the serial system case. Another advantage of the parallel scheme is the possibility of being able to avoid the use of equalisers when differential decoding is employed, thus severely reducing the complexity of the receiver's structure.

4.2. Impact of System Parameters

Unless otherwise stated, the main parameters used in the simulations here are summarised in Table 4.2.1 below. In addition, for the following simulations it is assumed that errors arising due to synchronisation, RF filtering and peak to average power ratio are assumed to be negligible.

Symbol Rate	*5Msps*	Maximum Delay-spread	*5μsec or 17.2μsec*
Mapping Scheme	*QAM16*	Cyclic Prefix	*5μsec or 17.2μsec*
Channel Type	*GSM 6 tap urban or 6 tap hilly*	Doppler Frequency	*100Hz*
No. of sub-carriers	*1024 or 512*	Symbol Duration	*200.48μsec 100.24μsec*
Coding Rate	*½ Rate Convolutional*	Constraint Length	*7*

Table 4.2.1: Simulation's Parameters

4.2.1. Number of Sub-carriers Versus Multipath

The aim of this section is to highlight the impact of varying the number of subcarriers in the presence of both time and frequency dispersion. To assess the degradation caused by each one, the simulation was repeated for each one individually and then for the combined effect of the two together. For the time dispersive scenario time-invariant channels with a maximum delay spread of $5\mu sec$ and $17.2\mu sec$ were used. On the other hand, for the frequency dispersive channels, a frequency-flat-time-selective channel with a Doppler frequency of 100Hz was used. It can be seen from Figure 4.2.1.1 (a) and (b) that the degradation caused by time dispersion decreases as the number of subcarriers increases. This is because the effect of the resulting ISI becomes negligible as the length of the data symbols increases in proportion to the increase in the number of subcarriers. It is worth noting that in the case of the urban channel, figure (b), the performance improvement is starting to saturate as the number of subcarriers reaches 4096. This implies that as the symbol duration to the

time dispersion ratio reaches a certain threshold (in this case about 164), very little improvement would be obtained by further increasing the number of subcarriers.

In the case of the time dispersive scenario, it can be seen that the detrimental effect takes an opposite direction. In other words, as the symbol period is increased more ICI is generated and hence a higher performance degradation. It can be seen from this figure that the impact of such channel impairment can degrade the system's performance from 10^{-3} to 10^{-1}, when the number of subcarriers is increased from 128 or below to 4096 subcarriers.

In order to find the optimum number of subcarriers that produces the best performance in the presence of both time and frequency dispersion, the simulation test was repeated in a time-varying-frequency selective fading channel. It was found that the best compromise corresponds to where the two performance lines cross, in this case 1024.
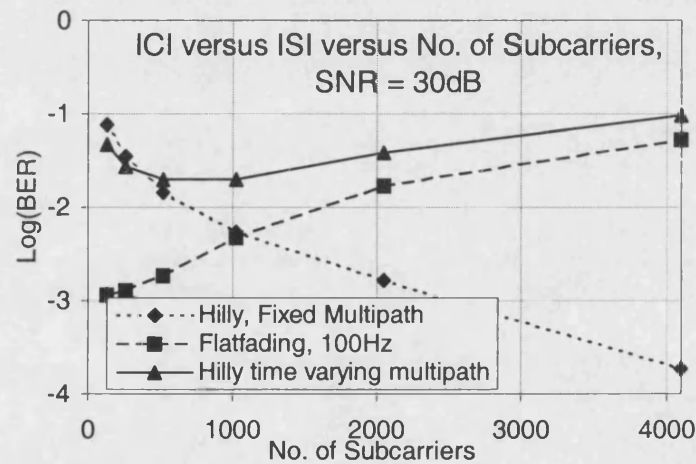
(a)
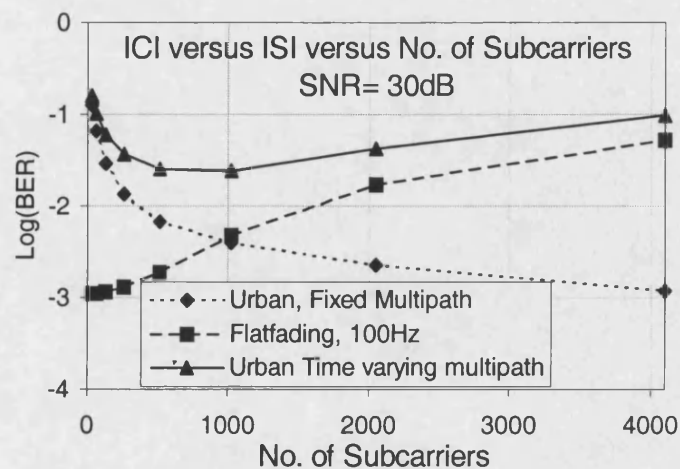
(b)

Figure 4.2.1.1 : Effect of No. of Sub-carriers in Both Hilly and Urban Channels

4.2.2. *Impact of the Cyclic Prefix*

In this section it is intended to highlight the impact of ISI, or alternatively the importance of the cyclic prefix on the OFDM system BER performance. The mathematical relationship relating the impact of the channel's delay spread to the theoretical BER performance of the OFDM system was presented in the previous chapter.

It is important to note that the use of the cyclic prefix is at least twofold. In addition to resulting in ISI-free OFDM blocks, the remaining impact of the channel's transient response on the individual sub-carriers may be resolved by a single multiplication operation using a copy of the inverse of the channel's frequency response. If however, a time guard-interval was used instead, i.e. during which no data is transmitted, the received OFDM blocks will be ISI free but in order to completely resolve the remaining impact of the channel on the individual sub-carriers, matrix inversion may be essential. Thus the number of multiplication operations is increased to *N* times that needed in the case of the cyclic prefix and that is excluding the number of multiplication and addition operations required in the matrix inversion process. In addition, because in the case of the time-guard-interval the ISI-free received OFDM blocks are masked with a waveform that contains high frequency components, this makes good channel estimation rather difficult and in the case of frequency domain differential modulation may result in higher bit error rates Figure 4.2.2.1 shows the time and frequency waveforms that mask each OFDM block in the presence of a cyclic prefix and a guard interval, respectively. It can be seen from (a) that unlike in the case of using a cyclic prefix, the frequency spectrum of the mask resulting from using a guard interval contains all frequency components up to the highest one in the available bandwidth.
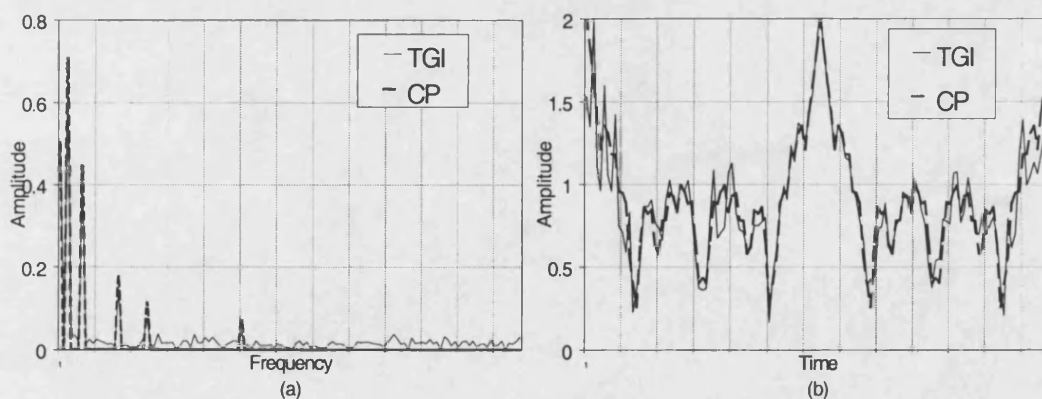
Figure 4.2.2.1:Comparsion Between the Cyclic Prefix and Guard Interval methods

Figure 4.2.2.2 shows the impact of ISI is the absence and presence of the cyclic prefix. It can be noted that the cyclic prefix offers a huge improvement even if its length is less than that of the maximum delay spread of the channel.

The graphs shown in Figure 4.2.2.3 are intended to highlight the impact of increasing the power of the secondary paths in a multipath environment. In this case a simple two-tap channel with a maximum delay spread of 17.2μsec was used and the power of the second path was varied from 20dB below the power of the main path to 0dB. It can be seen from this figure that when the power concentration in the main path is significantly higher than that in the secondary path, the impact of ISI is not severe and the cyclic prefix may be unnecessary.

(a)   (b)
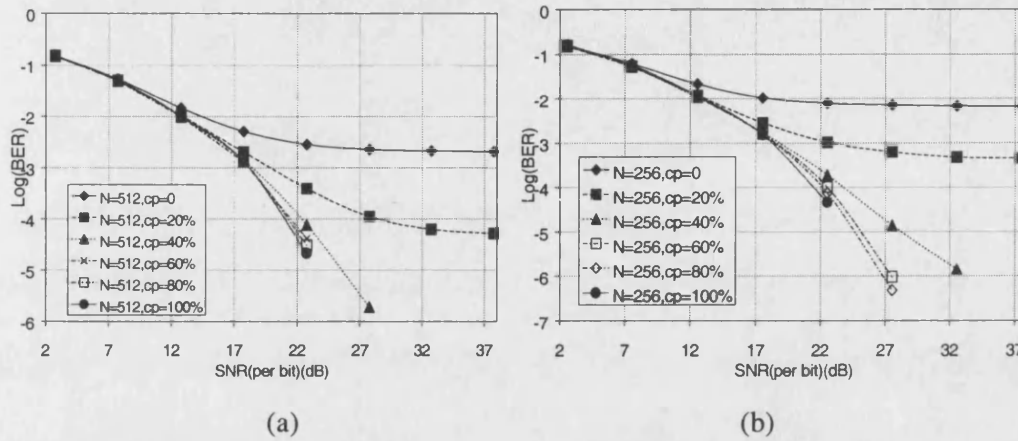
Figure 4.2.2.2: Impact of the Cyclic Prefix in 6 Taps Urban Channel Model, (a) N=512, (b) N=256

On the other hand, when the power in the second path starts approaching the level of power in the main path, the impact of ISI is more pronounced and the use for the cyclic prefix becomes important.
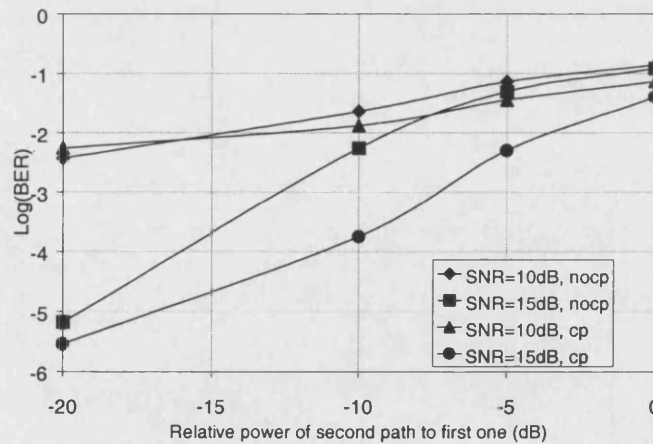
Figure 4.2.2.3: Impact of Multipath in the Presence and Absence of a Cyclic Prefix (CP) for Different E_b/N_o Ratios, Maximum delay = 17.2μs.

4.2.2.1. Alternative solution to the Cyclic Prefix

The use of a cyclic prefix entails penalties in the form of bandwidth and energy. Besides, the maximum delay spread of the channel may sometimes in practice exceed the length of the cyclic prefix resulting in a higher irreducible bit error rate floor. In addition, in cases where privacy is of prime importance, the use of a cyclic prefix is totally undesirable as it increases the probability of intercept. In view of this, in this work a method has been investigated where no cyclic prefix is needed and thus bandwidth, energy and privacy may be conserved. This method is feedback based as it performs tail cancellation using information from previous OFDM blocks [1]. One big advantage of the cyclic prefix is that provided that it completely absorbs the ISI term, the ISI free received OFDM block can then be easily equalised using an inverse of the channel frequency response. The frequency response of the channel usually contains a finite number of dominant frequency components and thus makes channel estimation an easier task. Because the alternative method discussed here does not use a cyclic prefix at the transmitter, the use of a simple equaliser that uses an estimate of the channel frequency response may not be sufficient and matrix inversion may be needed. However, this weakness of the feedback tail cancellation method may be overcome by re-storing the cyclic nature of the transmitted symbol before the receiver's FFT. Following from the analysis in chapter three, assuming that the OFDM block duration is long enough such that ISI can only exist between contiguous pairs of OFDM blocks, the received OFDM signal can be represented as follows:

$$r_{j,i} = \underbrace{x_{j,i} \cdot h_{j,0}}_{\substack{desired \\ sample}} + \underbrace{\sum_{k=0}^{i-1} x_{j,k} \cdot h_{j,i-k}}_{\substack{ISI, \\ within \quad the \quad block}} + \underbrace{\sum_{k=i+1}^{N-1} x_{j-1,k} \cdot h_{j,N+i-k}}_{\substack{ISI, \\ due \quad to \quad previous \quad block}} + \underbrace{n_{j,i}}_{\substack{additive \\ noise}} \qquad 4.2.2.1.1$$

where

r is the received symbol before the FFT,

x is the transmitted time domain data sample,

h is the channel impulse response

n is the additive white Gaussian noise.

and j is the OFDM block index.

If a good estimate of the channel impulse response and the previous OFDM block is available, the ISI term on the received symbol can be removed by reconstructing the third term at the receiver and subtracting it from 4.2.2.1.1. Although in practice, a perfect estimate of the channel impulse response and the previous block may not be available, it will be shown that using estimates will produce good performance especially at high SNRs. Once

the ISI term due to the previous OFDM block is removed, the periodicity of the received symbol may be restored using the following formula:

$$\hat{r}_{j,i} = \hat{r}_{j,i} + \sum_{m=1}^{L} x_{j,N-m} \cdot h_{j,m+i}$$ 4.2.2.1.2

where

         $\hat{r}$ is the ISI free received samples,

         L is the maximum delay spread of the channel.

It can be seen from equation 4.2.2.1.2 that in order to restore periodicity of the transmitted symbol knowledge of the actual symbol itself is needed. This condition is met in certain receivers discussed in [5] where the exact symbol may be known in advance. In this case however no knowledge of the actual symbol is available *a priori* and an estimate has to be established. An estimate can be established by first equalising the received signal using the simple channel frequency response based equaliser then reconstructing the time domain samples which are fed back to be used in the periodicity restoration process. Some of the samples will be in error and therefore the cyclic restoration is imperfect.

This technique of ISI removal and periodicity restoration may be summarised in the following steps:

         1: An initial estimate of the channel impulse response and the previous symbol is obtained from sending one comb of frequency-domain pilot tones at the beginning of transmission.

         2: Use the reconstructed time domain samples of the previous block, $\hat{x}_{j-1,i}$ to remove the ISI term from the newly arriving time domain samples, $x_{j,i}$ using the following relationship:

$$\hat{r}_{j,i} = r_{j,i} - \sum_{n=i+1}^{N-1} \hat{x}_{j-1,n} \cdot h_{N+i-n}$$ 4.2.2.1.3

         3: These ISI free samples are then converted back to the frequency domain using the receiver's FFT, equalised and used to construct an estimate of the originally transmitted symbols, $\hat{X}_j$. These are then converted back to the time domain using the IFFT, $\hat{x}_{j,i}$, in order to use in the periodicity restoration process as shown below:

$$\hat{r}_{j,i} = \hat{r}_{j,i} + \sum_{m=1}^{L} \hat{x}_{j,N-m} \cdot h_{j,m+i}$$ 4.2.2.1.4

4: The resulting time domain samples are then converted to the frequency domain using the FFT, equalised and demapped to recover the transmitted data bits. A copy of these bits is fed back and used for removing the ISI term on the next symbol.

A simplified block diagram of the part of the OFDM receiver that deals with the ISI removal and periodicity restoration processes is presented in Figure 4.2.2.1.1.
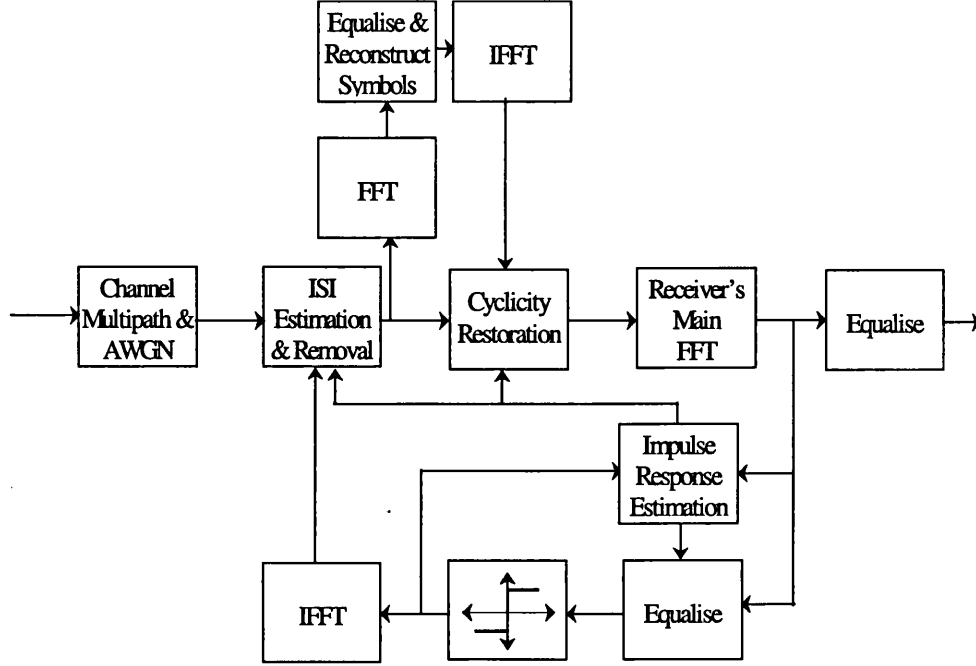
Figure 4.2.2.1.1: Part of the OFDM Receiver that Deals with ISI Removal

The process of ISI cancellation and periodicity restoration can also be done in the frequency domain after the receiver's FFT using the following relationships:

$$\hat{R}_{j,k} = \tilde{R}_{j,k} - \frac{1}{N} \cdot \sum_{m=0}^{N-1} \left[\underbrace{\left[\sum_{t=0}^{N-1} \left(e^{2j\pi kt/N} \cdot \sum_{p=t+(N-M)}^{N-1} h_{N+t-p} \cdot e^{2j\pi mp/N} \right) \right]}_{ISI} \cdot \hat{X}_{j-1,m} \right] \qquad 4.2.2.1.5$$

$$\hat{R}_j^{CYC} = \hat{R}_j + V \cdot \hat{R}_j$$

$$V_{k,m} = \frac{1}{N} \cdot \sum_{n=0}^{N-1} \left(e^{j2\pi kn/N} \cdot \sum_{p=n+1}^{N} h_{j,n-p} e^{-j2\pi mp/N} \right) \qquad 4.2.2.1.6$$

Its clear from both equation 4.2.2.1.5 and 4.2.2.1.6 that the frequency domain based method of tail cancellation and periodicity restoration requires more calculations and entails a higher risk of making errors since now the whole symbol is being operated upon, rather than just the fraction of the symbol that corresponds to the maximum delay spread of the channel as is the case with the time domain method. Therefore if an error is made it will affect the whole

symbol and then due to the feedback nature of the process, the error will propagate to the other symbols causing catastrophic failure. In addition the periodicity restoration process is useful for simplifying the feedback channel impulse response estimation process.

4.2.2.2.   Adaptive Algorithm

Because of the nature of the method used to cancel the ISI term and to restore the periodicity of the received signals, a good estimate of the channel impulse response is vital. In this section we examine the performance of the least mean square, LMS, CIR estimation on the systems performance, see appendix at the end of the chapter. The method implemented here to estimate the channel response uses an LMS algorithm for each sub-carrier as given by 4.2.2.2.1:

$$W_{i+1,n} = W_{i,n} + 2 \cdot \mu \cdot E_{i,n} \cdot X_{i,n}^*$$

4.2.2.2.1

$$E_{i,n} = Z_{i,n} - W_{i,n} \cdot X_{i,n}$$

where, i is a time index,

n is a frequency index,

W is the tap weight,

X^* is the complex conjugate of the transmitted symbol, in the frequency-domain.

μ is speed of convergence control factor.

and Z is the received corrupted symbol after ISI cancellation and periodicity restoration.

The LMS algorithm is used in a feedback channel modelling mode as shown in figure . In order to achieve a fast start of the algorithm, an initial estimate of the coefficients is established by dividing the first received block of frequency domain pilot tones by its corresponding transmitted one. It will be shown this will reduce the conversion time of the LMS algorithm significantly. After each block update of the LMS algorithm, the frequency-domain coefficients of the transfer function should be inverse FFT transformed to the time domain for use in the ISI cancellation and periodicity restoration processes. In addition, this set of time domain coefficients should be windowed by a rectangular window of length equal to the maximum delay spread of the channel, M. Then the coefficients should be replaced by the FFT transform of the windowed time domain coefficients. This process has the advantage of reducing the residual noise resulting from imperfect ISI cancellation and

periodicity restoration as well the receiver's additive noise, by as much as $10\log(M/N)$ dB. Therefore, the effective update including the effects of windowing is given by:

$$W_{i+1,n} = W_{i,n} + 2 \cdot \mu \cdot \alpha \cdot E_{i,n} \cdot X_{i,n}^*$$

<div align="right">4.2.2.2.2</div>

$$\alpha = \sqrt{M/N}$$
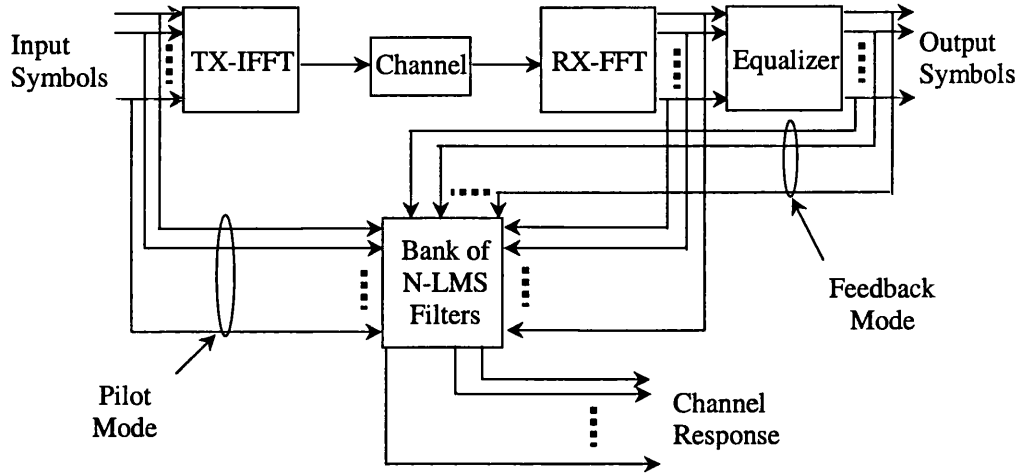
Figure 2.2.2.1: Schematic of LMS-Channel Estimator

4.2.2.3.   Simulation Results

Except for the Doppler frequency, the simulation parameters used in the simulation below are given in Table 4.2.1 provided before. The Doppler frequency was chosen to be 25Hz for the purpose of allowing an adaptive algorithm such as the LMS algorithm to converge. Figure 4.2.2.3.1 below shows the advantage of initialising the LMS weights by directly dividing the received signal by the transmitted one at the beginning of transmission. The advantage of using such initialisation technique however only pays off at high SNR (> 10dB), as shown in figure 4.2.2.3.1 part (b).

The choice of the control factor μ is very important in the presence of time-varying multipath channels. For the simulation results below, the optimum value for μ was found by trial and error to be 0.05. Figure 4.2.2.3.2 shows a few samples of the tests carried out to examine the impact of different μ values on the convergence rate of the LMS algorithm in the type of channel used here.

(a)   (b)
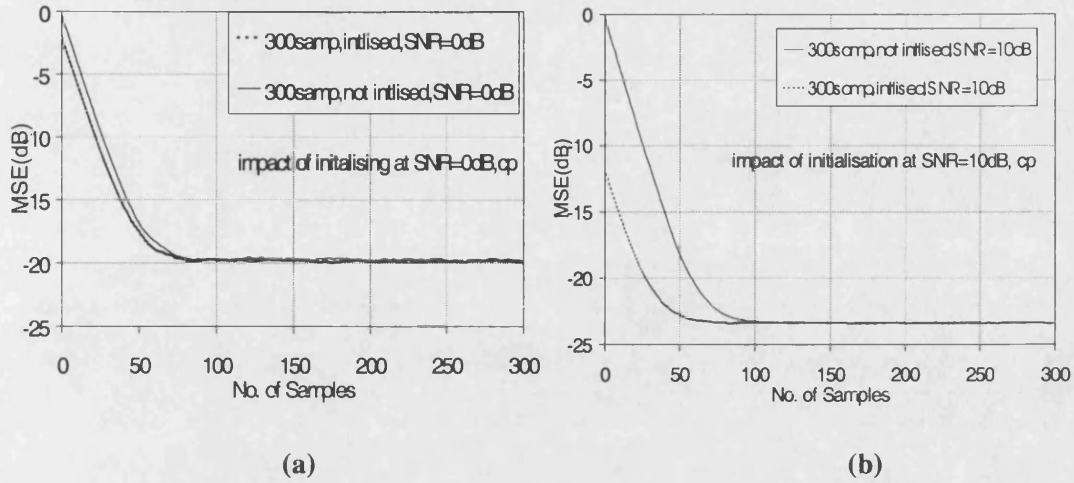
Figure 4.2.2.3.1: Convergence Time of the LMS Algorithm in Static Typical Urban GSM

Channel, (a) at SNR= 0dB, (b) at SNR =10dB
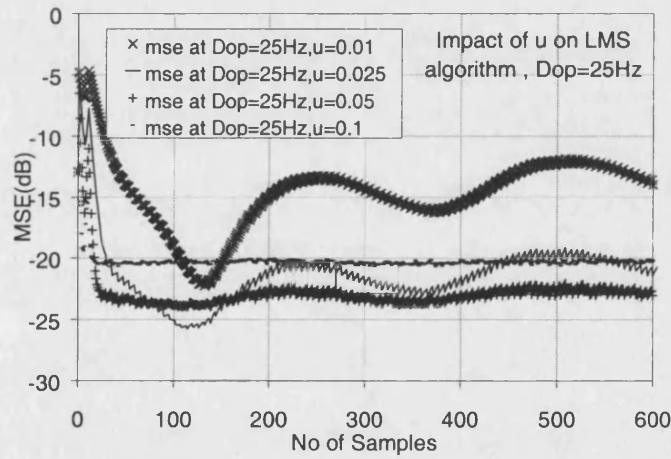
Figure 4.2.2.3.2: Convergence Time of the LMS Algorithm in Time-Varying Typical Urban

GSM Channel at SNR= 10dB, Doppler=25Hz

where the MSE on the *y-axis* is defined as the time-average of the difference between the estimated and actual channel estimate.

Figure 4.2.2.3.3 and Figure 4.2.2.3.4 illustrate the performance of the feedback-based ISI cancellation technique and compare it to the cyclic prefix method in both static and time-varying channels, respectively. The comparison on both figures includes results LMS algorithm, averaging technique and perfect channel knowledge. For the averaging technique, the channel estimate was obtained by averaging over a hundred samples for the static channel and only one sample for the time varying channel. The feedback-based ISI cancellation technique offers a good performance and may be considered as a potential

alternative to the cyclic prefix technique if the extra computational complexity is not of paramount importance. The secret of a successful implementation of this technique however lies in the availability of a good channel estimate as can be seen form Figure 4.2.2.3.4.
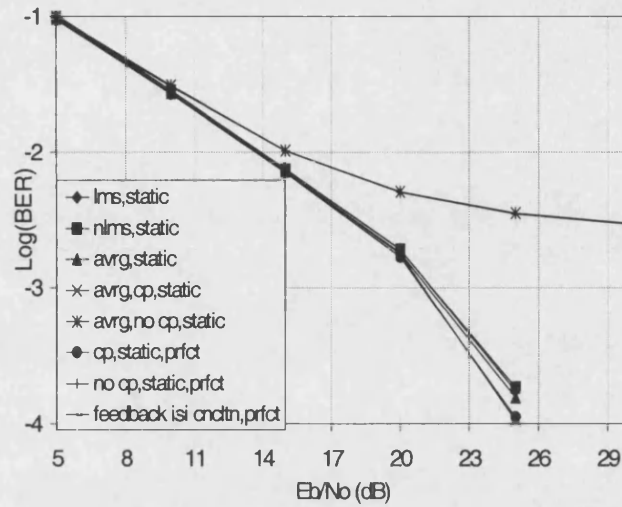
Figure 4.2.2.3.3: Comparison in the Presence and Absence of the Cyclic Prefix in Static 6 tap Typical Urban Multipath GSM Channel
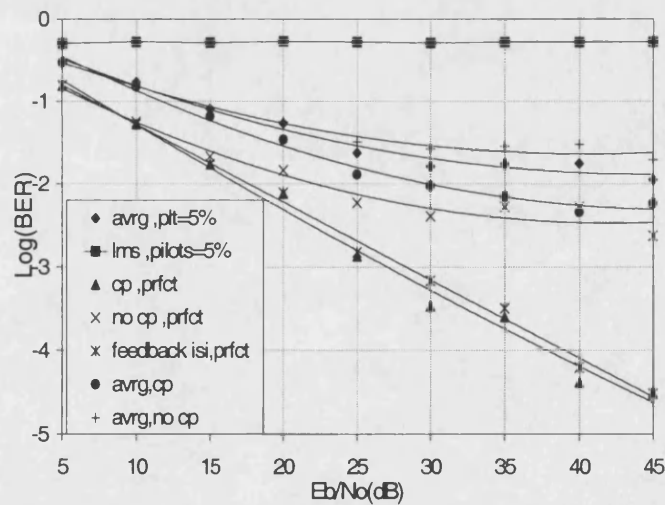
Figure 4.2.2.3.4: Comparison in the Presence and Absence of the Cyclic Prefix in Time-Varying 6 tap Urban Multipath Channel

In order to prevent instability due to erroneous ISI cancellation and periodicity restoration, pilot sequences were periodically transmitted at a rate of 5% of the used bandwidth. The pilot sequences were also used for preventing the channel estimate from diverging catastrophically from the correct one.

4.2.3.   Synchronisation Issues

The sensitivity of OFDM based systems to synchronisation errors, in particular frequency errors, is one of the major drawbacks of this technique. In this section a brief overview of the main synchronisation errors is presented. This includes frequency synchronisation, time synchronisation and phase noise.

4.2.3.1.   Frequency Synchronisation

Frequency offset between the transmission frequency, f_T, and the receiving frequency f_R, ($f_{offset} = f_T - f_R$), is generally caused by a synchronisation mismatch of the two oscillators at the transmitter and receiver. One of the principal disadvantages of OFDM is its high sensitivity to frequency offset. Such impairment is exacerbated in the case of asynchronous transmission, where subcarriers are shared by more than one user. In such a case, the oscillators of all users must be matched, [16]. In this section, however, the frequency offset is assumed to be the same for all subcarriers.

Furthermore, it is frequently stated that the time variant influence of the radio channel in the form of Doppler shifts also contributes to frequency offsets [17].

There are a few detrimental effects associated with frequency offset. These include phase rotation and amplitude reduction of signal at each of the subcarriers (the sinc functions are shifted and are no longer sampled at the peak) as illustrated in Figure 4.2.3.1.1. In addition, frequency offset results in introducing ICI between the subcarriers and hence causes loss of orthogonality. Because in OFDM the carriers may be very closely spaced in frequency compared to the channel bandwidth, the tolerable frequency offset becomes a very small fraction of the channel bandwidth. Maintaining sufficient open loop frequency accuracy can therefore become difficult in links, such as, satellites with multiple frequency translations or in mobile radio links that can introduce significant Doppler shifts.
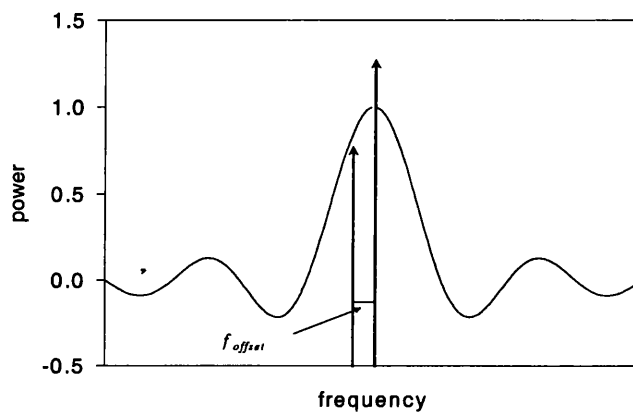
Figure 4.2.3.1.1: Impact of Frequency Offset

After passing through the channel, the complex envelope of the received sequence can be expressed as:

$$r_n = \frac{1}{N} \cdot \left(\sum_{k=0}^{N-1} X_k \cdot H_k \cdot e^{2j\pi nk/N} \cdot e^{2j\pi n\varepsilon/N} \right),$$

4.2.3.1.1

where

ε is the ratio of the actual frequency offset to the intercarrier spacing.

The use of a cyclic prefix in this situation merely helps maintain adjacent frames orthogonal, but the orthogonality with each frame is no longer complete due to the frequency offset. The signal at the output of the FFT is therefore:

$$R_k = \sum_{n=0}^{N-1} r_n \cdot e^{-2j\pi kn/N}$$

$$= (X_k \cdot H_k) \cdot \left[\frac{\sin(\pi\varepsilon)}{N \cdot \sin(\pi\varepsilon/N)} \right] \cdot e^{j\pi\varepsilon(N-1)/N} + I + \eta$$

4.2.2.3.2

The first term of equation 4.2.2.3.2 is the wanted signal modified by the channel transfer function. This component is also amplitude and phase shifted due to the frequency offset. The second term is the ICI term, which (assuming that the impulse response of the channel is fixed over one frame) is entirely due to frequency offset and is given by:

$$I_k = \sum_{\substack{l=0, \\ l\neq k}}^{N-1} (X_l H_l) \cdot \left[\frac{\sin(\pi\varepsilon)}{N \sin(\pi(l-k+\varepsilon)/N)} \right] \cdot e^{j\pi\varepsilon(N-1)/N} \cdot e^{-j\pi(l-k)/N},$$

4.2.2.3.3

In [19], an analytical expression for the SNR degradation due to carrier frequency offset and carrier phase noise was derived. It is found that an OFDM based system is much more sensitive than a single-carrier based system. The SNR degradation due to the frequency offset can be approximated by:

$$D_{awgn}(dB) = \frac{10}{3\ln(10)} \cdot (\pi\varepsilon)^2 \frac{Es}{N_o},$$

4.2.2.3.4

In the presence of fading and dispersive channels, the impact of frequency offset is slightly different. An upper bound for the degradation caused in such environment is given by [22]:

$$D_{fading}(dB) \leq 10\log_{10}\left(\frac{1 + 0.5947 \cdot \dfrac{Es}{N_o} \cdot \sin(\pi\varepsilon)}{\sin c^2(\varepsilon)} \right),$$

4.2.2.3.5

In Figure 4.2.2.3.2, the associated SNR degradation is plotted as a function of the normalised frequency offset for both AWGN and dispersive channels. It can be concluded from this

figure that a synchronisation accuracy of as good as within 2% of the actual subcarrier frequency may be needed to avoid severe SNR degradation.
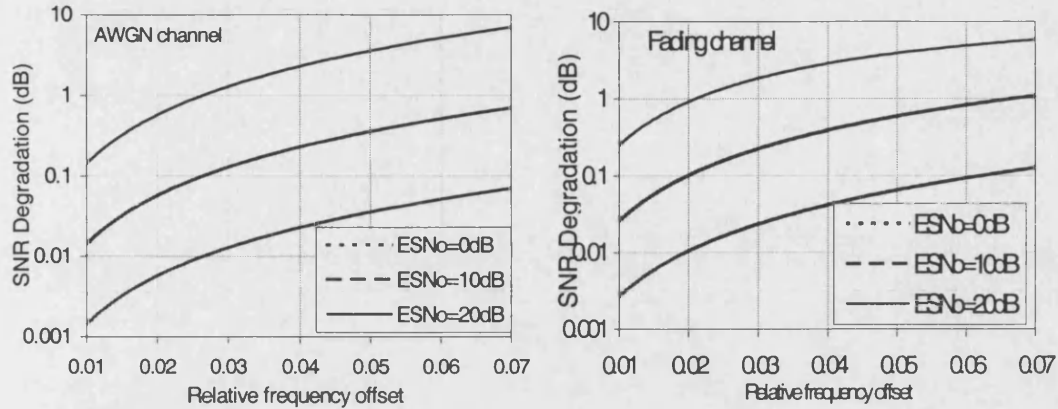
Figure 4.2.2.3.2: Degradation in SNR Due to Frequency Offset

Most, if not all, frequency offset estimation algorithms are based on using training sequences, or pilot tones. In [22] a maximum likelihood algorithm that involves repetition of a data symbol and comparison of the phases of each of the subcarriers between the successive symbols is presented. Since the modulation phase values are not changed, the phase shift of each of the subcarriers between successive repeated symbols is due to the frequency offset. It was shown that the estimate obtained using this technique is conditionally unbiased and is consistent in the sense that the variance is inversely proportional to the number of subcarriers in the OFDM signal. In [23][24] an algorithm that is based on scanning a certain frequency range for the training data distributed evenly over the subcarriers was suggested. The most difficult aspect of this algorithm however is to find a scanning range and step-size that time allow a precise-enough estimation and a fast search at the same time. This method was found to be successful at finding large frequency offsets, as long as they are within the search range, even in difficult mobile environments.

4.2.3.2.   Carrier Phase Noise

In the absence of frequency offset, phase shifts can occur due to phase noise, which arises due to imperfections in the transmitter and receiver oscillators. An analysis of the impact of phase noise on the system's BER performance was carried out in [19]-[21]. There it was modelled as a Wiener process $\theta(t)$ with $E\{\theta(t)\} = 0$ and $E\{(\theta(t_0 + t) - \theta(t_0))^2 = 4\pi\beta|t|\}$, where β denotes the one sided 3 dB linewidth of the Lorentzian power density spectrum of the free running oscillator.

The degradation in SNR due to such impairments was approximated to be [20]:

$$D(dB) = \frac{11}{6\ln(10)} \cdot \left(4\pi N \frac{\beta}{W}\right) \cdot \frac{Es}{No},$$ 4.2.2.3.1

where W is the subcarrier bandwidth.

Equation 4.2.2.3.1 implies that the impact of phase noise increases in proportion to increasing the number of subcarriers.

As the statistical characteristics of such noise are usually device dependent, a white Gaussian noise generator was used for the purpose of illustrating the impact of such effect. Figure 4.2.2.3.1 shows how the BER performance of an OFDM-16QAM system is degraded as the variance of the phase noise is increased from 0.0 to 0.25. It can be seen from these figures that the performance of the system is rapidly degraded, as the phase noise variance is increased.
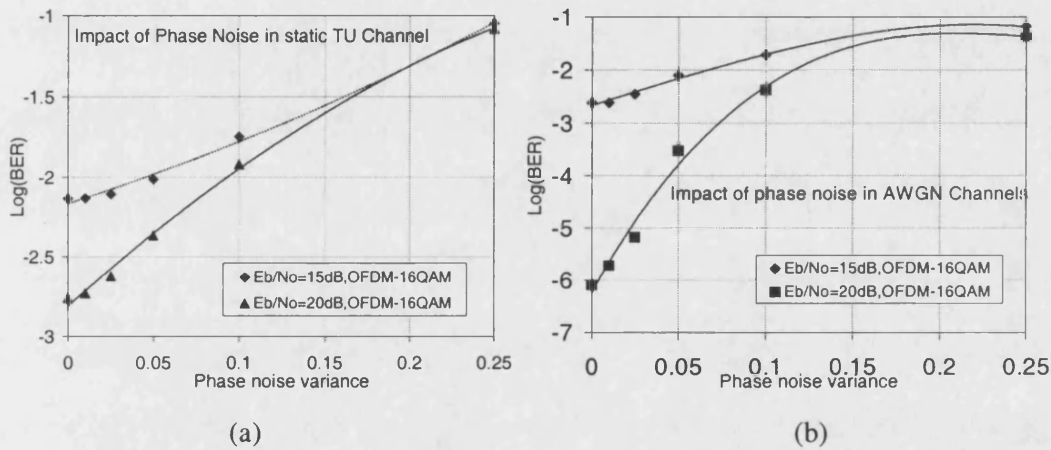
Figure 4.2.2.3.1: Impact of Phase Noise on Parallel QAM, (a) Static Urban & (b) AWGN

4.2.3.3.   Frame Synchronisation

In general, every OFDM block contains $N + G$ number of samples (useful + cyclic prefix samples). For correct reception, only the useful N samples have to be detected. If the detected samples contained some of the cyclic prefix components or even samples from an adjacent block, then a timing synchronisation error is caused. Assuming that the cyclic prefix is longer than the impulse response of the channel, then frame misalignment will be contained within one OFDM block. If the samples of the cyclic prefix included in the detection are contaminated with samples from an adjacent block, then the detected block will be ISI infected making the problem even more serious. Some effects of the transmission channel can also be seen as frame synchronisation errors as, for example, in the presence of a line of sight that is suddenly shadowed [17].
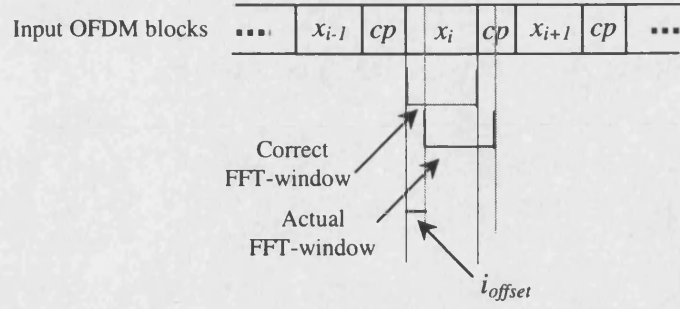
Figure 4.2.3.3.1: Frame Offset

A timing offset of $t_{offset} > 0$ causes the received OFDM signal to have the following form:

$$r_{m,i} = \sum_{k=0}^{N-1-i_{offset}N} x_{k+i_{offset}\cdot N,i} \cdot e^{-j2\pi mk/N} + \sum_{k=N-i_{offset}N}^{N-1} x_{k,i_{offset}N-N,i+1} \cdot e^{-j2\pi mk/N} \qquad 4.2.3.3.1$$

where

$i_{offset} = t_{offset}/Ts$ is the discrete time shift of the block.

Assuming that the frame offset does not contain any ISI, the degradation in SNR can be approximated by [18]:

$$D_{frame-offset} = \frac{1}{\left(1 - i_{offset}\right)^2} - 1 \qquad 4.2.3.3.2$$

It can be seen from equation 4.2.3.3.2, which is plotted in Figure 4.2.3.3.2 that the performance of OFDM based systems degrades in proportion to increasing the frame offset.
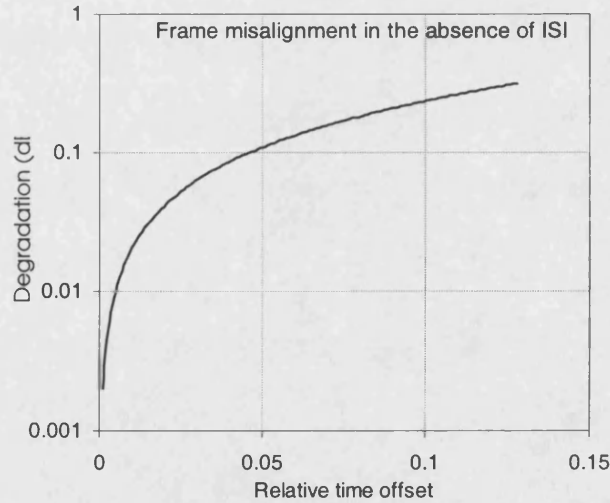
Figure 4.2.3.3.2: Impact of Frame Misaligment in the Absence of ISI

Several methods for frame synchronisation have been investigated [25]-[32]. The use of pilot tones was one of the first techniques proposed. It is based on sending known symbols in certain positions in the time-frequency grid [25][26]. As well as assisting in estimating the frame position, such technique can also provide an estimate of the channel transfer function.

The drawbacks of this technique however lie in the fact that precious bandwidth is used up by the insertion of the pilot tones. In addition, when frequency offset is present, it can become very difficult to detect the pilot tones after the receivers FFT due to the resulting loss of orthogonality.

The other most common technique investigated is based on the cyclic prefix [29][32]. This method relies on the fact that the cyclic prefix carries repeated data and therefore can be used as a reference. In [32] the difference between the received samples spaced N samples apart is calculated, $r_k - r_{k+N}$ and when one of the samples belong to the cyclic prefix and the other one to the useful OFDM symbol, the difference should be small. Otherwise the difference will have twice the power. By windowing this difference with a rectangular window of the same length as that of the cyclic prefix, the output will have a minimum when a new OFDM symbol starts.

4.2.4. Impact of Coding and Interleaving

The use of forward error correction coding [31] combined with interleaving to combat fading in the mobile channel is a key feature of the OFDM technique. Fades will always be present and when they occur they can result in the destruction of many contiguous sub-carriers, causing erroneous bits in the receiver. To prevent this, the information bits are protected with a suitable code, usually convolutional or may be even a concatenation of convolutional and Reed-Solomon codes. Prior to transmission, the coded bits are interleaved in time (over several OFDM blocks) or frequency (within the same OFDM block) or even both depending on the type of channel encountered. These two interleaving processes will ensure that most of the bursts of errors produced in the channel will be reduced to single random errors in the receiver after the de-interleaving process taking place. The single errors may then be more easily corrected using the decoder.

Time and frequency interleaving provide the OFDM system with both time and frequency diversity, respectively. In the presence of dominantly frequency selective channels, however, (i.e. when the receiver is not in motion), time interleaving becomes much less effective and therefore may be avoided. On the other hand, frequency interleaving in this type of channels is essential as it averages the impact of the nulls in the frequency response of the channel over many bits making it easier for the decoder at the receiver to recover the transmitted data. From this viewpoint, the presence of multipath is an advantage for the COFDM system as it makes the channel frequency selective and hence brings in frequency diversity.

Two types of interleavers have been examined. The first is a block interleaver in which the data is stored in a $(N \times N)$ matrix row-wise and read out column-wise. At the deinterleaver, the reverse process is implemented. The other type of interleavers examined here uses a special relationship to link between the interleaved bits. This relationship given by [4]:

For the interleaver $delay\_i(i)=$ *bit reverse* $(i \bmod N_{OFS})$ 4.2.4.1

For the deinterleaver $delay\_d(i)= N_{OFS} - 1 - delay\_i(i)$ 4.2.4.2

where:

N_{OFS} is the number of OFDM blocks involved in the interleaving process.

mod stands for modulo N_{OFS} operation, in this case used as modulo N_{OFS} addition, which is defined as:

modulo (i/N_{OFS}) = *remainder*(i/N_{OFS})

reverse bit operation swaps around the binary-representation of $(i \bmod N_{OFS})$. e.g. if the binary representation of $(i \bmod N_{OFS})$ is 1010, the *reverse bit* operation would produce 0101. i.e. it swapped the leftmost with the rightmost and the second leftmost with the second rightmost.

The number of OFDM blocks involved in the interleaving process determines the minimum number of binary bits required to represent the value of $(i \bmod N_{OFS})$. For example if N_{OFS} was 32 blocks, then the minimum number of bits required is 5.

The interleaver randomises the coded bits over the specified number of OFDM blocks. The total number of bits involved in the interleaving process is given by:

$$N_T = N_{OFS} \times N \times l \qquad\qquad 4.2.4.3$$

where:

N is the number of sub-carriers,

l is related to the mapping scheme used, i.e. number of bits per sub-carrier

The position of a given bit in a frame, e.g. i, determines the delay, in number of frames, to be applied to this bit before transmission. At the deinterleaver a complementary delay is applied to the incoming bits in order to restore the original bit order before interleaving. **Table 4.2.4.1** lists the delays to be applied to the first 16 bits entering the interleaver and deinterleaver as a function of bit index i. Because of the cyclic nature of the modulo-16 operation, the delays to be applied for the next 16 bits are identical.

i mod 16	delay_i(i)	delay_d(i)
0	0	15
1	8	7
2	4	11
3	12	3
4	2	13
5	10	5
6	6	9
7	14	1
8	1	14
9	9	6
10	5	10
11	13	2
12	3	12
13	11	4
14	7	8
15	15	0

Table 4.2.4.1: Delays Applied to Bits Entering the Interleaver and Deinterleaver

In order to show the effectiveness of both frequency and time interleaving, a number of simulations have been conducted for both static and dynamic channels. In Figure 4.2.4.1 the impact of interleaving in a static channel is presented. A considerable improvement is obtained at SNR > 10dB when interleaving is used. This figure also shows that the use of time interleaving in this type of channel results in an insignificant improvement over the frequency interleaving.

In a dynamic multipath channel however the situation is rather different. Figure 4.2.4.2 shows how time interleaving is vital in this type of channel as it results in significant improvement in terms of SNR.
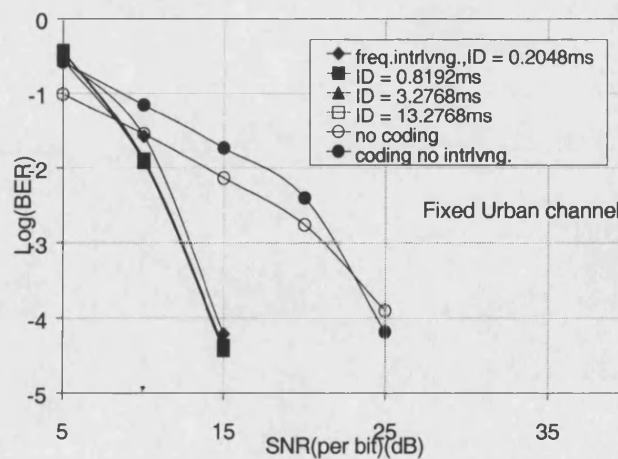
Figure 4.2.4.1: Impact of Coding and Interleaving in Static COST'207 Typical Urban Channel

The purpose Figure 4.2.4.3 is to provide a measure of the optimum interleaving depth for the systems parameters used here, highlight the impact of frequency interleaving on both interleaver types and compare the performance of both interleavers under such conditions. It is evident from this figure that the optimum interleaving depth to obtain a BER of 10^{-3} is about 400 msec. It is also clear that frequency interleaving increases the convergence rate of the non-block interleaver. Finally, this figure suggests that the non-block interleaver combined with frequency interleaving can outperform the block interleaver by about 1dB.
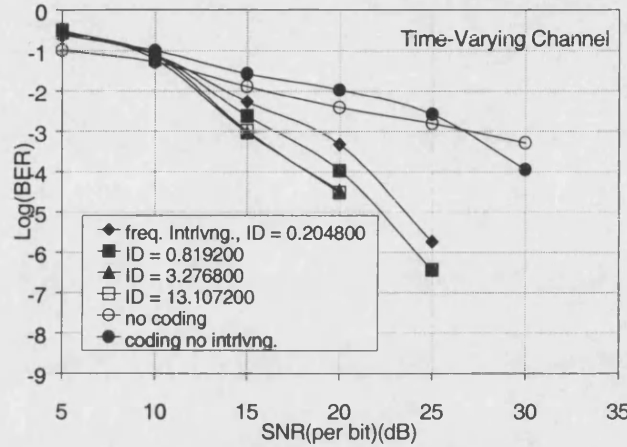
Figure 4.2.4.2: Impact of Coding and Interleaving in Time-Varying COST'207 Urban Channel
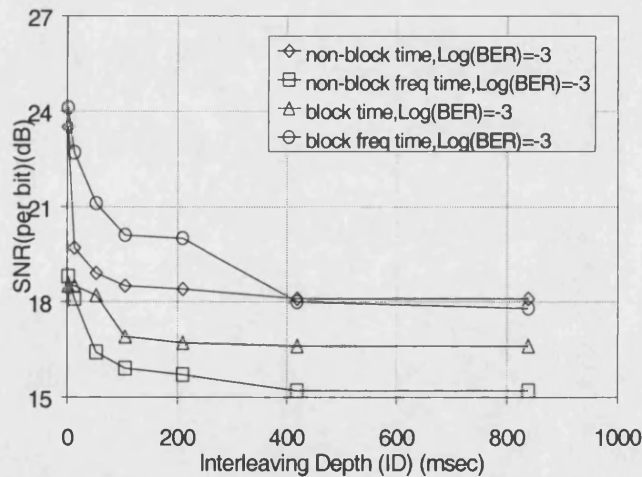
Figure 4.2.4.3: Impact of Interleaving Depth in Urban COST'207 at Doppler = 200Hz

4.3.   Non-Coherent OFDM modulation

The main reason for using non-coherent/differential modulation is because differential modulation techniques do not require any information about the channel and thus result in less computational complexity and overhead at the receiver. A classical and well-known

example of differential modulation technique is the differential phase shift keying, DPSK, technique which only requires the phase information for encoding and decoding the data bits. Other differential techniques include differential amplitude phase modulation, DAPM [9].

The use of differential encoding with OFDM systems may be implemented in two ways. The first is referred to as parallel implementation, in which the symbols in one block are differentially encoded with the corresponding symbols in the previous block. In other words, N differential encoders are required in this case, where N is the number of sub-carriers used. This form of DPSK/OFDM encoding is depicted in Figure 4.3.1.

Transmitter   Receiver
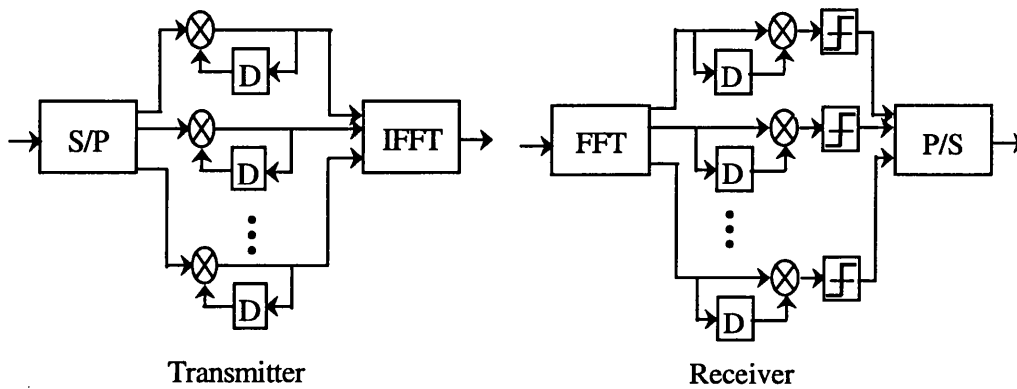
Figure 4.3.1: Schematic of the DBPSK (in Parallel) Encoder/Decoder

The other way of implementing DPSK/OFDM may be referred to as serial implementation, in which only one encoder is used before the serial to parallel converter at the transmitter and one decoder after the parallel to serial converter at the receiver. In other words, the parallel DPSK scheme is a time domain based one as it links between consecutive symbols in time whereas the serial scheme is based on the frequency domain as it links between symbols in frequency. The two implementations have both their advantages and disadvantages. In the parallel scheme case, the advantages are high tolerance of the system to the coherence bandwidth of the channel and secondly the high bandwidth efficiency achieved as it only requires one single block of reference symbols at the beginning of transmission. On the other hand, the disadvantages of this scheme are the higher complexity resulting from the use of N encoders/decoders at both the transmitter and receiver and the higher sensitive to Doppler effects due to its time dependence.

The advantages of using the serial scheme are the much simpler transmitter and receiver structures as it only requires one encoder/decoder and its high tolerance to Doppler effects. However, the disadvantages of this scheme are its high sensitivity to the coherence bandwidth of the channel and its bandwidth inefficiency as it requires to devote one sub-carrier with ever OFDM block throughout transmission as a reference symbol.

The differential encoding and decoding of the data may be described in the following steps:

Encoding:

1- separate the data bits into groups of m bits

2- translate each group of m bits into a complex number, $B_{j,i}$, according to a certain predefined constellation

3- the differentially encoded complex symbol is given by:

$$X_{j,i} = X_{j,i-1} \cdot B_{j,i} \qquad \text{for serial implementation or}$$

$$X_{j,i} = X_{j-1,i} \cdot B_{j,i} \qquad \text{for parallel implementation}$$

At the receiver the data bits are extracted from the received symbols, $R_{j,i}$, by using the following:

$$D_{j,i} = \frac{R_{j,i}}{R_{j,i-1}} = \frac{X_{j,i} \cdot H_{j,i}}{X_{j,i-1} \cdot H_{j,i-1}} = \frac{B_{j,i} \cdot X_{j,i-1} \cdot H_{j,i}}{X_{j,i-1} \cdot H_{j,i-1}}$$

$$= B_{j,i} \cdot \frac{H_{j,i}}{H_{j,i-1}}$$

$$\cong B_{j,i}, \qquad H_{j,i} \approx H_{j,i-1}$$

where $H_{j,i}$ is the channel frequency response

Due to the interdependency of the differentially encoded symbols, errors occur in pairs resulting in performance loss of about 3dB when compared to its coherent counterpart. Figure 4.3.2 shows a comparison between the performance of BPSK and DBPSK in an additive white Gaussian noise channel, AWGN. It is clear from this figure that BPSK outperforms its differential counterpart by about 3dB at low E_b/N_o values. As the noise power decreases with respect to the signal power, the performance difference between BPSK and DBPSK shrinks gradually to less than 1dB.

In multipath channels, coherent modulation requires an estimate of the channel frequency response and therefore the performance of the system is governed by the goodness of the channel estimate provided. On the contrary, differential modulation does not require knowledge of the channel but may suffer from error propagation between pairs of symbols as explained earlier. In order to eliminate errors due to imperfect channel estimation, perfect knowledge of the channel is assumed for the coherent modulation case.

In Figure 4.3.3, a comparison of both parallel and serial DBPSK at a BER of 10^{-3} and 10^{-4} as a function of E_b/N_o versus number of subcarriers is shown. A number of conclusions may be drawn from those figures. Firstly, the fact that BPSK outperforms both DBPSK schemes by

as much as 3-4 dB at BER=10^{-3}, figure (b). In practice however, this penalty may be less than 3dB, as the channel estimate used to equalise the multipath effect cannot be perfect.

It can also be seen that at BER = 10^{-4}, the difference in performance between BPSK and both parallel and serial DBPSK shrinks to about 1dB especially at $N>512$.
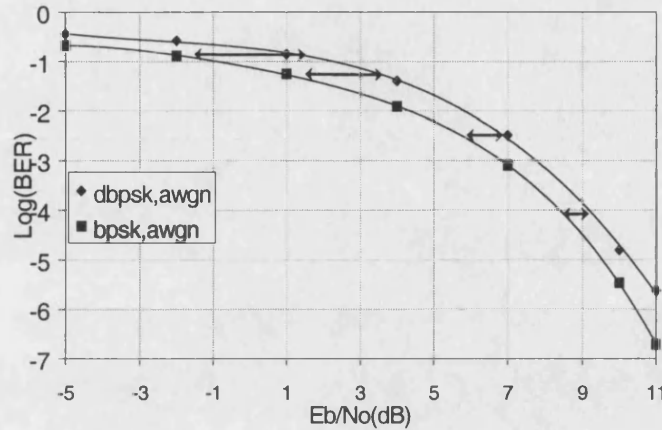
Figure 4.3.2: Comparison between BPSK and DBPSK in AWGN Channel

The final conclusion that may be drawn from this figure is the fact that the parallel DBPSK scheme outperforms the serial one when $N<512$, a direct result of the higher sensitivity of the serial scheme to the coherence bandwidth of the channel. The impact of the channel's frequency selectivity on the serial scheme is more destructive as it will subject consecutive pairs of DBPSK symbols to significantly different fades which will result in erroneous decoding of the symbols at the receiver.

(a)   (b)
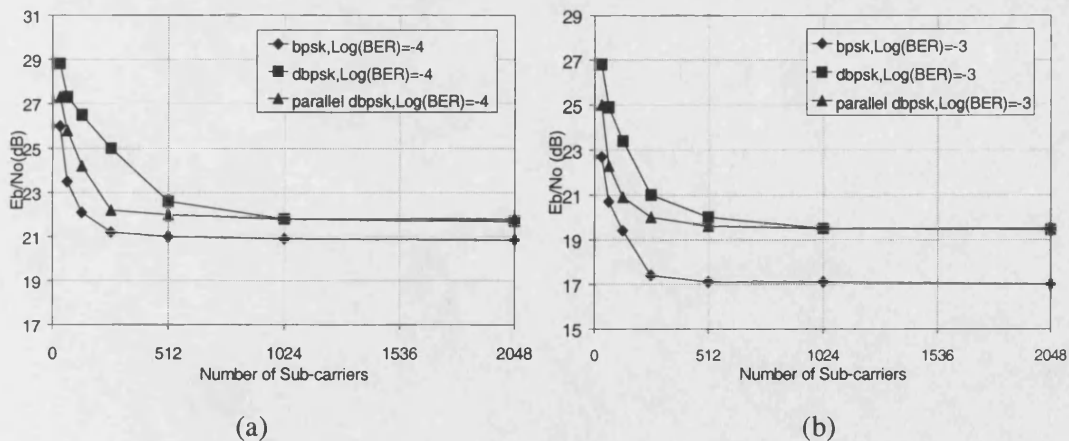
Figure 4.3.3: Performance Comparison Between Coherent and Differential BPSK in 6 tap Urban GSM Channel, (a) Log(BER)=-4, (b) Log(BER)= -3

Figure 4.3.4 gives a comparison between the two schemes for different E_b/N_o ratios and reveals the significant improvement in terms of BER obtained when using the parallel

scheme especially at N< 256. It is evident from this figure that the improvement of the parallel scheme over the serial one becomes more significant as the BER sought is lower. For example, if the BER required is between 10^{-4} and 10^{-5}, this can be achieved at $E_b/N_o \le$ 25dB using $N<256$ when the parallel scheme is employed whereas if the serial scheme is to be used then an average N value of 512 is to be considered for the same E_b/N_o.
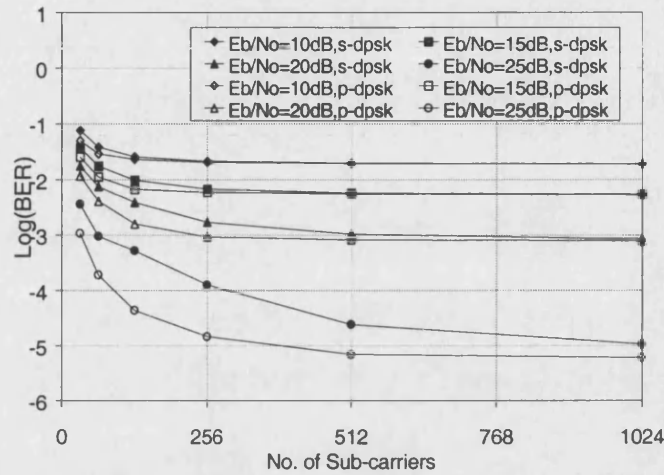
Figure 4.3.4: Comparison Between Parallel and Serial DBPSK for Different E_b/N_o

4.3.1. Impact of Doppler Frequency

In order to emphasise on the effect of the channel's time variations on the OFDM system BER performance, a flat-fading-time-varying channel was used here. The fading encountered in such a channel is classified as time selective (and frequency non-selective). Generally in designing OFDM based systems the duration of each OFDM symbol is such that the channel is effectively time-invariant during the transmission of each symbol. Nevertheless, it is intended here to produce a measure of when a significant degradation begins to occur in relation to a fixed Doppler frequency and variable number of sub-carriers when using the parallel DBPSK/OFDM scheme. Since this scheme relates the samples of one OFDM symbol to their corresponding ones in the previous symbol, it will be shown how the BER performance of the system degrades as the number of sub-carriers is increased. This is because an increase in the symbol duration means more time for the channel to change significantly. It can be seen from Figure 4.3.1.1 how the impact of the Doppler frequency becomes more evident at large N values. Unlike in the case of the static multipath channel, the serial scheme outperforms the parallel one in this type of channels, especially at large values of N. This is because the time delay between the pairs of DBPSK symbols for the serial scheme is N times less than that for the parallel scheme.
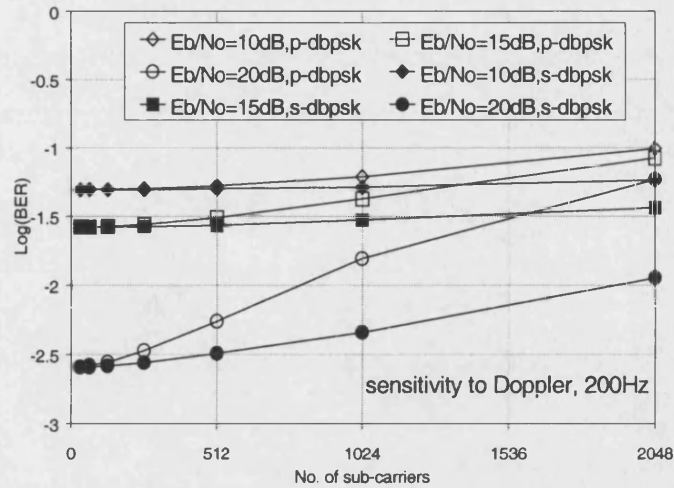
Figure 4.3.1.1: Comparison Between Parallel and Serial DBPSK

in the Presence of Multipath

Figure 4.3.1.2 further highlights the higher sensitivity of the parallel scheme to Doppler as a function of E_b/N_o versus number of subcarriers.
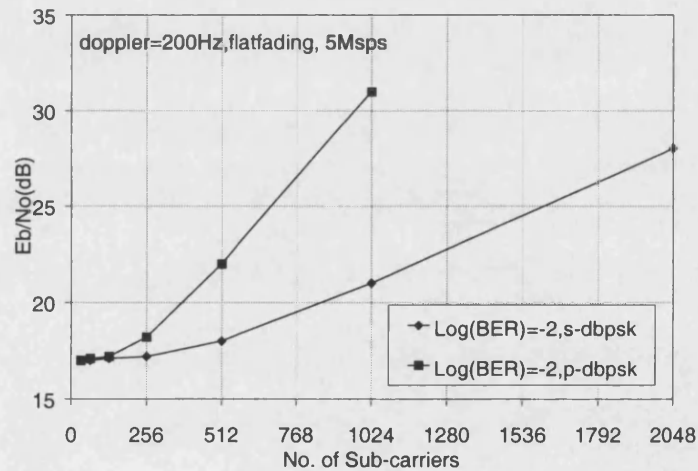
Figure 4.3.1.2: Sensitivity of DBPSK Schemes to Doppler

Therefore, it can be said that the use of the serial DBPSK/OFDM scheme in time varying and frequency selective fading channels not only produces a much less complicated and more commercially economical system but also may outperform its parallel DBPSK/OFDM counterpart.

4.3.2. Impact of time-varying multipath

In this section the combined effect of multipath and Doppler on both the serial and parallel DPSK schemes is investigated. The channel used in the simulation below is the urban GSM model with a maximum delay spread of 5μsec. As can be seen from Figure 4.3.2.1, the two

schemes behave in a completely opposite sense to each other. In the case of the parallel scheme the performance degrades rapidly as soon as the number of sub-carriers exceeds 256. On the contrary, in the case of the serial scheme, the performance significantly improves as the number of sub-carriers reaches 512 and beyond. This figure also suggests that both schemes can be applied in such channel provided that the necessary measures in choosing the right number of sub-carriers are met. If the number of sub-carriers to be used is small such as in the cases where it is essential to keep the size of the FFT as small as possible to reduce the computation overhead, then the parallel scheme must be used. On the other hand, if its necessary to have many sub-carriers such as in the case of DAB, then the serial scheme would be the better option.

(a)   (b)
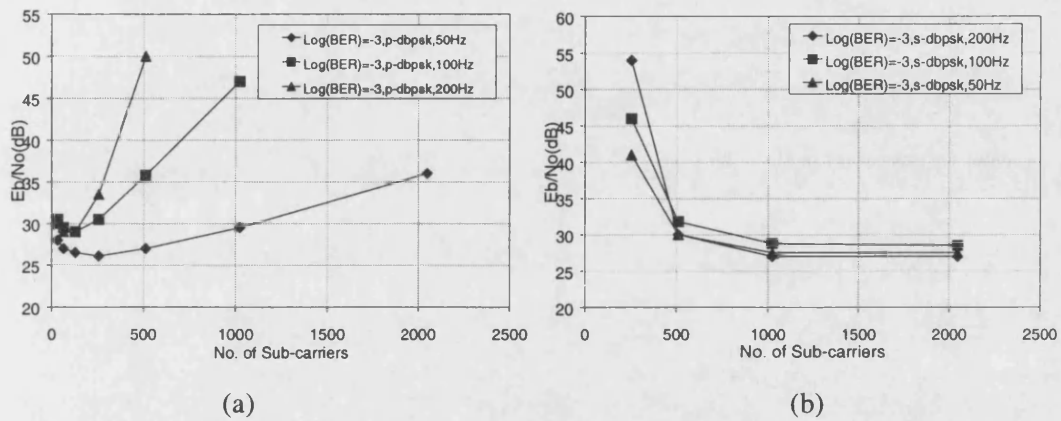
Figure 4.3.2.1: Impact of Time-Varying Multipath Channel on Both DBPSK Schemes, (a) Parallel DBPSK and (b) Serial DBPSK

4.4.   Conclusion

The behaviour of OFDM in multipath fading channels was studied in this chapter. The performance of OFDM in terms of bit error versus signal to noise ratio was evaluated over two types of GSM channel models, namely urban and hilly channels, and the impact of increasing the number of subcarriers in time static and time variant channels was investigated. It was shown how the performance improves by increasing the number of subcarriers when the channel is time-static and degrades when the channel is mainly time variant. In the presence of a time varying multipath channel, the choice of the number of subcarriers has a major impact on the system's BER performance.

The use of a cyclic prefix for combating ISI was investigated along with an alternative solution based on feedback echo cancellation. It was concluded that some form of ISI combating technique must be used when the ratio of the channel's maximum delay spread to

the OFDM block duration is significant. The use of a cyclic prefix is the simplest and safest technique, but only at the expense of bandwidth and energy. Feedback echo cancellation works very well provided that a good channel estimate is obtainable.

A brief overview of the main synchronisation issues concerned with OFDM was presented. The presence of frequency offset was shown to have the highest impact on the system's performance making the use of frequency offset estimation techniques a necessity. The influence of carrier phase noise on the OFDM system performance was simulated. It was shown that for a fixed bit rate the performance degradation of OFDM due to carrier phase noise is higher than single carrier transmission.

The importance of coding and interleaving in time varying frequency selective fading channels was examined. It was shown how frequency interleaving may be sufficient in dominantly frequency selective fading channels. The time diversity achieved through time interleaving is very effective in time varying channels. The optimal interleaving depth is a function of the coherence time of the channel as well as the minimum distance of the channel coding scheme used. Generally speaking, the optimal interleaving depth is that depth after which no further significant improvement is achieved. A comparison between the performance of an OFDM system and a single carrier system showed that OFDM outperforms the single carrier only when combined with coding and interleaving. Finally a comparison between differential and coherent modulation was presented. In the presence of a perfect channel estimate, coherent modulation outperforms its non-coherent counterpart by as much as 3dB at relatively low signal to noise ratio due to the error propagation associated with differential modulation. The performance difference gradually shrinks to about 1dB at higher SNRs. A comparison between the two different ways of implementing differential modulation techniques was presented. It was shown that the serial implementation is more appropriate in the presence of rapidly time varying channels especially when the coherence bandwidth of the channel is much bigger than that of the individual sub-channels. On the other hand, the parallel implementation is the better choice when the channel's coherence bandwidth is relatively small.

4.5. References

[1] W. Webb and L. Hanzo, *"Modern Quadrature Amplitude Modulation, Principles and Applications for Fixed and Wireless Channels"*, IEEE press, 1994

[2] L Vandendrope, *"Multitone Transmission in Multipath Rician Fading Channels"*, Proceedings of the IEEE 1st Symposium on Communications and Vehicular Technology, Benelux, Delft, the Netherlands, pp. 2.1.1-2.1.6., Oct., 1993

[3] H. Nikookar, *"Wireless Channel Modelling and Code Division Multiple Access for Indoor Communications"*, Ph.D. Thesis, Delf University, the Netherlands, 1996.

[4] D. Pommier and B. LeFloch, *"Method of Broadcasting of Digital Data, Notably for Radio Broadcasting at High Throughput Rate Towards Mobile Receivers, with Time-Frequency Interlacing and Analogue Synchronisation "*, US Patent 5,191,576, March 2, 1993.

[5] J. M. Cioffi and A. C. Bingham, *"A data-Driven Multitone Echo Canceller "*, IEEE Transactions on Communications, Vol. 42, pp. 2853-2869, Oct. 1994.

[6] T. C. Chen, *"One Dimentional Signal Processing"*, Marcel Decker: New York & Basel, Chapter 13, 1978.

[7] N. J. Bershad, *"On The Real and Complex Mean Square Adaptive Filter Algorithm "*, Proceedings of the IEEE, Vol. 69, pp. 469-470, Apr. 1981.

[8] S. Haykin, *"Adaptive Filter Theory"*, Prentice-Hall, 2nd edition, 1991.

[9] V. Engels and H. Rohling, *"Multilevel Differential Modulation Techniques (64-DASK) for Multicarrier Transmission Systems "*, European Transactions on Communications, Vol. 6. No. 6, pp.633-640, Nov-Dec. 1995.

[10] J. Sklar, *"Digital Communications Fundamentals and Applications"*, Prentice Hall International Edition, 1995.

[11] H. Rohling and T. May, *"Comparison of PSK and DPSK Modulation in Coded OFDM Systems"*, Proceedings of the IEEE VTC'97, pp. 870-874, 1997.

[12] M.Okada, S. Hara and N. Morinaga, *"Bit Error Rate Performance of Multicarrier Modulation Radio Transmission Systems"*, IEICE Transactions on Communications, Vol. E76-B, No. 2, pp. 113-119, Feb. 1993.

[13] J. G. Proakis, *"Digital Communications"*, McGraw-Hill, 3^{ed} 1993.

[14] H. Sari, G. Karam and I. Jeanclaude, *"Transmission Technique for Digital Terrestrial TV Broadcasting "*, IEEE Communications Magazine, Vol. 33, No. 2, pp. 100-109, Feb. 1995.

[15] Ifeachor and Jervis, *"Digital Signal Processing A Practical Approach "*, Addison Wesley, 1992.

[16] D. Dardari, "*MCM Systems with Waveform Shaping in Multiuser Environments: Effects of Fading, Interference and Timing Errors*", Proceedings of the IEEE Global Telecommunication Conference, Phoenix, pp.21-26, 1997.

[17] M. Gudmundson and Per-Olof Anderson, "*Adjacent Channel Interference in an OFDM System*", Proceedings of the IEEE VTC'96, pp. 918-922, Atlanta, 1996.

[18] K. Matheus and K. Kammeyer, "*Optimal Design of Multicarrier Systems With Soft Impulse Shaping Including Equalisation in Time and Frequency Direction*", Proceedings of OFDM-Fachgesprach, Braunschweig, Germany, Sept. 1997.

[19] T. Pollet, M. Bladal and M. Moeneclaey, "*The Effect of Carrier Frequency Offset and Phase Noise on the BER Performance of OFDM Signals*", Proceeding of the IEEE 1st Symposium on Communications and Vehicular Technology, pp. 4.2-1 – 4.2.4, Delft, The Netherlands, Oct. 1993.

[20] T. Pollet and M. Moeneclaey, "*Carrier Phase Jitter Sensitivity for Single Carrier and Multicarrier QAM Systems*", Proceeding of the IEEE 2nd Symposium on Communications and Vehicular Technology, pp. 174 – 181, Louvain la Neuve, Belgium, Nov. 1995.

[21] T. Pollet, M. Bladal and M. Moeneclaey, "*BER Sensitivity of OFDM Systems to Carrier Frequency Offset and Wiener Phase Noise*", IEEE Transactions on Communications, vol. 43, No. 2 - 4, pp. 191 – 193, Feb. – Apr. 1995.

[22] P. H. Moose, "*A Technique for Orthogonal Frequency Division Multiplexing Frequency Offset Correction*", IEEE Transactions on Communications, vol. 42, No. 10, pp. 2908 – 2914, Oct. 1994.

[23] F. Classen and M. Meyr, "*Frequency Synchronisation Algorithms for OFDM Systems Suitable for Communication over Frequency Selective Fading Channels*", Proceedings of the IEEE VTC'94, pp. 1655-1659, June 1994.

[24] M. Luise and Ruggero Reggiannini, " *Carrier Frequency Acquisition and Tracking for OFDM-Systems*", IEEE Transactions on Communications, 44(11):1590-1598, Nov. 1996.

[25] W. D. Warner and C. Leung, "*OFDM/FM Frame Synchronisation for Mobile Radio Data Communication*" IEEE Transactions on Communications Technology, 42(3):302-313, Aug. 1993.

[26] M. Wahlqvist, R. Larsson and C. Ostberg, "*Time Synchronisation in the Uplink of an OFDM System*", Proceeding of IEEE VTC'96, pp. 918-922, Atlanta, 1996.

[27] P. R. Chevillat, D. Maiwald and G. Ungerboek, "*Rapid Training of a Voiceband Data Modem Receiver Employing an Equaliser with Fractional T-Spaced Coefficients*", IEE Transactions on Communications, COM-35(9):869-876, Sept. 1987.

[28] T. M. Schmidl and Donald C. Cox, "*Low-Overhead, Low-Complexity [Burst] Synchronisation for OFDM* ", Proceedings of the IEEE International Conference on Communications, Dallas, pp.1301-1306, June 1996.

[29] J-J Beek, M. Sandell, M. Isaksson and P. O. Borjesson, "*Low-Complexity Frame Synchronisation in OFDM Systems*", Proceedings of the IEEE International Conference on Personal and Wireless Communications, pp. 982-986, Nov. 1995.

[30] vandeBeek_JJ, Sandell_M, Borjesson_PO, "*ML estimation of time and frequency offset in OFDM systems*", IEEE Transactions on Signal Processing, Vol.45, No.7, pp.1800-1805, 1997

[31] S. Lin and D. Costello, "*Error Control Coding Fundamentals and Applications*", Prentice Hall, 1983.

[32] P. J. Tourtier, R. Monnier and P. Lopez, "*Multicarrier Modem for Digital HDTV Terrestrial Broadcasting*", Signal Processing: Image Communications, 5(5-6): 379-403, Dec. 1993.

Chapter Five

Channel Estimation for OFDM

5 Chapter Five

5.1 Introduction

Modulation can be classified as differential or coherent. When differential modulation is used, channel estimation is not necessary as the information is encoded in the difference between consecutive symbols. This is a common technique in wireless communications, which reduces the overall complexity of the system by eliminating the need for equalisation. Differential modulation is used in the European DAB standard [1]. The drawback of using differential modulation is a SNR loss of about 1-3dB. An interesting form of differential modulation is the differential amplitude and phase shift keying (DAPSK), where a greater spectral efficiency is achieved by using differential coding of amplitude as well as phase [2][3]. Coherent modulation allows a greater range of different signal constellations to be used and therefore is normally chosen when the channel is static or very slowly changing in time such as the fixed wireless channels. Coherent modulation is used in the European DVB standard [4][5].

There are mainly two problems in the design of channel estimators for coherent OFDM systems. The first problem is the choice of a suitable technique to obtain an initial estimate of the channel and the second one is the choice of the optimum criteria within fixed complexity and performance for utilising this initial estimate to obtain an improved one.

One way of estimating the channel frequency domain transfer function is to insert multiples of pilot tones (known symbols) in the spectrum of the transmitted signal. From these symbols all the channel attenuations can be estimated using an interpolating filter. This technique is called pilot symbol assisted modulation (PSAM) and was introduced for single carrier systems by [6]. Since each channel in OFDM is flat fading, PSAM can be generalised in two dimensions where pilots are transmitted in certain positions in the time and frequency grid of the OFDM signal. An estimate of the full channel response can then be obtained by using a single or two-dimensional interpolating filter.

There are a number of parameters that need to be correctly determined in order to use this technique efficiently. Such parameters include the optimum pilot tone pattern, estimation criteria, pilot tone power level and interpolation order. Correct choice of such parameters is very important as they have a direct impact on the system's efficiency and BER performance.

In this chapter, the basic principle of the scattered pilots based channel estimation for OFDM transmission is presented. The use of different estimation criteria, such as, zero forcing, ZF, minimum mean square error, MMSE, and Fourier transform domain, FTD, are discussed and a comparison on the basis of BER performance is given in both urban and hilly channels. The impact of increasing the pilot tones power level on the system's overall BER performance was evaluated. The sensitivity of such channel estimation technique to frame misalignment and its impact on the system performance are analysed using computer simulation. Finally, a new alternative method that is based on orthogonal code spreading for simultaneous channel estimation and data transmission is presented. Such method allows the transmission of 100% pilot tones without altering the data throughput. Thus alleviating some of the problems associated with the scattered pilot tone technique.

5.2   System Description

Channel estimators usually need some kind of pilot information as points of reference. In the case of a time varying fading channel, constant tracking is necessary so pilot signals may have to be continuously transmitted. An efficient way of continuously tracking the time varying channel is to transmit pilot symbols instead of data at certain locations of the OFDM time- frequency lattice, examples of this are shown in Figure 5.2.1, where both scattered and continual pilot symbols are shown.

In general, the fading channel frequency domain transfer function can be viewed as a two-dimensional signal (time and frequency) which is sampled at pilot positions, and the channel's induced attenuations and phase shifts between pilots are estimated by interpolation. This allows us to use the two-dimensional sampling theorem to put limits on the density of the pilot tone patterns. However, as in the single carrier transmission case, the pilot pattern should be designed so that the channel is not under-sampled at the receiver [7].

When estimating the channel, the pilot tones are firstly extracted from the received signal and used along with their known actual values to estimate the channel's frequency response at their positions. Then the channel response over the subcarriers that carry data is estimated by interpolation using the estimates provided by the closest neighbouring pilots. This is depicted in Figure 5.2.2.
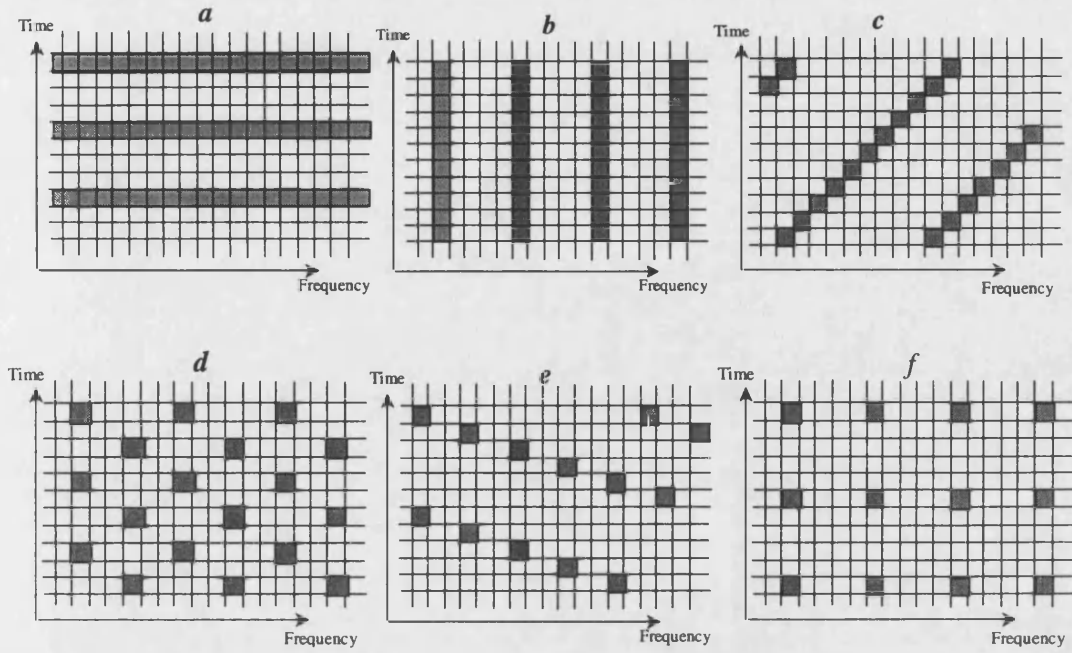
Figure 5.2.1: Examples of Scattered Pilot Tone Patterns
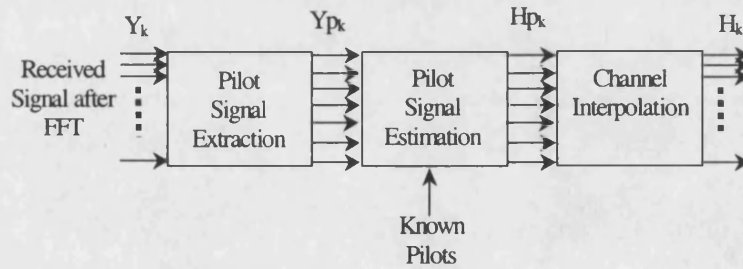
Figure 5.2.2: Schematic of Channel Estimator Based on Scattered Pilot Pattern

Mathematically, the channel estimation may be described as follows. It is assumed here that the received OFDM blocks are independent of each other; in other words the channel impulse decayed to near zero during the cyclic prefix. It is also assumed that the scattered pilots are evenly spaced in frequency and time. In such a pilot arrangement, the N subcarriers are divided into Np groups, each with $L=N/Np$ adjacent subcarriers. In each group the first subcarrier is used to transmit a pilot signal. The OFDM signal modulated on the kth subcarrier can be expressed as:

$$X_k{}^` = X_{mL+l} \qquad m = 0,1,\cdots Np-1$$

$$= \begin{cases} Xp_m & l = 0 \\ Information\ data & l = 1,2\cdots,L-1 \end{cases} \qquad 5.2.1$$

101

The pilot signals Xp_m can be either equal to fixed complex values to reduce the computational complexity or random generated data that can also be used for synchronisation as well as channel estimation.

Let Hp be the channel response of the pilot subcarriers where,

$$Hp = \begin{bmatrix} Hp_0 & Hp_1 & \cdots Hp_{N-1} \end{bmatrix}^T$$
$$= \begin{bmatrix} H_0 H_{L-1} \cdots H_{((Np-1)\cdot L-1)} \end{bmatrix}^T , \qquad\qquad 5.2.2$$

and Yp be the vector of received pilot signals, where this can be expressed in the following format:

$$Yp = \begin{bmatrix} Yp_0 & Yp_1 & \cdots Yp_{(Np-1)} \end{bmatrix}^T \qquad\qquad 5.2.3$$

$$Yp = Xp \cdot Hp + Np, \qquad\qquad 5.2.4$$

where

$$Xp = \begin{bmatrix} Xp_o & \cdots & 0 \\ & \ddots & \\ 0 & & Xp_{(Np-1)} \end{bmatrix}$$

and Np is the vector of Gaussian noise on the pilot subcarriers. Assuming zero-forcing criteria, the channel response at the position of the pilot tones is given by:

$$Hp^{ZF} = Xp^{-1} \cdot Yp$$

$$= \begin{bmatrix} \dfrac{Yp_0}{Xp_0} & \dfrac{Yp_1}{Xp_1} & \cdots & \dfrac{Yp_{(N_p-1)}}{Xp_{(Np-1)}} \end{bmatrix}^T , \qquad\qquad 5.2.5$$

Which corresponds to dividing the received symbols (which are masked by the channel frequency domain transfer function) by a copy of the actual transmitted symbols.

To obtain the full channel response, a first or second order polynomial interpolator can be used according to equation 5.2.6 and 5.2.7 as shown below.

$$\hat{H}_k = \hat{H}_{mL+l} = \left(1 - \frac{l}{L}\right) \cdot \hat{H}p_m + \frac{l}{L} \cdot \hat{H}p_{m+1} \quad 0 \le l \le L, \qquad\qquad 5.2.6$$

and

$$\hat{H}_k = C_0 \cdot \hat{H}p_m + C_1 \cdot \hat{H}p_{m+1} + C_2 \cdot \hat{H}p_{m++2}$$

$$\begin{cases} C_0 = (1-\alpha)\left(1-\dfrac{\alpha}{2}\right) \\ C_1 = \alpha \cdot (2-\alpha) \\ C_2 = \dfrac{\alpha}{2}(\alpha-1) \\ \text{and} \\ \alpha = 1/N \end{cases} \qquad , \qquad 5.2.7$$

5.3   Alternative Estimation Criteria

The ZF method of estimating the channel frequency response is susceptible to noise and intercarrier interference, ICI. Because the estimation of the full channel response is obtained by interpolation using the channel response samples obtained at the pilots positions, the performance of such OFDM system is highly dependent on the goodness of the estimate of the pilot samples.

The minimum mean-square error (MMSE) estimator has been shown to provide a much better performance than the ZF estimator at low SNR [8]. The major drawback of the MMSE estimator, however, is its high complexity, which grows exponentially with the number of observation samples. The mathematical representation for the MMSE estimator of pilot signals is [9]:

$$\begin{aligned} \hat{H}p_{lmmse} &= R_{HpHp^{ZF}} R^{-1}_{HpHp^{ZF}} \hat{H}p^{ZF} \\ &= R_{HpHp}\left(R_{HpHp} + \sigma_n^2 \left(XpXp^H\right)^{-1}\right)^{-1} Hp^{ZF} \end{aligned} \qquad , \qquad 5.3.1$$

where $\hat{H}p^{ZF}$ is the initial estimate of H_p, σ_n^2 is the variance of the additive noise and the covariance matrices are defined by:

$$R_{Hp,Hp} = E\{HpHp^H\},$$
$$R_{Hp,Hp^{ZF}} = E\{HpHp^{ZF^H}\},$$
$$R_{Hp^{ZF},Hp^{ZF}} = E\{Hp^{ZF}Hp^{ZF^H}\},$$

The above implies that there is a matrix inversion involved in calculating the MMSE estimate of the channel, which must be calculated every time. This problem however, can be avoided by using fixed pilot positions resulting in a simplified linear MMSE estimator [9]:

$$\hat{H}p = R_{HpHp}\left(R_{HpHp} + \frac{\beta}{SNR}I\right)^{-1}\hat{H}p^{ZF}, \qquad 5.3.2$$

where $SNR = \dfrac{E|Xp_k|^2}{\sigma_n^2}$ is the average signal to noise ratio and

$\beta = E|Xp_k|^2 E\left|\dfrac{1}{Xp_k}\right|$ is a constant depending on the signal constellation.

Provided that the autocorrelation matrix of the channel, R_{HpHp}, and the SNR are known in

advance, $R_{HpHp}\left(R_{HpHp} + \dfrac{\beta}{SNR} I \right)^{-1}$ will only need to be calculated once.

Although the MMSE estimator may be implemented without repetetive evaluation of matrix inversion, the number of caculations involved may be considered to be very high for many applications and the performance of the algorithm depends heavily on the goodness of the predetermined statistics of the channel.

Another technique, which is a compromise between the MMSE and ZF techniques, is the Fourier Transform Domain, FTD, technique described in chapter six and [10]. This technique simply works by taking the inverse Fourier transform of the pilot tones and zero padding the transformed components that extend beyond the impulse response of the channel. When the channel is sample-spaced and the maximum delay spread of the channel is known, this technique is "almost" equivalent to the MMSE method. On the contrary, when the channel is not sample-spaced and the maximum delay spread of the channel approaches the duration of the OFDM block, this technique becomes equivalent to ZF. If the zero-padded region is extended such that the total size of the block becomes equal to N samples, taking the Fourier transform of this block will give the full channel response and no further interpolation will be required. The interpolated samples will have to be scaled by the square root of the sampling period to compensate for the difference between the two transforms.
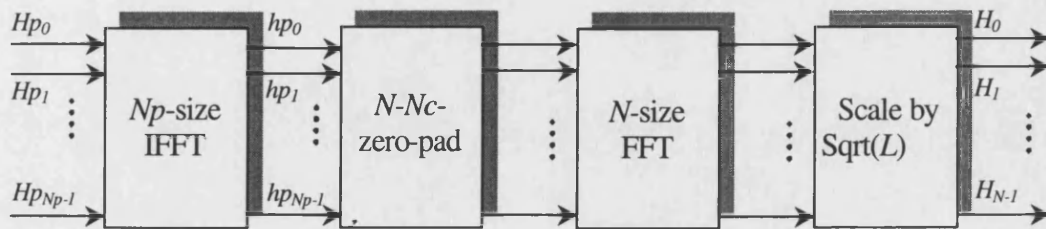
Figure 5.3.1: Schematic of FTD Channel Estimator

As shown in figure 5.3.1, the FTD method works as follows. The received pilots are firstly grouped into one group of Np and transformed to the time domain. Zero-padding is then applied to eliminate the noise-dominant samples. The zero-padding operation takes place

over *Nc* samples where *Nc* is chosen such that *Np* + *Nc* = *N*. Finally, the inverse Fourier transform is invoked producing a down scaled version of the channel frequency response. To get the exact channel frequency response, a scaling factor equal to the square root of *N/Np*.

In Figure 5.3.2 a comparison between the three different techniques in time-invariant urban and hilly GSM environments is presented. It can be seen that the performance of the FTD technique closely matches that of the MMSE in the urban channel but does not perform as well in the hilly channel. This is due to the fact that hilly channels have a much longer maximum delay spread and therefore the FTD generated estimate is subjected to more noise.

(a)   (b)
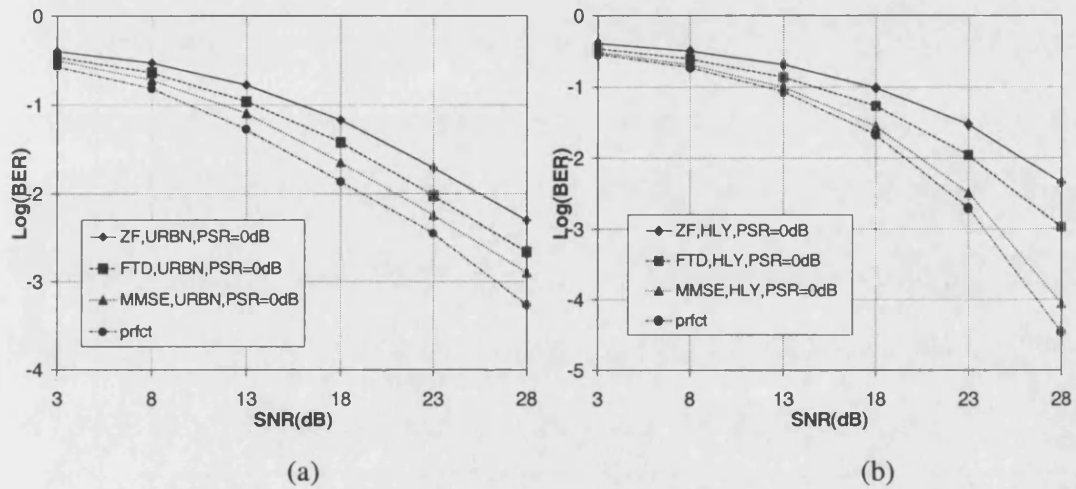
Figure 5.3.2: Comparison between ZF, MMSE and FTD, (a) Hilly Channel, (b) Urban Channel

The issue of two dimensional channel estimators has been addressed in [16][19]. A number of techniques such as using 2-Dimentsional and separable one-dimensional filters have been examined. The employment of separable filters instead of 2-D filters is a standard technique used to reduce computational complexity in multidimensional signal processing [20][22]. Using this technique the estimation is first obtained in the frequency direction using a 1-D filter and then in the time direction using a second 1-D filter. This restricts the obtainable 2-D impulse responses to those that are the outer product of the two 1-D filters.

A comparison between 2-D separable and non-separable classes of filters based on the FIR Wiener filters and low-rank approximations of the linear MMSE estimators was conducted by [16]. While the 2-D Wiener filter is considered to be the optimal solution in a Gaussian environment, the low-rank 2-D estimator is an approximation of such filter, which is derived using the theory of optimal rank reduction [22].

Through analytical calculations of the MSE and simulation results of the BER, [16] showed that the separable estimators provided the best performance for a fixed complexity. Two levels of complexities were investigated, 3 and 13 multiplications per estimated channel transfer function attenuation, and it was found that the low-rank separable Wiener filter provided the best system performance within about 1dB of that obtained using a perfect channel estimate.

5.4 Pilot tone Pattern

Pilot spacing has an optimum value, which represents a trade off between, wasting energy in unnecessary pilot symbols and sampling the fading process just often enough for good channel estimation. By viewing the channel in the time-frequency grid as a two-dimensional interpolation, fundamental limits on the minimum separation between pilots can be derived. The scattered pilot symbols can be seen as noisy samples of a two-dimensional image. In order to avoid aliasing, these samples have to be placed close enough to fulfil the sampling theorem which constraints both, the maximum tolerable excess delay of the channel and the maximum tolerable Doppler frequency. It is important to note that the effective SNR is lowered as the percentage of pilots used is increased since this corresponds to a decrease in the power transmitted in the useful data symbols.

In order to fulfil the sampling theorem [23], in the time-direction, the maximum Doppler frequency, f_D, has to be smaller than:

$$f_D \leq \frac{1}{2 \cdot N_t \cdot T_s \cdot (1 + \Delta)} \qquad\qquad 5.4.1$$

Where T_s is the OFDM symbol duration, Δ is the guard interval and N_t is the pilot spacing in the time direction. Similarly, when the interpolation is to be performed in the frequency direction, the maximum excess delay of the channel, τ_{max} has to be smaller than:

$$\tau_{max} \leq \frac{T_s}{N_f} \qquad\qquad 5.4.2$$

where N_f is the pilot spacing in the frequency direction.

Figure 5.4.1 and Figure 5.4.2 show the sensitivity of an OFDM system to the spacing between the pilot tones in both urban and hilly GSM environments using a MMSE based estimator for both 16QAM and BPSK modulation schemes. The pilots where chosen to be equally spaced in the frequency direction. Not surprisingly, the BER rises steeply when the separation between the pilots causes sampling to fall below the Nyquist rate. It can be seen

that the optimum sampling duration of pilot tones is independent of the modulation scheme used and in this case, for both the 16QAM and BPSK schemes, is about 32 samples for the urban channel and 8 samples for the hilly channel. It is also clear that when the channel is unnecessarily over-sampled, the performance of the system degrades due to the corresponding reduction in the effective SNR.

(a)   (b)
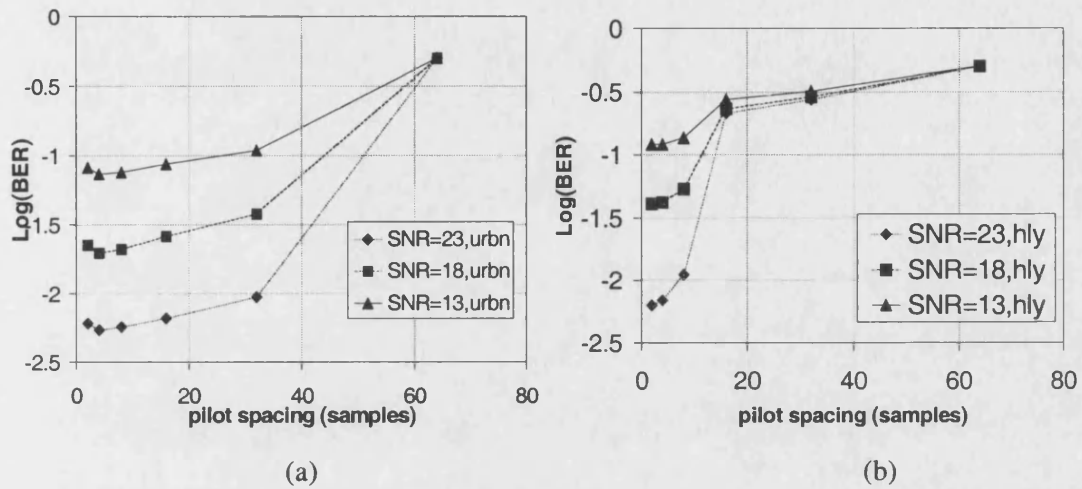
Figure 5.4.1: Impact of Pilot Tone Spacing Using 16QAM Modulation(a) Urban GSM, (b) Hilly GSM for Varuous SNR's Expressed in dB

(a)   (b)
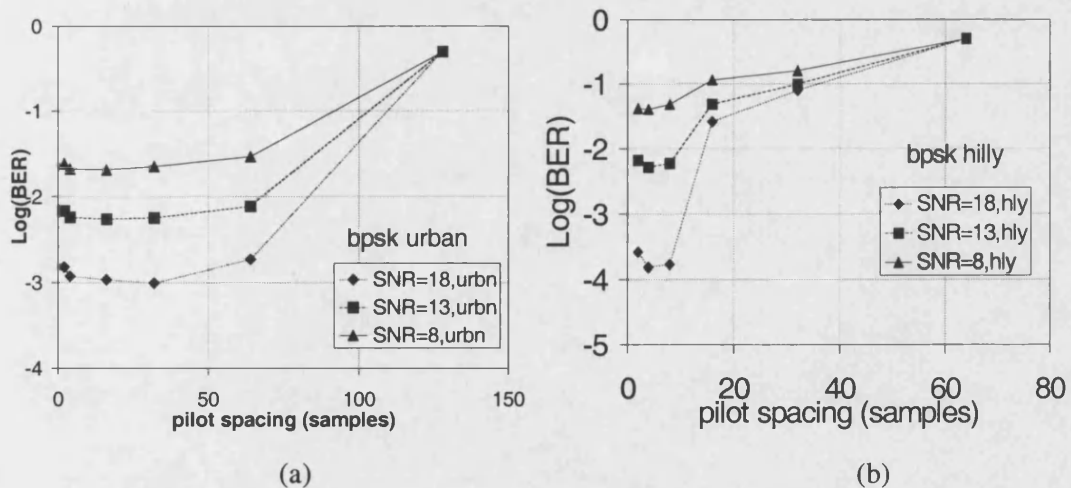
Figure 5.4.2: Impact of Pilot Tone Spacing Using BPSK Modulation(a) Urban GSM, (b) Hilly GSM for Varuous SNR's Expressed in dB

Figure 5.4.3 shows the impact of varying the amount of pilot-tones in the time direction. It can be seen that as the percentage of pilots is increased beyond a certain value, the system's performance degrades as the effective SNR decreases. Similarly, if the percentage of pilots is well below that value serious performance degradation is incurred. In this case, because the Doppler frequency considered is 100Hz, a pilot spacing of 8 seems to provide the best

compromise between performance and bandwidth. This corresponds to about 5 times the sampling frequency of equation 5.4.1. The interpolation in the time direction was done in the time domain in order to keep the amount of interpolation needed to a minimum.
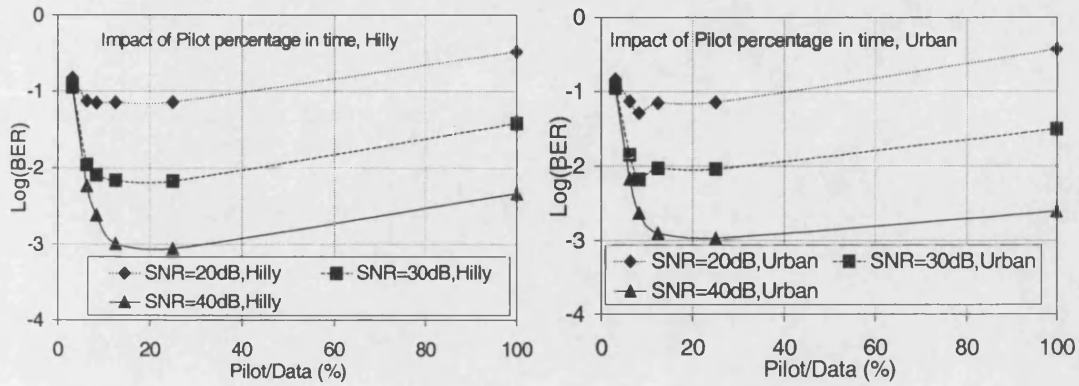
Figure 5.4.3: Impact of Spacing of Pilots in the Time Direction

As it can be seen from the above results, over-sampling the channel beyond the optimum value not only results in a reduction of the system's efficiency but also a further degradation in performance due to a corresponding reduction in the effective SNR of the system. Once the optimum pilot tone percentage is obtained, further improvement may be achieved by varying the power of the pilots with respect to that of the data signal. Figure 5.4.4 gives a measure of the impact of varying the power of the pilot tones with respect to that of data signal, PSR. From these results it can be seen that increasing the pilot tone power by 3 to 6 dB above the signal power results in a significant improvement in the system's performance. It is worth noting that decreasing the pilot tone power much below the optimum level have worse consequences than increasing the pilot power beyond the optimum value. This is because when the pilots become more sensitive to noise the entire channel estimate is affected as the noise power propagates to the interpolated values and therefore the system's performance is degraded. In order to highlight the impact of PSR, the results in Figure 5.4.4 where shown in two forms, one as a function of Log(BER) versus PSR and the other as Log(BER) versus SNR, for both the urban and hilly channels.

When these simulations were repeated for BPSK modulation, similar results were obtained giving an optimum value for PSR at around 3 to 6dB.

Urban Channel

Hilly Channel
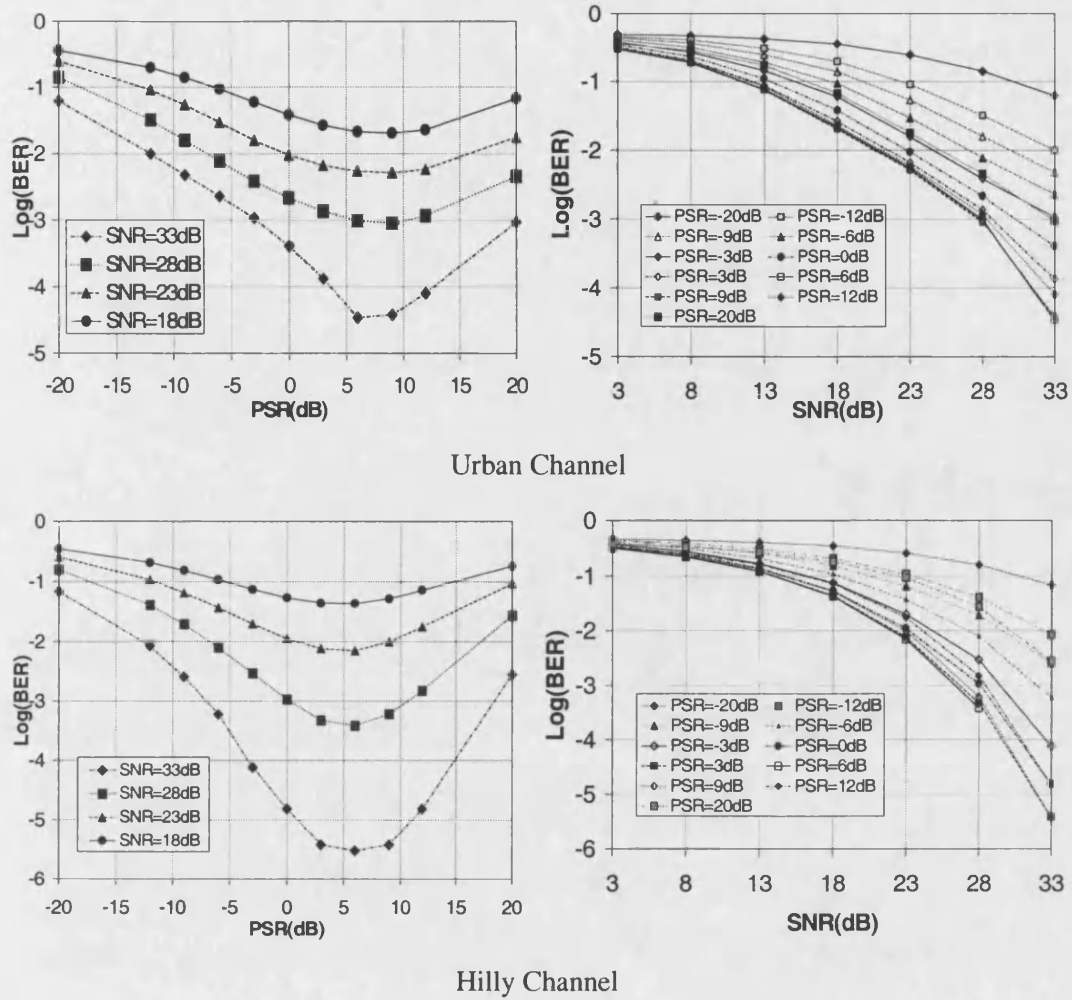
Figure 5.4.4: Impact of Increasing Pilot Tone Power Level with Respect to the Data Signal Power Using 16QAM

Urban Channel

Hilly Channel
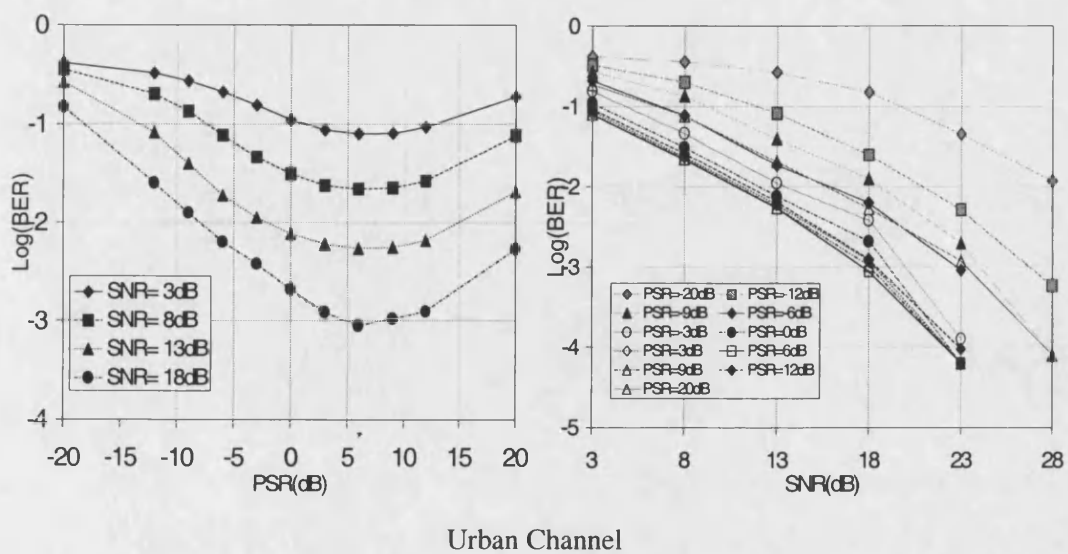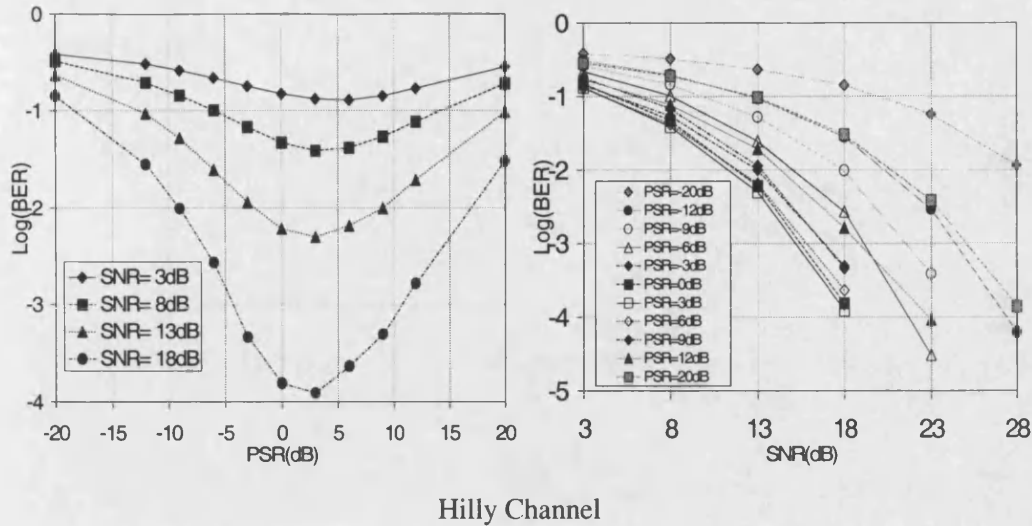
Figure 5.4.5 Impact of Increasing Pilot Tone Power Level with Respect to the Data Signal Power Using BPSK

5.5   Sensitivity to frame timing synchronisation

In OFDM systems detecting the correct beginning and end of every OFDM symbol is very important as the impact of any misjudgement may not only be on the data to be conveyed but also on the channel estimation which can in some circumstances result in a catastrophic failure of the system. Using a cyclic prefix of appropriate length at the beginning of every block, however, will significantly reduce the impact of ISI as well as help relax the timing requirements of the system. As briefly discussed in chapter four, methods for timing synchronisation have been investigated by [25] and [27]. The algorithm suggested by [25] uses the difference between the received samples spaced N samples apart to locate the beginning of a new OFDM symbol. When one of the samples belongs to the cyclic prefix and the other one to the OFDM symbol from which it is copied, the difference should be small otherwise the difference will be relatively larger. By windowing the difference with a rectangular window of the same length as the cyclic prefix, the output signal has a minimum when a new symbol starts. The impact of timing errors has been analysed by many authors [28][29][30].

Assuming that the cyclic prefix is longer than the maximum delay spread of the channel, then timing errors may occur in two forms as depicted in Figure 5.5.1. If the start position of the FFT window is within region A, then the only effect suffered by the subcarrier symbols including the pilot symbols is a change in phase that increases with the subcarrier index. If however, the start position were .within region B then the symbols will suffer from ISI as well as a phase rotation and the orthogonality of the entire system is degraded.

110
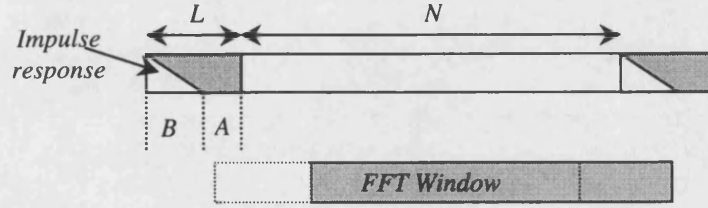
Figure 5.5.1: Principle of Frame Synchronisation

The aim of this section is to investigate the impact of timing misalignment on the scattered pilots-based channel estimation technique. A shift in the time domain introduces a phase shift in the frequency domain. It is argued in [14] that such a phase shift gives rise to a model mismatch between the correct channel model and estimated one regardless of whether its in the ISI region or outside it. In [12], however, it is stated that so long as the timing error does not spill into the ISI contaminated region, the timing error has no effect on the channel estimate and may not need to be compensated for. To establish when can timing errors have a serious impact on the channel estimate in relation to the interpolation technique used we simulated the system with and without frame misalignment.

Assuming that the frame misalignment does not exceed region A, the received signal after the FFT may be given by [12]:

$$Y_k = X_k \cdot H_k \cdot e^{-j\phi^p \cdot k} + W_k \cdot e^{-j\phi^p \cdot k},$$ 5.5.1

where $\phi^p = 2\pi(p_\varepsilon - L)/N$ and p_ε is the frame start position within region A, i.e. $p_\varepsilon < L$.

It was found that when a trigonometric interpolator similar to that of Figure 5.3.1 was used, the impact of the timing error only occurred when the misalignment included the ISI region. On the other hand, when a polynomial interpolator was used, the effect of timing error was very serious. The polynomial interpolation was investigated for both real and imaginary as well as phase and amplitude. It was found that in both cases, unless the phase shift was compensated for before interpolation, significant performance degradation would be incurred.

In order to compensate for the frame mismatch in the absence of ISI, for the pilot symbols, an estimate of the phase rotation is required. Considering only the pilot tones, the estimated channel frequency response in the presence of group delay can be given by:

$$\hat{H}p_m = Hp_m \cdot e^{-j\phi^p m} + E_m^{Hp}$$ 5.5.2

Where ϕ^p is the change in phase caused by the frame error and E_m^{Hp} is the estimation error.

Assuming that the pilot tones are scattered in the time domain, then $\hat{H}p_m$ is a sequence with

a single frequency and therefore ϕ^p can be estimated using the estimator presented in [13]:

$$\hat{\phi}^p = \sum w_m \angle (\hat{H}p_m)^* \cdot (\hat{H}p_{m+1})^*$$

where   5.5.3

$$w_m = \frac{\frac{3}{2}Np}{Np^2 - 1}\left\{ 1 - \left[\frac{m - \frac{Np}{2} + 1}{\frac{Np}{2}} \right]^2 \right\}$$

Once an estimate of the ϕ^p has been obtained, it is then used to compensate the channel

transfer function at the pilot-tones positions as given below:

$$\hat{H}p_m = \hat{H}p_m \cdot e^{j\hat{\phi}_m^p}$$ 5.5.4

The phase change on the interpolated values is then re-introduced using:

$$\hat{H}_k = \hat{H}_k \cdot e^{-jk\hat{\phi}^p / L}$$ 5.5.5
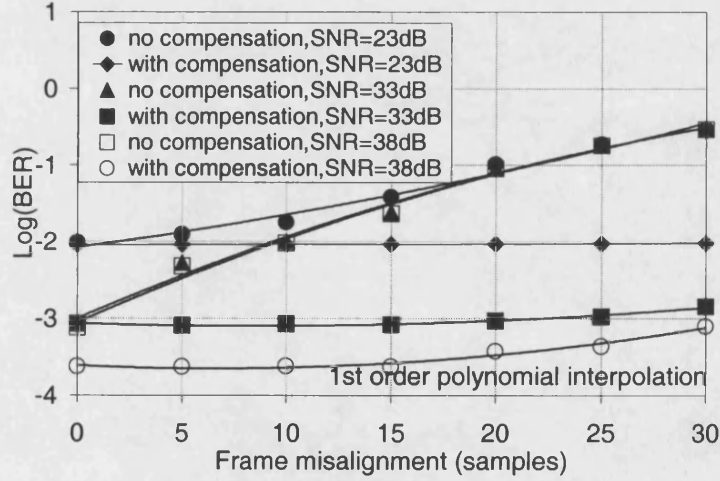
(a)
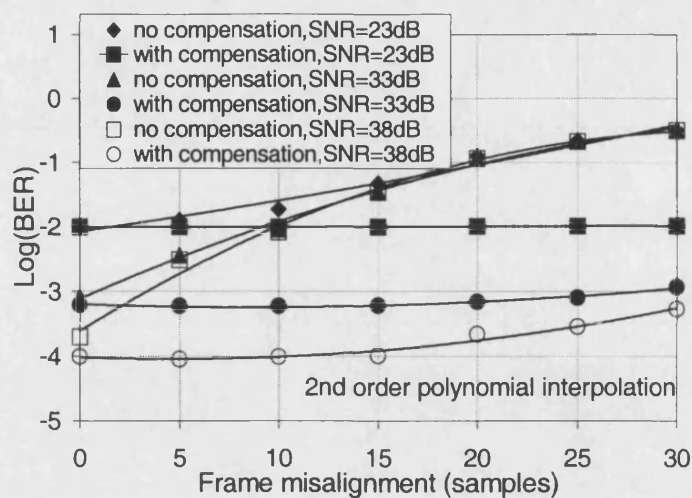
(b)
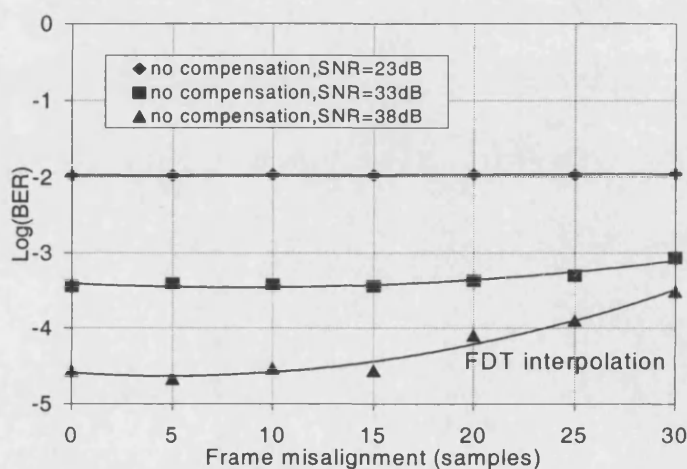
(c)

Figure 5.5.2: Impact of Group Delay Compensation (16QAM in TU-GSM) Using (a) 1st Order Polynomial Interpolation, (b) 2nd Order Polynomial Interpolation (c) FDT Interpolation

It is obvious from Figure 5.5.2 that severe performance degradation is incurred in proportion to increases in the group delay. When the group delay exceeds the cyclic prefix, ISI arises and even when the delay is compensated for, the system performance will degrade due to the ISI effect. This however is only obvious at high SNR's as can be seen form the above figures.

5.6 Orthogonal Code Channel Estimator

The scattered pilot-tones channel estimation technique is suitable for situations when the channel coherence time and bandwidth are relatively large. For example, systems such as the DVB-T [1] find such technique highly applicable, since the application uses very large FFT

sizes which corresponds to a large channel coherence bandwidth and the application is limited to static or, very slowly time varying channels. In applications that involve vehicular receivers, however, much smaller FFT sizes are used to accommodate for high velocities and keep ICI to a manageable level, making such technique less suitable due to the excessive overhead required for a good channel estimate.

In this section we propose and analyse a new channel estimation technique aimed at providing an instantaneous channel estimate without reducing the total data throughput. This is achieved by simultaneously transmitting the pilot tones and information signal using two orthogonal codes. Ideally two one-chip orthogonal codes would be used for the spreading, but because this is not possible two two-chip orthogonal codes are the second best alternative.

Figure 5.6.1 depicts a functional block diagram of the OFDM system proposed. The figure has two main branches, one for the data symbols and the other for the pilot tone symbols. In each branch, the incoming signal is spread by a unique two-chip orthogonal code where the code Cd_1Cd_2 is for the data symbols and Cp_1Cp_2 is for the pilot tones. After the spreading, in each branch, the chips representing the symbols are separated such that the first chips are kept in one block and the second chips are in a second block. The first block of chips representing the data symbols is summed with the first block of chips representing the pilot tones and similarly the second block of chips representing the data symbols are summed with the second block of chips of pilot tones. In other words, the chips representing each symbol are transmitted in series on a single sub-carrier. This is in a way analogous to a spread spectrum system in which each user is allocated one sub-carrier and a code of length two-chips. Therefore, the signal transmitted has the following format:

$$X_{j,k} = Cd_1 \cdot Xd_{j,k} + Cp_1 \cdot Xp_{j,k} \qquad 0 \leq k < N$$

$$X_{j+1,k} = Cd_2 \cdot Xd_{j,k} + Cp_2 \cdot Xp_{j,k} \qquad -\infty < j < \infty$$

$$X_{j+2,k} = Cd_1 \cdot Xd_{j+1,k} + Cp_1 \cdot Xp_{j+1,k} \qquad\qquad 5.6.1$$

$$X_{j+3,k} = Cd_2 \cdot Xd_{j+1,k} + Cp_2 \cdot Xp_{j+1,k}$$

$$\vdots$$

where Xd and Xp represent the data and pilots frames respectively.

At the receiver, the inverse process is implemented. Since the pairs of chips representing the parallel symbols are transmitted serially, the receiver requires having two blocks of sub-carriers before recovering the data and pilot symbols. Thus, a buffer is used to store pairs of blocks of chips representing the transmitted data symbols. The received signal is then passed

through two branches, one is for extracting the data by correlating the received signal with a replica of the data spreading code and the other is for extracting the pilot tones by correlating the data with a replica of the pilot tone spreading code. Assuming that there is no ISI present and that the channel is time-invariant over the duration of two OFDM blocks, then the channel transfer function may be obtained by dividing the received pilot tones with the originally transmitted pilot tone sequence. Further refinement of the channel estimate may be obtained by using one of the estimation techniques described above.
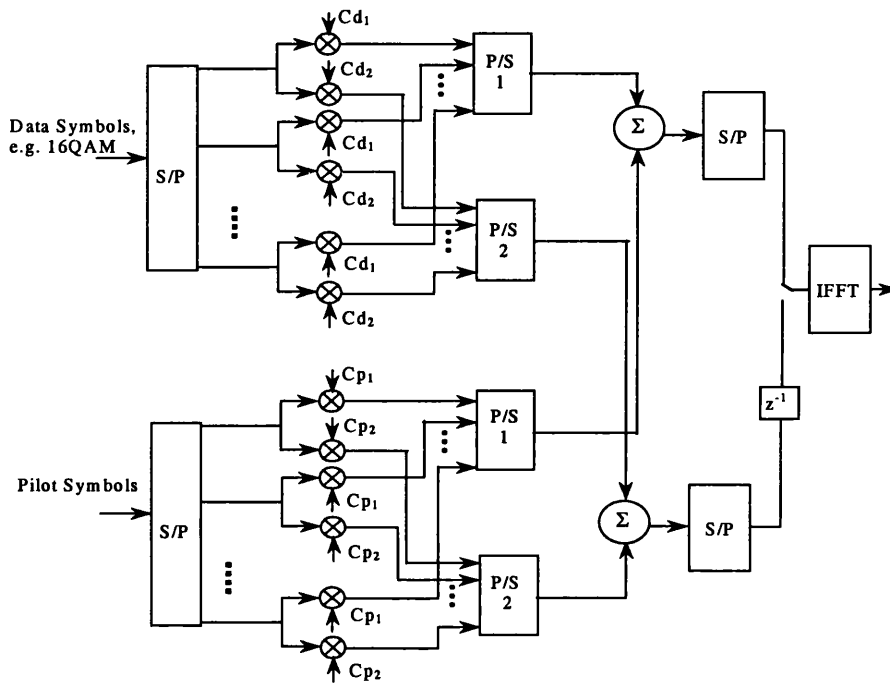
Figure 5.6.1: Schematic of the OFDM Modulator
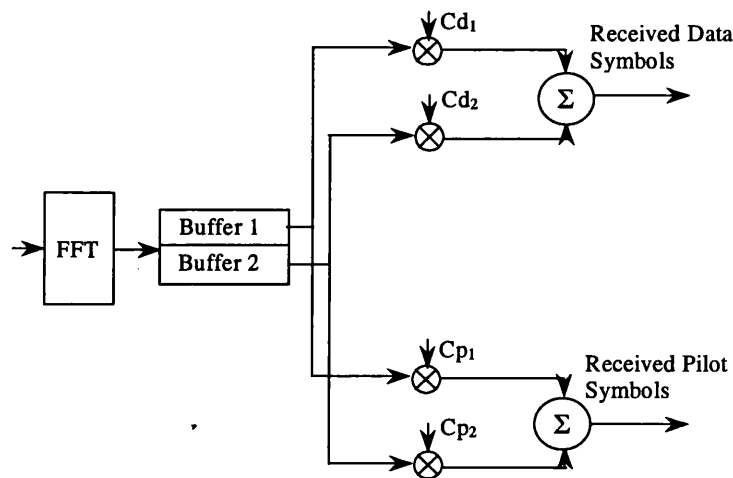
Figure 5.6.2: Schematic of the OFDM Receiver

5.6.1 Analysis of the Received Signal

In this analysis it is assumed that the maximum channel dispersion does not exceed the OFDM block duration.

Following the analysis in chapter 3, assuming that ISI only occures between pairs of consecutive OFDM symbols, the received time domain samples of the combined signal can be given by:

$$
r_{j,i} = \underbrace{\sum_{k=0}^{i} x_{j,k} \cdot h_{j,i-k}}_{\text{required signal}} + \underbrace{\sum_{k=i+1}^{N-1} x_{j-1,k} \cdot h_{j,N+i-k}}_{\text{ISI}} + n_j ,
\qquad 5.6.1.1
$$

Since the data symbols are now delivered over two OFDM blocks instead of one, it will be assumed that the data is transmitted in two-block frames. Each OFDM frame is therefore $2N$ samples/chips in duration.

$$
X_{f,j,k} = \begin{cases} Cd_1 \cdot Xd_{f,j,k} + Cp_1 \cdot Xp_{f,j,k} \\ Cd_2 \cdot Xd_{f,j,k} + Cp_2 \cdot Xp_{f,j,k} \\ \qquad\qquad\qquad 0 \le k < N \end{cases} ,
\qquad 5.6.1.2
$$

where f, j and k are the frame, time and frequency indices, respectively. By combining equation 5.6.1.1 and 5.6.1.2, the received time domain OFDM frame can therefor be given by the two equations below:

$$
r_{f,j} = \underbrace{\overset{m1}{h_j} \cdot CDFT^{-1} \cdot \left(Cd_1 \cdot Xd_{f,j} + Cp_1 \cdot Xp_{f,j} \right)}_{\text{required data + innerblock ISI}} +
$$

$$
\underbrace{\overset{m2}{h_j} \cdot CDFT^{-1} \cdot \left(Cd_2 \cdot Xd_{f-1,j-1} + Cp_2 \cdot Xp_{f-1,j-1} \right)}_{\text{interframe ISI}} + n_j
\qquad , \qquad 5.6.1.3
$$

$$
r_{f,j+1} = \underbrace{\overset{m1}{h_{j+1}} \cdot CDFT^{-1} \cdot \left(Cd_2 \cdot Xd_{f,j} + Cp_2 \cdot Xp_{f,j} \right)}_{\text{required data + interblock ISI}} +
$$

$$
\underbrace{\overset{m2}{h_{j+1}} \cdot CDFT^{-1} \cdot \left(Cd_1 \cdot Xd_{f,j} + Cp_1 \cdot Xp_{f,j} \right)}_{\text{interblock ISI}} + n_{j+1}
$$

where

$$
\overset{m1}{\mathbf{h}} = \begin{bmatrix} h_0 & 0 & 0 & \cdots \\ h_1 & h_0 & 0 & \cdots \\ \vdots & \vdots & \ddots & \ddots \\ h_{N-1} & h_{N-2} & \cdots & h_0 \end{bmatrix}
\qquad
\overset{m2}{\mathbf{h}} = \begin{bmatrix} 0 & h_{N-1} & h_{N-2} & \cdots & h_1 \\ 0 & 0 & h_{N-1} & \cdots & h_2 \\ \vdots & \vdots & \vdots & \ddots & \vdots \\ 0 & 0 & 0 & \cdots & 0 \end{bmatrix}
$$

$$\mathbf{CDFT^{-1}} = \begin{bmatrix} D_N^{0\cdot0} & D_N^{1\cdot0} & D_N^{2\cdot0} & \cdots & D_N^{(N-1)\cdot0} \\ D_N^{0\cdot1} & D_N^{1\cdot1} & D_N^{2\cdot1} & \cdots & D_N^{(N-1)\cdot1} \\ D_N^{0\cdot2} & D_N^{1\cdot2} & D_N^{2\cdot2} & \cdots & D_N^{(N-1)\cdot2} \\ \vdots & \vdots & \vdots & \vdots & \vdots \\ D_N^{0\cdot(N-1)} & D_N^{1\cdot(N-1)} & D_N^{2\cdot(N-1)} & \cdots & D_N^{(N-1)\cdot(N-1)} \end{bmatrix}$$

$$D_N = \frac{1}{\sqrt{N}} \cdot e^{2j\pi/N}$$

and j and f are the block and frame index respectively.

The presence of interblock and interframe ISI terms result in the loss of orthogonality between the consecutive OFDM symbols, frames and consequently the spreading codes. At the receiver, the frequency domain symbols with each frame can be given by:

$$R_{f,j} = \underbrace{(CDFT \cdot \overset{m1}{h}_j \cdot CDFT^{-1}) \cdot Cd_1 \cdot Xd_{f,j} + (CDFT \cdot \overset{m1}{h}_j \cdot CDFT^{-1}) \cdot Cp_1 \cdot Xp_{f,j}}_{\text{required data+innerblock ISI}} +$$

$$\underbrace{(CDFT \cdot \overset{m2}{h}_j \cdot CDFT^{-1}) \cdot Cp_1 \cdot Xd_{f-1,j-1} + (CDFT \cdot \overset{m2}{h}_j \cdot CDFT^{-1}) \cdot Cp_2 \cdot Xp_{f-1,j-1}}_{\text{interframe ISI}} +$$

$$CDFT \cdot n_j$$

$$R_{j+1}^f = \underbrace{(CDFT \cdot \overset{m1}{h}_{j+1} \cdot CDFT^{-1}) \cdot Cd_2 \cdot Xd_{f,j} + (CDFT \cdot \overset{m1}{h}_{j+1} \cdot CDFT^{-1}) \cdot Cp_2 \cdot Xp_{f,j}}_{\text{required data+innerblock ISI}} +$$

$$\underbrace{(CDFT \cdot \overset{m2}{h}_j \cdot CDFT^{-1}) \cdot Cd_1 \cdot Xd_{f,j} + (CDFT \cdot \overset{m2}{h}_{j+1} \cdot CDFT^{-1}) \cdot Cd_1 \cdot Xp_{f,j}}_{\text{interblock ISI}} +$$

$$CDFT \cdot n_{j+1}$$

Rewriting the above:

$$R_{f,j} = M1 \cdot (Cd_1 \cdot Xd_{f,j} + Cp_1 \cdot Xp_{f,j}) +$$
$$M2 \cdot (Cd_2 \cdot Xd_{f-1,j-1} + Cp_2 \cdot Xp_{f-1,j-1}) + CDFT \cdot n_j$$

$$\qquad\qquad\qquad 5.6.1.4$$

$$R_{f,j+1} = M1 \cdot (Cd_2 \cdot Xd_{f,j} + Cp_2 \cdot Xp_{f,j}) +$$
$$M2 \cdot (Cd_1 \cdot Xd_{f,j} + Cp_1 \cdot Xp_{f,j}) + CDFT \cdot n_{j+1}$$

where

$$M1 = CDFT \cdot \overset{m1}{h}_j \cdot CDFT^{-1},$$
$$M2 = CDFT \cdot \overset{m2}{h}_j \cdot CDFT^{-1}$$

Expanding equation 5.6.1.4 and rearranging produces:

$$R_{f,j} = \mathbf{M1} \cdot Cd_1 \cdot Xd_{f,j} + \mathbf{M2} \cdot Cd_2 \cdot Xd_{f-1,j-1} + \mathbf{M1} \cdot Cp_1 \cdot Xp_{f,j} + \mathbf{M2} \cdot Cp_2 \cdot Xp_{f-1,j}$$

$$R_{f,j+1} = \mathbf{M1} \cdot Cd_2 \cdot Xd_{f,j} + \mathbf{M2} \cdot Cd_1 \cdot Xd_{f,j} + \mathbf{M1} \cdot Cp_2 \cdot Xp_{f,j} + \mathbf{M2} \cdot Cp_1 \cdot Xp_{f,j}$$

At the receiver, a correlator is used to separate the data symbols from the pilot symbols by utilising the orthogonality relationship between the two codes. Assuming that a fixed pilot tone sequence was used, ignoring the additive noise term, the data and pilot symbols at the output of the correlator are given by:

$$\hat{X}d_{j,k} = \mathbf{M1} \cdot Xd_{f,j,k} \cdot (Cd_1^{\,2} + Cd_2^{\,2}) + \mathbf{M2} \cdot Cd_1 \cdot Cd_2 (Xd_{f-1,j,k} + Xd_{f,j,k}) +$$
$$\mathbf{M1} \cdot Xp_{f,j,k} \cdot (Cd_1 \cdot Cp_1 + Cd_2 \cdot Cp_2) + \mathbf{M2} \cdot Xp_{f,j,k} \cdot (Cd_1 \cdot Cp_2 + Cd_2 \cdot Cp_1)$$
$$\hat{X}p_{j} = \mathbf{M1} \cdot Xp_{f,j,k} \cdot (Cp_1^{\,2} + Cp_2^{\,2}) + \mathbf{M2} \cdot Xp_{f,j,k} \cdot (Cp_1 \cdot Cp_2 + Cp_1 \cdot Cp_2) +$$
$$\mathbf{M1} \cdot Xd_{f,j,k} \cdot (Cd_1 \cdot Cp1 + Cd_2 \cdot Cp2) + \mathbf{M2} \cdot (Cp_1 \cdot Cd_2 \cdot Xd_{f-1,j,k} + Cd_1 \cdot Cp_2 \cdot Xd_{f,j,k})$$

$$5.6.1.5$$

5.6.2 Simulation Results

Since in this channel estimation technique, the SNR is effectively halved due to the insertion of 100% pilots, the aim of the first simulation test was to find out the best trade off between PSR and BER performance of the system. The effective SNR used here includes the signal power due to the data symbols, pilots, cyclic prefix and processing gain of the spreading code. Figure 5.6.2.1 shows the relationship between PSR, SNR and BER for the system parameters used here for both the urban and hilly channels. It can be seen from these figures that for both, the urban and hilly channels, the best system BER performance is obtained when PSR is kept at around –8dB. In contrary to the scattered pilot tone method, a worsened BER performance is incurred when the power of the pilots is increased beyond the power of the actual signal. This is because no interpolation is involved with this technique, therefore noise on the individual pilots will only affect the subcarrier at that position, unlike in the case of the scattered pilots where the impact of the noise is propagated to the entire OFDM block through the interpolation process.
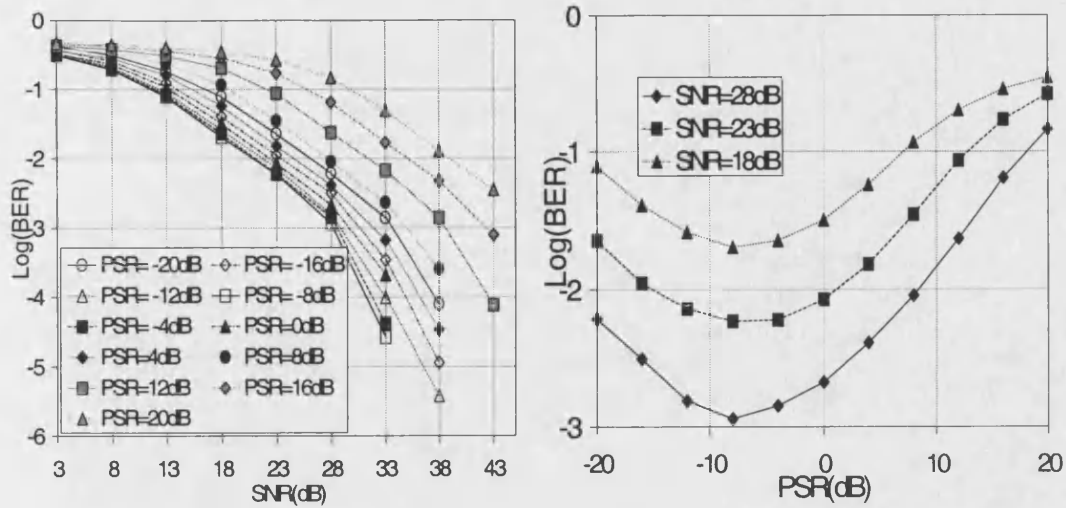
Urban Channel
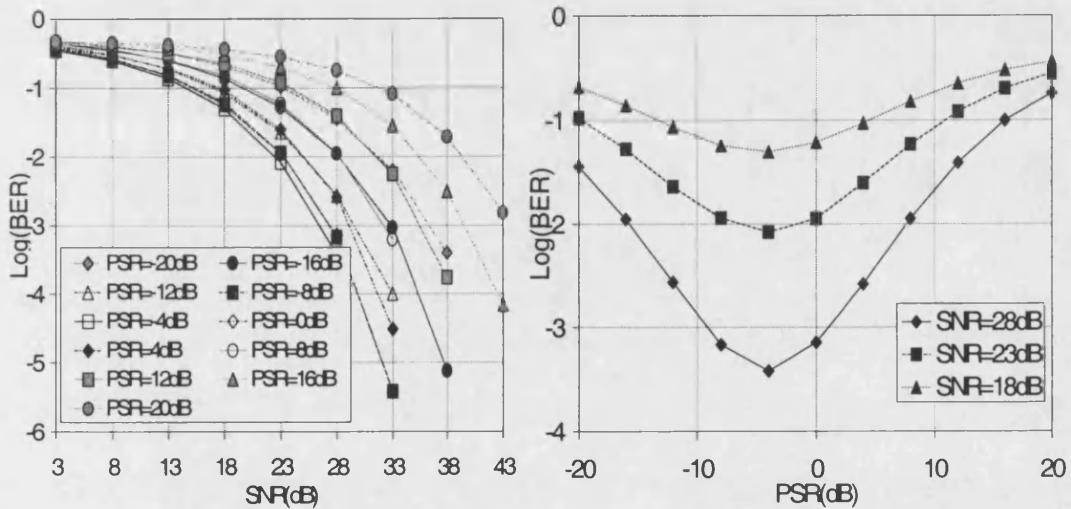
Hilly channel

Figure 5.6.2.1: Impact of Varying PSR for Urban and Hilly Channels

The aim of the rest of the simulations is to compare the performance of this technique to that of the scattered pilots and feedback techniques under a variety of different Doppler conditions and different number of subcarriers. The type of channel used here is the hilly 6-tap GSM model. Throughout the simulation, the bit rate was fixed at 20Mbps regardless of the amount of pilot tones inserted. In the case of the scattered pilot tone method, the pilots were spaced uniformly in the frequency direction.

Figure 5.6.2.2 and Figure 5.6.2.3 show a comparison between the above three channel estimation techniques in a fixed/static channel when the number of subcarriers is kept at 256 and 1024, respectively. It can be seen from Figure 5.6.2.2 that the scattered-pilots method results in the worst performance even when the amount of pilot tones used was increased to

50% of the total transmitted data. This is because of the rapid variations in the channel's frequency response that even when the percentage of pilot tones was increased to 50% no improvement was obtained. When the number of subcarriers was increased to 1024, however, the performance of the scattered pilot tone method has improved significantly. These two figures suggest that the feedback channel estimation technique is the most robust in time invariant channels.
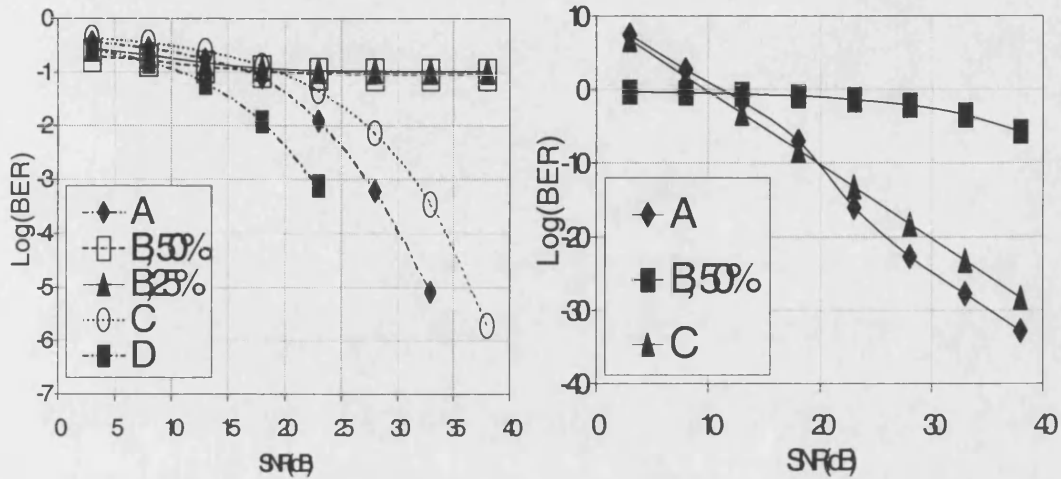
Figure 5.6.2.2: Comparison Between Feedback (A), Scattered Pilot (B) and Orthogonal Code (C) Relative to Perfect Channel Estimate (D), Channel Type is Static Hilly GSM, Block Length is 256
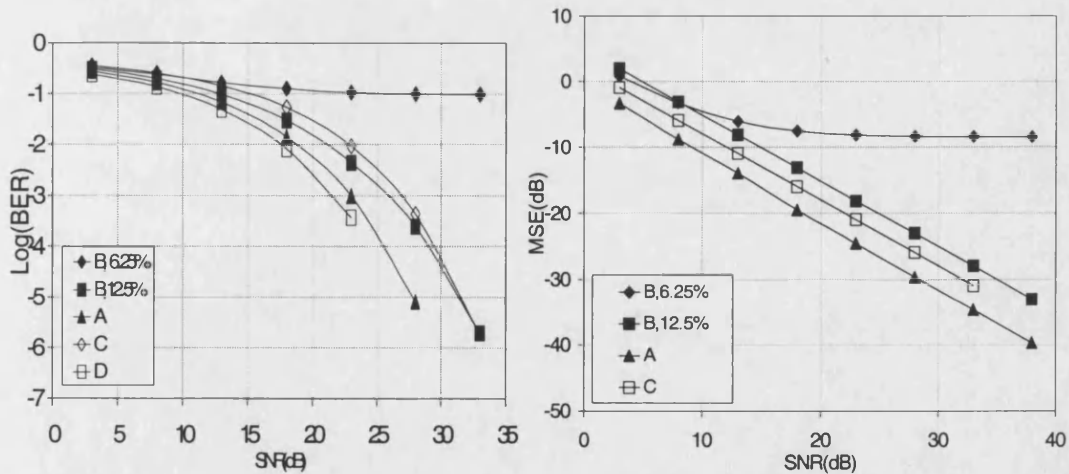
Figure 5.6.2.3: Comparison Between Feedback (A), Scattered Pilot (B) and Orthogonal Code (C) Relative to Perfect Channel Estimate (D), Channel Type is Static Hilly GSM, Block Length is 1024

In order to test the stability of this new channel estimation technique, the above tests were repeated under time variant conditions. Figure 5.6.2.4 to Figure 5.6.2.7 show a comparison between the performance of this technique and that of the pilot assisted and feedback

channel estimation techniques for a Doppler frequency of 50Hz and 100 Hz and FFT length of 256 and 1024 points. As in the static channel case, the pilot assisted technique has the worst performance when the number of subcarriers is 256 due to the rapid changes in the frequency response of the channel. It can also be seen that the feedback technique is more sensitive to the time variation of the channel as can be seen from Figure 5.6.2.4 and Figure 5.6.2.5.
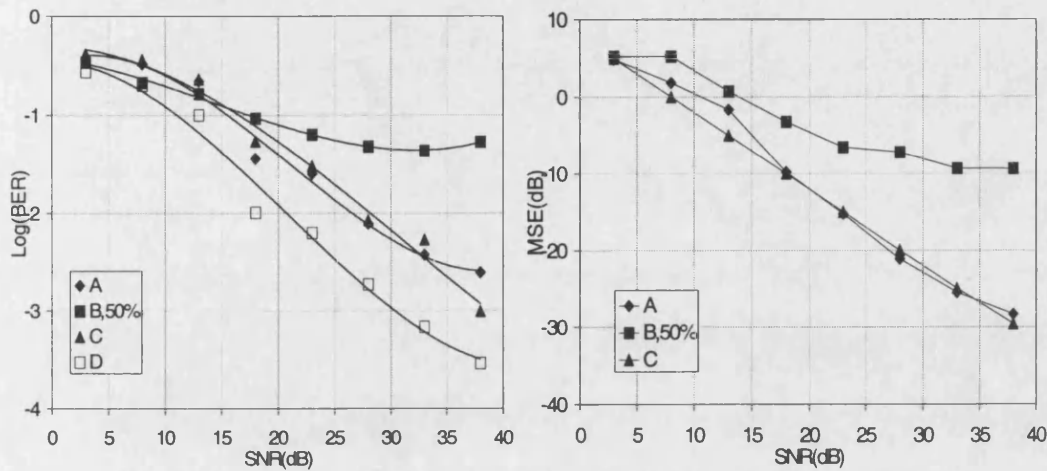
Figure 5.6.2.4: Comparison Between Feedback (A), Scattered Pilot (B) and Orthogonal Code (C) Relative to Perfect Channel Estimate (D), Channel Type is Dynamic Hilly GSM, Block Length is 256, Doppler Frequency is 50Hz
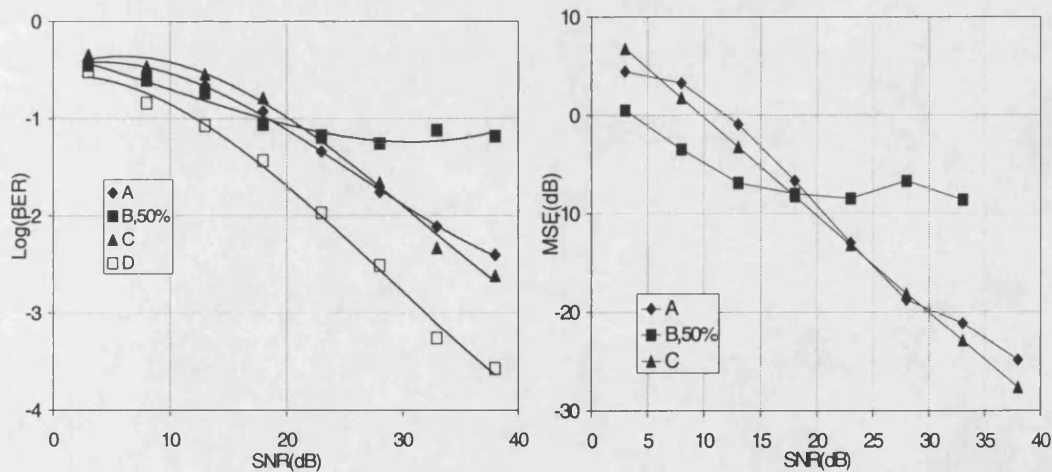
Figure 5.6.2.5: Comparison Between Feedback (A), Scattered Pilot (B) and Orthogonal Code (C) Relative to Perfect Channel Estimate (D), Channel Type is Dynamic Hilly GSM, Block Length is 256, Doppler Frequency is 100Hz

When the number of subcarriers has been increased to 1024, the performance of the pilot assisted technique improved significantly. On the other hand, both the new technique and the feedback technique have suffered from the time delay imposed by the block length and

therefore degraded in performance. Having said that, it can be seen that the feedback technique is more sensitive to time variations than the new channel estimation technique.
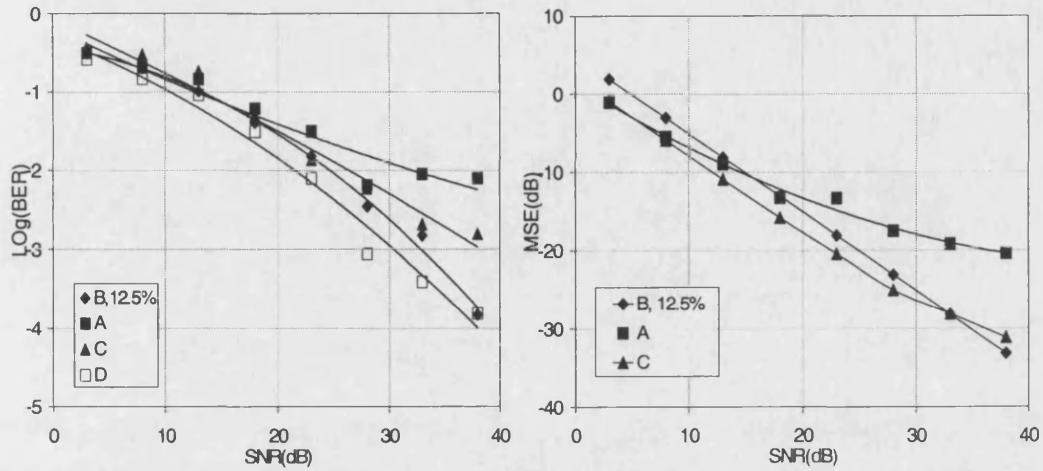
Figure 5.6.2.6: Comparison Between Feedback (A), Scattered Pilot (B) and Orthogonal Code (C) Relative to Perfect Channel Estimate (D), Channel Type is Dynamic Hilly GSM, Block Length is 1024, Doppler Frequency is 50Hz
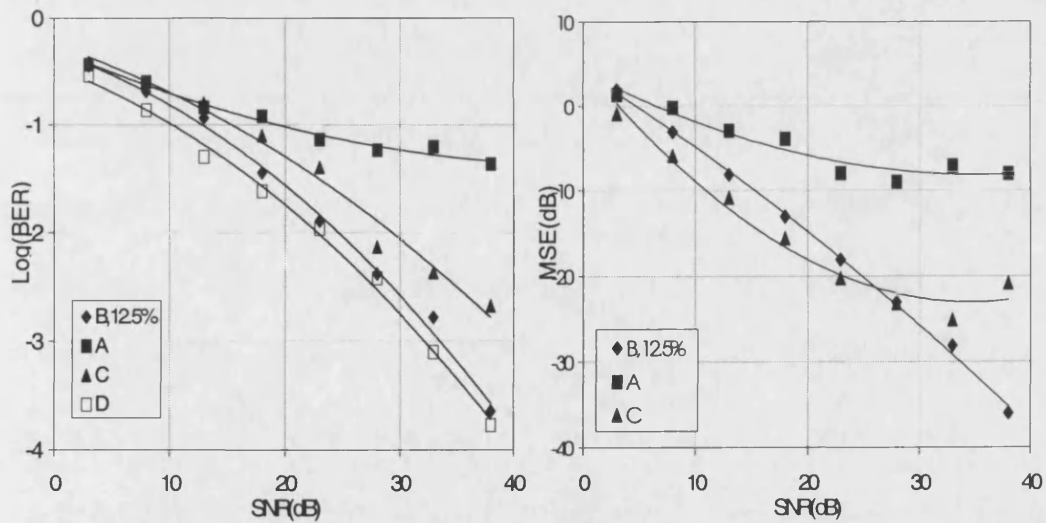
Figure 5.6.2.7: Comparison Between Feedback (A), Scattered Pilot (B) and Orthogonal Code (C) Relative to Perfect Channel Estimate (D), Channel Type is Dynamic Hilly GSM, Block Length is 1024, Doppler Frequency is 100Hz

The above results suggest that under completely unknown and unpredictable channel conditions, the new channel estimation technique may be the safest choice. If however, the channel is known to be very slowly time variant, such as the fixed wireless channel, then the feedback technique is the best choice. Alternatively, if the channel is highly time variant and

the maximum delay spread of the channel is known, then by careful selection of the FFT length, pilot tone separation and PSR, the pilot assisted technique may be customised to provide the best overall performance.

5.7 Conclusion

In this chapter, various key issues of the pilot assisted channel estimation technique were investigated. This included the impact of pilot tone spacing, power level and sensitivity to timing errors. It was shown that by increasing the pilot tone power by about 3 to 6 dB above that of the signal, a significant performance improvement is achieved. On the contrary, increasing the percentage of pilot tones beyond a certain level degrades the systems capacity as well as performance due to unnecessary transmission of redundant symbols, which in turn reduces the effective SNR of the system. It was also shown that certain types of channel interpolators are much more sensitive to timing errors than others. Using the FTD based channel interpolator, eliminates the need to phase compensate the pilots prior to interpolation, consequently reducing the risk of miss-estimating the phase shift introduced by the frame misalignment.

The scattered pilot-tones channel estimation technique is suitable for situations when the channel coherence time and bandwidth are relatively large. For example, systems such as the DVB-T find such technique very applicable since the application uses very large FFT sizes which corresponds to a large channel coherence bandwidth and the application is limited to static or, very slowly time varying channels. In applications which involve vehicular receivers that require using much smaller FFT sizes to accommodate for high velocities, such technique may not be the most suitable due to the excessive overhead required to ensure that the channel is oversampled adequately. In view of this a new channel estimation technique aimed at providing an instantaneous channel estimate without reducing the total data throughput was investigated. This is based on the simultaneous transmission of the pilot tones and information signal using two two-chip orthogonal codes. It was shown that under unknown channel conditions, the new channel estimation technique is the safest choice. If however, the channel is known to be very slowly time variant, such as the fixed wireless channel, then the feedback technique will result in the best overall performance provided that consecutive OFDM blocks are.perfectly synchronised. Finally, if the channel is highly time variant and the coherence bandwidth of the channel is relatively large, then by careful selection of the FFT length, pilot tone percentage and PSR, the pilot assisted technique may be customised to provide the best overall performance.

5.8 References

[1] P. Dambacher, *"Digital Broadcasting"* IEE Press, English addition, 1996.

[2] V. Engels and H. Rohling, "Multilevel Differential Modulation Technique (64-DAPSK) for Multicarrier Transmission Systems" Eur. Trans. on Rel. Technol. 6(6) pp. 633-640, Nov. 1995.

[3] C. Reiners and H. Rohling, "Multicarrier Transmission Technique in Cellular Mobile Communication Systems", Proceedings of the IEEE Vehic. Technol. Conf., pp. 1645-1649, Stockholm, June 1994.

[4] Digital Broadcasting Systems for Television, Sound and Data Services. European Telecommunications Standard, prETS 300 744 (Draft, version 0.0.3), Apr. 1996.

[5] T. de Couasnon, R. Monnier and J. B. Rault, *"OFDM for Digital TV Broadcasting"*, Signal Proc. 39(1-2), pp. 1-32, Sept. 1994.

[6] M. L. Moher and J. H. Lodge, "TCMP- A Modulation and Coding Strategy for Ricean Fading Channels", IEEE Journal of Selected Areas in Communications, 7(9), pp. 1347-1355, Dec. 1989.

[7] J. K. Cavers, *"An Analysis of Pilot Symbol Assisted Modulation for Rayleigh Fading Channels "*, IEEE Transactions on Vehicular Technology, 40(4), pp. 686-693, Nov. 1991.

[8] J. J. van de Beek, O. Edfors, M. Sandell, S. K. Wilson and P. O Borjesson, *" On Channel estimation in OFDM Systems"* Proceedings of the IEEE 45th VTC, Chicago, IL, USA, pp. 815-819, July 1995.

[9] O. Edfors, M. Sandell, J. J. van de Beek, S. K. Wilson and P. O Borjesson, *"OFDM Channel Estimation By Singular Value Decomposition"* Proceedings of the IEEE 46th VCT, Atlanta, GA, USA, pp. 923-927, Apr. 1996.

[10] E. Al-Susa and R.F. Ormondroyd *"A Predictor - Based Decision Feedback Channel Estimation Method for COFDM with High Resilience to Rapid Time Variations "*, Proceedings of the VTC'99 Fall, the Netherlands, Sept. 1999.

[11] V. Mignone and A. Morello, *"CD3-OFDM: A novel demodulation scheme for fixed and mobile receivers"*, ", IEEE Transactions on Communications, Vol. 44, No 9, pp. 1144-1151, Sept. 1996.

[12] M. Speth, F. Classen and H. Meyr, *"Frame Synchronisation of OFDM Systems in Frequency Selective Fading Channels"*, Proceedings of the IEEE 47th VTC, Phoenix USA, pp. 1807-1811, May 1997.

[13] S. Kay, *" A Fast and Accurate Single Frequency Estimator"*, IEEE Transactions on Acoustics, Speech and Signal Processing, Vol. 37, no. 12, pp. 1987-1990, Dec. 1989.

[14] M. H. Hsieh and C. H. Wei, *"Channel Estimation For OFDM Systems Based on Combed-Type Pilot Arrangememnts in Frequency Selective Fading Channels"*, IEEE Transactions on Consumer Electronics, Vol. 44, pp. 217-225, Feb. 1998.

[15] R.F. Ormondroyd and E. Al-Susa, "*A High Efficiency Channel Estimation and Equalisation Strategy for a broadband COFDM System*", ISSSE'98, pp.471-475, 1998.

[16] M Sandell, "*Multicarrier Modulation*", Ph.D. Thesis, 1996, Lulea University of Technology.

[17] Y. Li, L. J. Cimini and N. R. Sollenberger, "*Robust Channel estimation for OFDM Systems with Rapid Dispersive Fading Channels* ", IEEE Transactions on Communications, Vol. 46, No. 7, pp. 902-915, July 1998.

[18] Y. Wu and W.Y. Zou, "*Performance Simulation of COFDM for TV Broadcast Application*", Conference Proceedings of the SMPTE Technical Conference, pp.258-261, Oct. 1994.

[19] P. Hoher, "*TCM on Frequency-selective Land Mobile Fading Channels*", Proceedings of Tirrenia International Workshop on Digital Communications, Tirrenia, Italy, Sept. 1991.

[20] D. E. Dudgeon and R. M. Mersereau. "*Multidimentional Digital Signal Processing*", Prentice-Hall Englewood Cliffs, NJ, 1984.

[21] F. Tufvesson and T. Maseng, "*Pilot Assisted Channel Estimation for OFDM in Mobile Cellular Systems* ", Proceedings of the IEEE47th Vehicular Technology Conference, Phoenix, USA, pp. 1639-1643, May 1997.

[22] L. L. Scharf, "*Statistical Signal Processing: Detection, Estimation and Time Series Analysis* ", Addison-Wesley, 1991.

[23] A. Oppenheim and R. Schafer, "*Discrete-Time Signal Processing*", Prentice-Hall, 1989.

[24] John G. Proakis, "*Digital Communications*", third edition, 1995.

[25] P. J. Tourtier, R. Monnier and P. Lopez, "*Multicarrier Modem for Digital HDTV Terrestrial Broadcasting*", Signal Processing: Image Communications, vol. 5, part (5-6), pp. 379-403, Dec. 1993.

[26] W. H. Press, S. A. Teukolsky, W. T. Vetterling and B. P. Flannery, "*Numerical recipes in C*", 2nd edition, Cambridge, 1993.

[27] W. D. Warner and C. Leung, "OFDM/FM Frame Synchronisation for Mobile Radio Data Communications", IEEE Transactions on Vehicular Technology, Vol, 42, part 3, pp. 302-313, 1993.

[28] T. Pollet and M. Moeneclay, "Synchronizability of OFDM Signals" In Proceedings of GlobCom'95, Vol. 3, pp. 2054-2058, Singapore, Nov. 1995.

[29] H. Nogami and T. Nagashima, "*A Frequency and Timing Period Acquisition Techniques for OFDM Systems*", IEEE Proceedings of VTC'95, pp. 1010-1015, 1995.

[30] L. Wei and C. Schlegel, " *Synchronisation Requirements of Multiuser OFDM on Satellite Mobile and Two-path Rayleigh Fading Channels* ", IEEE Transactions on Communications, Vol. 43 (2/3/4), pp. 887-895, 1995.

[31] J-J Beek, M. Sandell, M. Isaksson and P. O. Borjesson, "*Low-Complexity Frame Synchronisation in OFDM Systems*", Proceedings of the IEEE International Conference on Personal and Wireless Communications, pp. 982-986, Nov. 1995.

Chapter Six

Feedback Equalisation for OFDM Systems

6 Chapter Six

6.1 Introduction

To operate digital terrestrial television broadcasting, high data rates need to be guaranteed with high quality of service. In order to achieve that, multi-level QAM or PSK modulation is normally employed [1]. The important challenge for these systems is the choice of an appropriate channel estimation technique that combines the best trade-off between performance and bandwidth efficiency.

In order to avoid the need for channel estimation and continuous tracking, OFDM has to use non-coherent modulation techniques, which suffers a significant loss in SNR compared to the coherent ones. For example, differential phase shift keying (DPSK) has a 3dB SNR loss compared with coherent phase shift keying (PSK).

The use of scattered pilot tones has been investigated by a number of researchers as a potential technique for channel estimation [2]-[4]. In this technique, pilot tones (known symbols) are periodically inserted between the data symbols for the purpose of providing an estimate of the channel response at the frequency corresponding to the position of that tone. At the receiver, these pilots are recovered and used in establishing the full channel response using interpolation. In order to fully utilise this technique, the use of two-dimensional channel estimation methods may have to be used as this will allow the technique to be more efficiently implemented with respect to bandwidth and performance.

An alternative to using scattered pilot tones is the use of decision directed feedback based techniques [6][8][16][17][19]. As such techniques rely mainly on the data itself in tracking the channel variations, the channel estimate provided is usually a one-block-delayed-noisy version of the actual channel transfer function. Initially, an estimate of the channel frequency response is obtained using a training signal consisting of either a known modulated sequence on each of the subcarriers or unmodulated subcarriers to start off the feedback process. Assuming that the channel time variations are slow compared to the data transmission bandwidth, it is possible to track the time variations by using decisions at the output of the detector or the decoder in a decision directed fashion.

In this chapter, the use of decision directed adaptive feedback based channel estimation and tracking technique that provide a very high bandwidth efficiency rate is investigated. The

structure of the system that uses such technique is first presented and described. Then, a mathematical model of the mean square error (*MSE*) of the produced channel estimate and the bit error rate (*BER*) performance for QPSK is derived. The performance of the system is then more comprehensively analysed using computer simulations. This includes the effect of increasing the time variation of the channel through increasing the Doppler frequency or increasing the block duration. An estimate of the best compromise between the bandwidth efficiency and training sequence channel estimation is also given. It will be shown that filtering the channel estimate is essential and hence some sub-optimal filtering techniques will be analysed in terms of the mean square error. The analysis is based on a transmission rate of 25Mbps (which is in the range of DVB) in an AWGN and time varying frequency selective fading channel using QPSK and DQPSK. Finally the impact of using a time domain based predictor on the estimators performance will be investigated.

6.2 System model and description

Three feedback channel estimation modes are discussed in this chapter. The first is the standard feedback mode, which is referred to here as the *uncoded* mode. In this mode the recovered baseband modulated signal is directly fed back to the channel estimator for use in channel tracking. The second channel estimation mode uses the binary error corrected bits for channel tracking. This mode, which is referred to as the *coded* channel estimation mode uses the error correction capability of the decoder in order to establish a more reliable estimate of the transmitted baseband signal. Finally, the dual channel estimator mode uses both the uncoded and coded modes for tracking the channel variations. It selects the most appropriate mode depending on the state of the decoder and the available signal to noise ratio.

For clarity, the uncoded channel estimator mode is described first. A description of the other two modes then follows. A schematic block diagram of this type of estimator is depicted in Figure 6.2.1 below.
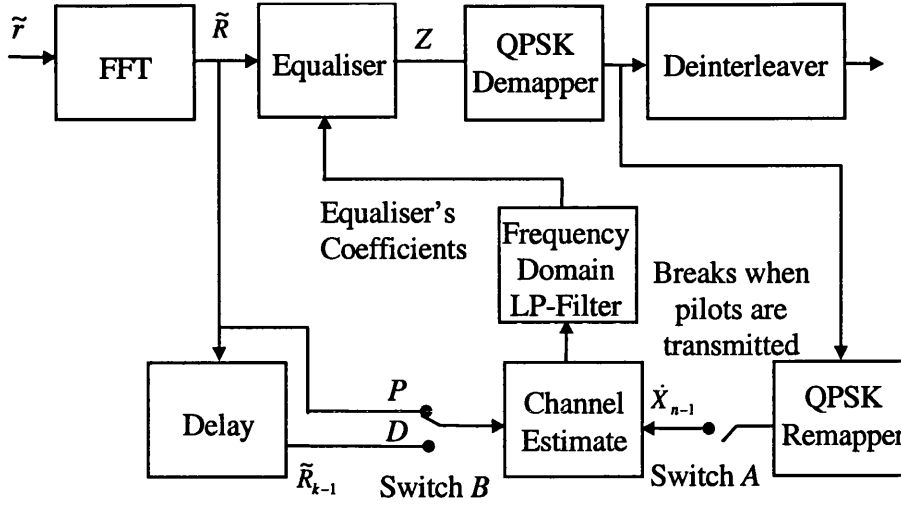
Figure 6.2.1: Schematic Diagram of the Channel Estimator

By ensuring that the maximum delay spread of the channel is fully absorbed by the appended *cyclic-prefix*, the signal samples at the output of the FFT represent the transmitted complex symbols multiplied by the frequency response of the channel and also corrupted by the additive noise of the receiver. This is expressed as:

$$\tilde{R}_n = X_n \cdot H_n + N_n \,, \qquad\qquad\qquad 6.2.1$$

where

$\tilde{R}_n$ is the nth symbol of the received OFDM block prior to equalisation,

X_n is the nth symbol of the transmitted OFDM block,

H_n is the nth sample of the channel's frequency response,

and N_n is n^{th} the additive white Gaussian noise.

For the full OFDM block, the received signal may be represented in a vector form as shown below:

$$\tilde{R} = X \cdot H + N \,, \qquad\qquad\qquad 6.2.2$$

Assuming that an initial estimate of the channel transfer function is already established, for example, using a training sequence, the received OFDM block of data may be equalised and de-mapped. Then, as well as sending a copy of the de-mapped data to the deinterleaver, a copy is fed back to the channel estimator, which in turns re-maps the data in order to re-construct the originally transmitted baseband OFDM block symbols, in this case $\dot{X}$. The reason for de-mapping and then re-mapping of the equalised symbols is to hard limit the additive noise corrupting the received symbols and consequently improve the channel

estimate. An initial noisy estimate of the channel is then obtained by dividing the re-mapped symbols, $\dot{X}$, by the received corresponding ones at the output of the FFT, $\tilde{R}$, as shown in 6.2.3:

$$\overset{n}{H} = \left(\frac{\tilde{R}}{\dot{X}} \right) = \left(\frac{X \cdot H + N}{\dot{X}} \right), \qquad\qquad 6.2.3$$

The noisy estimate of the channel is then refined using a frequency domain low-pass filter, which has a cut-off frequency of the order of the reciprocal of the maximum delay spread, which corresponds to the coherence bandwidth of the channel. Consequently, this results in reducing the noise power by a factor equal to the ratio of the useful OFDM block duration to the time guard-interval. The low-pass filter used here is depicted in Figure 6.2.2 below.
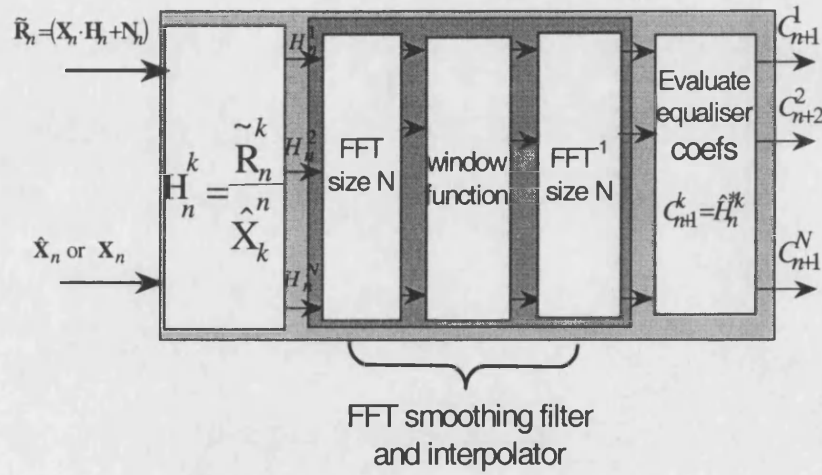
Figure 6.2.2: Schematic Diagram of the Frequency Domain Noise Canceller

In order to prevent serious error propagation and ensure conversion of the equaliser's coefficients, pilot tones may be sent periodically to assist the channel estimator. When the pilot tones are transmitted, swich A on figure 6.2.1 is left open while switch B is connected to point P, otherwise, switch A is closed and switch B is connected to point D. By now it should be clear that the decision vector is given by the ratio of the received vector to the filtered frequency response of the channel estimate delayed by one OFDM block duration. Therefore, the equalised k^{th} decision vector, Z_k, can be expressed in the following manner:

$$Z_k = \tilde{R}_k \cdot \dot{H}_{k-1}^* = \left(X_k \cdot H_k \cdot (H_{k-1} + \eta)^* + N_k \cdot (H_{k-1} + \eta)^* \right), \qquad 6.2.4$$

where

η is the additive noise component on the delayed channel estimate and * stands for the complex conjugate.

In equation 6.2.4 only phase compensation is applied, since the transmitted signal is assumed to be phase modulated.

The coded channel estimation technique is very similar to the first one except that the channel estimate is made after the received signal has been symbol-deinterleaved and decoded, thus making fuller use of the error correction code. Once the received bits are decoded and the original data bits are recovered, the inverse process is implemented in which the data is re-encoded, symbol-interleaved and modulated in order to re-establish an estimate of the originally transmitted baseband signal. This is then used for channel tracking.

The third technique, dual mode, combines the former two techniques in order to achieve the best performance. It uses the coded technique if the error correction decoder was successful in decoding the received signal, otherwise the uncoded technique is employed. In the case of a block code, it is easy to determine how successful the FEC decoder is. On the other hand in the case of a convolutional code, the SNR may be the only way to predict how successful the decoder would be. The full block diagram of this is depicted in Figure 6.2.3.
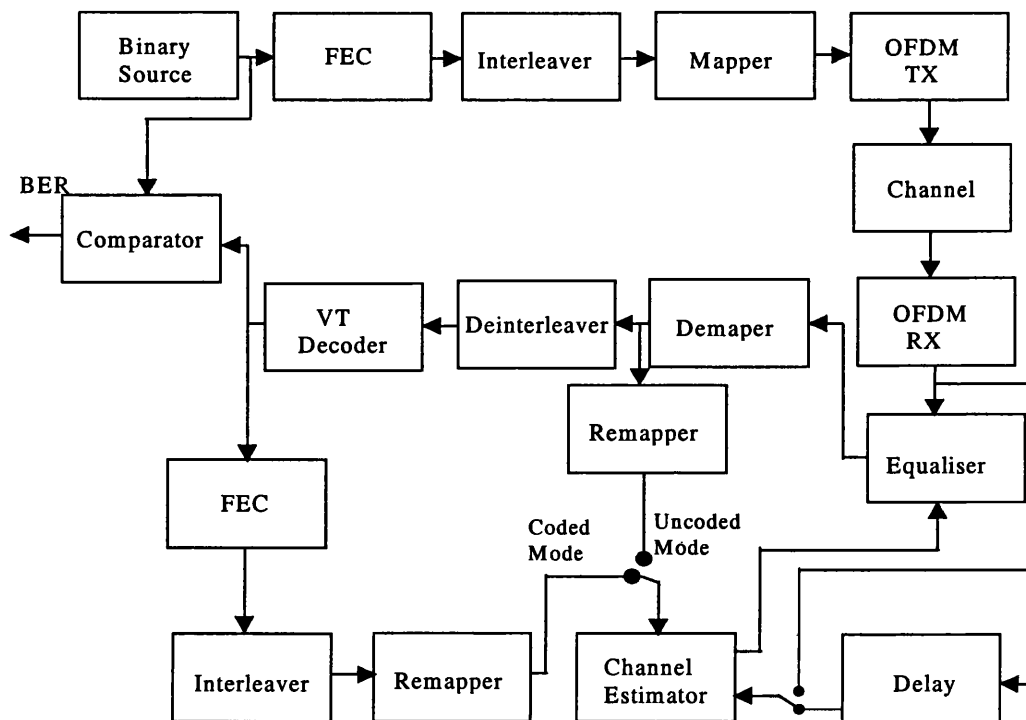
Figure 6.2.3 : Schematic Block Diagram of the Full Channel Estimator

6.3   Mean Square Error (MSE) calculation

In order to calculate the *MSE* of the estimator, it is first assumed that the channel is static. Once an expression for the static channel is established it will be shown how the time variations of the channel can be accounted for. Every OFDM signal consists of F complex values grouped in one block, where F is the number of sub-carriers used. The mean square error of the channel estimator is defined as [5],

$$MSE(\overset{n}{H}) = E\left\{\left(\overset{n}{H} - H\right)^2\right\},$$
6.3.1

where the noisy channel estimate, $\overset{n}{H}$, and the actual channel estimate, H, may be given by:

$$\overset{n}{H} = \frac{\tilde{R}}{X} \quad \& \quad H = \frac{R}{X},$$
6.3.2

Therefore the *MSE* may be written in the following form:

$$MSE(\overset{n}{H}) = E\left\{\left(\overset{n}{H} - H\right)^2\right\} = E\left\{\left(\left(\frac{X \cdot H}{X} + \frac{N}{X}\right) - \frac{X \cdot H}{X}\right)^2\right\} = E\left\{\left(\frac{N}{X}\right)^2\right\},$$
6.3.3

Since N and X are independent random variables, the above equation may be rewritten as:

$$MSE(\overset{n}{H}) = E\{(N)^2\} \cdot E\{(X^{-1})^2\},$$
6.3.4

where

$$E\{(N)^2\} = 2\sigma^2 \text{ is the noise power}$$

and $E\{(X^{-1})^2\} = \alpha$ is the modulation noise enhancement factor [6]. Thus, *MSE* may be given by:

$$MSE(\overset{n}{H}) = 2\sigma^2 \cdot \alpha,$$
6.3.5

Assuming that the average power of the transmitted symbols are normalised to unity and so is the channel frequency response, then the resulting *SNR* is given by the reciprocal of the average noise power as shown below:

$$SNR = \frac{1}{2\sigma^2} = \gamma \quad \Rightarrow \quad E\{(N)^2\} = \gamma^{-1},$$
6.3.6

This leads to the conclusion that, the mean square error of the channel estimator due to the additive noise only is given by:

$$MSE(\overset{n}{H}) = \alpha \cdot \gamma^{-1},$$ 6.3.7

6.4 Impact of noise cancellation

Since OFDM systems are designed such that the symbol time is significantly longer than the duration of the channel impulse response, the inverse of the channel attenuation vector, *H*, has most of its power concentrated in a relatively few samples. In Figure 6.4.1 the power distribution of two types of channels, namely the sample-spaced and non-sample spaced channels is presented. Sample spaced channels are those channels that have all fading impulses at integer multiples of the systems sampling rate and for which the FFT gives the optimal power concentration [10].
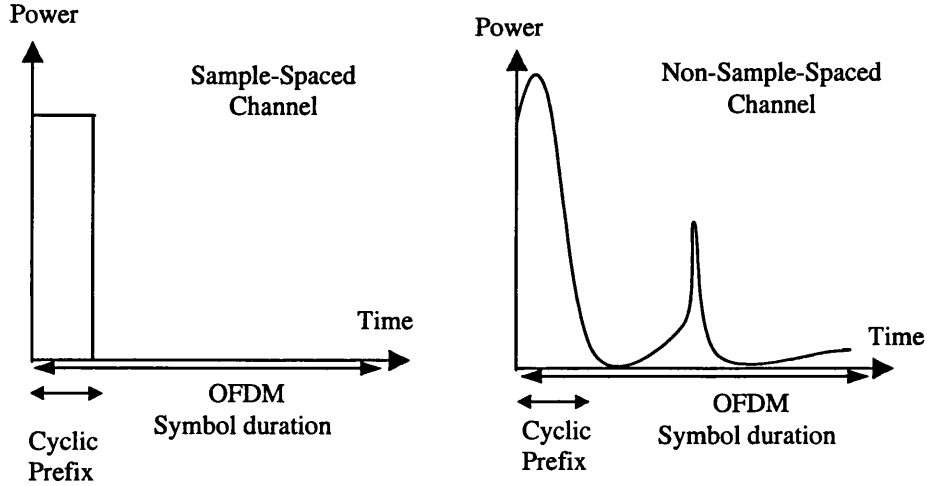
Figure 6.4.1 Example of the time domain power distribution of two channel types (IFFT(*H*))

The effect of low-pass filtering using the FFT based filter on the channel estimate is a further reduction in the noise power by a factor of (*L/F*), where *F* is the number of sub-carriers and *L* is the *cyclic prefix* duration. The impact of this on the mean square error is thus a reduction of (*L/F*), giving:

$$MSE(\dot{H}) = \frac{L}{F} \cdot \alpha \cdot \gamma^{-1},$$ 6.4.1

6.4.1 Impact of time variation and Doppler

The impact of the time-varying channel due to Doppler can be assessed as follows. The channel coefficients for the kth block are related to the channel coefficients for the $(k-1)^{th}$ block if there is no differential Doppler by [7]:

$$H_k = H_{k-1} \cdot \exp(-j2\pi f_D T_L),$$ 6.4.1.1

where f_D is the Doppler frequency shift, and T_L is the duration of the *OFDM* block. Assuming that $E\{H^2\} = 1$, it can be shown that the mean square error due to the time variation can be given by:

$$MSE^{DT}(\breve{H}_k) = E \leq \{(H_{k-1} - H_k)\}^2$$
$$= E\{(1 - \exp(2\pi f_D T_L))^2\},$$ 6.4.1.2
$$\approx (2\pi f_D T_L)^2$$

6.4.2   Loss in received SNR

Using equation 6.4.1 and 6.4.1.2, the total mean square error can be given by

$$MSE^{tot}(\dot{H}) = \left(\frac{L}{F} \cdot \alpha \cdot \gamma^{-1} + (2\pi f_D T_L)^2 \right),$$ 6.4.1.3

As can be seen from Figure 6.4.2.1, a plot of the theoretical performance using the above equation and the simulated performance shows close resemblance especially when the percentage of pilot tones is increased. Where the pilot tones are used to break any propagation of errors that might occur.
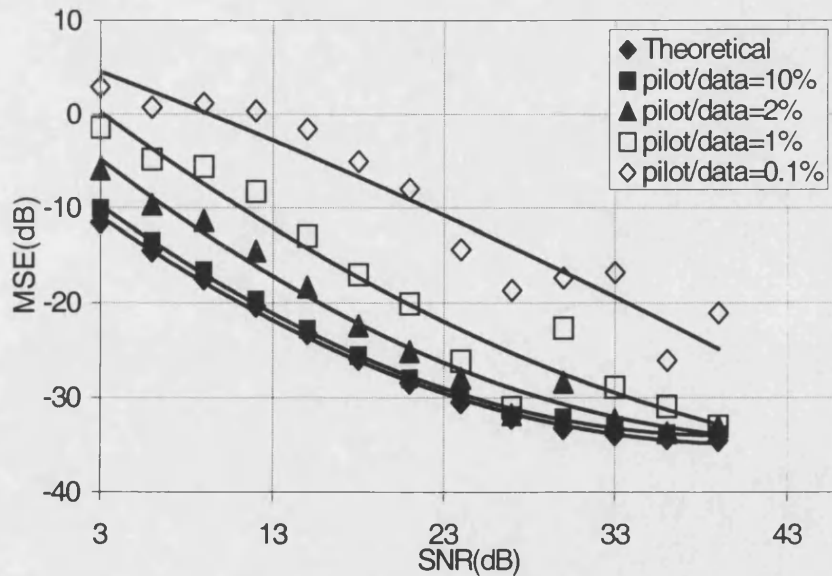
Figure 6.4.2.1: Comparison Between Simulation and Theorectical Performance

Thus, the loss in the received *SNR*, *ΔSNR*, due to the channel transfer function estimation errors can be approximated using

$$\Delta SNR = 10 Log \left(\frac{Noise \quad power + MSE^{tot}(\dot{H})}{Noise \quad power} \right)$$

$$= 10 Log \left(1 + \frac{\left(\sqrt{\frac{L}{F}} \cdot \alpha \cdot \gamma^{-1} + 2\pi f_D T_L \right)^2}{\gamma} \right), \qquad 6.4.1.4$$

6.5 Theoretical analysis of Bit Error Rate (BER) performance

When the number of sub-channels used for transmitting the OFDM signal is large, each sub-channel will have a narrow bandwidth and therefore the impact of the frequency selective fading channel on the individual sub-channels will become flat fading [8]. This implies that each sub-carrier will be multiplied by a complex value, H_n, that on the average has a Rayleigh distributed density function. Having an estimate of this channel gain, the probability of bit error for a coherent QPSK detector using the decision variable given by 6.5.1, may be calculated.

$$Z = \tilde{R} \cdot \dot{H}^* \qquad\qquad 6.5.1$$

The *BER* analysis for this detector is based on appendix C of [9], which results in the following expression:

$$P_{BER} = \frac{1}{2} \cdot \left(1 - \frac{\mu c}{\sqrt{2 - \mu c^2}} \right), \qquad 6.5.2$$

where

$$\mu c = \frac{\bar{\gamma}}{1 + \bar{\gamma}} \quad \text{is the cross-correlation coefficient}$$

and $\bar{\gamma}$ is the average received *SNR* that includes the loss due to estimation errors of the channel response.

The full derivation of the *BER* is presented in appendix *G*.

The *BER* performance comparison between the theoretical and simulated OFDM system in multipath fading is shown in Figure 6.5.1.
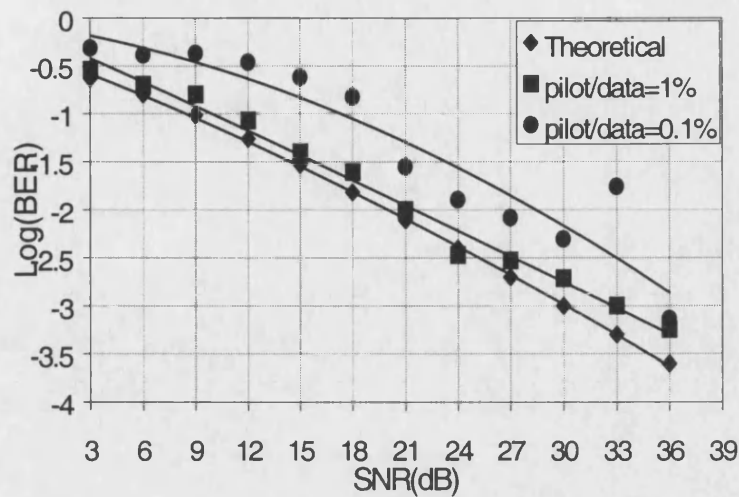
Figure 6.5.1: Theoretical and simulated performance of OFDM in multipath fading

This figure shows close agreement between the theoretical and simulated performance especially as the pilot tone percentage is increased.

6.6   Simulation Results and Discussion

The primary objective of this section is to demonstrate the performance achieved using feedback channel estimation techniques. The work here is specifically set to investigate a best compromise between pilot tone percentage and bandwidth efficiency. It is also intended to give a measure of the impact of time delay on such system and investigate a way of reducing the system's susceptibility to such limiting problem

6.6.1   System Parameters

The simulation parameters used in the tests here are all summarised in Table 6.6.1 below.

Parameter	Value	Parameter	Value
Number of Subcarriers	512	Pilot to Data Ratio ($1/K$)	2%
Transmission Rate	25Mbps	Cyclic Prefix	5 μsec
Doppler Frequency	100Hz	Modulation Scheme	QPSK
Prediction Length	100 Samples	Prediction Order	4
Maximum Delay Spread	5 μsec	Coding Rate	½ Rate Convolutional

Table 6.6.1: Simulation Parameters

The type of channel used is the six-tap-delay-line GSM urban model [11]. For consistency of the results, the data throughput was kept constant and therefore a variable transmission bandwidth was used. Since the purpose of the simulation is to be able to test the performance of the system at a fixed data throughput of 25Mbps, the transmission bandwidth has to be altered to accommodate for the redundancy imposed by the *cyclic prefix* whenever the number of subcarriers used is changed. For example, if the number of subcarriers used is 128, the corresponding OFDM symbol duration is $10.24\mu sec$ and when a *cyclic prefix* of length $5\mu sec$ is appended, the resulting OFDM symbol duration will be increased to $15.24\mu sec$. This implies that in this case about one third of every OFDM block transmitted is redundant information and thus in order to keep the data throughput fixed at 25Mbps the transmission rate of the OFDM symbols has to be increased by one third of the original rate.

To compare the performance of the OFDM system with and without the channel estimation, PSK modulation with coherent demodulation and differential PSK, (DPSK), modulation with differential demodulation, are used, respectively. Convolutional rate-half encoding and the Viterbi decoding algorithm was also implemented at the transmitter and receiver, respectively. Hence, the simulated system can transmit about 12Mbps of actual data. The data symbols are assumed to be transmitted in frames of *M* OFDM blocks with each frame carrying a block of pilot tones as shown in Figure 6.6.1.1. In addition, the channel is assumed to be static throughout the duration of the OFDM block.

The channel transfer function estimators considered here are:

The uncoded channel estimator mode: The channel estimate is derived from the demaped symbols without making use of the forward error correction code.

The coded channel estimator mode: Here the channel is estimated after the received data has been equalised and decoded using the Viterbi decoder making a fuller use of the forward error correction code.

The coded/uncoded dual mode: If the Viterbi decoder was successful in decoding the OFDM block the coded mode in estimating the channel response is used, otherwise the uncoded mode is used.
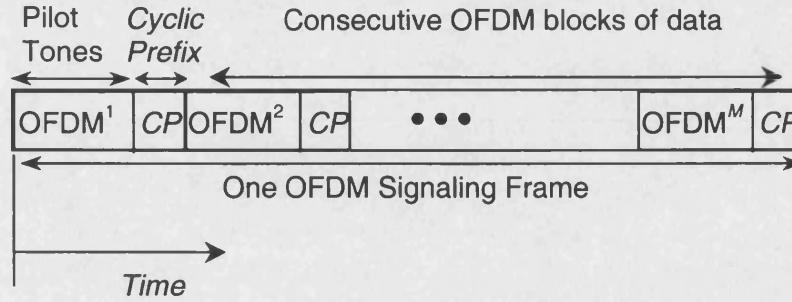
Figure 6.6.1.1: Schematic of the OFDM Frame Structure

6.6.2   **Simulation Results**

The simulation results presented here provide a measure of the *BER* performance of the estimators under a variety of different conditions. To get an insight into the average behaviour of the estimators, the *BER* performance was averaged over 50 000 OFDM blocks.

The sensitivity of both the uncoded and coded estimators to different pilot to data ratios, ρ, is shown in Figure 6.6.2.1 and Figure 6.6.2.2, respectively. As it can be seen from these two figures, both estimator modes are sensitive to ρ, which controls the propagation of feedback errors. It is evident from the two figures that both system modes, in particular the coded one, can still give an acceptable performance even at as low ρ as 0.4% giving a bandwidth efficiency of almost 100%. It can also be concluded that the significance of high ρ becomes less important as the *SNR* increases. From Figure 6.6.2.2 it is evident that the BER performances of the coded mode for different values of ρ become identical at *SNR* greater than 21dB. This comparison shows that the coded mode outperforms the uncoded one only at high *SNR* (>17dB).
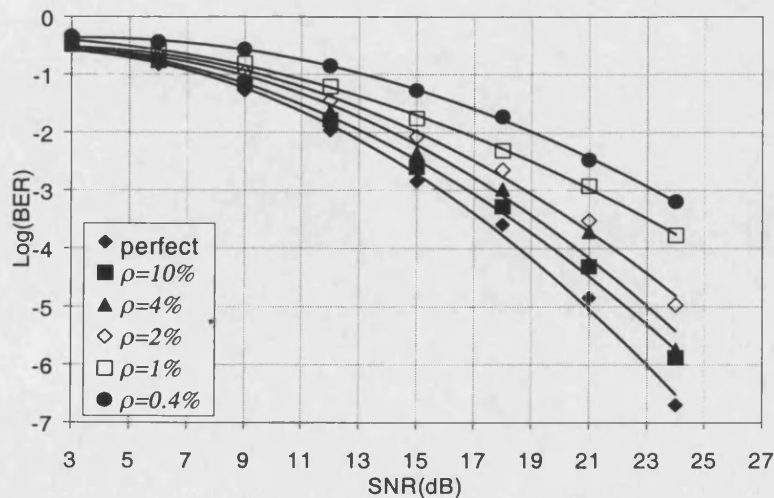
Figure 6.6.2.1: Performance of the Uncoded Estimator Mode with Respect to ρ

138
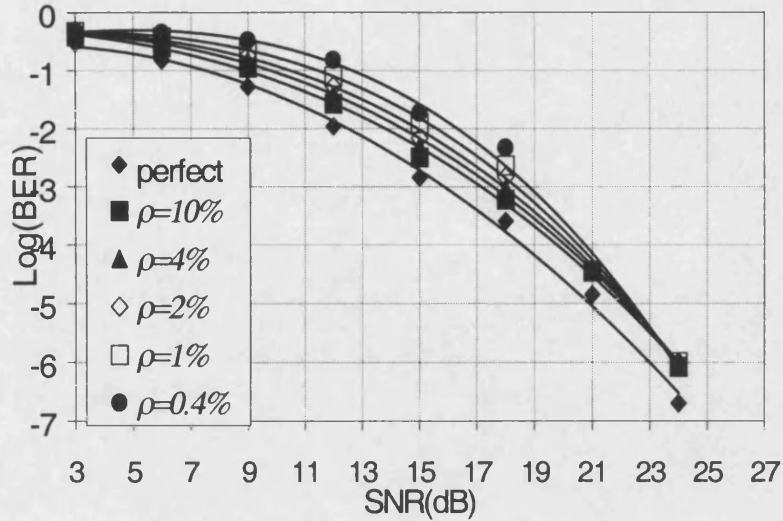
Figure 6.6.2.2: Performance of the Coded Estimator Mode with Respect to ρ

In Figure 6.6.2.4 the estimators *BER* performance with respect to different numbers of subcarriers is assessed. Theoretically, the OFDM system performance should improve as its symbol duration is increased. However, since the channel estimation method examined here is sensitive to the feedback delay which is governed by the block duration and transmission rate, an extra constraint on the maximum number of subcarriers that can be used is imposed. It can be seen from the two figures how the *BER* performance initially improves as the number of subcarriers is increased, but soon starts to degrade as the feedback delay becomes more significant. Although both modes are sensitive to the block duration, it is evident that the uncoded mode is more susceptible to time delay.
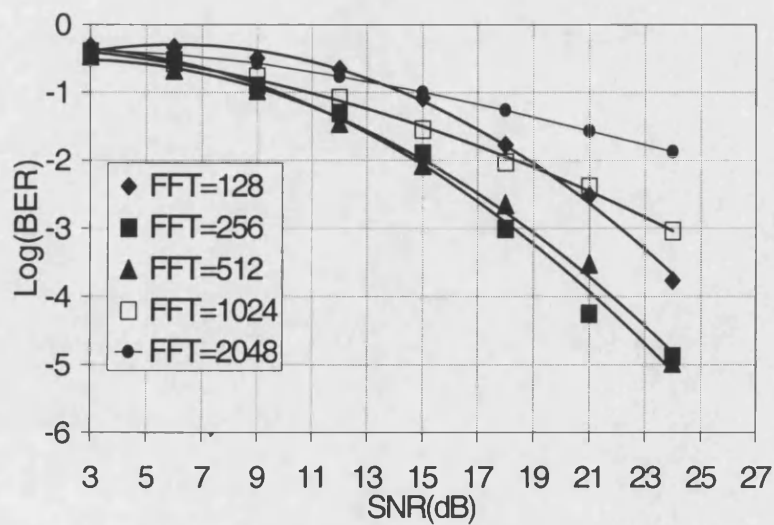
Figure 6.6.2.3: Performance of the Uncoded Mode with Respect to the Number of
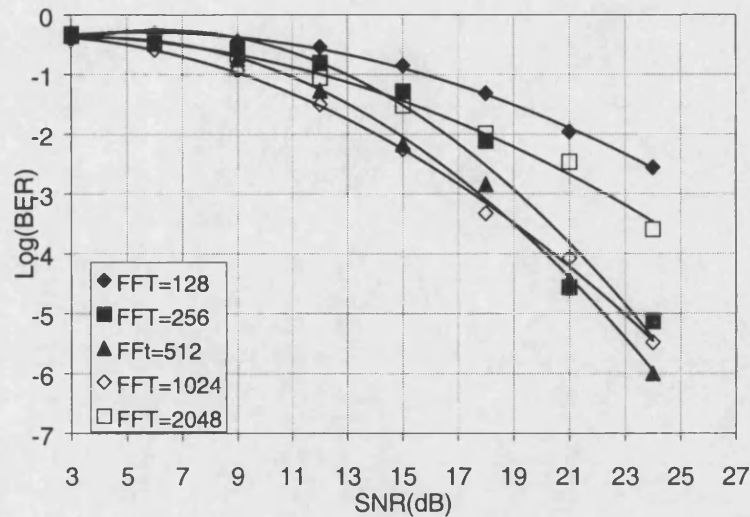
Subcarriers

Figure 6.6.2.4: Performance of the Coded Mode with Respect to the Number of Subcarriers

In Figure 6.6.2.5, the system performance using differential Phase Shift Keying, DQPSK, where channel estimation is not needed, is examined. It can be seen from this figure how the *BER* performance is improved as the number of subcarriers used is increased. This improvement in performance is due to a corresponding increase in the system's frequency diversity. The only main constraints on the maximum number of subcarriers are the computational time required and Doppler frequency shift, which is related to the vehicle speed. It is clear from these three figures that the use of this type of differential modulation only outperforms the two estimator modes when the number of subcarriers used is >2048.
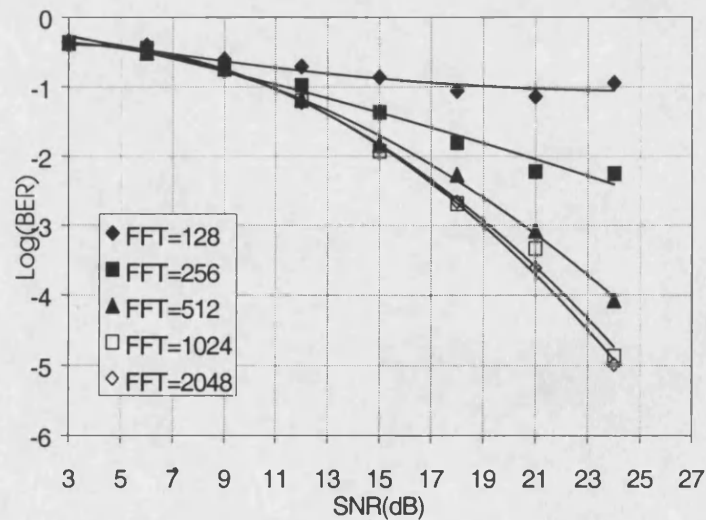
Figure 6.6.2.5: Performance of the Differential QPSK with Respect to the Number of Subcarriers

Increasing the Doppler frequency results in increasing the speed of variation of the channel response and hence making the mismatch between the estimated and actual channel response greater. In Figure 6.6.2.6, Figure 6.6.2.7 and Figure 6.6.2.8 the *BER* performance of the uncoded, coded and differential modes under different Doppler frequencies are presented, respectively. It can be seen that of the three modes, the uncoded mode is the most sensitive to the Doppler frequency. The differential mode only outperforms the coded mode at Doppler frequencies in excess of 200Hz.
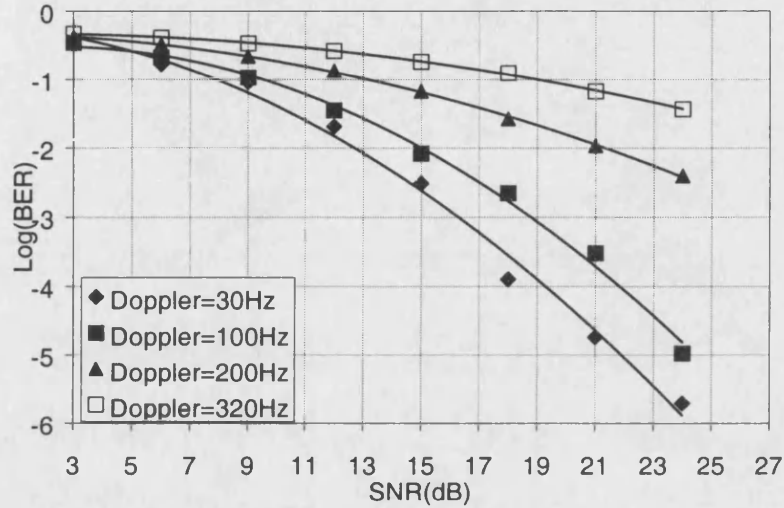
Figure 6.6.2.6: Performance of the Uncoded Estimator Mode with Respect to Doppler
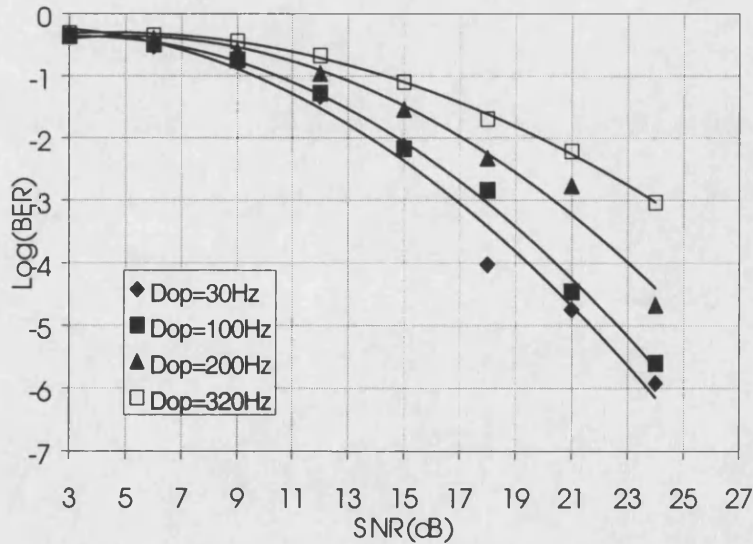
Figure 6.6.2.7: Performance of the Coded Estimator Mode with Respect to Doppler

こ
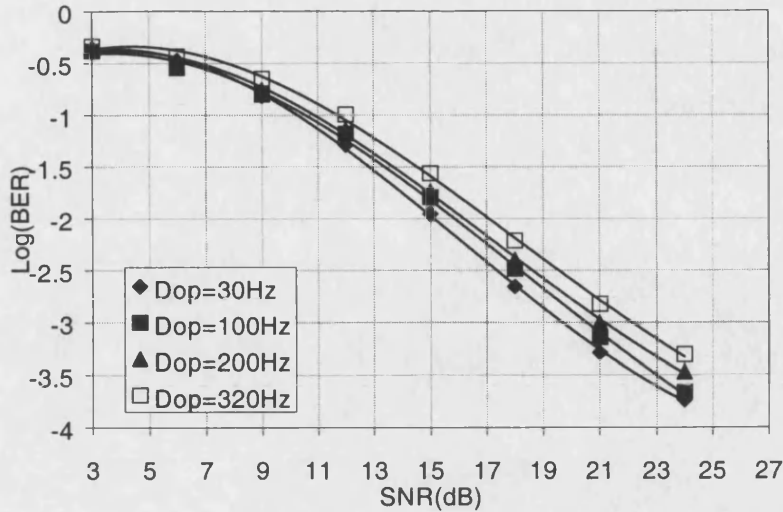
Figure 6.6.2.8: Performance Differential QPSK with respect to Doppler

In Figure 6.6.2.9, a comparison, based on the system parameters presented in Table 6.6.1 between the four modes is shown. It is evident from this figure that for such system parameters, the best performance is obtained when the dual mode is used, followed by the coded mode, uncoded mode and the differential mode, respectively.
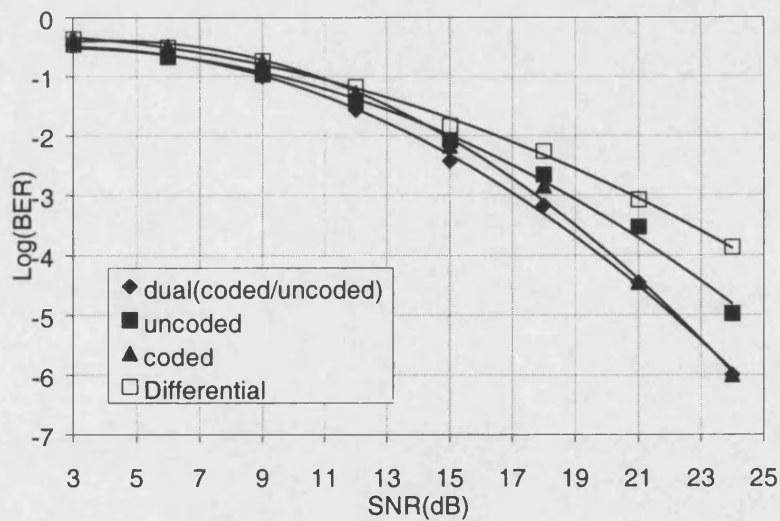
Figure 6.6.2.9: Comparison Between the Four Modes

6.7   Impact of Linear Prediction

As could be seen from the previous results, both estimator modes (coded and uncoded) suffer performance degradation as the mismatch between the estimated and actual channel response increases due to either high Doppler frequencies or long block duration. In this section we propose the use of a prediction algorithm that is based on the time domain correlation vector

between the estimated samples in order to improve the channel estimate. Since the intention here is to reduce the mismatch between the estimated and actual channel response, the results are shown in terms of mean square error (*MSE*) which is defined as the time averaged error energy per OFDM symbol between the estimated transfer function and the actual one.

Linear prediction is especially successful at extrapolating oscillatory signals that are not necessarily periodic. It is based upon the concept of estimating the value of the Mth sample of a signal from the *M-1* previous samples. Thus, given a set of data $h_{t-1}, h_{t-2}, \cdots, h_{t-M}$, for a predictor of order *M*, the predicted value of h_t is given by:

$$\hat{h}_t = \sum_{k=1}^{M} -a_k \cdot h_{t-k} ,$$

6.7.1

The prediction error is defined as the difference between the predicted and actual values, ε, given by:

$$\varepsilon_t = h_t - \hat{h}_t = h - \sum_{k=1}^{M} -a_k \cdot h_{t-k}$$

$$= \sum_{k=0}^{M} a_k \cdot h_{t-k}, \qquad a_0 = 1$$

6.7.2

To obtain the predictor coefficients that minimise the mean square prediction error, $E(\varepsilon)^2$, we differentiate 6.7.2 with respect to a_j, and equate the partial derivatives to zero. This produces:

$$\frac{\partial E(\varepsilon_t)^2}{\partial a_j} = 2E\left(\frac{\partial \varepsilon_t}{\partial a_j} \cdot \varepsilon_t \right) = 2E\left(h_{t-j} \cdot \sum_{k=0}^{M} a_k \cdot h_{t-k} \right)$$

$$= 2\sum_{k=0}^{M} a_k E\left(h_{t-j} \cdot h_{t-k} \right) = 2\sum_{k=0}^{M} a_k \cdot \phi_{t-k} = 0, \qquad 1 \le t \le M$$

6.7.3

Using the fact that a_0 =1 and the even property of the autocorrelation vector, $\phi_j = E[h_t \cdot h_{t+j}]$, equation 6.7.3 can be written in a matrix form as shown in equation 6.7.4 which when solved produces the best predictor's coefficients, in the minimum mean square sense:

$$\begin{bmatrix} \phi_0 & \phi_1 & \cdots & \phi_{M-2} & \phi_{M-1} \\ \phi_1 & \phi_0 & \cdots & \phi_{M-3} & \phi_{M-2} \\ \vdots & \vdots & \vdots & \vdots & \vdots \\ \phi_{M-2} & \phi_{M-3} & \cdots & \phi_2 & \phi_1 \\ \phi_{M-1} & \phi_{M-2} & \cdots & \phi_1 & \phi_0 \end{bmatrix} \cdot \begin{bmatrix} a_1 \\ a_2 \\ \vdots \\ a_{M-1} \\ a_M \end{bmatrix} = - \begin{bmatrix} \phi_1 \\ \phi_2 \\ \vdots \\ \phi_{M-1} \\ \phi_M \end{bmatrix}, \qquad 6.7.4$$

To obtain an estimate of the auto-covariance matrix and the cross-covariance vector previously estimated channel transfer functions are used. Where the first initial estimate is obtained using a comb of pilot tones.

It is well known that the performance of the predictor is remarkably sensitive to exactly how the autocorrelation vector is estimated [10]. Two of the most popular algorithms used to estimate the predictor coefficients are the Levinson-Durbin and Burg algorithms [12][13][14]. The Burg algorithm is in fact a development of the Levinson-Durbin algorithm. It is based on minimising the backward and forward prediction errors simultaneously in for calculating the predictor coefficients using a recursive procedure. This procedure exploits the Toeplitz symmetry of the autocorrelation matrix to proceed recursively beginning with a predictor of order one (ie. One coefficient) and to increase the order recursively using the low order solutions to obtain the solutions to the next higher order. This method has been proven to be generally a more accurate method than the Levison-Durbin method. For a more in depth discussion of these two algorithms and more, references [5][12][13][14] are recommended. The steps for implementing the Burg's algorithm are summarised below:

1. *Initial conditions*

$$\hat{\pi}_0 = \phi(0),$$

$$e_0^f(n) = h(n), \qquad n = 1,2,...,N-1,$$

$$e_0^b(n) = h(n), \qquad n = 0,1,...,N-2.$$

2. *Reflection Coefficients for p = 1,2,..., P,*

$$\hat{\pi}_p = \frac{-2\sum_{n=p}^{N-1} e_{p-1}^f(n) e_{p-1}^b(n-1)}{\sum_{n=p}^{N-1}\left(e_{p-1}^f(n)\right)^2 + \left(e_{p-1}^b(n-1)\right)^2},$$

$$s_p^2 = \left(1 - |\hat{\pi}_p|^2\right)s_{p-1}^2$$

For *p = 1:*

$$\hat{a}_1(1) = \hat{\pi}_1$$

For *p > 1:*

$$a_p(i) = \begin{cases} a_{p-1}(i) + \hat{\pi}_p a_{p-1}(p-i) & for \quad i = 1,2,...,p-1 \\ \hat{\pi}_p & for \quad i = p \end{cases}$$

3. Prediction errors for next order

$$e_p^f = e_{p-1}^f(n) + \hat{\pi}_p e_{p-1}^b(n-1), \qquad\qquad n = k+1,...,N-1$$

$$e_p^b = e_{p-1}^b(n-1) + \hat{\pi}_p e_{p-1}^f(n) \qquad\qquad n = k+1,...,N-2$$

6.7.1   Performance of the Prediction Algorithm

In order to implement the technique more efficiently, the prediction was applied on the time domain CIR samples of the channel as shown in Figure 6.7.1.1. By doing so, only a small fraction of the transformed samples are used and thus the number of calculations is greatly reduced. Assuming that the number of samples involved per each predicted value is M, then $M \, X \, L$ samples were stored in a matrix, A, as shown below. Then, prediction is performed on a row by row basis to produce the time domain samples of the channel estimate. These are then passed onto the N size (N-L zero padded) FFT to produce the full channel response, where L is the length of the cyclic prefix [19][20].
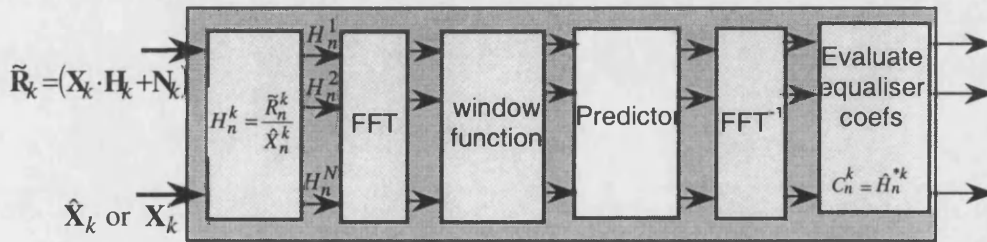
Figure 6.7.1.1: Schematic of Estimator with Prediction

The results here are given in terms of MSE versus SNR only. Provided that the relationship between BER and MSE are known the system performance of any modulation scheme may be deduced. Since QPSK modulation was used here, a graph relating MSE to BER of QPSK is provided.

$$A = \begin{bmatrix} h_0^0 & h_0^1 & \cdots & h_0^{M-2} & h_0^{M-1} \\ h_1^0 & h_1^1 & \cdots & h_1^{M-2} & h_1^{M-1} \\ \vdots & \vdots & \vdots & \vdots & \vdots \\ h_{L-1}^0 & h_{L-11}^1 & \cdots & h_{L-1}^{M-2} & h_{L-1}^{M-1} \\ h_L^0 & h_L^1 & \cdots & h_L^{M-2} & h_L^{M-1} \end{bmatrix}$$

In Figure 6.7.1.2 and Figure 6.7.1.3, the impact of the predictor on the system's performance is presented. It can be seen that, especially in the case of the uncoded mode, a very significant improvement is achieved (about 20dB at $MSE = -10$dB) in the case when the FFT length is 2048. The other conclusion that can be drawn from these two figures is the fact that the performance of both the coded and uncoded modes became almost identical at $SNR > 15$dB when prediction is used.

Similarly, Figure 6.7.1.4 and Figure 6.7.1.5 show the significant improvement achieved by using a predictor in the presence of very high Doppler frequencies. These two figures also confirm that the performance of the both estimator modes become almost identical at *SNR >* 15dB.
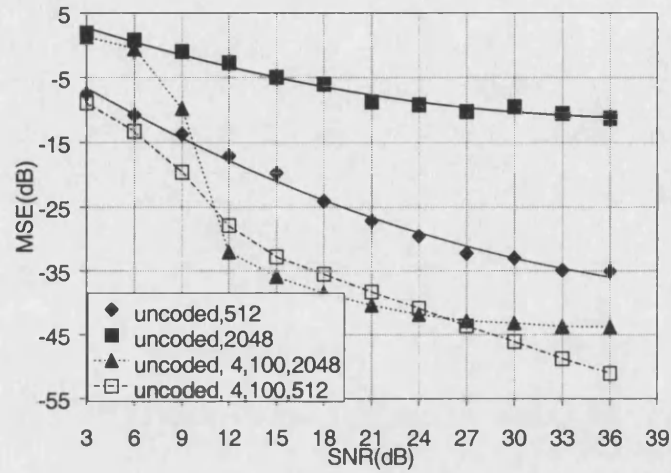
Figure 6.7.1.2: Comparison on the Uncoded Mode with Respect to the Block length
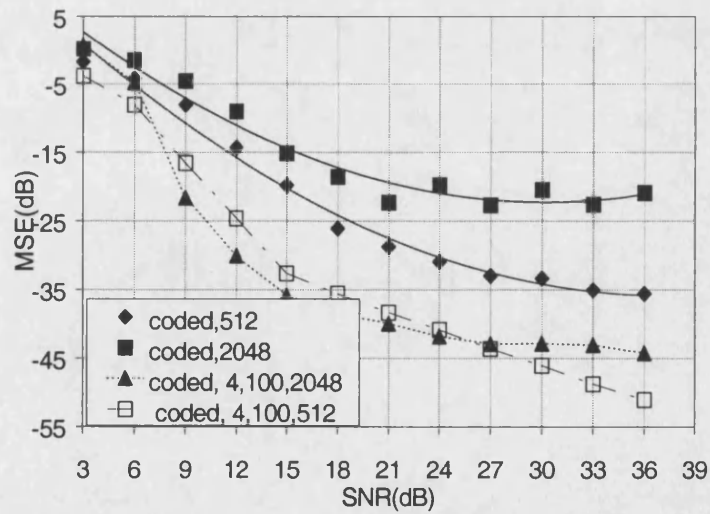
Figure 6.7.1.3: Comparison of the Coded Mode with Respect to the Block length
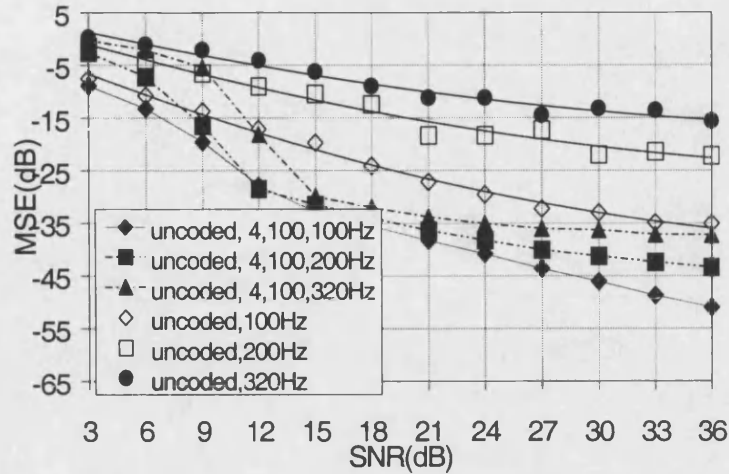
Figure 6.7.1.4: Comparison of the Uncoded Mode with Respect to Doppler
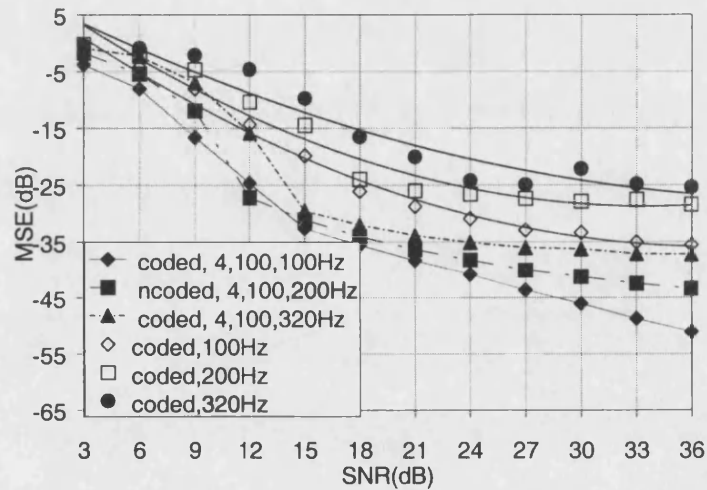
Figure 6.7.1.5: Comparison of the Coded Mode with Respect to Doppler

It was initially thought that a better estimate of the predictor weights is achieved when the number of samples involved is large. However, it was found that the improvement becomes much less significant after a certain number. As can be seen from Figure 6.7.1.6, especially at *SNR* > 15dB, the improvement achieved by increasing the number of samples is decreasing in an exponential manner.
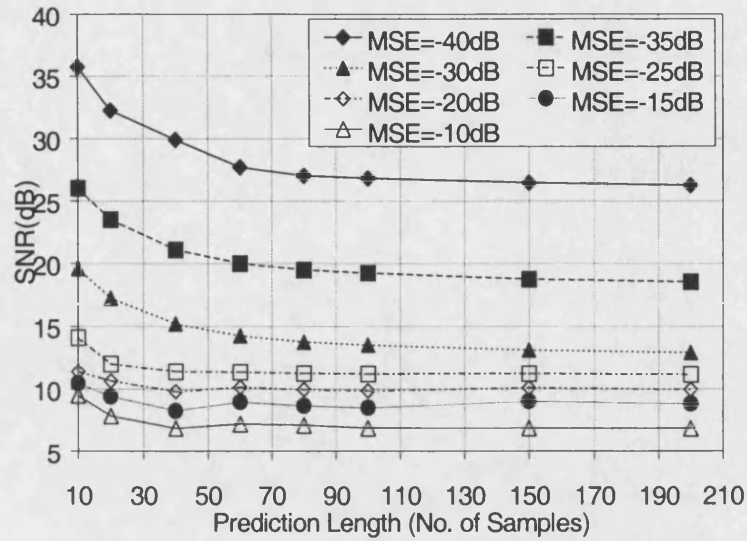
Figure 6.7.1.6: Effect of Increasing the Prediction Length

A similar test was carried out to investigate the effect of increasing the order of the predictor. The results are shown in Figure 6.7.1.7 and it can be seen that at low signal to noise ratio there is a performance improvement achieved by increasing the order from two to four, however by increasing the order to higher than four the improvement achieved is much less significant.
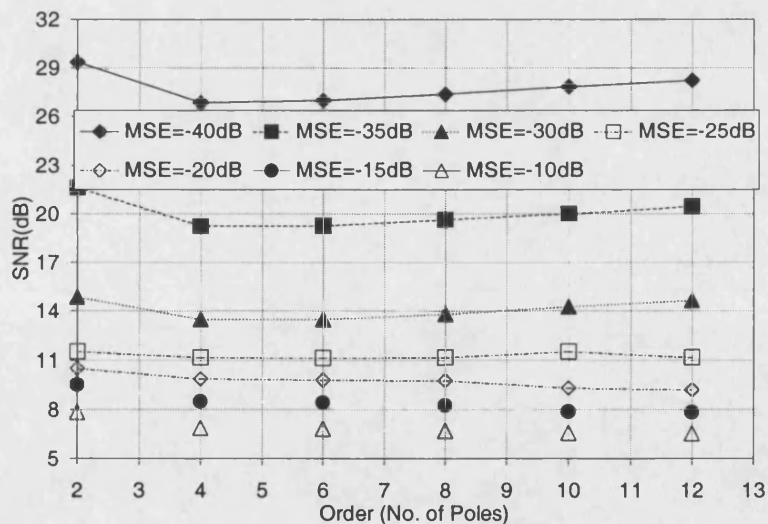
Figure 6.7.1.7: Effect of Increasing the Order of the Filter

Figure 6.7.1.8 is shows the relationship between the channel MSE and BER performance. It can be seen from this figure that the use of a predictor makes it possible to use feedback channel tracking and achieve BER of less than 10^{-5} even under severeconditions.
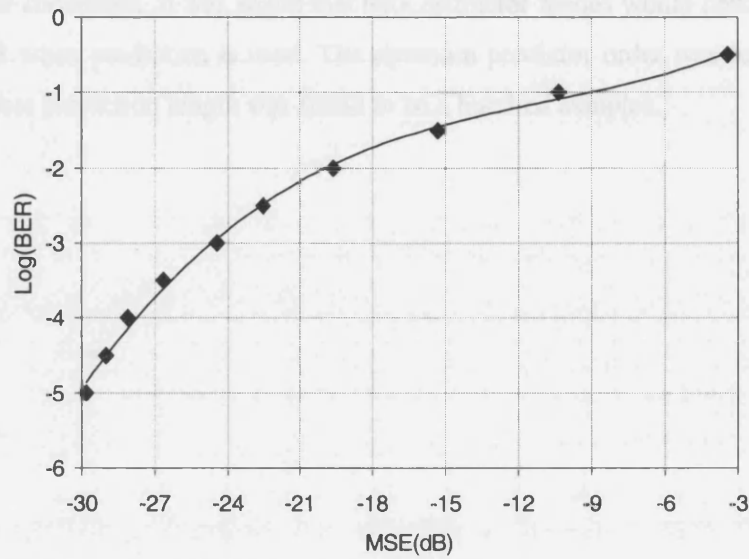
Figure 6.7.1.8: Relation of Average BER to the MSE

6.8 Conclusion

The use of decision directed feedback channel estimation was investigated in this chapter. It was shown that under certain circumstances this technique can provide a bandwidth efficiency of nearly 99% while maintaining acceptable BER performance. The use of coded feedback channel estimation was shown to be superior to the uncoded mode under various channel conditions. Having said that it was also found that both the coded and uncoded channel estimator modes are susceptible to the time delay imposed by the joint effect of the duration of the data block and the Doppler effect. The impact of filtering the channel estimate was also investigated and it was found to be essential especially at low SNR. A theoretical analysis of the system was also presented and an upper bound formula was given.

When compared to the performance of DQPSK under the same conditions, it was realised that the choice of such technique may be the best one when the block duration is of the order of 2048 and higher or the Doppler frequency in the range of about 200Hz. It was also found that this technique is much less sensitive to Doppler shifts than both the coded and uncoded modes.

The use of time domain based prediction in view to improve the performance of both the coded and uncoded channel estimation modes was found to be significantly helpful.

Considerable improvement was obtained especially in the case of the uncoded mode under severe channel conditions. It was found that both estimator modes would perform identically at SNR>15dB when prediction is used. The optimum predictor order was found to be four whereas the best prediction length was found to be a hundred samples.

6.9 Reference

[1] Y. Wu and W.Y. Zou, *"Performance Simulation of COFDM for TV Broadcast Application"*, Conference Proceedings of the SMPTE Technical Conference, pp.258-261, Oct. 1994.

[2] F. Tufvesson and T. Maseng, *"Pilot Assisted Channel Estimation for OFDM in Mobile Cellular Systems "*, Proceedings of the IEEE47th Vehicular Technology Conference, Phoenix, USA, pp. 1639-1643, May 1997.

[3] J. Rinne and M. Renfors, *"Pilot Spacing in Orthogonal Frequency Division Multiplexing Systems on Practical Channels"*, IEEE Transactions on Consumer Electronics, Vol. 42, No. 4, Nov. 1996.

[4] M.H. Hsieh and C.H. Wei, *"Channel estimation For OFDM Systems on Comb Type Pilot Arrangement in Frequency Selective Fading Channels "*, IEEE Transactions on Consumer Electronics, Vol. 44, No. 1, pp. 217-225, 1998.

[5] Steven M. Kay, *"Fundamentals of Statistical Signal Processing"*, PTR Prentice Hall, Chap. 2, pp. 19, 1987.

[6] A. Chini, Y. Wu, M. El-Tanny and S. Mahmoud, *"Filtered decision feedback channel estimation for OFDM based digital DTV terrestrial broadcasting system "*, IEEE Transactions on Broadcasting, Vol. 44, No. 1, pp. 2-11, Mar. 1998.

[7] A. Chini, *"Multi-carrier Modulation in Frequency Selective Fading Channels "*, Ph.D. dissertation, Carleton University, Canada, 1994.

[8] P. Frenger and A. Svensson, *"A Decision Directed Coherent Detector for OFDM"*, Proceedings of the IEEE VTC'96, Vol. 3, pp. 1584-1593, 1996.

[9] John G. Proakis, *"Digital Communications"*, third edition, 1995.

[10] W. H. Press, S. A. Teukolsky, W. T. Vetterling and B. P. Flannery, *"Numerical recipes in C"*, 2nd edition, Cambridge, 1993.

[11] R. Steele, *"Mobile Radio Communications"*, 3ed edition, IEEE press, 1991.

[12] G. B. Ribicki, *"Computers in Physics"*, Vol. 3, no. 2, pp. 85-87, G. B 1989.

[13] R. Shiavi, *"Introduction to Applied Statistical Signal Analysis"*, Aksen Associates Incorporated Publishers, Chap. 8, 1991.

[14] J. Proakis, C. M. Rader, F. Ling and C. L. Nikias, *"Advanced Digital signal Processing"*, Maxwell Macmillan International, Chap. 8, 1992.

[15] B. Porat, *"A Course in Digital Signal Processing"*, John Wiley and Sons, INC. 1997.

[16] Y. Li, L. J. Cimini and N. R. Sollenberger, *"Robust Channel estimation for OFDM Systems with Rapid Dispersive Fading Channels "*, IEEE Transactions on Communications, Vol. 46, No. 7, pp. 902-915, July 1998.

[17] R.F. Ormondroyd and E. Al-Susa, "*A High Efficiency Channel Estimation and Equalisation Strategy for a broadband COFDM System*",ISSSE'98, pp.471-475, Piza-Italy, 1998.

[18] V. Mignone and A. Morello, "*CD3-OFDM: A novel demodulation scheme for fixed and mobile receivers* ", IEEE Trans. on Comms. Tech., Vol. 44, No 9, Sept. 1996.

[19] E. Al-Susa and R.F. Ormondroyd, "*Improved Equalisation for a Broadband COFDM System in a Time-Varying Frequency Selective Fading Channel Using Predictor Based Channel Estimation*", Submitted to the IEEE Transactions on Vehicular Technology.

[20] M Sandell, "*Multicarrier Modulation*", Ph.D. Thesis, 1996, Lulea University of Technology.

Chapter Seven

Adaptive OFDM Modulation

7 Chapter Seven

7.1 Introduction

The transmission of data over the Rayleigh mobile radio channels is subjected to random error bursts due to the presence of deep fades. These fades take two forms; one in the frequency domain and the other is in the time domain. The fades in the frequency domain are governed by the multipath strength, which is determined by the relative instantaneous power levels of the received rays. The time dependent fades are, on the other hand, governed by the speed of the mobile station, which may be used to give a measure of the average rate and duration of such fades. The presence of such channel impairments alters the power of the received signal making the signal more or less vulnerable to noise. This leads to the notion of using adaptive modulation methods, which are based on monitoring the integrity of the channel and accordingly either increase the system's capacity without degrading its BER performance, or improve the BER performance without altering the required SNR, or a combination of both. In general this can be achieved by varying either: the transmitted power level of the transmitted carrier(s) according to some optimum criterion [1], the symbol transmission rate [2], the constellation order [3][4], the coding rate [5] or any combination of such parameters [6]-[8]. Such techniques are applicable to both single-carrier and multi-carrier systems and have attracted considerable attention for many applications such as digital subscriber line, satellite links and fixed wireless communication systems [9]-[21]. For instance, adaptive modulation is part of the V.34 modem standard [16], and is currently used in modems to maintain an acceptable BER performance over poor quality telephone lines. Also, in [17] a variable-rate QAM for third-generation wireless communication systems was proposed. The Enhanced Data rates for GSM Evolution, *EDGE*, [18][19], proposed as a wireless data enhancement for GSM and IS-136 (North American Time Division Multiple Access System) uses a combination of modulation and coding to achieve variable data rates. This was shown to be significantly more spectrum-efficient than the standard GSM currently in use [20].

If the adaptive modulation scheme used is based on producing a fixed BER, a variable data throughput is obtained. Alternatively, if the throughput is held constant, a variable BER results.

In general, an adaptive system can only work over a duplex transmission as some method of informing the transmitter of the current state of the channel or the quality of the received

signals required. The transmitter then adapts to such changes according to the criteria used. Successful implementation of adaptive OFDM requires that the channel changes slowly compared with the transmission rate of the OFDM blocks. Since OFDM is a wide-band system, normally adopted for high data rate transmission, such conditions should rarely cause any serious concern.

The simplest arrangement for an adaptive modem is Time Division Duplex, (TDD), where both the base station, *BS*, and mobile unit, *MU*, transmit over the same radio frequency channel, but at different times. In this case, both the *BS* and *MU* experience similar channel fading conditions as their transmissions are typically only one time slot apart. The transmission received by the *MU* is used to estimate the channel frequency response. In order to successfully demodulate the received signal, it is critical that both the *BS* and *MU* inform each other of the adaptation parameters used and that this information does not get corrupted by the channel. The other arrangement that can be used is based on the Frequency Division Duplex scheme (FDD). In FDD the uplink and the downlink use different propagation frequencies that are typically spaced by a few tens of MHz allowing both the transmitter and receiver to transmit simultaneously. Both the *BS* and *MU* must monitor their incoming channels and signal the required adaptation parameters to be used by the other on their outgoing channels.

In this chapter, a comparative study of three adaptive techniques, namely, adaptive constellation, adaptive power control using channel inversion and adaptive subcarrier allocation will be given. In addition, the impact of the channel variation and mismatch errors on such techniques will be evaluated using computer simulation.

7.2 Channel Capacity

7.2.1 *Ideal Channel (Gaussian Channel)*

A Gaussian channel is a combination of a linear filter and additive Gaussian noise. In the time domain the output of this channel is given by:

$$r(t) = x(t) * h(t) + n(t) \; ,$$ 7.2.1.1

where $x(t)$ is the transmitted signal,

$h(t)$ is the channel impulse response,

$*$ is a convolution operator,

          $n(t)$ is zero-mean additive Gaussian noise.

and $X(f)$, $H(f)$ and $N(f)$ is the Fourier transform of $x(t)$, $H(t)$ and $n(t)$, respectively.

The total transmit power is limited by an average power constraint, $\int X(f)df \leq P$.

The ideal Gaussian channel is characterised by a brickwall linear filter and by white Gaussian noise whose power spectrum $N(f)$ is equal to a constant $N_0/2$ over some frequency band B of width W Hz. In this type of channels the frequency response is constant over B, and equal to zero elsewhere.

Assuming perfect synchronisation and filtering, the sampled channel outputs r_k may be given by:

$$r_k = x_k + n_k,$$ 7.2.1.2

where

          r_k, x_k and n_k correspond to the discrete received signal, transmitted signal and AWGN sample, respectively.

The average energy per signal symbol, S_x, and noise sample, S_n, for this type of channel is given by:

$$\begin{aligned} S_x &= P/W \\ S_n &= N_0 \end{aligned}$$ 7.2.1.3

Under an average transmit power constraint, the channel capacity, C, of an ideal Gaussian channel may be given by [23]:

$$C = \ln\left(1 + \frac{S_x}{S_n}\right),$$ 7.2.1.4

bits per symbol (bits per second per Hz), or equivalently:

$$\tilde{C} = C \cdot W = W \cdot \ln\left(1 + \frac{S_x}{S_n}\right),$$ 7.2.1.5

Therefore, an ideal Gaussian channel can be characterised by two parameters, one is its bandwidth, W, and the other is its signal to noise ratio (SNR) S_x/S_n or equivalently its

capacity C in b/s/Hz. This is normally referred to as the Shannon's channel capacity, which is plotted as a function of bits versus SNR in **Figure 7.2.1.1** below.

Shanon's capacity
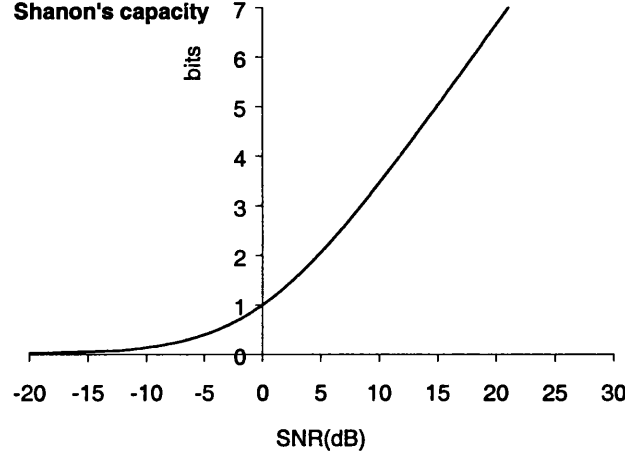
Figure 7.2.1.1: Channel Capacity (bits/Hz) Versus SNR(dB)

This is used as a benchmark to the best possible system performance achievable.

7.2.2   *Non-Ideal Channels (Frequency Selective)*

The capacity of an arbitrary channel may be determined as follows. Let $S(f)$ be an arbitrary transmit power spectrum over a transmission band B. Divide B into many sub-bands of width Δf, where Δf is chosen small enough so that the channel SNR function $|H(f)|^2/N(f)$ is approximately constant within any one sub-band. Then, given $S(f)$, the capacity within a sub-band of width Δf around frequency f_i is:

$$C(f_i) = \ln\left(1 + \frac{S(f_i)\cdot|H(f_i)|^2}{N(f_i)}\right),$$

         7.2.2.1

bits per symbol, or $C(f_i)\Delta f$ bits per second. The aggregate capacity across the whole band is given by integrating across the entire bandwidth:

$$\tilde{C} = \sum_i C(f_i)\Delta f \rightarrow \int C(f)df = \int \ln\left(1 + \frac{S(f)\cdot|H(f)|^2}{N(f)}\right)df,$$

         7.2.2.2

bits per second.

The optimum transmit power spectrum in this type of channels may be determined by *water-pouring* as shown in [22], and illustrated in Figure 7.2.2.1.

The optimum transmit spectrum $S(f)$ is nonzero over a band of frequencies $B = \{f: N(f)/|H(f)|^2 < K_0\}$, called the capacity achieving band, and within B is equal to:

$$S(f) = K_0 - N(f) / |H(f)|^2 \qquad\qquad 7.2.2.3$$

where K_0 is a threshold chosen so that the transmit power spectrum $S(f)$ satisfies the power constraint $\int S(f)df \leq P$

For ideal brickwall channel, for example, the optimum transmit spectrum is constant over the band where $|H(f)|2/N(f) > 0$ and zero elsewhere, and the capacity expression reduces to:

$$\tilde{C} = W \cdot \ln\left(1 + \frac{S_x}{S_n}\right), \qquad\qquad 7.2.2.4$$
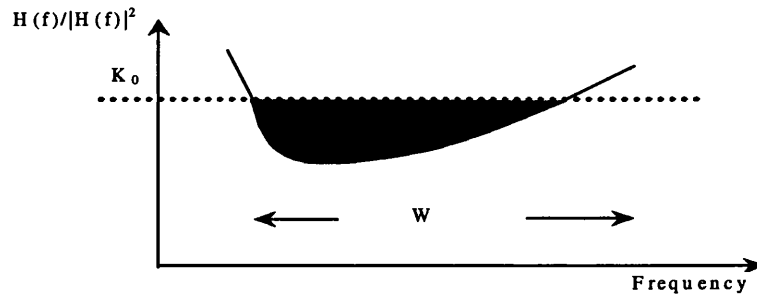
Figure 7.2.2.1: Determination of Optimum Water Pouring Spectrum

7.3 Constellation Order Selection

There are two main criteria that an adaptive modulator can use for selecting the constellation order. The first is based on the signal to noise ratio resulting in a variable BER performance and the second is based on achieving specified BER, resulting in a variable data throughput. In the case of the former, the channel frequency response is stylised in such a way that each zone corresponds to a different QAM level in the modem. Figure 7.3.1 shows an arbitrary segment of the frequency response of the channel and the corresponding number of bits per symbol selected per sub-channel.
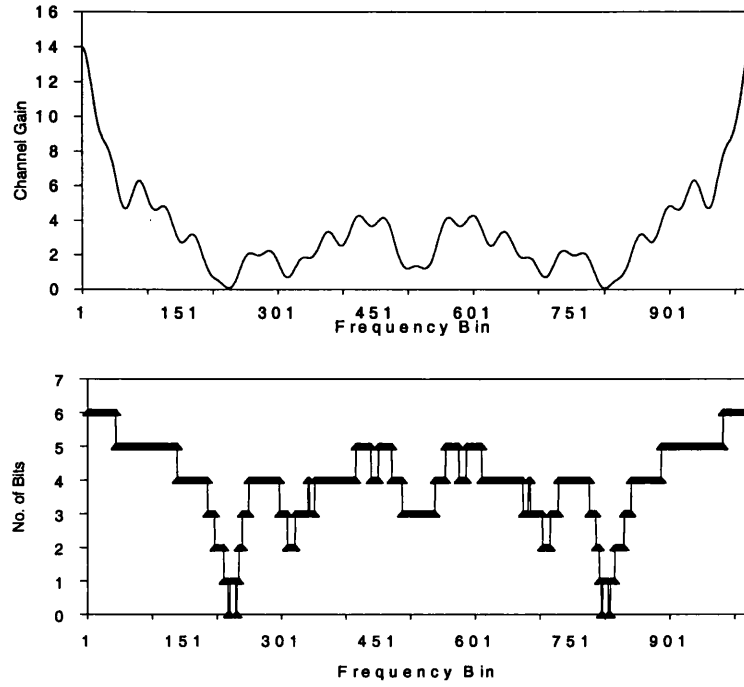
Figure 7.3.1: Channel Frequency Response for Adaptive Modulation and

Equivalent Bit Distribution

7.3.1   *Adaptive Modem Structure*

A typical OFDM adaptive modem structure is shown in Figure 7.3.1.1 below. The entire bandwidth is divided into F parallel sub-channels. An input bit stream of data rate R bits/sec is first buffered into blocks of $b = RT$ bits, where T is the symbol period. The adaptive algorithm assigns a certain number of bits, b_i, to each sub-channel where,

$$b = \sum_{i=1}^{N} b_i \,, \qquad\qquad\qquad 7.3.1.1$$

The encoder then translates the bits, b_i, into symbols, X_i, chosen from the appropriate constellations. These symbols are then OFDM transformed, cyclically prefixed and transmitted. At the receiver the inverse process is implemented where the cyclic prefix is ignored, the signal is OFDM demodulated and the symbols are decoded using simple memoryless decoder for each sub-channel. In the case of FDD-OFDM, the bit allocation parameters are passed to the receiver separately. On the other hand, in TDD-OFDM, the receiver can estimate the bit allocation parameters independently. If the bit allocation is updated every OFDM block, then a one-block delay of the channel estimate is imposed at the receiver to eliminate the mismatch between the channel parameters used at the transmitter and those used at the receiver to estimate the bit allocation parameters.
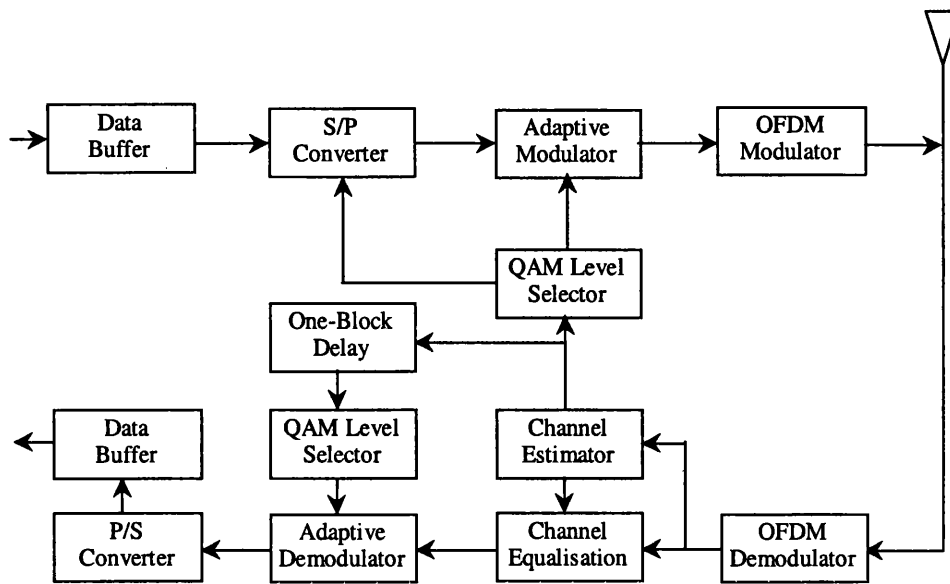
Figure 7.3.1.1: Transceiver Block Diagram of An Adaptive Modulator

7.3.2 *Existing Bit Loading Algorithms*

It has long been known that the capacity achieving energy distribution for a spectrally shaped channel corresponds to a '*water pouring*' distribution [23]. However, while the water pouring energy allocation will yield the optimal solution, it may be difficult to compute and it requires infinite granularity in constellation size, which is not realisable.

There are, at least, three multicarrier bit loading algorithms in use today, all of which are sub-optimal relative to the water pouring. These are the Hughes-Hartogs [13], Chow [14] and Fisher [15].

The Hughes-Hartogs algorithm assigns the bits successively to the sub-carriers until the target bit rate is reached. Thereby, that sub-channel is selected, for which the transmission of an additional bit can be done with the smallest additional transmit power in order to guarantee a desired performance. Unfortunately, due to the extensive sorting and searching needed with this algorithm, it is rendered as very slow for applications like mobile radio communications, where the channel may be changing very rapidly and the number of subcarriers used may be relatively high.

Chow's algorithm omits most of the extensive sorting and exploits the fact that the difference between the optimal water-pouring distribution and the flat-energy distribution is minimal. Thus the same amount of energy is assigned to all the channels used:

$$\varepsilon_n = \frac{\varepsilon}{N}$$

7.3.2.1

and the number of bits in each sub-channel is given by:

$$b_i = \log_2\left(1 + \frac{SNR_i}{\Gamma + \gamma_m}\right),$$

7.3.2.2

where SNR_i is the signal to noise ratio on sub-channel i, Γ is the SNR gap representing how far the system is from achieving capacity, and γ_m is the system performance margin, which is defined as the amount of noise that the system can tolerate while still achieving the desired bit error rate requirement. This iterative algorithm is repeated with a different set of sub-channels turned off at each step, until the optimal margin is achieved and the sum of the bits in each sub-channel equals the required target. The results presented in [14] show that the Chow's *et al* algorithm gives a very similar performance to that of [13] under a variety of conditions.

The disadvantage of the Chow's algorithm is mainly concerned with the part of the algorithm designed to establish an optimum value of γ_m which determines the speed of bit-allocation. When the wanted optimum value of γ_m is not found, this results in the possibility of having to perform extensive searching and sorting before completing the bit allocation process.

The aim of the third algorithm, proposed by Fischer *et al*, is to minimise the probability of error on each sub-channel given by:

$$P_e = K_n \cdot Q\left(\sqrt{\frac{d_n}{2\sigma_n}}\right)$$

7.3.2.3

for QAM modulated systems. K_n is the number of nearest neighbours, d_n is the minimum distance between constellation points and σ_n^2 is the variance of the noise in sub-channel i. The minimum is achieved when all the sub-channels have the same probability of error. Setting equal the error probabilities, Fischer arrives at the following equation for determining the best bit allocation per sub-carrier:

$$b_i = \frac{TBR}{F} + \frac{1}{F} \cdot \log_2\left(\frac{\prod N}{N_i^N}\right)$$

7.3.2.4

where F is the block length, TBR is the total bit rate per block and N_i is the noise power on channel i.

The simulation results of this algorithm show that its performance is almost identical to that of Chow *et al* [14].

The other algorithm examined here is based on the same principle as that of Fisher *et al* in the sense that it aims at achieving a fixed data rate using the best combination of constellations. The algorithm establishes a relationship using the information relating the BER performance of the modulation schemes to be used with the expected SNR at the receiver. In [24], the BER for an AWGN channel with MQAM modulation and identical coherent phase detection is bounded by:

$$BER \leq 2 \cdot e^{-1.5\bar{\gamma}/(M-1)},$$ 7.3.2.5

Where $\bar{\gamma}$ is the average SNR of the received signal.

A tighter bound to within 1 dB, for $M \geq 4$ and $0 \leq \bar{\gamma} \leq 30$ dB is [8]:

$$BER \leq 0.2 \cdot e^{-1.5\bar{\gamma}/(M-1)},$$ 7.3.2.6

A plot of equation 7.3.2.6 is given in Figure 7.3.2.1.
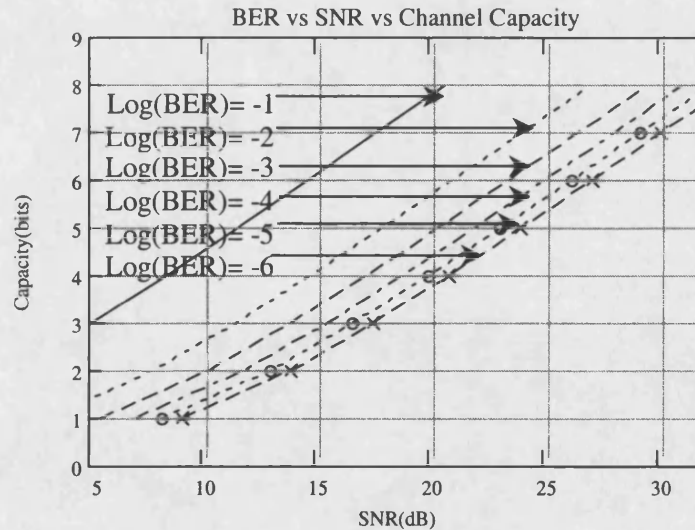
Figure 7.3.2.1: MQAM BER *vs* Es/No(dB) *vs* Capacity

The adaptive algorithm examined here utilises this relationship to allocate a suitable number of bits to every usable subcarrier. The first step however is to determine the average SNR available as well as an average bit constellation order to fulfil the required target bit rate. The

latter is a function of both the target bit rate and the number of subcarriers used. Once those two parameters are estimated the next step would be to determine an average expected BER using equation **7.3.2.6**. After determining all three parameters, the bit allocation is achieved by using the following relationship:

$$b_i = \log_2\left(1 - \frac{1.5 \cdot SNR_i}{\ln\left(\frac{BER}{0.2}\right)}\right),$$ 7.3.2.7

The scheme may be summarised in two main steps. First, it determines the (approximately) best system performance using the average SNR and constellation order required, then it guarantees that the target bit rate is reached using a sub-optimal loop.

Algorithmically, the procedure can be summarised as follows:

1. Compute the average constellation order (*AveOrder*) required to achieve the target bit rate (*TBR*) using the following:

    AveOrder = (TBR/F)

2. Compute the individual signal to noise ratios *SNR(i)* and determine the average SNR, *AveSNR*, assuming that all sub-channels, *F*, are used with a normalised energy level of unity.

3. Using the above two parameters find an estimate to the average BER using

    $$BER \le 0.2 \cdot e^{-1.57/(M-1)}$$

4. For *i=0 to F*, calculate *b(i)*, *b'(i)* and *dif(i)* according to the following:

    $$b_i = \log_2\left(1 - \frac{1.5 \cdot SNR_i}{\ln\left(\frac{BER}{0.2}\right)}\right)$$

    b'(i)= 0   *if b(i)<0*

    =MAXMAP   *if b(i)>MAXMAP*

    = RoundDown(b(i)) if (ceil(b(i))-b(i)>0.5))

    = RoundUp(b(i)) otherwise

    dif(i)= b(i) – b'(i)

    (*MAXMAP=* Maximum constellation order used)

5. Calculate the total number of bits allocated, *Btot*.

6. If *Btot > TBR*, then subtract one bit at a time from *b'(i)* on the carrier that has the smallest *dif(i)*, adjust *dif(i)* for that particular carrier and repeat until *Btot = TBR*.

7. If *Btot* > *TBR*, then add one bit at a time from b'(i) on the carrier that has the largest *dif(i)*, adjust *dif(i)* for that particular carrier and repeat until *Btot* = *TBR*.

8. Determine which subcarriers are not used and evenly distribute the power of those subcarriers over the used ones.

The determination of an average value for the SNR and the constellation order helps in achieving quick convergence to the target bit rate after the first initial bit allocation. In the presence of time-varying frequency selective fading channels, the speed of convergence of the algorithm may be vital. A comparison between the proposed algorithm and that of Fisher shows that both algorithms give similar convergence properties. As can be seen from Figure 7.3.2.2, the convergence to the targeted bit rate after the initial bit allocation is within about 90% when the target bit rate is within (20 − 90)% of the maximum achievable bit rate per block. The Chow's algorithm however, even when using 10 loops to establish an optimum value for γ_m, show erratic behaviour compared to the other two algorithms with regard to the initial bit allocation. The convergence rate for the three algorithms was measured over several different channels with different number of rays and found to be similar to that shown in Figure 7.3.2.2. The convergence rate was averaged over a period of one second of transmission time for every measurement.

(a)

163
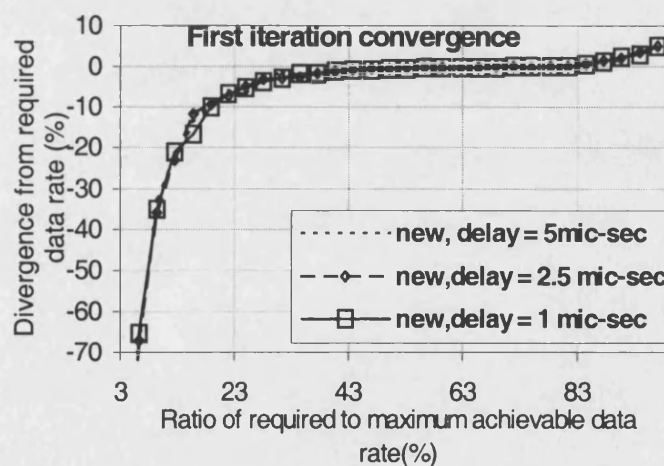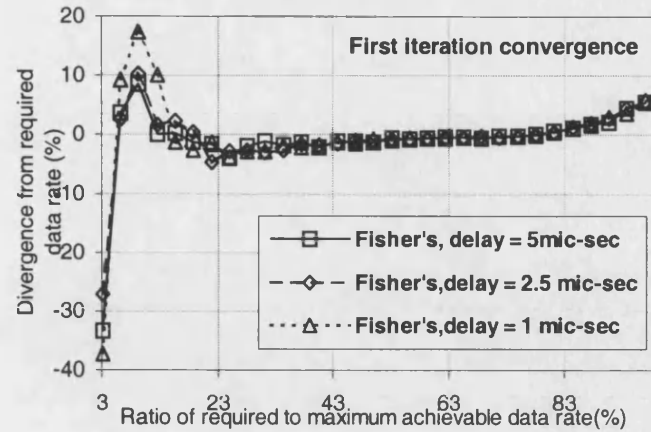
(b)
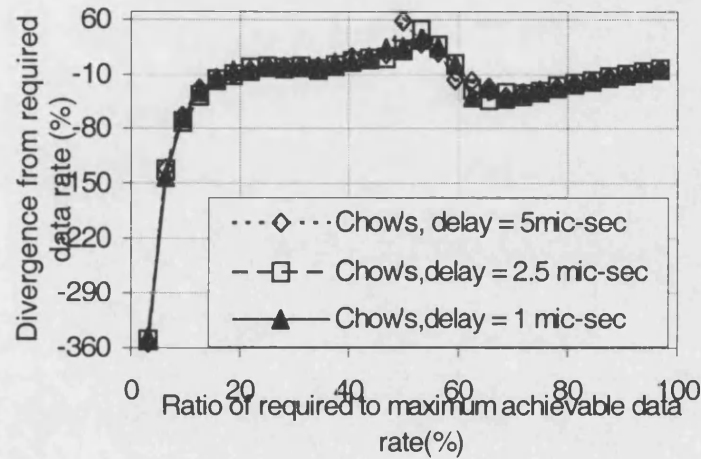
(c)

Figure 7.3.2.2: Convergence rate of the Algorithm, 6-tap TU GSM channel, Doppler = 100Hz

7.4   Constellation Schemes

The constellations used here range from 1 bit/symbol corresponding to BPSK to 8 bits/symbol corresponding to 256QAM. These are shown in Figure 7.4.1. The choice of square QAM constellations was based on their inherent spectral efficiency and ease of implementation [25]. Each constellation scheme was appropriately scaled such that the symbols corresponding to different constellation order have the same average power of unity. This ensures that all subcarriers are used with the same average power.
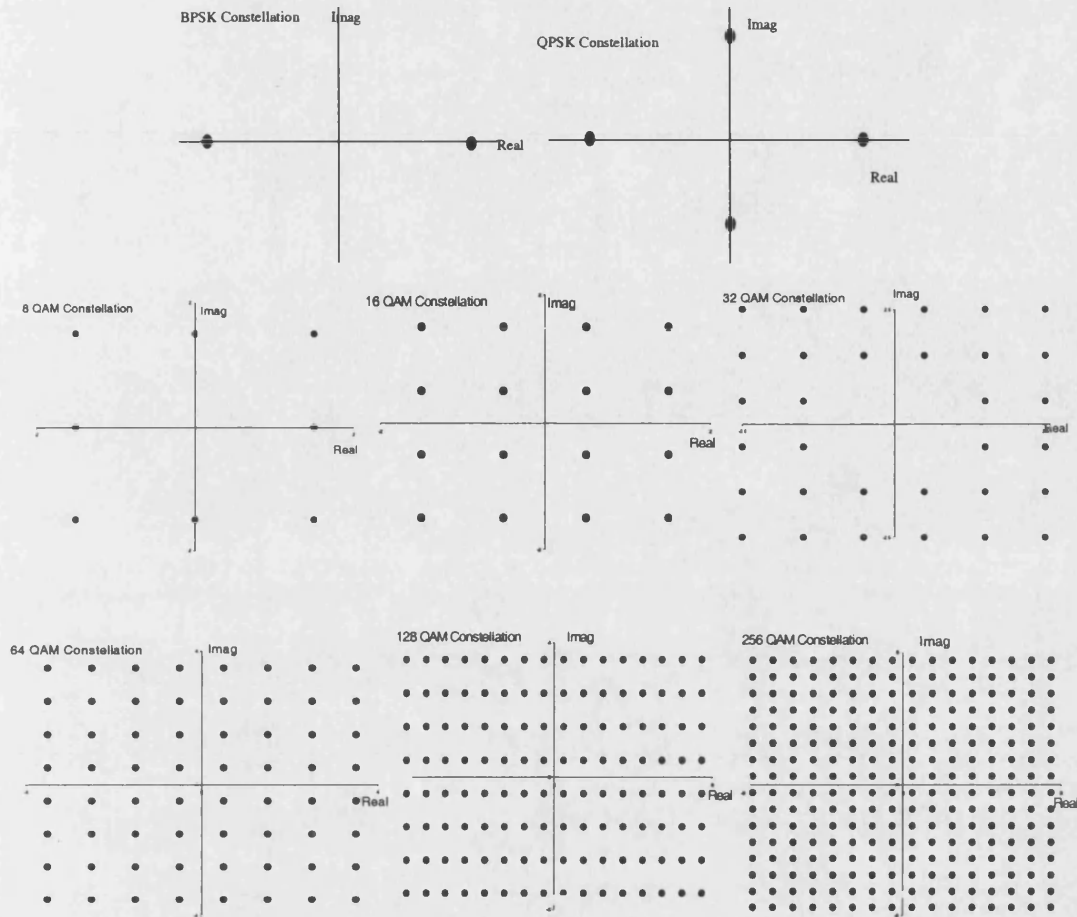
Figure 7.4.1: Constellation Diagrams of the Modulation Schemes Used

7.5 Pre-equalisation Based OFDM Systems [31]

Pre-equalisation is based on the principle of channel compensation of the data symbols prior to transmission. This will not only result in a simpler receiver structure, since no equalisation will be needed, but also protect the otherwise deeply faded symbols from being completely buried in noise. The penalty of such a technique however, is the need to have a good up to date estimate of the channel transfer function prior to transmission. Assuming that an estimate of the channel response is available and that the channel is ISI free, the optimum way of implementing pre-equalisation is to multiply the data symbols by the inverse of the channel response. If the estimate of the channel response is perfect, the received symbols would be independent of the fading statistics and only suffer from the AWGN present at the receiver. The power control policy for channel inversion is:

$$\overline{S} = \sum_{i=0}^{F-1} \hat{S}_i = \sum_{i=0}^{F-1} \frac{S_i}{\alpha_i},$$

7.5.1

Where $\overline{S}, \hat{S}_i, S_i$ = constant and α_i are the average total transmit signal power, signal power of the ith sub-carrier, the power level of the ith sub-carrier before adaptation and the channel fading level at the ith sub-carrier. The channel capacity of such system with this power adaptation strategy is derived from the capacity of an AWGN channel with a fixed received SNR:

$$C = B \log_2 (1 + SNR), \qquad\qquad\qquad 7.5.2$$

However, with channel inversion, much of the transmit-power may be used to compensate for deep fading. This has at least two major effects. The first is the fact that it might lead to producing large peak to average power ratios, PAPR, making it necessary to use non-linear amplifiers with large dynamic range. The other disadvantage is related to making the symbols which are not in deep fade more vulnerable to noise as most of their power may be compromised in the process of rescuing the symbols most affected by the deep fades. To reduce the impact of such drawbacks of this technique, two approaches can be taken [32]. The first approach is to detect the sub-carriers that are most affected by deep fades and prohibit their use. This works by monitoring the gain/attenuation of the channel and disabling the subcarriers that happen to be affected by the channel attenuations that are below a certain threshold as shown in 7.5.3

$$\hat{S}_i = \begin{cases} \dfrac{S_i}{\alpha_i} & \text{if } \alpha_i \geq \alpha_{thrsh} \\ 0 & \text{Otherwise} \end{cases}, \qquad\qquad 7.5.3$$

This technique may sometimes be referred to as *adaptive power allocation with sub-carrier blocking*. Since only sub-channels where the fading level is $\geq \alpha_{thrsh}$ are used, the average power is given by:

$$\overline{S} = \int_{\alpha_{thrsh}}^{\infty} \frac{S}{\alpha} p(\alpha) d\alpha, \qquad\qquad\qquad 7.5.4$$

Where $p(\alpha)$ is the probability of $\alpha \geq \alpha_{thrsh}$

In order to keep the average transmit power constant regardless of the number of useful sub-carriers, after power allocation, all the used sub-carriers are scaled by a factor such that the total transmit power is kept unchanged.

Because some of the subcarriers will not be used, this results in a variable bit rate transmission, which may not be a useful technique for applications that require a constant bit

rate. In other words, this approach compromises the system's capacity to minimise the BER performance of the system.

The second technique that can be used in conjunction with pre-equalisation uses a threshold-based estimate of the inverse of the channel transfer function as shown in **7.5.5** below.

$$\hat{S}_i = \begin{cases} \dfrac{S_i}{\alpha_i} & \text{if} \quad \alpha_i > \alpha_{thrsh} \\[2mm] \dfrac{S_i}{\alpha_{thrsh}} & \text{Otherwise} \end{cases}, \qquad\qquad 7.5.5$$

Such system uses what is called *controlled channel inversion*, and the average transmitted power of this system is given by:

$$\overline{S} = \int_{-\infty}^{\alpha_{thrsh}} \frac{S}{\alpha_{thrsh}} p(\alpha) d\alpha + \int_{\alpha_{thrsh}}^{\infty} \frac{S}{\alpha} p(\alpha) d\alpha, \qquad\qquad 7.5.6$$

In the simulation used here, the complex alphabets representing the modulated symbols are modified as shown below according to the channel inversion technique used.

Total Channel Inversion:

$$X_i = \frac{X_i}{H_i},$$

Sub-carrier Blocking:

$$X_i = \begin{cases} \dfrac{X_i}{H_i} & \text{if } |H_i| > thrsh \\[2mm] 0 & \text{Otherwise} \end{cases},$$

Controlled Channel Inversion:

$$X_i = \begin{cases} \dfrac{X_i}{H_i} & \text{if } |H_i| > thrsh \\[2mm] \dfrac{X_i}{thrsh \cdot e^{\angle H_i}} & \text{Otherwise} \end{cases},$$

Where, X_i is the symbol transmitted on the ith subcarrier and H_i is the corresponding channel response at that subcarrier. The threshold level depends on the peak to average power ratio of the system. If the mapping used is only phase dependent, the mismatch between the actual channel response and that used at the transmitter, produced by the threshold operation, will not result in any performance degradation. If, on the other hand, a mapping scheme that uses amplitude and phase is used, such as QAM modulation, this mismatch will result in irreducible BER floors, unless compensated for at the receiver.
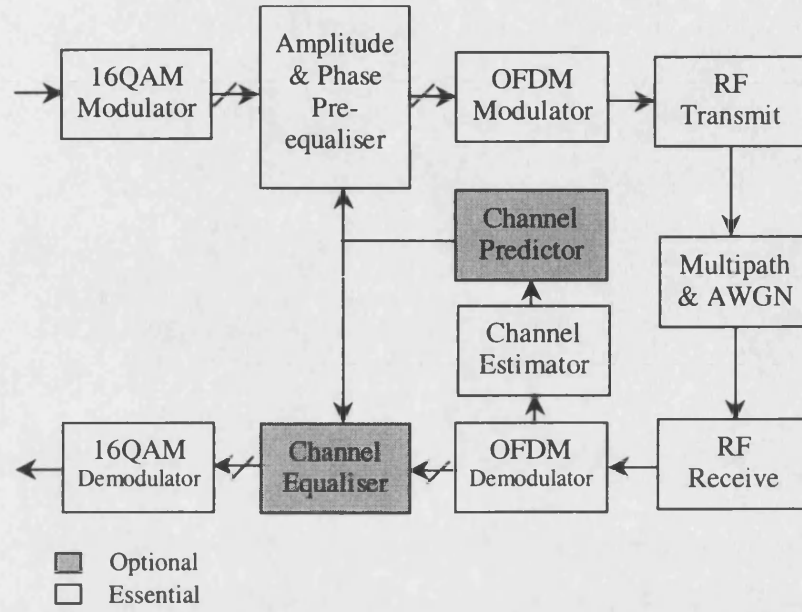
Figure 7.5.1: Schematic Block Diagram of Pre-Equalisation Based OFDM System

7.5.1 *Theoretical BER Performance*

For the full channel inversion, the theoretical BER performance is the same as that of an AWGN channel. In [8] the BER for an AWGN channel with MQAM modulation and ideal coherent phase detection is tight bounded to within 1dB for $0 \leq SNR \leq 30$ dB by:

$$BER_{AWGN} \approx \frac{1}{5} \cdot \exp\left(\frac{-3 \cdot SNR}{2 \cdot (M-1)} \right),$$
7.5.1.1

In fact **7.5.1.1** serves as a lower bound for $M = 2$ and an upper bound for $M \geq 4$.

For the sub-carrier blocking technique, the average SNR of the system is increased in accordance with number of disused sub-carriers. Therefore, assuming a Rayleigh fading environment the BER performance may be given by:

$$BER_{AWGN} \approx \frac{1}{5} \cdot \exp\left(\frac{-3 \cdot SNR \cdot (1+\rho)}{2 \cdot (M-1)} \right)$$

$$\rho = \int_{\alpha=-\infty}^{\alpha < \alpha_{thrsh}} \frac{\alpha}{\sigma^2} \cdot \exp\left(\frac{-\alpha^2}{2\sigma^2} \right) d\alpha$$
7.5.1.2

where $0 \leq \rho < 1$ is the probability of $\alpha < \alpha_{thrsh}$,

In the case of controlled channel inversion, the received SNR of some of the sub-carriers will be set by the fixed threshold used and the corresponding channel fade at that position. Using **7.5.1.1** and assuming that the sub-carriers which are affected by the threshold have a constant SNR, the BER performance of the controlled channel inversion method can be approximated by:

$$BER \approx \frac{1}{5} \cdot \left(\exp\left(\frac{-3 \cdot SNR_1}{2 \cdot (M-1)} \right) \cdot (1 - \rho) + \exp\left(\frac{-3 \cdot SNR_2}{2 \cdot (M-1)} \right) \cdot \rho \right), \qquad 7.5.1.3$$

Where ρ is as defined in **7.5.1.2** and SNR_1 and SNR_2 correspond to the average SNR of the sub-carriers which are above the threshold and those which are below it, respectively.

7.6 Adaptive Subcarrier Allocation

The idea of adaptive subcarrier allocation is based on assigning the subcarriers according to the channel transfer function of all users such that the total power received by all users is the global maximum. In other words, given the channel transfer function of all users, what is the best way of allocating the subcarriers such that the total power required at the transmitter to achieve a certain performance is the absolute minimum. Mathematically, this can be stated as follows:

$$P_R = \max \sum_{i=0}^{N-1} \sum_{n=0}^{Nu-1} \alpha_{i,n} \cdot \chi_{i,n}, \qquad 7.6.1$$

where

P_R is the total power received by all users

$\alpha_{i,n}$ is the channel gain of the ith user at the nth subcarrier and

$\chi_{i,n}$ is a binary number to insure that users do not share the same subcarrier and is defined by the following:

$$\sum_{n=0}^{N-1} \chi_{i,n} = Nsu_i \quad \& \quad \sum_{i=0}^{Nu-1} \chi_{i,n} = 1,$$

where

Nsu_i is the total number of subcarriers of the ith user.

Nu is the total number of users

The conditions and assumptions sought here are:

1- No more than one user can use the same sub-carrier at the same time.

2- Subcarriers are equally distributed between users

3- Subcarriers are allocated based on maximising the total power received by all users

4- Users have equal data throughput and fixed constellation order

Although different conditions and assumptions may be used in practice, for example allocate different number of subcarriers or allow different quality of services to the active users, the basic principle remains valid and is flexible enough to be used under a variety of conditions. Once the optimum allocation has been determined, the transmitted power for the individual users is adjusted according to the required performance. In this analysis we assume, without loss of generality, that all users have equal quality of service and have the same noise power level at the receiver. Therefore, the power at the transmitter is distributed between the users such that the power received by the individual users is identical.

It is clear form equation 7.6.1 that this is a constrained non-linear optimisation problem for which it may be difficult to give a closed-form solution. Instead, iterative numerical solutions are normally used. In here we examine two iterative methods of finding an optimum distribution of the subcarriers. The first is based on finding the global maximum through extensive searching. If equation 5.6.1 is rewritten in the following matrix format:

$$P_R = \sum (\aleph \cdot A) = \sum P_R ,$$

7.6.2

Where:

A, $\aleph$ and P_R are $N \times Nu$, $Nu \times N$ and $1 \times Nu$ matrices, respectively.

$$A = \begin{bmatrix} \alpha_{0,0} & \alpha_{0,1} & \cdots & \alpha_{0,N-1} \\ \alpha_{1,0} & \alpha_{1,1} & \cdots & \alpha_{1,N-1} \\ \vdots & \vdots & \vdots & \vdots \\ \alpha_{Nu-1,0} & \alpha_{Nu-1,1} & \cdots & \alpha_{Nu-1,N-1} \end{bmatrix}, \aleph = \begin{bmatrix} \chi_{0,0} & \chi_{1,0} & \cdots & \chi_{Nu-1,0} \\ \chi_{0,1} & \chi_{1,1} & \cdots & \chi_{Nu-1,1} \\ \vdots & \vdots & \vdots & \vdots \\ \chi_{0,N-1} & \chi_{1,N-1} & \cdots & \chi_{Nu-1,N-1} \end{bmatrix}$$

$$P_R = \begin{bmatrix} P_0 & P_1 & \cdots & P_{Nu} \end{bmatrix}$$

Each row of $\aleph$ contains one 1 and $Nu-1$ 0s where each column contains Nus 1s and $N - Nus$ 0s. The idea is to find all the possible forms of $\aleph$ and work out the total corresponding power using equation 7.6.2. The algorithm keeps a record of only the form of $\aleph$ that produces the largest total power. The position of the ones for each user determines the allocated subcarriers for that user. Therefore in order to insure that the global maximum is reached, all the different combinations must be tested exhaustively. This technique is based on the maximum likelihood criterion in the sense that it searches through all possible combinations to find the optimum one. Clearly, when the number of users and the number of subcarriers are large, such searching method becomes computationally cumbersome.

In a time variant channel, the subcarrier allocation process may be repeated continuously every t interval of time. Thus a fast converging algorithm is very desirable. In order to

achieve a fast subcarrier allocation, a sub-optimal algorithm is sought. The sub-optimal algorithm used here is based on searching through every column of **A**, starting from column one, and assigning the best subcarrier to its corresponding user. Once the total number of subcarriers for that user is reached, this user is dropped from the rest of the search. Once all the users are assigned their subcarriers, the process is repeated starting from the second column onwards, and so on. At each stage, only one subcarrier allocation that results in the largest total power is kept. The process is then repeated from the Nth subcarrier backwards, repeating the same process as before. In other words, this algorithm finds the subcarrier allocation that produces the best local maximum out of $2N$ local maximums. This algorithm may be summarised in steps as shown below:

1- Starting from subcarrier one, allocate that subcarrier to the user that has the highest channel gain at this position.

2- Repeat step one until all subcarriers are allocated.

3- If the total number of subcarriers is reached for one user, this user is dropped from the rest of the search.

4- Once all subcarriers are allocated, find the total power (channel gain)

5- Repeat the above steps, starting from the next subcarrier downwards

6- Compare the total power and keep the subcarrier allocation with the highest total power

7- Once all possibilities up to N are examined the search starts again in the opposite direction, i. e the Nth downwards repeating step 1 to 6.

To speed up this algorithm, not all the combinations may be used. This however might reduce the accuracy of the optimisation algorithm.

When this adaptive technique is used, the users have to be continuously informed of their corresponding subcarriers every time the subcarriers are redistributed.

7.7 Simulations and Results

The simulation parameters used are summarised in **Table 7.7.1** below. We assume a downlink TDD-OFDM multi-user scheme. The symbol rate was chosen such that the system can provide twenty users at 2Mbps each at full stretch. It is assumed that the block processing time is equal to the block transmission time and that synchronisation errors are negligible.

Symbol Rate	10Msps	Maximum Delay	5μsec
Mapping Scheme	QAM16, Variable	Cyclic Prefix	5μsec
Channel Type	GSM 6 tap urban	Doppler Frequency	100Hz
No. of sub-carriers	1024	Symbol Duration	100.48μsec
Coding Rate	½ Rate Convolutional	Constraint Length	7

Table 7.7.1: Simulation's Parameters

7.7.1   *Estimation of Channel Gain and Noise Power*

An initial estimate of the channel frequency response and the noise power level at the receiver is established using a PN sequence, which is known at both the transmitter and the receiver. Once the initial estimate of the channel response is established, the noise power level can be determined by equalising the received PN sequence and then correlating it with an orthogonal PN sequence of the same length. To up date the channel at both the transmitter and receiver, the scattered pilot tone channel estimation technique was used. The percentage of pilot tones used is 10% for urban channels and 25% for hilly channels The interpolation and filtering was carried out using the FTD based technique described in chapter five. To obtain an estimate of the noise power level at the receiver the received symbols are equalised and a new estimate of the channel frequency response is generated using decision directed feedback. This is then inverse Fourier transformed and the samples beyond the maximum delay spread of the channel are then considered to be purely noise and therefore the maximum likelihood estimate of the noise variance, σ^2, is given by:

$$\sigma^2 = \frac{1}{2} \cdot \frac{\sum_{i=M}^{F} h_i \cdot h_i^*}{F - M},$$
       7.7.1.1

where F and M are the total number of sub-carriers and maximum delay spread of the channel, respectively. Such method is usable when the number of subcarriers is large and the maximum delay spread of the channel is relatively short.

7.7.2   *BER Performance of the Adaptive Modulation Scheme*

A comparison between the Chow's method, Fisher's method and the proposed algorithm is presented in Figure 7.7.2.1 (a), (b), (c) and (d) below. From these figures, it is evident that the Chow *et al* algorithm slightly outperforms the other two. This is however due to the fact

that Chow's algorithm includes power adjustment after the bit allocation process. The power adjustment is achieved by comparing the allocated number of bits and their corresponding SNR on every sub-channel to the required average BER and then adjusting the total average power such that it remains unchanged. It can also be seen from these figures that at SNR >20dB an average improvement of about 4 – 10dB is obtained over the fixed modulation scheme, depending on the type of channel encountered. For these simulations, the received symbols were equalised using a perfect channel estimate.
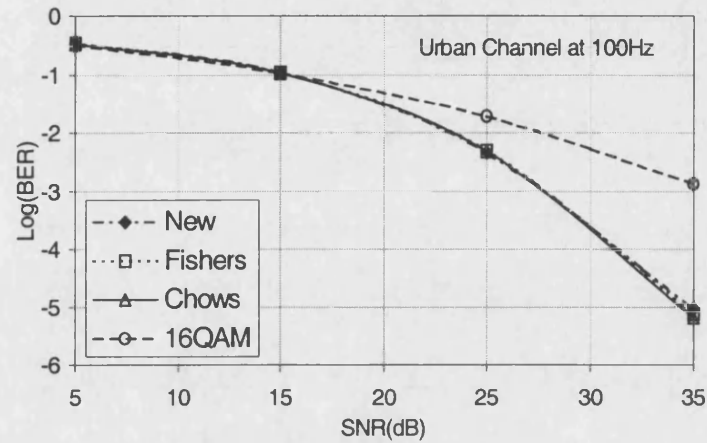
(a)
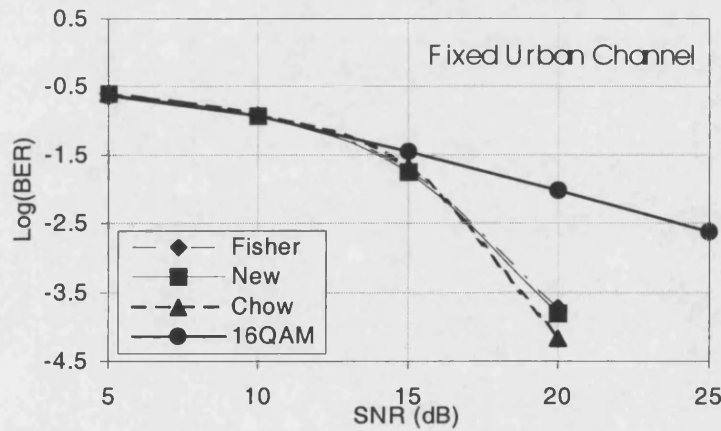
(b)

Figure 7.7.2.1: Comparison Between Existing and Proposed Algorithm, (a) at Doppler = 100Hz in Urban Channel and (b) in a Static Urban Channel
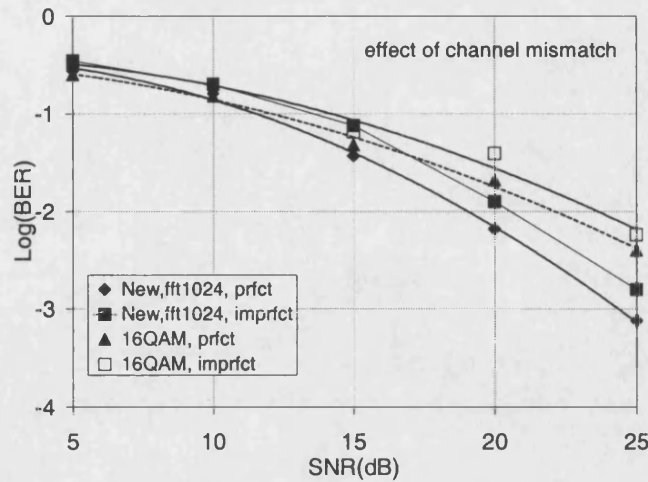
Figure 7.7.2.2: Impact of Channel Mismatch

The wider the constellation range that can be used, the closer to optimum the bit allocation will become. However, the complexity of such an adaptive system increases in proportion to the maximum constellation order used. Thus, it would be useful to determine a maximum constellation order such that the resulting BER degradation incurred by imposing such limitation may be considered negligible. Unfortunately, this is largely channel dependent as the distribution of power amongst the subcarriers is determined by the relative strength of the multipath rays. For both the urban and hilly channels used in these simulations, it was found that negligible performance improvement is obtained when the constellation range is increased by more than an order of two beyond the minimum constellation order required. For instance, in Figure 7.7.2.3 (a), the minimum constellation order required to fulfil the bit rate per block of 2048 bits, is 2 bits per symbol corresponding to QPSK modulation. It can be seen from this figure that when the constellation range is increased beyond 4 bits per symbol, the improvement obtained is hardly noticeable. Similar results were obtained when the minimum required constellation order is increased to 4 (16QAM) and 5 (32QAM) as can be seen from Figure 7.7.2.3 (b) and (c) below.

(a)

(b)

(c)
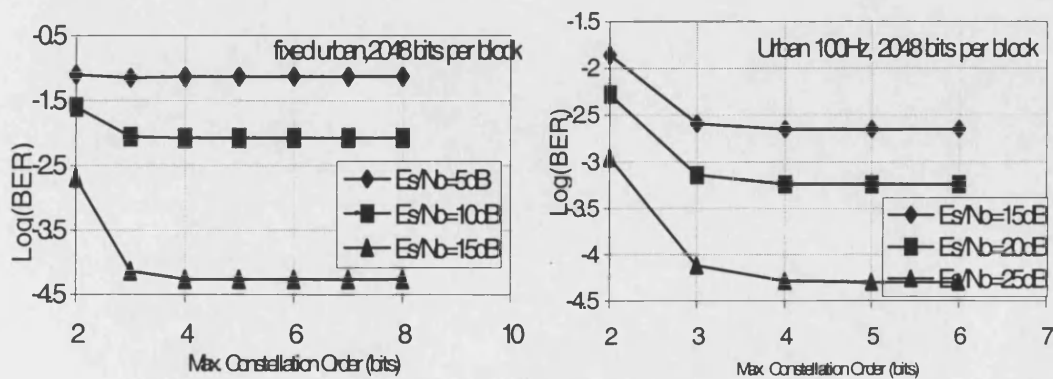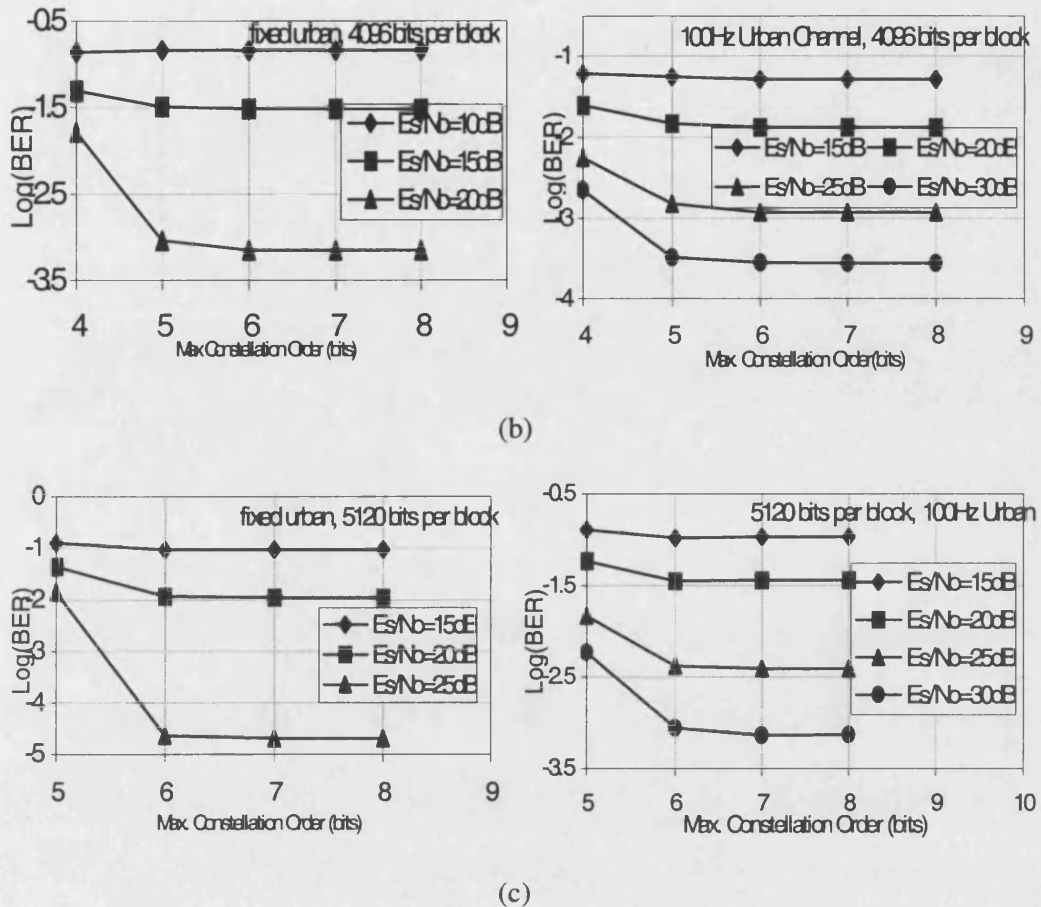
Figure 7.7.2.3: Sensitivity to Modulation Diversity Range

The above experiments were repeated using the other two bit-loading algorithms and were found to give a similar performance.

In mobile radio communications, the speed of the bit-loading algorithm is vital. Since the target bit rate of the system simulated here falls within the 20-90 % of the maximum achievable bit rate only a maximum of 10% of the target bit rate is required to be added/removed to reach the target bit rate. This is done by recursively adding/removing one bit at a time to the subcarrier that requires the least/most amount of energy. Every time one bit is added/removed, the subcarriers are re-indexed according to the least/most required energy level to add/remove one bit. In order to reduce the repetition of such process to a single iteration only, the subcarriers that require the least/most amount of energy are used simultaneously to reach the target bit rate in after a single indexing operation only. In Figure 7.7.2.4 it can be seen that limiting the sorting operation to a single iteration almost makes no difference to the systems performance.
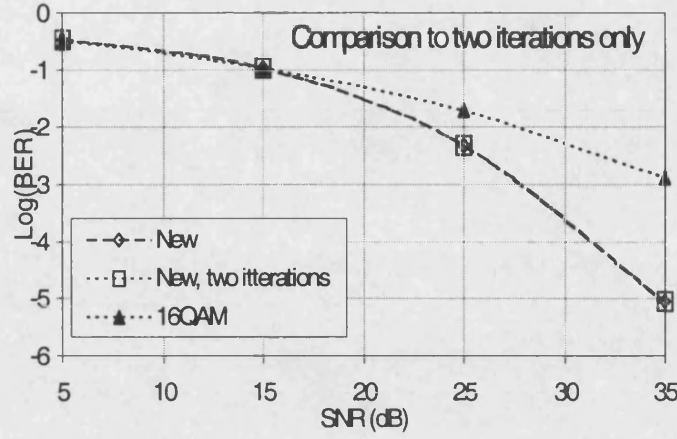
Figure 7.7.2.4: Effect of Two-Time-Fill Adaptive OFDM Using the New Technqiue in Urban Channel at Doppler = 100Hz

Determining how long the channel gains remain within specific regions is of great importance when using adaptive modulation as this impact on the total number of calculations needed per block. The aim is to establish a theoretical measure of the rate of change of the channel such that it can be used as a guide to control the rate of adaptation. Lee, [29], gives a measure of the average time that the channel amplitude stays below a certain level, better known as the average fade duration, AFD. What is required in this case however is the average time, τ_{av}, during which the channel amplitude stays between two certain levels. This will be referred to here as the average fade region duration, AFRD. Using the finite state Markov channel model derived in [30], Goldsmith *et al* [8] established a relationship relating the AFD of [29] to the average fade region duration. Since the fading in [30] was assumed to remain within one region over a symbol period and can only transition to the same region or adjacent regions, this assumption is consistent with the model used here. The transition probabilities between regions under such assumption are given as:

$$p_{j,j+1} = \frac{lcr_{j+1}T_s}{\pi_j}, \quad p_{j,j-1} = \frac{lcr_j T_s}{\pi_j}$$

$$p_{j,j} = 1 - p_{j,j+1} - p_{j,j-1}$$

7.7.2.1

where $lcr_j = f_D e^{-L_j/\bar{\gamma}} \cdot \sqrt{2\pi L_j / \bar{\gamma}}$ is the level crossing rate at level L_j for Rayleigh channels and π_j is the steady state distribution corresponding to the jth region. Assuming that the time in which the Markov process stays in a given state is geometrically distributed, the value of τ_{av} is given by [8]:

$$\tau_{av} = \frac{\pi_j}{lcr_{j+1} + lcr_j}$$

7.7.2.2

176

Table presents the values of AFRD corresponding to five regions (M_j=0,2,4,16,64) in Rayleigh fading for f_D = 100Hz and two average power levels $\bar{\gamma}$ =10dB and $\bar{\gamma}$ =20dB. Because in OFDM transmission all the modulation schemes used are transmitted in parallel, to reduce the risk of performance degradation, the adaptation rate must not exceed the lowest value of AFRD at the corresponding $\bar{\gamma}$.

Region(j)	$\bar{\gamma}$ =10 dB	$\bar{\gamma}$ =20 dB
0	2.23ms	0.737ms
1	0.830ms	0.301ms
2	3.0ms	1.06ms
3	2.83ms	2.28ms
4	1.43ms	3.84ms

Table 7.7.2.2: AFRD at f_D = 100Hz for rayleigh Fading

It can be seen from Figure 7.7.2.5 that the systems performance degrades as the re-adaptation rate is increased beyond the maximum theoretical value, in this case 0.301ms and the block length is 0.1024ms. When the re-adaptation rate reaches the coherence time of the channel the performance degradation incurred almost saturates around a fixed value.
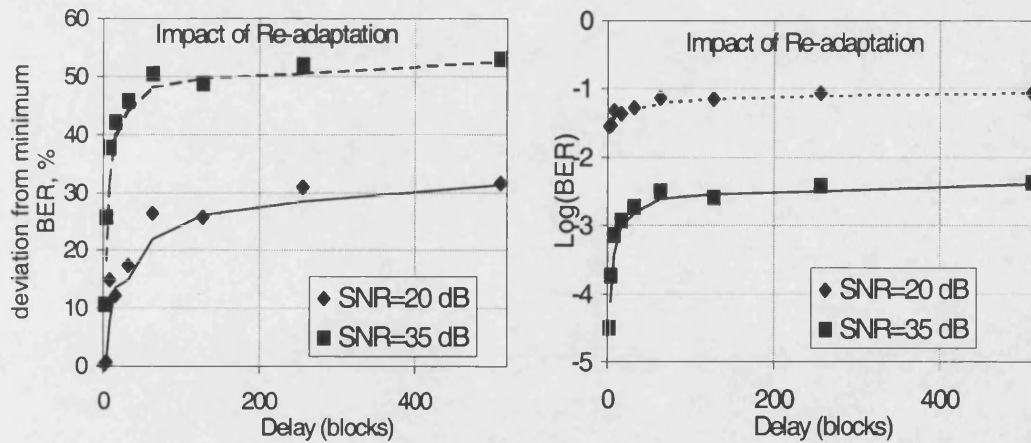
Figure 7.7.2.5: Sensitivity Adaptation Time to Doppler

7.7.3   *BER Performance of the Pre-equalisation Scheme*

Figure 7.7.3.1 shows the impact of using pre-equalisation under static channel conditions. It is self evident from this figure that the advantage of employing such technique is considerable. It can also be seen that the performance of such system, under the assumption

177

of a perfect channel estimate, is equivalent to that of the same mapping scheme in an AWGN channel. To reduce the maximum dynamic range of the transmitter's amplifier, the threshold technique of equation 5.5.5 was implemented for two dynamic ranges of 5 dB and 10 dB. The results shown in Figure 7.7.3.1and Figure 7.7.3.2 show the impact of using a threshold based technique and highlight the importance of compensation for the threshold operation, which becomes more important as the dynamic range is reduced. A close inspection of these figures shows that although threshold compensation at the receiver significantly improves the system's performance, some degradation (about 6 dB for the 5 dB dynamic range and SNR = 20dB) is incurred due to the strength of the deep fade at that location.

The other major drawback of pre-equalisation is its sensitivity to time variations. The impact of such drawback becomes more pronounced in proportion to the time variation of the channel and increased modulation order. In Figure 7.7.3.4 it can be seen that a time delay of one block duration results in severe performance degradation. In fact in such situation pre-equalisation performs much worse than using equalisation at the receiver. In order to make use of pre-equalisation without allowing the time variation influence of the channel to degrade its performance, equalisation at the receiver was also used to compensate for the channel variation. A one block delayed copy of the channel transfer function is first used to undo pre-equalisation, this is then followed by normal equalisation using an up to date estimate of the channel response. By doing so, the impact of the noise on the subcarriers falling in the deep fade region is reduced by the first step, then the equalisation process takes care of the channel induced amplitude and phase shifts.

It can be seen from Figure 7.7.3.4 that channel prediction may be successfully used to overcome the effect of time variation on the channel inversion method. It is however clear from this figure that although such a technique considerably improves the performance of a channel inversion based system, it leads to irreducible BER floors. This is due to the residual mismatch between the true channel transfer function and the predicted one.
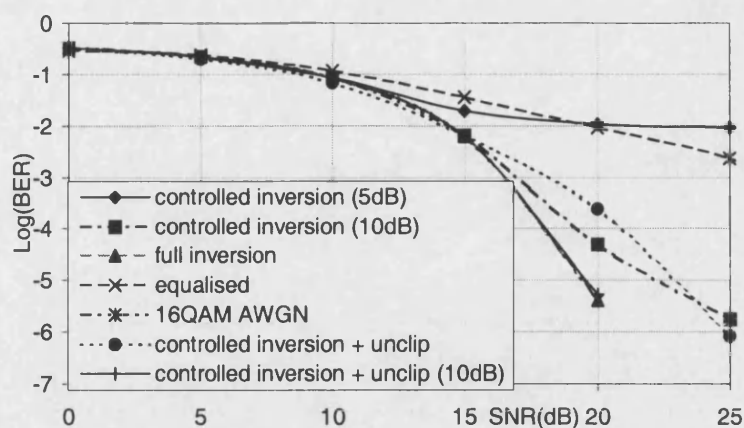
Figure 7.7.3.1: Impact of Channel Inversion Under Static Conditions (i.e 0 Hz Doppler)
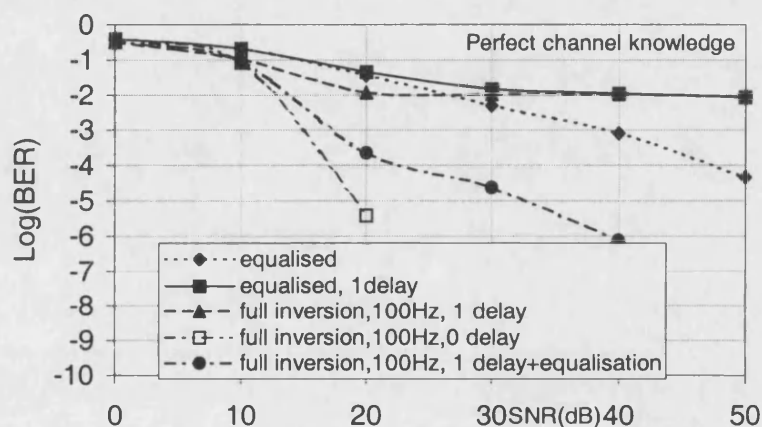
Figure 7.7.3.2: Impact of Time-Variation
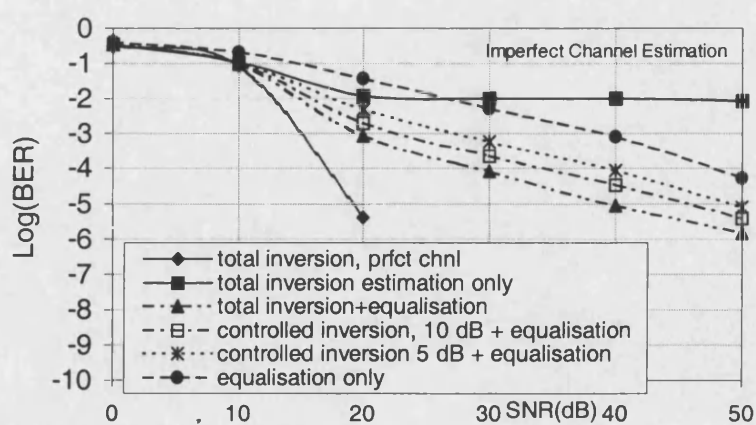
Figure 7.7.3.3: Imperfect Channel Estimation
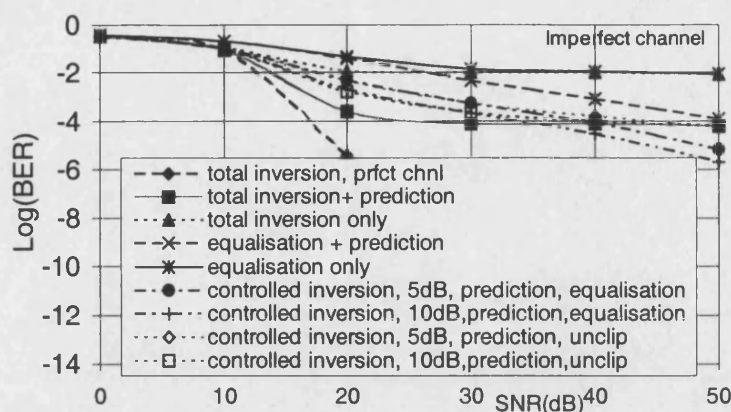
Figure 7.7.3.4: Channel Inversion with Prediction

7.7.4 *Adaptive Subcarrier Allocation*

To keep the computational load feasible, the optimum subcarrier allocation method was examined under time invariant conditions where the subcarrier allocation needs only to be evaluated once. In addition, the number of subcarriers was kept at 64 and the number of users at 6. In Figure 7.7.4.1 it can be seen that degradation incurred by using the sub-optimal method is about 1dB. It can also be seen that the improvement obtained by using such technique is over 10dB in terms of SNR. The same simulation test was then redone in a time variant channel using only the sub-optimal technique and the parameters given in **Table 7.7.1**. It can be seen from Figure 7.7.4.2 that the improvement gained in this environment is in the order of 7 dB. To keep the simulation running-time to a minimum, the sub-optimal searching algorithm was set to look through only 100 possible maximums.
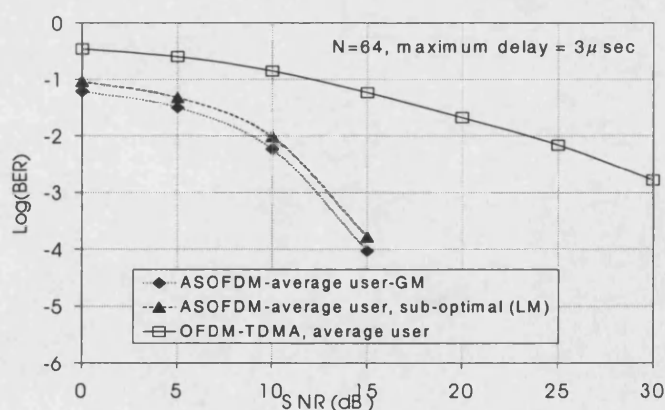
Figure 7.7.4.1: With Subcarrier Allocation, N=64, No. Of Users =6, Perfect Channel

Estimate
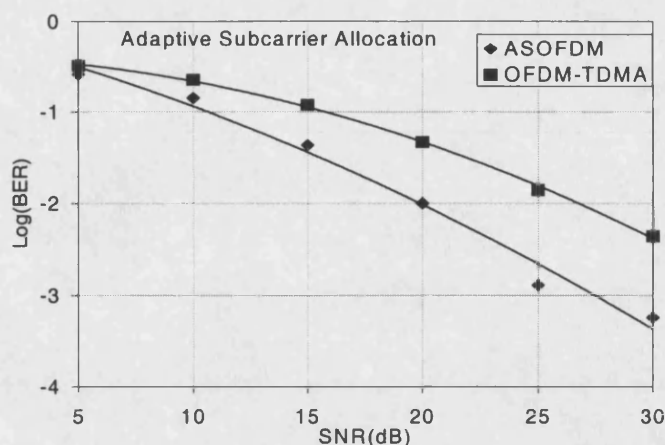
Figure 7.7.4.2: With Subcarrier Allocation in Time Variant Channels,
N=1024, No. of Users = 10, Perfect Channel Estimate

7.8 Conclusion

In this chapter the use of adaptive OFDM techniques was examined. In particular three adaptation strategies were compared. These were the fixed-power adaptive-constellation, fixed-constellation adaptive-power using channel inversion and adaptive subcarrier allocation.

For the adaptive constellation scheme, three adaptation algorithms were examined. It was shown that all three algorithms have almost identical BER performance. When compared on the basis of speed of convergence however, it was found that the Chow's algorithm can be the slowest. This is because there is no guarantee that the sub-optimal loop designed to speed up the convergence rate of the algorithm will always converge to the correct starting value. We also explored the impact of restricting the number of constellation levels and found that minimum improvement is obtained when the number of levels is increased by more than two levels above the average required constellation level. It was shown that using fixed power adaptive modulation provides as much as 7dB-performance improvement at BER = 10^{-3} over fixed power fixed modulation techniques. A measure of how fast the transmitter needs to adapt to the continuously changing channel was also given. The feasibility of such measure is however dictated by hardware constraints.

The use of adaptive power control using channel inversion has shown very promising results. An improvement of as much as 15 – 20 dB was obtained compared with fixed power techniques. Such technique is however sensitive to channel variations unless this is compensated for at the receiver. The use of controlled channel inversion combined with compensation at the receiver has been shown to be a good compromise that provides

considerable improvement over fixed power techniques as well as limited peak to average power ratio. Channel prediction was also examined and it was shown that although it provides significant improvement in the absence of channel compensation at the receiver, it also leads to irreducible BER floors. This is because of the residual difference between the actual and predicted channel transfer function.

The use of subcarrier allocation in a multi-user environment was also investigated. An optimum algorithm was suggested. This algorithm however requires a large number of computations that may not be desirable especially in a time variant channel. Instead, a sub-optimal iterative algorithm that is based on finding the best subcarrier allocation out of $2N$ possibilities was given. Using this scheme an improvement of about 7dB is obtained over non-adaptive schemes.

It can be concluded that the adaptive power technique is the simplest to implement and provides the best overall performance improvement. Adaptive subcarrier allocation was found to be the second best even when using a sub-optimal allocation algorithm. In addition, these two techniques only need the channel transfer function and do not require information about the noise level at the receiver that the adaptive constellation technique requires.

7.9 Reference

[1] J. F. Hays, " *Adaptive Feedback Communications*", IEEE Transactions on Communications, vol. COM-16, pp. 29-34, Feb. 1968.

[2] J.K Cavers, "*Variable Rate Transmission for Rayleigh Fading Channels*", ", IEEE Transactions on Communications, vol. COM-20, pp. 15-22, Feb. 1972.

[3] W. T. Webb, and R. Steele, "*Variable Rate QAM for Mobile Radio*", IEEE Transactions on Communications, Vol. 43, pp. 2223-2230, July 1995.

[4] J. M. Torrance and L. Hanzo, "*Optimisation of Switching Levels for Adaptive Modulation in Slow Rayleigh Fading*", IEE Electronics Letters, pp. 1167-1169, June 1996.

[5] B. Vucetic, "*An Adaptive Coding Scheme for Time Varying Channels*", IEEE Transactions on Communications, Vol. 49, pp. 653-663, May 1991.

[6] S. M. Alamouti and S. Kallel, "*Adaptive Trellis-Coded Multiple Phased Shift Keying for Rayleigh Fading Channels*", IEEE Transactions on Communications, Vol. 42, pp. 2305-2304, July 1994.

[7] T. Ue, S. Sampie, and N. Morinaga, "*Symbol Rate and Modulation Level Controlled Adaptive Modulation/TDMA/TDD for Personal Communications*", Proceedings of VTC'95, pp. 306-310, July 1995.

[8] A. J. Goldsmith and S-G. Chua, "*Variable Rate Variable Power MQAM For Fading Channels*", IEEE Transactions on Communications, Vol. 45, pp. 1218-1230, Oct. 1997.

[9] A.M Monk and L. B. Milstein, "*Open-loop Power Control Error in a Land Mobile Satellite System*", IEEE JSAC, Vol. 13, pp.205-212, Feb. 1995.

[10] J.L. Rose, "*Optimum Utilisation of the Channel Capacity of A Satellite Link in the Presence of Amplitude Scintillations and Rain Attenuation*", IEEE Transactions on Communications, Vol. 38, pp. 1958-1965, Nov. 1990.

[11] R.V. Cox, J. Hagenauer, N. Seshadri and C. E. W. Sundberg, "*Subband Speech Coding and Matched Convolutional Channel coding for Mobile Radio Channels*", IEEE Transactions on Signal Processing, Vol. 39, pp. 1717-1731, Aug. 1991.

[12] W.T. Webb and L. Hanzo, "*Modern Quadrature Amplitude Modulation, Principles and Applications for Fixed and Wireless Channels*", IEEE Press, 1994.

[13] D. Hughes-Hartogs, "*Ensemble Modem Structure For Imperfect Transmission Media*", US Patent, Nos. 4679227,.July 1987, 4731816 March 1988 and 4833706 May 1989.

[14] P. S. Chow, J. M. Cioffi and J. A. C. Bingham, "*A Practical Discrete Multitone Transceiver Loading Algorithm for Data Transmission Over Spectrally Shaped Channels*", IEEE Transactions on Communications., 43(2/3/4), pp. 773-775, Feb. /March/Apr. 1995.

[15] R. F. H. Fischer and J. B. Huber, "*A New Loading Algorithm for Discrete Multitone Transmission*", Proceedings of IEEE Globcom'96, pp. 724-728, London, Nov. 1996.

[16] CCITT Draft Recommendation V.34: "*A Modem Operating at Data Signalling Rates of up to 28800 bits/s for Use on the General Switched Telephone Network and on Least Point to Point 2-Wire Telephone Type circuits* ", 1993.

[17] IMT-2000: Standards Efforts of the ITU, IEEE Personal Communications, vol. 4, Aug. 1997.

[18] ETSI Tdoc SMG2 95/97, EDGE Feasability Study, Work Item 184: " *Improved Data Rates Through Optimised Modulation*", version 0.3, Dec. 1997.

[19] P. Schramm, H. Andereasson, C. Edholm, N. Edvardssona, M. Hook, S. Javerbring, F. Muller and J. Skold, "*Radio Interface Performance of EDGE, A Proposal for Enhanced Data Rates in Existing cellular Digital Systems*", Proceedings of the IEEE VTC'98, pp. 1064-1068, 1998.

[20] A. Furuskar, M. Frodigh, H. Olofsson and J. Skold, " *System Performance of EDGE, A proposal for Enhanced Data Rates in Existing Digital Cellular Suystems*", Proceedings of the IEEE VTC'98, pp. 1284-1289, 1998.

[21] R. Steele and W.T. Webb, "*Variable Rate QAM for Data Transmission Over Rayleigh Fading Channels*", Keynote Paper, Wireless'91, Calgary Alberta, July 1991.

[22] R. G. Gallager, "*Information Theory and Reliable Communication*", Wiley, 1968.

[23] G. D. Forney and M. V. Eyuboglu, "*Combined Equalisation and Coding using Precoding*", IEEE Communications Magazine, pp. 25-33, Dec. 1991.

[24] G. J. Foschini and J. Salz, "*Digital Communications Over Fading Radio Channels*", Bell Systems Technology Journal, pp. 429-456, Feb. 1983.

[25] J. G. Proakis, "*Digital Communications*",2nd edition, New York McGraw Hill, 1989.

[26] J. A. C. Bingham, "*Multicarrier Modulation for Data Transmission: An Idea Whose Time Has Come*", IEEE Communications Magazine, pp. 7-12, May 1990.

[27] K. Hamaguchi and E. Moryiyama, "*Performance of Multi-level QAM Controlled Adaptive Modulation for Land Mobile Communication Systems* ", IEICE Transactions on Communications, Vol. E81-B, No. 4, pp. 771-776, Apr. 1998.

[28] T. Ue, S. Sampei, N. Morinaga and K. Hamaguchi, "*Symbol Rate and Modulation Level Controlled Adaptive Modulation/TDMA/TDD System for High Bit Rate Wireless Data Transmission*", IEEE Transactions on Vehicular Technology, Vol. 47, No. 4, pp. 1134-1147, Nov.1998.

[29] W. C. Lee, "*Mobile communications, design and fundamentals*", John Wiley and Sons, 2ed 1993.

[30] H. S. Wang and N. Moayeri, "*Finite-State Markov Channel- A useful Model for radio Communication Channels*", IEEE Transactions on Vehicular Technology, vol. 44, pp. 163-171, Feb. 1995.

[31] E. A. Al-Susa and R.F. Ormondroyd, "*An Improved Channel Inversion Based OFDM System In the Presence of Channel errors and Rapid Time variations*" Accepted to be published in the IEEE VTC'2000, Boston-USA, Sept. 2000.

[32] T. Keller and L Hanzo, "*Sub-Band Adaptive Pre-Equalised OFDM Transmission*", Proceedings of VTC'99 falls, pp. 334-338, Sept. 1999.

Chapter Eight

Conclusions and Future Work

8 Chapter Eight

8.1 Conclusions

The vision of being able to have information "*any-form-anytime-anywhere*" has been the driving force behind the implementation and deployment of wireless-mobile communication systems. The challenge faced however is to be able to provide such facility with a high quality using the minimum possible resources (power, bandwidth complexity, etc). The main obstacle to overcome at the physical layer is the transmission channel, which imposes serious constraints on the data throughput. The transmission channel is characterised by two major categories. These are the time dispersion due to multipath, which makes the channel frequency selective and thus causes parts of the transmitted signal's spectrum to undergo severe fading as well as produces ISI. The second category is the time variation of the channel due to the relative movement between the transmitter and the receiver, which makes the channel frequency dispersive and gives rise ICI.

In order to overcome such problems, two air-interface techniques have been the subject of extensive investigation recently. These are the spread spectrum and the multicarrier (in the form of orthogonal frequency division multiplexing, OFDM) techniques. The two techniques work in opposite sense in order to achieve the same aim. While spread spectrum systems spread the data across a multiple of the original data bandwidth (hence stretching the data in frequency), the multicarrier systems divide the original bandwidth into many narrow subchannels (hence stretching the data in time). The two techniques allow different channel equalisation and receiver structures to establish an efficient and robust communication link. The advantages of the OFDM technique include simpler equalisation strategies, robustness against time-dispersive channels and inherent frequency diversity when combined with the relevant channel coding and interleaving. However, these advantages do not all occur without some drawbacks. These include redundancy introduced by the cyclic prefix, channel estimation and higher sensitivity to synchronisation.

Due to its robustness against ISI and spectral efficiency the OFDM technique has now found many applications for high data rates modems such as DAB, DTVB and DSL in Europe and Japan. In addition, it has also been standardised for other applications such as the HIPERLANII, and was also proposed for wireless and personal communication systems.

An OFDM system can be realised using a bank of coherent modulators equally spaced in frequency. This however is not the common method of realising such system. Instead the FFT transform is used due to its efficiency and relative ease of implementation especially when the number of subcarriers needed is large. The main disadvantage of the FFT method is the increased sensitivity of the system to amplifier non-linearity.

Current demand for wireless internet access is such that there is likely to be a pressing need for more bandwidth to be available for the fourth generation cellular radio systems to provide WAP and multimedia facilities. This is the issue considered in this thesis.

Following the brief description of the mobile radio channel and the relevant basic communication techniques in chapter two, this thesis has focussed on studying mainly coherent OFDM systems for applications which require high bit rate modems.

A brief analytical description of the principle of OFDM modulation scheme has then been presented in chapter three where it was shown that OFDM could make wideband transmission over frequency selective fading channels achievable. Typical system waveforms were shown and the system capacity was discussed. It has also been shown analytically that in order to preserve the orthogonality between the subcarriers and prevent significant ISI, the use of a cyclic prefix is indispensable. A simplified description of the mathematical representation of an OFDM signal in the presence of time and frequency selective fading channel was also given. In addition, a theoretical analysis of the BER performance of MQAM/OFDM has been provided, which could be used to show the trade off between the system BER performance, number of subcarriers and duration of the cyclic prefix.

An FFT based OFDM system was described and modelled in a multipath-fading environment in chapter four. In this chapter the relationship between the FFT-size, channel time selectivity and frequency selectivity was established using computer simulation. It was concluded that when time selectivity is the dominant factor of the channel, ICI dominates and increases in proportion to the number of subcarriers. ICI is not removed by the cyclic prefix and can only be reduced by increasing the separation between the subcarriers. In contrast, when the channel is dominantly frequency selective, the time selectivity may be ignored. The frequency selectivity of the channel yields ISI, which decreases in proportion to increasing the number of subcarriers or the duration of the cyclic prefix. In a time-selective-

frequency-selective channel, the optimum number of subcarriers can be approximated to be the crossing point between the performance of the time-flat limit and the frequency-flat limit of the considered channel. It was also shown that the use of a cyclic prefix is indispensable, especially when using high order modulation. There are however two disadvantages associated with using a cyclic prefix. One of these problems is the reduction in spectral efficiency and the other is the reduction in effective SNR. As an alternative a feedback based technique was proposed which removes the need for a cyclic prefix and this has showed encouraging results. This was based on removing the ISI term prior to the receiver's FFT using an estimate of the previous transmitted symbol. The performance of such a technique however was found to be highly dependent on the goodness of the channel estimate and therefore is recommended for slowly time variant channels where a good channel estimate can more easily be obtained. A brief review of the sensitivity of the OFDM system to synchronisation errors was also presented in this chapter along with some of the current synchronisation techniques proposed in the literature. Coded OFDM was also examined, in particular its relationship to interleaving. It was shown that as much as 5-7dB improvement is achieved when combining coding with interleaving. The exact interleaving depth is mainly a function of the channel Doppler spread and code free distance. The optimum interleaving depth is that depth beyond which no further performance improvement is obtained. In slowly time varying channels this optimum depth may not be feasible as the delay imposed may be very significant and intolerable for real time applications. A comparison between a single carrier and an OFDM system in multipath fading showed that only when the OFDM system is combined with coding and interleaving it becomes superior to the single carrier system. The performance of parallel DPSK/OFDM and serial DPSK/OFDM was studied using computer simulation. It was observed that in a dominantly time selective channel, the serial DPSK/OFDM is a better method as it relies on consecutive symbols in the encoding and decoding operations and therefore $1/N$ times less sensitive to time variations. On the other hand, in a dominantly frequency selective channel the parallel DPSK/OFDM is the better choice when the coherence bandwidth of the channel is relatively large compared to the frequency separation between the subcarriers. This is because the correlation between the channel response across the time direction is much higher than that across the frequency direction.

Chapter 5 focussed on the pilot-symbol-assisted channel estimation technique for OFDM. It provided a comparison between three practical estimators and discussed the relative merits of each. In this chapter, various key issues of the pilot assisted channel estimation technique were investigated. This included the impact of pilot tone spacing, power level and sensitivity

to timing errors. It was shown that by increasing the pilot tone power by about 3 to 6 dB above that of the signal, a significant performance improvement is achieved. In contrast, increasing the percentage of pilot tones beyond a certain level degrades the systems capacity as well as BER performance due to unnecessary transmission of redundant symbols, which in turn reduces the effective SNR of the system. The impact of timing misalignment on this channel estimation method was also examined. It was shown that certain types of interpolators are much more sensitive to timing errors than others. Using the FTD based channel interpolator, eliminates the need to phase compensate the pilots prior to interpolation, consequently reducing the risk of incorrectly estimating the phase shift introduced by the frame misalignment.

The scattered pilot-tones channel estimation technique is suitable for situations when the channel coherence time and bandwidth are relatively large. For example, systems such as the DVB-T find such technique very applicable since the application uses very large FFT sizes which corresponds to a large channel coherence bandwidth and the application is limited to static or, very slowly time varying channels. For applications which involve vehicular receivers on the other hand, much smaller FFT sizes are used to accommodate for high velocities, such technique may not be the most suitable due to the excessive overhead required for a good channel estimate. In view of this a new channel estimation technique aimed at providing an instantaneous channel estimate without reducing the total data throughput was investigated. This is based on the simultaneous transmission of the pilot tones and information signal using two two-chip orthogonal codes. It was shown that under unknown channel conditions, the new channel estimation technique is the safest choice. If however, the channel is known to be very slowly time variant, such as the fixed wireless channel, then the feedback technique will result in the best overall performance provided that consecutive OFDM blocks are perfectly synchronised. Finally, if the channel is highly time variant and the coherence bandwidth of the channel is relatively large, then by careful selection of the FFT length, pilot tone percentage and PSR, the pilot assisted technique may be customised to provide the best overall performance.

A highly bandwidth-efficient channel estimator was studied in chapter six. This estimator tracks the variations after the initial estimation in a decision directed feedback fashion. Two forms of this estimator were examined. The coded mode, which utilises the error correction capability of the Viterbi decoder to improve the channel estimate, and the uncoded mode, which uses the hard-decision symbols directly before error correction takes place. The coded feedback channel estimator was shown to be superior to the uncoded mode under various

189

transmitter needs to adapt to the continuously changing channel was also given. The feasibility of such measure is however dictated by hardware constraints.

The use of adaptive power control using channel inversion has also shown very promising results. An improvement of as much as 15 – 20 dB was obtained over fixed power techniques. Such a technique is however sensitive to channel variations unless this is compensated for at the receiver. The use of controlled channel inversion combined with compensation at the receiver has been shown to be a good compromise that provides considerable improvement over fixed power techniques as well as limited peak to average power ratio. Channel prediction was also examined and it was shown that although it provides significant improvement in the absence of channel compensation at the receiver, it also leads to irreducible BER floors. This is because of the residual difference between the actual and predicted channel transfer function.

The use of subcarrier allocation in a multi-user environment was also investigated. An optimum algorithm was suggested. This algorithm however requires a large number of computations that may not be desirable especially in a time variant channel. Instead, a sub-optimal iterative algorithm that is based on finding the best subcarrier allocation out of $2N$ possibilities was given. Using this scheme an improvement of about 7dB is obtained over non-adaptive schemes.

It can be concluded from this study that the adaptive power technique is the simplest to implement and provides the best overall performance improvement. Adaptive subcarrier allocation was found to be the second best even when using a sub-optimal allocation algorithm. In addition, these two techniques only need the channel transfer function and do not require information about the noise level at the receiver that the adaptive constellation technique requires.

8.2 Future Work

This work has highlighted a number of potential areas for further research, which will be listed below.

8.2.1 Practical Synchronisation Algorithms

It was shown in chapter four that preserving the orthogonality of an OFDM system is a formidable task but one that is vital for maintaining the BER performance at the required

level. It was shown how a small phase offset due to either frequency mismatch or phase noise can lead to higher ICI, which ultimately degrades the system performance. Although a number of algorithms have been investigated by, for example, [1]-[5], the need for a simpler and more effective algorithm is far from over yet.

8.2.2   Multicarrier Techniques

Much research into multicarrier CDMA systems has been focussed on synchronous systems, appropriate mainly for a downlink transmission. Meanwhile, there has been comparatively little research on asynchronous systems that are appropriate for uplink channels. The justification for this is the fact that many of the benefits of the MC-CDMA technique, such as the simple detector/equaliser structures, may be lost when an asynchronous approach is considered. In the asynchronous case, the required matrix inversions required to implement the optimal linear receiver are as complex as those required for DS- CDMA [6]. These receivers require near-perfect channel estimation as the performance degrades severely with imperfect channel information [7]. If MC-CDMA modulation were to be considered for future mobile communication systems, further research into such area would be needed.

8.2.3   Adaptive OFDM Techniques

As OFDM has now become the standard air-interface technique for many applications such as DVB, DAB and HIPERLANII, which require high bit rates, the need to maximise the spectrum efficiency of such technique is even greater. Adaptive modulation is a key area that has lately surfaced again. As DVB and DAB are a one-to-many channel, only adaptive techniques that do not require a duplex link are considered useful. On the other hand, communication systems that involve a duplex link give more flexibility in the choice of an appropriate adaptive scheme.

8.2.4   Diversity Techniques Using Space-time Codes

Space-time codes are designed for efficient transmission using multiple transmit antennas. It was shown in [8][9] that the use of multiple transmit and receive antennas along with intelligent signal processing can result in enormous capacities. OFDM systems have the potential to benefit from such technique.

Appendices

Appendices

A. Box-Muller Algorithm [1]

The Box-Muller algorithm is formulated as follows:

1. Generate two random variables u_1 and u_2 and let

$$s = u_1^2 + u_2^2$$

2. While $s \geq 1$ discard s and recompute u_1, u_2 and s

3. If $s < 1$ is satisfied compute the I and Q components of the noise as follows:

$$n_i = u_i \sqrt{\frac{-2\sigma^2}{s} \log_e(s)}$$

$$n_q = u_q \sqrt{\frac{-2\sigma^2}{s} \log_e(s)}$$

σ is the standard deviation of the AWGN.

B. 2nd Order Cascaded Butterworth Filter Design [2]

The steps involved are outlined below:

1. Prewarp the critical frequency of the digital filter. In this case the critical frequency is the maximum Doppler frequency. This is done as follows:

$$w_p = \tan\left(\frac{w_p}{2f_s}\right) \tag{B.1}$$

Where $w_p = 2\pi f_m$, the critical frequency before prewarpping.

f_m = Maximum Doppler frequency.

f_s = Sampling frequency.

2. Denormalise by frequency scaling $H(s)$. This is implemented by replacing s by $\dfrac{s}{w_p}$.

3. Transform from the s-domain to the z-domain using the Bilinear Transformation to obtain the digital filter transfer function $H(z)$. This is done by replacing s by $(z-1)/(z+1)$.

The resulting z-domain transfer function of the above frequency domain transfer function is

$$H(z) := \frac{(z+1)^4}{\left[\left[\alpha^2 \cdot (z-1)^2 + \sqrt{2} \cdot \alpha \cdot (z-1) \cdot (z+1) + (z+1)^2\right] \cdot \left[\alpha^2 \cdot (z-1)^2 + 2 \cdot 10^{-2} \cdot \alpha \cdot (z-1) \cdot (z+1) + (z+1)^2\right]\right]}$$

Where

$$\alpha := \frac{1}{\tan\left(\pi \cdot \frac{fd}{fs}\right)}$$

Using the z-domain transfer function, the difference equation that can be used to model the filter can be found as follows:

$$H(z) = \frac{Y(z)}{X(z)} \qquad\qquad\qquad \text{B.2}$$

Rearranging the above equation and substituting for *H(z)* produces

$$Y(z) = \frac{1}{k}\left[\left[\left(1 + 4 \cdot z^{-1} + 6 \cdot z^{-2} + 4 \cdot z^{-3} + z^{-4}\right) \cdot X(z) - \left(\beta1 \cdot z^{-1} + \beta2 \cdot z^{-2} + \beta3 \cdot z^{-3} + \beta4 \cdot z^{-4}\right) \cdot Y(z)\right]\right]$$

From which the difference equation below is deduced.

$$y(n) = \frac{1}{k} \cdot (x(n) + 4 \cdot x(n-1) + 6 \cdot x(n-2) + 4 \cdot x(n-3) + x(n-4) - \beta1 \cdot y(n-1) - \beta2 \cdot y(n-2) - \beta3 \cdot y(n-3) - \beta4 \cdot y(n-4))$$

Where $k := \alpha^4 + \left(2.0 \cdot 10^{-2} + \sqrt{2}\right) \cdot \alpha^3 + \left(2.0 \cdot 10^{-2} \cdot \sqrt{2} + 2.\right) \cdot \alpha^2 + \left(2.0 \cdot 10^{-2} + \sqrt{2}\right) \cdot \alpha + 1.$

$\beta1 := -4. \cdot \alpha^4 + \left(-2. \cdot \sqrt{2} - 4.0 \cdot 10^{-2}\right) \cdot \alpha^3 + \left(2. \cdot \sqrt{2} + 4.0 \cdot 10^{-2}\right) \cdot \alpha + 4.$

$\beta2 := \left(6. \cdot \alpha^4 - 4. \cdot \alpha^2 - 4.0 \cdot 10^{-2} \cdot \sqrt{2} \cdot \alpha^2 + 6.\right)$

$\beta2 := 6. \cdot \alpha^4 + \left(-4. - 4.0 \cdot 10^{-2} \cdot \sqrt{2}\right) \cdot \alpha^2 + 6.$

$\beta3 := -4. \cdot \alpha^4 + \left(2. \cdot \sqrt{2} + 4.0 \cdot 10^{-2}\right) \cdot \alpha^3 + \left(-2. \cdot \sqrt{2} - 4.0 \cdot 10^{-2}\right) \cdot \alpha + 4.$

$\beta4 := \alpha^4 + \left(-2.0 \cdot 10^{-2} - 1. \cdot \sqrt{2}\right) \cdot \alpha^3 + \left(2.0 \cdot 10^{-2} \cdot \sqrt{2} + 2.\right) \cdot \alpha^2 + \left(-2.0 \cdot 10^{-2} - 1. \cdot \sqrt{2}\right) \cdot \alpha + 1$

C. Important Channel Parameters

a) Root Mean Square, (rms), Delay Spread Calculation

Although the power delay profile of a channel describes completely the variations of the received power with time, it is often more convenient to simplify this to a single quantity known as the rms delay spread which is expressed as follows:

$$\tau_{rms} = \sqrt{\overline{\tau^2} - \overline{\tau}^2} \qquad\qquad\qquad \text{C.1}$$

Where $\overline{\tau^2}$ and $\overline{\tau}^2$ are the mean square excess delay and the square mean excess delay, respectively.

$$\overline{\tau} = \frac{\sum_{n=1}^{N} \tau_n \cdot \alpha_n^2}{\sum_{n=1}^{N} \alpha_n^2} \quad , \quad \overline{\tau^2} = \frac{\sum_{n=1}^{N} \tau_n^2 \alpha_n^2}{\sum_{n=1}^{N} \alpha_n^2}$$

C.2

b) Capacity of Frequency Selective Fading Channels

In this section the capacity of frequency selective fading channels is reported. The derivation of such parameter has been provided by Holsinger in 1964 and reprinted in H.

$$C_S = W \cdot Log_2 \left(GM \cdot \left(1 + \gamma \mid C(f) \mid^2 \right) \right)$$

$$GM \left(1 + \gamma \mid C(f) \mid^2 \right) = \exp \left(\frac{1}{W} \cdot \int_W \ln \left(1 + \gamma \mid C(f) \mid^2 \right) df \right)$$

C.1

For a time invariant frequency selective channel, the capacity is given by:

Where W is the available bandwidth of the channel, $C(f)$ is the frequency response of the channel and γ is the signal to noise ratio.

For a time variant Rayleigh frequency selective fading channel it can be shown that the capacity can be given by:

$$C_{T.V.R.} = \frac{W}{\ln(2)} \cdot \int_a^\infty x^{-1} \cdot \exp(-x) dx$$

C.2

Where a is a threshold and may be calculated using:

$$\gamma = \int_a^\infty x^{-2} \cdot \exp(-x) dx$$

c) Level Crossing Rate and average Duration of fades

The level crossing rate, (lcr), may be defined as the number of times the envelope of a signal crosses a certain level per second. It is defined by [4] as:

$$n(R) = n_0 \cdot n_R$$

Where $n_0 = \sqrt{2\pi} \dfrac{V}{\lambda}$, and $n_R = \dfrac{1}{2} \cdot p(R)$, V is the vehicle speed, λ is the wavelength and $p(R)$ is Rayleigh PDF. For example the expected level crossing rate at 10dB below the average signal's power level is $0.71 \cdot \left(\dfrac{V}{\lambda} \right)$ crossings per second.

The average duration of fades, (*adf*), is defined as the sum of N fades at a certain level, A, divided by N. The average duration of fades may be given by:

$$adf = \frac{\int_0^R p(x)dr}{lcr} \qquad\qquad C.1$$

Where the numerator represents the cumulative Rayleigh distribution function (CPD). For the previous example it can be shown that the *adf* is equal to $0.132 \cdot \frac{\lambda}{V}$ sec.

D. The LMS algorithm [2][9]

A common method of optimising adaptive filter parameters is to minimise the mean square error, which is defined as the square of the difference between the filter's output and the desired signal. When the mean square error is plotted as a function of the filter's coefficients vector it forms a multidimensional parabolic, (performance surface), with a unique minimum corresponding to the Wiener Solution. The Wiener solution can be derived easily as follows. Since the error, e, between the desired output, y, and the filter's output, $\hat{y}$, is given by:

$$e_k = y_k - \hat{y}_k = y_k - \mathbf{W}^T \cdot \mathbf{X}_k = y_k - \sum_{i=0}^{N-1} w_i \cdot x_{k-i} \qquad\qquad D.1$$

where $\mathbf{W}^T$ is the transpose of the filter's coefficients vector,

                 $\mathbf{X}$ is a vector of the received signal samples.

and N is the number of filter's coefficients.

The square of the error is given as:

$$e_k^2 = y_k^2 - 2y_k \mathbf{X}_k^T \mathbf{W} + \mathbf{W}^T \mathbf{X}_k \mathbf{X}_k^T \mathbf{W} \qquad\qquad D.2$$

Assuming that both the received and desired signals are stationary and ergodic processes, then the mean square error, J, is obtained by taking the expectation of both sides of the above equation giving:

$$J = E[e_k^2] = E[y_k^2] - 2E[y_k \mathbf{X}_k^T \mathbf{W}] + E[\mathbf{W}^T \mathbf{X}_k \mathbf{X}_k^T \mathbf{W}] = \sigma^2 + 2\mathbf{P}^T \mathbf{W} + \mathbf{W}^T \mathbf{R} \mathbf{W} \quad D.3$$

where

       $\sigma^2 = E[y_k^2]$ is the variance of y_k

       $\mathbf{P} = E[y_k \mathbf{X}_k]$ is the cross-correlation vector,

       $R = E[X_k \dot{X}_k^T]$ is the NxN correlation matrix.

The gradient of the performance surface, Δ, is given by:

$$\Delta = \frac{\partial J}{\partial \mathbf{W}} = -2\mathbf{P} + 2\mathbf{RW} \qquad\qquad \text{D.4}$$

At the minimum point of the performance surface, the gradient is zero and therefore, the filter weight vector has its optimum value given by:

$$\mathbf{W}_{opt} = \mathbf{R}^{-1}\mathbf{P} \qquad\qquad \text{D.5}$$

Widrow and Hopf, have developed a recursive algorithm based on the standard steepest decent method to obtain the optimum weights without the need to matrix inversion which is a necessity in the direct method discussed above. The steepest decent method is given by :

$$\mathbf{W}_{k+1} = \mathbf{W}_k - \mu\Delta_k \qquad\qquad \text{D.6}$$

where μ controls the stability and rate of convergence of the algorithm and must satisfy the following relationship [7].

$$\frac{1}{\mu_{\text{max}}} > \mu > 0$$

where μ_{max} is the maximum eigenvalue of $\mathbf{R}$.

In the LMS algorithm instantaneous estimates are used for Δ. Thus

$$\begin{aligned}\Delta_k &= -2\mathbf{P}_k + 2\mathbf{R}_k\mathbf{W}_k = -2\mathbf{X}_k y_k + 2\mathbf{X}_k\mathbf{X}_k^T\mathbf{W}_k \\ &= -2\mathbf{X}_k(y_k - \mathbf{X}_k^T\mathbf{W}_k) = -2e_k\mathbf{X}_k \end{aligned} \qquad\qquad \text{D.7}$$

Substituting the above equation into the steepest decent algorithm results in the Widrow-Hopf LMS algorithm:

$$\mathbf{W}_{k+1} = \mathbf{W}_k + 2\mu e_k\mathbf{X}_k \qquad\qquad \text{D.8}$$

The Widrow-Hopf LMS algorithm can be extended to complex forms where all the signals are complex numbers and the complex conjugate of the reference input is used [8].

$$\mathbf{W}_{k+1} = \mathbf{W}_k + 2\mu e_k\mathbf{X}^*_k \qquad\qquad \text{D.9}$$

In this simple form of the LMS recursion the correction applied to the tap weight is proportional to the input vector which can give rise to convergence problems when the input power is high. It is therefore usual to normalise the adaptation constant μ to the input power to give the normalised LMS algorithm [9].

$$\mathbf{W}_{k+1} = \mathbf{W}_k + 2\frac{\mu}{|\mathbf{X}_k|^2}e_k\mathbf{X}^*_k \qquad\qquad \text{D.10}$$

E. Performance of Non-coherent OFDM

The system BER performance derived here is based on a differential binary phase shift keying, DBPSK, modulation scheme. Assuming that the decision variable at the receiver is D, the steps involved in deriving the BER performance of such system can be summarised in the following steps:

1. Find the characteristic function of the decision variable D, $\psi(\zeta)$.

2. Calculate the inverse Fourier transform of ψ to find the probability density function, *pdf*, of D, $p(D)$.

3. Assuming that one has been transmitted, the BER probability is obtained by integrating $p(D)$ over the period of $-\infty$ to 0.

The method used in deriving the BER performance here follows the same idea as that used in [5][6].

Since the decision variable, D, may be given by:

$$D_{j,i} = \Re\left(R_{j,i} \cdot R_{j,i-1}^*\right) \qquad \text{E.1}$$

assuming that a 1 has been transmitted implies that $R_{j,i} = R_{j,i-1}$, then the characteristic function, $\psi(\zeta)$, of this variable is given by [10]:

$$\psi(\zeta) = \frac{1}{\det(I - j2\zeta C^* F)} \qquad \text{E.2}$$

Where

$$C = \frac{1}{2}E[R^* \cdot R^T] = a \cdot \begin{bmatrix} 1 & \rho \\ \rho^* & 1 \end{bmatrix} \qquad \text{is the covariance matrix of } R$$

$$\rho = \frac{E[R_{j,i} \cdot R_{j,i-1}^*]}{E[R_{j,i} \cdot R_{j,i}^*]} \qquad \text{is the correlation factor between } R_{j,i} \text{ and } R_{j,i-}$$

$$_l$$

$$F = \begin{bmatrix} 0 & 1 \\ 1 & 0 \end{bmatrix} \qquad \text{is a 2X2 matrix.}$$

Substituting for R and C into equation **E.2** and calculating the inverse Fourier transform of the resulting equation produces the probability density function of D, $p(D)$ as shown below:

$$p(R) = \frac{1}{2\pi} \cdot \int \psi(\zeta) e^{-j\zeta \mathfrak{I}} d\zeta$$

$$= \frac{B}{\sqrt{A^2 + 4B}} \cdot \left\{ e^{0.5\left(A + \sqrt{A^2+4B}\right) \cdot R} \cdot u(-D) + e^{0.5\left(A - \sqrt{A^2+4B}\right) \cdot R} \cdot u(D) \right\}$$

E.3

Where $u(x)$ is a unit step function and

and

$$A = \frac{\mathfrak{R}(\rho)}{a \cdot (1 - |\rho|^2)}$$

$$B = \frac{1}{4a^2 \cdot (1 - |\rho|^2)}$$

The bit error rate is found by integrating $p(D)$ over the period of $-\infty$ to 0 as shown below:

$$P(e) = P(D_{j,i} < 0) = \int_{-\infty}^{0} p(D) dD$$

$$= \frac{(1 - \rho^2) \cdot (\rho + 1)}{2}$$

E.4

The correlation coefficient of, R, in the presence of a frequency selective fading channel may be given in terms of the powers of the different paths and delay spreads as shown below:

$$\rho = \frac{b_0}{b_0 + \sigma_I^2 + \sigma_n^2}$$

E.5

Where

$$b_0 = \sum_{l=1}^{M1} p_l + \sum_{l=M1+1}^{M1+M2} \left(\frac{T_u - \tau_l + CP}{T_u} \right)^2 \cdot p_l \quad \text{is the power of the desired signal,}$$

$$\sigma_I^2 = \sum_{l=M1+1}^{M1+M2} \left(\frac{\tau_l - CP}{T_u} \right)^2 \cdot p_l \cdot \left(\sum_{k=0}^{N-1} \sin c^2 \left(\frac{\pi(k-m)(\tau_l - CP)}{T_u} \right) - \frac{1}{2} \right) \quad \text{is the power}$$

related to ICI and ISI

τ_l is the delay of the lth path.

and $M1$ and $M2$ are the length of the cyclic prefix and the length of the useful symbol duration, respectively.

The correlation coefficient for a time selective channel is given by [11]:

$$\rho = \frac{b_1}{b_0 + \sigma_c^2 + \sigma_n^2}$$

E.6

Where b_0, b_1 and σ_c^2 in this case are defined as:

$$b_0 = \frac{1}{T_u^2} \cdot \int_0^{T_u}\int_0^{T_u} Cr(\zeta - \eta) d\zeta d\eta$$

$$b_1 = \frac{1}{T_u^2} \cdot \int_0^{T_u}\int_{-T_{TOT}}^{T_u-T_{TOT}} Cr(\zeta - \eta) d\zeta d\eta$$

$$\sigma_c^2 = \sum_{\substack{k=0 \\ k \neq m}}^{N-1} \frac{1}{T_u} \int_0^{T_u}\int_0^{T_u} Cr(\zeta - \eta) e^{-j\frac{2\pi(m-k)(\zeta-\eta)}{T_u}} d\zeta d\eta$$

Where $Cr(\tau)$ is the autocorrelation function of the channel, which assuming the use of an omni-directional antenna may be given as:

$$Cr(\tau) \approx a\left(1 - (\pi f_D \tau)^2\right) \tag{E.7}$$

Substituting the definition of $b0$, $b1$, σ_c^2 and $Cr(\tau)$ in equation E.5 results in:

$$\rho = \frac{1 - (\pi f_D)^2 \cdot \left(\frac{T_u^2}{6} + T_{ToT}^2\right)}{1 + \frac{(\pi f_D T_u)^2}{6} + \sum_{\substack{k=0 \\ k \neq i}}^{N-1} \frac{(f_D T_u)^2}{2 \cdot (k-m)^2} + \sigma_n^2} \tag{E.8}$$

Where

T_u, T_{TOT} and f_D are the useful symbol duration, the total symbol duration and the Doppler frequency, respectively.

F. Channel Autocorrelation Function

The autocorrelation function of the channel is given by [12]:

$$R_{HH}(\Delta f, \Delta t) = E\{H(f;t) \cdot H^*(f - \Delta f; t - \Delta t)\}$$

$$= E\left\{\frac{1}{M} \cdot \sum_{n,n'=1}^{M} e^{j(\theta_n - \theta_{n'})} \cdot e^{j2\pi(F_{Dn} \cdot t - F_{Dn'} \cdot (t - \Delta t))} \cdot e^{-j2\pi(f\tau_n - (f - \Delta f)\tau_{n'})}\right\} \tag{F.1}$$

Since all random variables are independent, equation F.1 can be written as:

$$R_{HH}(\Delta f, \Delta t) = \frac{1}{M} \cdot \sum_{n=1}^{M} E\{e^{j2\pi F_{Dn}\Delta t}\} E\{e^{-j2\pi\Delta f\tau_n}\}$$

$$= E\{e^{j2\pi F_{Dn}\Delta t}\} E\{e^{-j2\pi\Delta f\tau_n}\} = R_f(\Delta f) R_t(\Delta t) \tag{F.2}$$

Equation **F.2** implies that the channel correlation is separable. The expectation can be found from a standard Fourier transformation:

$$R_t(\Delta t) = E\{e^{j2\pi F_D \Delta t}\} = J_o(2\pi F_{D,max}\Delta t)$$

$$R_f(\Delta f) = E\{e^{j2\pi\Delta f \tau_n}\} = \frac{\left(1 - e^{-T_{cp}(1/\tau_{rms} + j2\pi\Delta f)}\right)}{\left(1 - e^{-T_{cp}/\tau_{rms}}\right)\left(1 + j2\pi\Delta f \tau_{rms}\right)} \qquad \text{F.3}$$

where

$$J_o(.) \text{ is the Bessel function of the first kind.}$$

The correlation function for a uniform power delay profile can be obtained by letting $\tau_{rms} \to \infty$:

$$R_f^{uniform}(\Delta f) = E\{e^{j2\pi F_D \Delta t}\} = \frac{1 - e^{-j2\pi\Delta f T_{cp}}}{j2\pi\Delta f T_{cp}} \qquad \text{F.4}$$

Therefore, the correlation between channel attenuations separated by k subcarriers and l OFDM symbols is:

$$E\{h_{k',l'}h^{*}_{k'-k,l'-l}\} = r_f(k)r_t(l)$$

where

$$r_f(k) = R_f\left(\frac{k}{NT_s}\right) = \frac{\left(1 - e^{-L(1/\tilde{\tau}_{rms} + j2\pi k/N)}\right)}{\left(1 - e^{-L/\tilde{\tau}_{rms}}\right)\left(1 + j2\pi k\tilde{\tau}_{rms}/N\right)}$$

$$r_t(l) = R_t(l(N+L)T_s) = J_o\left(2\pi f_D, \max\left(1 + \frac{L}{N}\right)l\right) \qquad \text{F.5}$$

where

$\tilde{\tau}_{rms} = \tau_{rms}/T_s$ is the RMS-spread relative to the sampling interval.

G. Performance of QPSK/OFDM using feedback channel estimation

The *BER* probability for OFDM signals using phase shift keying modulation is calculated here. As already been mentioned earlier in the thesis, each symbol in the OFDM block is subjected to flat fading as shown in the expression below:

$$\tilde{R} = X \cdot H + \tilde{N} \qquad \text{G.1}$$

and therefore, the multiplicative channel coefficient, H, is estimated using

$$\overset{n}{H} = \frac{\tilde{R}}{X} - \frac{N}{X} = H - \frac{N}{X} \qquad \text{G.2}$$

Since this analysis is for *PSK*, only phase equalisation is required and thus the decision

variable, Z, is given by

$$Z = \tilde{R} \cdot \overset{n}{\tilde{H}}* = \tilde{R} \cdot Y* = Z_r + Z_i \qquad \text{G.3}$$

where

$$Z_r = \Re\{Z\}$$
$$Z_i = \Im\{Z\}$$

and the phase, θ, of the decision variable, Z, is given by

$$\theta = \tan^{-1}\left(\frac{Z_i}{Z_r}\right) \qquad \text{G.4}$$

In calculating the *BER* probability, we are assuming that the symbols carried by the different

sub-carriers have equal probability of being in error. To find *BER*, it is required to calculate

the probability density function (*pdf*) of the phase θ. This is calculated using the following

steps:

1. Find the characteristic function of the joint *pdf* of Z_r and Z_i, ψ.

2. Find the double Fourier transform of ψ to find the joint *pdf* of Z_r and Z_i, $p(Z_r, Z_i)$.

3. Use the equality, $r = \sqrt{Z_r^2 + Z_i^2}$ and $\theta = \tan^{-1}(Z_i / Z_r)$ to find the *pdf* of the envelope r

   and phase θ, $p(r, \theta)$.

4. Integrate over r the joint *pdf*, $p(r, \theta)$, to find the *pdf* of θ, $p(\theta)$.

When the above steps are carried out, the results are as follows:

1) The joint *pdf* function of Z_r and Z_i can be expressed as

$$\psi(jv_1, jv_2) = \left[\frac{\dfrac{4}{m_{xx}m_{yy}(1-|\mu|^2)}}{\left(v_1 - j\dfrac{2|\mu|\cos\varepsilon}{\sqrt{m_{xx}m_{yy}}(1-|\mu|^2)}\right)^2 + \left(v - j\dfrac{2|\mu|\sin\varepsilon}{\sqrt{m_{xx}m_{yy}}(1-|\mu|^2)}\right)^2 + \dfrac{4}{m_{xx}m_{yy}(1-|\mu|^2)^2}}\right]^L$$

$$\text{G.5}$$

where

$$m_{xx} = E\{|\tilde{R}|^2\}$$

$$m_{yy} = E\{|Y|^2\}$$

$$m_{xy} = E\{\tilde{R} \cdot Y\}$$

$$\mu = \frac{m_{xy}}{\sqrt{m_{xx}m_{yy}}} = |\mu| e^{-j\varepsilon}$$

and L is the number of diversity antennas used.

2) Taking the double Fourier transform of G.5 produces,

$$p(Z_r, Z_i) = \frac{(1-|\mu|^2)^L}{(L-1)!\pi 2^L} \left(\sqrt{Z_r^2 + Z_i^2}\right)^{L-1} \cdot e^{[|\mu|(Z_r \cos\varepsilon + Z_i \sin\varepsilon)]} \cdot K_{L-1}(\sqrt{Z_r^2 + Z_i^2}) \qquad \text{G.6}$$

where

$K_n(x)$ is the modified Hankel Function [5] of order n.

3) Substituting r and θ in G.6 gives

$$p(r,\theta) = \frac{(1-|\mu|^2)^L}{(L-1)!\pi 2^L} \cdot r^L \cdot e^{[|\mu|r\cos(\theta-\varepsilon)]} \cdot K_{L-1}(r) \qquad \text{G.7}$$

4) Integrating over r produces the marginal *pdf* function of θ, $p(\theta)$, which is given by [5]:

$$p(\theta) = \frac{(-1)^{L-1} \cdot (1-|\mu|^2)^L}{2\pi(L-1)!} \cdot \left\{ \frac{\partial^{L-1}}{\partial b^{L-1}} \left[\frac{1}{b-|\mu|^2 \cos^2(\theta-\varepsilon)} + \frac{|\mu|\cos(\theta-\varepsilon)}{[b-|\mu|^2 \cos^2(\theta-\varepsilon)]^{3/2}} \cdot \cos^{-1}\left(-\frac{|\mu|\cos(\theta-\varepsilon)}{b^{1/2}}\right) \right] \right\}_{b=1} \qquad \text{G.8}$$

where

$\dfrac{\partial^L}{\partial b^L} f(b,\mu)\big|_{b=1}$ denotes the Lth partial derivative of the function $f(b,\mu)$ evaluated at $b=1$.

The *BER* for any *M*-phase signalling is given by:

$$P_{MPSK} = 2 \int_{\pi/M}^{\pi} p(\theta)d\theta \qquad \text{G.9}$$

Since we are only interested in the *BER* of QPSK modulation, it is the only *BER* probability that is reported here. Assuming that the signal sent represents the code word 00 and that Grey coding is used, a single error will occur if $\pi/4 < \theta < 3\pi/4$ and a double error if $3\pi/4 < \theta < \pi$. Thus, of a binary digit error is

$$P_{QPSK} = \int_{\pi/4}^{3\pi/4} p(\theta)d\theta + 2\int_{3\pi/4}^{\pi} p(\theta) \qquad \text{G.10}$$

Using G.10 to substitute for q, and assuming no antenna diversity ($L = 1$), the probability of *BER* for *QPSK* may be given by

$$P_{QPSK} = \frac{1}{2}\cdot\left[1 - \frac{\mu}{\sqrt{2-\mu^2}}\right] \qquad \text{G.11}$$

The cross-correlation coefficient, μ, may be approximated by:

$$\mu = \frac{\bar{\gamma}}{1+\bar{\gamma}} \qquad \text{G.12}$$

where

$$\bar{\gamma} = \frac{E_b}{N_0}\cdot E\{\ \overset{n}{(H)}^2\} \quad \text{is the average received } SNR.$$

H. References

[1] W.T. Webb and L. Hanzo, *"Modern Quadrature Amplitude Modulation, Principles and Applications for Fixed and Wireless Channels"*, IEEE Press, 1994.

[2] E. C. Ifeature and B. W. Jervis, *"Digital Signal Processing, A Practical approach"*, Addison Wesley publishers ltd, 1993.

[3] R. G. Gallager, *"Information Theory and Reliable Communication"*, John Wiley, 1968.

[4] W. C. Lee, *"Mobile Communications, Design and Fundamentals"*, John Wiley and Sons, 2ed 1993.

[5] J. G. Proakis, *"Digital Communications"*, 3ed, McGraw Hill, 1992.

[6] R. C. V. Macario, *"Modern Personal Radio Systems "*, IEE, 1996.

[7] T. C. Chen, *"One Dimentional Signal Processing"*, Marcel Decker: New York & Basel, Chapter 13, 1978.

[8] N. J. Bershad, *"On The Real and Complex Mean Square Adaptive Filter Algorithm "*, IEEE Proceedings, Vol. 69, pp. 469-470, April 1981.

[9] S. Haykin, *"Adaptive Filter Theory"*, Prentice-Hall, 2nd edition, 1991.

[10] M. Schwartz and W. R. Bennet, *"Communication Systems and Applications"*, 2^{ed}, 1987.

[11] M. Okada, S. Hara and N. Morinaga, *"Bit error Rate Performance of Multicarrier Modulation Radio Transmission Systems"*, IEICE Transactions on Communications, Vol. E76-B, No. 2, pp. 113-119, Feb. 1993.

[12] J. J. van de Beek, O. Edfors, M. Sandell, S. K. Wilson and P. O Borjesson, *" On Channel estimation in OFDM Systems"* Proceedings of the IEEE 45th VTC, Chicago, IL, USA, July 1995, pp. 815-819.

Publications

The following paper was accepted to be published in the proceedings of the IEEE VTC'00, Sept. 2000

An Improved Channel Inversion Based Adaptive OFDM System in the Presence of Channel Errors and Rapid Time variations

E A Al-Susa
University of Bath
Department of Electronic and Electrical
Engineering
Bath BA2 2AY
e.alsusa@bath.ac.uk

R F Ormondroyd
Cranfield University
Communications & Wireless Networks
Group
Royal Military College of Science, Shrivenham,
Swindon, SN6 8LA, UK
r.f.ormondroyd@rmcs.cranfield.ac.uk

Abstract

The use of channel inversion for adaptive pre-equalised OFDM-based systems has been introduced by Keller and Hanzo [1] and was shown to be very sensitive to time variations and power clipping at the transmitter. In this paper we examine a fixed bit-rate channel inversion-based OFDM system and show that by combining such a technique with channel compensation at the receiver, a performance improvement in excess of 7 dB over standard OFDM transmission can be obtained when the channel characteristics are time varying

1. Introduction

For the past few years, intense interest has been focussed on adaptive modulation techniques in OFDM systems with the aim of achieving high-speed data trans-mission over mobile radio channels for applications including wireless multimedia, wireless internet access and future generation mobile communication systems. Adaptive modulation methods are based on monitoring the integrity of the channel and they generally increase either the system's capacity without degrading its BER performance, improve the BER performance without altering the required SNR, or they may be a combination of both.

This can be achieved by varying either: the transmitted power level of the transmitted carrier(s) according to some optimum criterion [1][2], the symbol transmission rate [3], the constellation order [4][5], the coding rate [6] or any combination of such parameters [7]-[9]. Most adaptive techniques are only applicable to systems with a duplex link as some means of informing the transmitter of the received signal quality is required, and this is assumed here.

The simplest of these adaptive modulation techniques is the variable transmitted power method. In this technique, the aim is to maintain the power of the received sub-carriers at a constant SNR so that the BER performance of all the sub-carriers is identical. The most efficient way of implementing such technique is by weighting the sub-carriers by a copy of the reciprocal of the channel frequency response. If ISI is negligible and the estimate of the channel frequency response is accurate, then no equalisation will be needed at the receiver. This technique of adaptive power transmission is sometimes referred to as pre-equalisation. A consequence of channel inversion pre-equalisation is that the peak to average power ratio (PAPR) of the transmitted signal is increased, requiring amplifiers with a large dynamic range otherwise signal clipping occurs. The aim of this paper is to investigate methods of improving the performance of a pre-equalisation based OFDM system in the presence of rapid variations of the channel characteristics.

2. System Description

Pre-equalisation is based on the principle of channel compensation of the data symbols prior to transmission. This not only results in a simpler receiver structure (since no equalisation is needed), but it also protects the otherwise deeply faded symbols from being completely buried in noise.

The penalty of this method however, is the need to have a good up-to-date estimate of the channel transfer function prior to transmission. Assuming that an estimate of the channel response is available and that the channel is ISI free, the optimum way of implementing pre-equalisation is to multiply the data symbols by the inverse of the channel response. If the estimate of the channel response is perfect, the received symbols are independent of the fading statistics and only suffer from the AWGN present at the receiver. The power control policy for channel inversion is:

$$\overline{S} = \sum_{i=0}^{F-1} \hat{S}_i = \sum_{i=0}^{F-1} \frac{S_i}{\alpha_i}$$

(1)

where $\overline{S}, \hat{S}_i, S_i$ are constant and represent respectively: the average total transmit signal power, the signal power of the ith sub-carrier after adaptation and the power level of the ith sub-carrier before adaptation and α_i is the channel fading level at the ith sub-carrier. The channel capacity of such system with this power adaptation strategy is derived from the capacity of an AWGN channel with a fixed received SNR:

$$C = B \log_2 (1 + SNR)$$

(2)

However, with channel inversion, much of the transmit-power may be used to compensate for deep fading. This has at least two major effects. The first is that it might lead to producing signals with large peak to average power ratios. The other disadvantage is that the symbols which are not in deep fades may be now more vulnerable to noise as most of the power in those sub-carriers may be reduced in the process of rescuing the symbols most affected by the deep fades.

To reduce the impact of the drawbacks of this technique, two approaches can be taken. The first approach is to detect the sub-carriers that are most affected by deep fades and not

use them. This is achieved by monitoring the gain/attenuation of the channel and disabling those sub-carriers affected by the frequency-selective channel attenuation where they fall below a certain threshold as shown in equation (3):

$$\hat{S}_i = \begin{cases} \dfrac{S_i}{\alpha_i} & \text{if } \alpha_i \geq \alpha_{thrsh} \\[2mm] 0 & \text{Otherwise} \end{cases}$$

(3)

This technique is sometimes referred to as *adaptive power allocation with sub-carrier blocking*. Since only sub-carriers where the fading level is $\geq \alpha_{thrsh}$ are used, the average power is given by:

$$\overline{S} = \int_{\alpha_{thrsh}}^{\infty} \frac{S}{\alpha} p(\alpha) d\alpha$$

(4)

where $p(\alpha)$ is the probability of $\alpha \geq \alpha_{thrsh}$. In order to keep the average transmit power constant, regardless of the number of useful sub-carriers after power allocation, all the used sub-carriers are scaled by a factor to keep the total transmit power unchanged. Because some of the sub-carriers may not be used, this results in a variable bit rate transmission. This is not very useful for applications requiring a constant bit rate.

The second technique that can be used in conjunction with pre-equalisation uses a threshold-based estimate of the inverse of the channel transfer function as shown in equation (5) below.

$$\hat{S}_i = \begin{cases} \dfrac{S_i}{\alpha_i} & \text{if } \alpha_i > \alpha_{thrsh} \\[2mm] \dfrac{S_i}{\alpha_{thrsh}} & \text{Otherwise} \end{cases}$$

(5)

This system uses *controlled channel inversion*, and the average transmitted power of this system is given by:

$$\bar{S} = \int\limits_{-\infty}^{\alpha_{thrsh}} \frac{S}{\alpha} p(\alpha < \alpha_{thrsh})d\alpha +$$

$$\int\limits_{\alpha_{thrsh}}^{\infty} \frac{S}{\alpha} p(\alpha \geq \alpha_{thrsh})d\alpha$$

(6)

In the simulations presented in this paper, the complex alphabets representing the modulated symbols are modified according to the channel inversion technique used as shown below:

(a) Total channel inversion:

$$X_i = \frac{X_i}{H_i}$$

(b) Sub-carrier blocking:

$$X_i = \begin{cases} \dfrac{X_i}{H_i} & \text{if } |H_i| > thrsh \\[2mm] 0 & \text{Otherwise} \end{cases}$$

(c) Controlled channel inversion:

$$X_i = \begin{cases} \dfrac{X_i}{H_i} & \text{if } |H_i| > thrsh \\[2mm] \dfrac{X_i}{thrsh \cdot e^{\angle H_i}} & \text{Otherwise} \end{cases}$$

where, X_i is the symbol transmitted on the ith sub-carrier and H_i is the corresponding channel response at that sub-carrier. The threshold level depends on the peak to average power ratio of the system. If the mapping used is only phase dependent, the mismatch between the actual channel response and that used at the transmitter, produced by the threshold operation, does not result in any performance degradation. If, on the other hand, a mapping scheme that uses amplitude and phase is used, such as QAM modulation, this mismatch will result in irreducible BER floors unless compensated for at the receiver.

3. Theoretical BER Performance

For the full channel inversion method, the theoretical BER performance is the same as that of an AWGN channel. In [9] the BER for an AWGN channel with MQAM modulation and ideal coherent phase detection is tight bounded to within 1dB for $0 \leq SNR \leq 30$ dB by:

$$BER_{AWGN} \approx \frac{1}{5} \cdot \exp\left(\frac{-3 \cdot SNR}{2 \cdot (M-1)} \right)$$

(7)

In fact (7) serves as a lower bound for $M = 2$ and an upper bound for $M \geq 4$.

For the sub-carrier blocking technique, the average SNR of the system is increased in accordance with the number of disused sub-carriers. Therefore, assuming a Rayleigh fading environment the BER performance may be given by:

$$BER_{AWGN} \approx \frac{1}{5} \cdot \exp\left(\frac{-3 \cdot SNR \cdot (1+\rho)}{2 \cdot (M-1)} \right)$$

$$\rho = \int\limits_{\alpha=-\infty}^{\alpha < \alpha_{thrsh}} \frac{\alpha}{\sigma^2} \cdot \exp\left(\frac{-\alpha^2}{2\sigma^2} \right) d\alpha$$

(8)

where $0 \leq \rho < 1$ is the probability of $\alpha < \alpha_{thrsh}$,

For the case of controlled channel inversion, the received SNR of some of the sub-carriers will be set by the fixed threshold used and the corresponding channel fade at that position. Using (7) and assuming that the sub-carriers affected by the threshold have a constant SNR, the BER performance of the controlled channel inversion method can be approximated by:

$$BER \approx \frac{1}{5} \cdot \left(\begin{array}{l} \exp\left(\dfrac{-3 \cdot SNR_1}{2 \cdot (M-1)} \right) \cdot (1-\rho) + \\[3mm] \exp\left(\dfrac{-3 \cdot SNR_2}{2 \cdot (M-1)} \right) \cdot \rho \end{array} \right)$$

(9)

where ρ is as defined in equation (8) and SNR_1 and SNR_2 correspond to the average SNR of the sub-carriers which are above the threshold and those which are below it, respectively.

4. Simulation Results

The performance of the proposed system was established using Monte-Carlo simulation.

A schematic diagram of the adaptive modulation system considered in this paper is shown in Figure 1. The sub-system blocks of the basic system are shown as white boxes. The additional blocks required to improve the system performance are shown as shaded boxes.
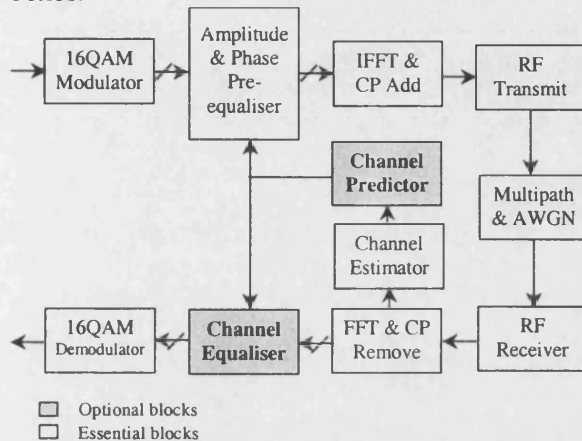

Figure 1. Schematic diagram of the system

The simulation parameters used are summarised in Table 1. We assume a duplex-link TDD-TDMA-OFDM multi-user scheme. The symbol rate was chosen such that the system can provide a maximum of twenty users at 2Mbps each when at full capacity. It is assumed that the block processing time is equal to the OFDM block transmission time and that synchronisation errors are negligible.

Symbol Rate	*10Msps*	Max. Delay	*5μsec*
Mapping Scheme	*QAM16*	Cyclic Prefix	*5μsec*
Channel Type	*GSM 6 tap TU*	Doppler Frequency	*100 (Hz)*
No. of sub-carriers	*1024*	Symbol Duration	*100.48μsec*

Table 1: Simulation Parameters

Figure (2) shows the impact of SNR on the probability of a bit error of using pre-equalisation under static multipath channel

conditions. The curves correspond to (a) controlled channel inversion with a threshold chosen to provide a 5dB dynamic range of the signal, (b) controlled channel inversion with threshold chosen to give a 10dB dynamic range, (c) full channel inversion pre-equalisation and (d) no power adaptation. For the case of full channel inversion, it can be seen by comparison of the BER performance of 16QAM in AWGN (curve (e)), that the performance of a full channel inversion scheme under the assumption of a perfect channel estimate is equivalent to that of the same mapping scheme in an AWGN channel. For the case of controlled channel inversion, the curves of Figure 2 show that while such a technique helps to maintain the dynamic range within a specific range it results in relatively high irreducible BER floors.
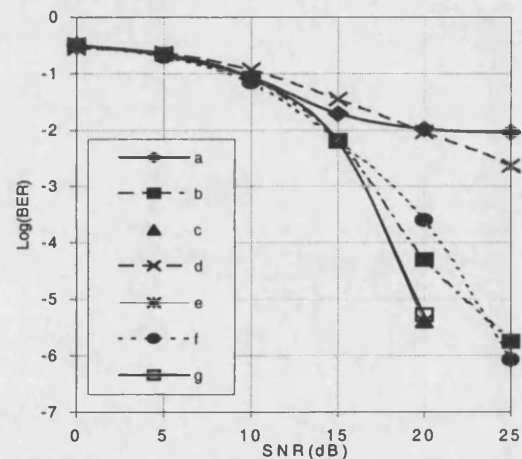
Figure 2. System performance with and without channel inversion under static multi-path channel conditions

To overcome this drawback, compensation for the threshold operation must be implemented at the receiver. The performance of the modified types of system are shown in curves (f) and (g) and described below. It can be seen from these curves that controlled threshold combined with compensation at the receiver produces a very good system performance. A close comparison between the full channel inversion graph (c) and the controlled inversion to 5dB with compensation (f) shows that a performance

degradation of about 4dB (at SNR = 20dB) is incurred. This is due to the strength of the deep fades at the location of the subcarriers affected by the threshold. When the threshold is increased to 10dB as shown in graph (g), the performance loss is hardly significant.

The other major drawback of pre-equalisation is its sensitivity processing delay when the channel character-istics are time-varying. The impact of such a drawback becomes more pronounced in proportion to the rate of time variation of the channel, the OFDM block length and increases in the modulation order. The graphs presented in Figure (3) are as follows: curve (a) standard non-adaptive OFDM system with zero-forcing equalisation and perfect channel knowledge, curve (b) standard non-adaptive OFDM system with zero-forcing equalisation and one-block delayed channel estimate, curve (c) full channel inversion with one-block delayed channel estimate, curve (d) full channel inversion with perfect channel knowledge and curve (e) full channel inversion with one-block delayed channel estimate and equalisation at the receiver.

It can be seen from this figure that using a one-block delayed version of the channel frequency response results in severe performance degradation for the time varying channel described by the parameters given in Table 1.

In order to make use of pre-equalisation without allowing the time variation of the channel to degrade its performance, equalisation at the receiver was also used to compensate for the time variation of the channel. Using this method, a one block delayed copy of the channel transfer function is first used to undo pre-equalisation, this is then followed by normal equalisation using an up-to-date estimate of the channel response. By doing so, the impact of the noise on the sub-carriers falling in the deep fade region is reduced by the channel inversion step, then the equalisation process takes care of the channel induced amplitude and phase shifts. It can be seen from Figure (3) curve (e) that using such technique results in a very significant

improvement over the standard non-adaptive technique shown in curve (a).

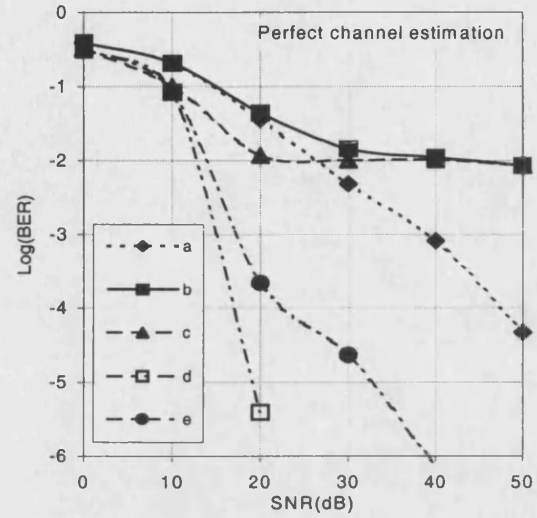**Figure 3: System performance with and without channel inversion in time-variant multi-path channels**

Figure (4) shows a similar comparison except that in this case the channel is estimated using scattered pilot tones. Only 6% of the total bandwidth was used for the pilot tone transmission. It can be seen from this figure that an improvement of about 10-20 dB is achieved when compared with the standard non-adaptive OFDM.

The use of equalisation at the receiver may be avoided by using a channel predictor at the transmitting end. The predictor used here is the same as that described in [10], where the predicted channel response, $\hat{h}$ is given by:

$$\hat{h}_t = \sum_{k=1}^{M} -a_k \cdot h_{t-k} \qquad (10)$$

and

$$\begin{bmatrix} \phi_0 & \phi_1 & \cdots & \phi_{M-2} & \phi_{M-1} \\ \phi_1 & \phi_0 & \cdots & \phi_{M-3} & \phi_{M-2} \\ \vdots & \vdots & \vdots & \vdots & \vdots \\ \phi_{M-2} & \phi_{M-3} & \cdots & \phi_2 & \phi_1 \\ \phi_{M-1} & \phi_{M-2} & \cdots & \phi_1 & \phi_0 \end{bmatrix} \cdot \begin{bmatrix} a_1 \\ a_2 \\ \vdots \\ a_{M-1} \\ a_M \end{bmatrix} = - \begin{bmatrix} \phi_1 \\ \phi_2 \\ \vdots \\ \phi_{M-1} \\ \phi_M \end{bmatrix}$$

(11)

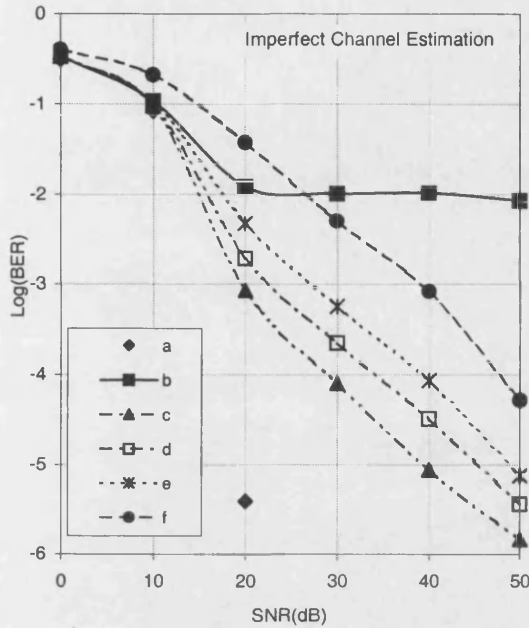where $\phi_j = E[h_t \cdot h_{t+j}]$, is the autocorrelation vector.

Figure 4: Impact of channel estimation errors, (a) total channel inversion using perfect channel estimate, (b) total channel inversion using noisy channel estimate, (c) total channel inversion + equalisation using noisy channel estimate, (d) controlled inversion 10dB dynamic range + compensation and equalisation using a noisy channel estimate, (e) controlled inversion 5dB dynamic range + compensation and equalisation using a noisy channel estimate, (f) non-adaptive OFDM using noisy channel estimate

In [10], it was shown that a prediction order and length of four poles and a hundred samples, respectively, produced the best compromise between complexity and system performance and hence such parameters were used in the simulations here. It can be seen from Figure (5) that the use of channel prediction may be successfully used to overcome the effect of time variation on the channel inversion method. It is also clear from this figure, however, that although such a technique considerably improves the performance of a channel inversion based

system, it leads to irreducible BER floors. This is due to the residual mismatch between the true channel transfer function and the predicted one.
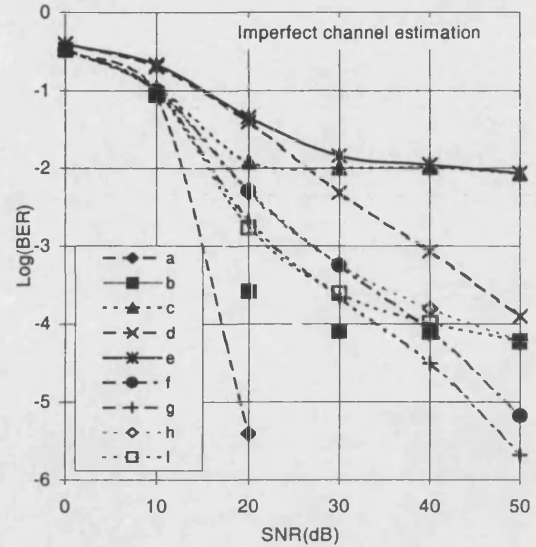

Figure 5: Channel inversion with channel prediction, (a) total channel inversion using perfect channel estimate, (b) total channel inversion using noisy channel estimate and prediction, (c) total channel inversion using noisy channel estimate, (d) non-adaptive OFDM using noisy channel estimate and prediction, (e) non-adaptive OFDM using noisy channel estimate, (f) controlled inversion 5dB dynamic range using noisy channel estimate prediction and equalisation, (g) controlled inversion 10dB dynamic range using noisy channel estimate prediction and equalisation, (h)) controlled inversion 5dB dynamic range using noisy channel estimate prediction and compensation only, (i) controlled inversion 10dB dynamic range using noisy channel estimate prediction and compensation only,

5. Conclusions

The use of channel inversion in conjunction with an adaptive OFDM system was examined. It is clear from the simulation results that such a technique is very sensitive to time variations in the channel characteristics and the technique must be aided with some form of compensation when it is used. Two solutions were examined, one based on equalisation at the receiver and the other based on prediction. While the former may result in extra signal processing at the receiver, the

latter suffers from irreducible BER floor. In either case however, considerable performance improvement is obtained. The choice of which technique to use is based on the required BER, the average SNR and the required level of receiver complexity that can be tolerated.

6. References

[1] T. Keller and L Hanzo, *"Sub-Band Adaptive Pre-Equalised OFDM Transmission"*, Proceedings of VTC'99 falls, 1999, pp. 334-338.

[2] J. F. Hays, *" Adaptive Feedback Communications"*, IEEE Transactions on Communications Technology, vol. COM-16, pp. 29-34, Feb. 1968.

[3] J.K Cavers, *"Variable Rate Transmission for Rayleigh Fading Channels"*, ", IEEE Transactions on Communic-ations Technology, vol. COM-20, pp. 15-22, Feb. 1972.

[4] W. T. Webb, and R. Steele, *"Variable Rate QAM for Mobile Radio"*, IEEE Transactions on Communications Technology, Vol. 43, pp. 2223-2230, July 1995.

[5] J. M. Torrance and L. Hanzo, *"Optimisation of Switching Levels for Adaptive Modulation in Slow Rayleigh Fading"*, IEE Electronic Letters, pp. 1167-1169, June 1996.

[6] B. Vucetic, *"An Adaptive Coding Scheme for Time Varying Channels"*, IEEE Transactions on Communications, Vol. 49, pp. 653-663, May 1991.

[7] S. M. Alamouti and S. Kallel, *"Adaptive Trellis-Coded Multiple Phased Shift Keying for Rayleigh Fading Channels"*, IEEE Transactions on Communications, Vol. 42, pp. 2305-2304, July 1994.

[8] T. Ue, S. Sampie, and N. Morinaga, *"Symbol Rate and Modulation Level Controlled Adaptive Modulation/ TDMA/TDD for Personal Communications"*, Proceedings of VTC'95, pp. 306-310, July 1995.

[9] A. J. Goldsmith and S-G. Chua, *"Variable Rate Variable Power MQAM For Fading Channels"*, IEEE Transactions on Communications, Vol. 45, pp. 1218-1230, October 1997.

[10] E. A. Al-Susa and R. F. Ormondroyd, *"'A Predictor-Based Decision Feedback Channel Estimation Method for COFDM with High Resilience to Rapid Time-Variations', Vehicular Technology Conference, Amsterdam, September 1999"*, Proceedings of the VTC'99 fall, the Netherlands, pp.273-278, Sept. 1999.

[11] G. J. Foschini and J. Salz, *"Digital Communications Over Fading Radio Channels"*, Bell Systems Technology Journal, pp. 429-456, Feb. 1983.

[12] J.G. Proakis, *"Digital Communications"*, 3ed edition, McGraw Hill, 1995.

The following paper was published in the proceedings of the
IEEE VTC'99, Sept. 1999

A Predictor-Based Decision Feedback Channel Estimation Method for
COFDM with High Resilience to Rapid Time-Variations

E Al-Susa

Department of Electronic and Electrical Engineering,
University of Bath, Bath BA2 7AY,UK.

R F Ormondroyd

Communications and Wireless Networks Group, Cranfield University,
RMCS, Shrivenham, Swindon, SN6 8LA, UK

Abstract: This paper investigates the performance of a coherent COFDM system in the presence of a time-varying frequency-selective fading channel using a predictor-based channel estimator. The channel estimation method is based on a decision-directed adaptive technique that uses decisions at the output of either the detector (uncoded mode) or the decoder (coded mode). The main aim is to investigate the effect of using a time-domain predictor on the performance of the channel estimator and to compare its impact on both the coded and uncoded estimator modes. It is found that the predictor significantly improves the estimator's performance, especially when the channel changes rapidly between consecutive OFDM symbols. It is also found that the performance of both the coded and uncoded estimator modes converge for SNR>15dB.

I. INTRODUCTION

Coded orthogonal frequency division multiplexing (COFDM) is an alternative approach to the design of a bandwidth efficient communication system in the presence of time-varying frequency-selective fading. It is based on the principle of transmitting a high-rate bit stream of data simultaneously on a number of parallel low-rate bit streams by sub-dividing the available bandwidth into many sub-channels. For maximum spectral efficiency, the sub-carriers are orthogonally spaced in frequency [1]-[3]. Forward error correction (FEC) coding and interleaving of the data bits provides frequency and time diversity. Since the data is now transmitted at a much lower rate, the impact of the inter-symbol interference (ISI) is significantly reduced. However, the ISI causes loss of orthogonality between OFDM blocks.

This may be maintained by the use of a cyclic prefix of a duration equal to the maximum delay spread of the channel [4]. Although the use of the cyclic prefix eliminates ISI between OFDM blocks, the impact of inter-channel interference (ICI) and local ISI remains and may need to be compensated by the use of channel equalisation, depending on whether coherent or non-coherent modulation is used. The penalty of using a non-coherent scheme, such as differential modulation, is the loss of about 3–4 dB in SNR to achieve a given bit error probability.

For a coherent modulation scheme, the use of decision-directed feedback adaptive channel estim-ation for the purpose of equalisation has been investigated by a number of authors [5][6][7]. The estimation of the channel may be obtained by using data-bit decisions at the output of the detector, prior to decoding (*uncoded mode*), or at the output of the decoder (*coded mode*), which, depending on the SNR, takes advantage of the FEC code.

In this paper we investigate the impact of using a prediction algorithm based on the time-domain autocorrelation function of samples of the previous estimates of the channel response. We also compare the performance of both the uncoded and coded channel estimator modes with and without the inclusion of the predictor.

In section two, a description of both the uncoded and coded channel estimator modes is presented. In sections three and four, we derive equations for the mean square error of the channel transfer function coefficients and bit error rate (BER) respectively. A description of the proposed prediction scheme and the simulation results are presented in

sections five and six. Finally, the conclusion is presented in section seven.

II Operation of Uncoded and Coded Channel Estimator Modes

The feedback channel estimator is shown in Figure 1. Both the coded and uncoded modes are based on the same principle, except that in the case of the coded mode the decisions for estimating the channel's response are taken after decoding the received symbols whereas for the uncoded mode they are taken immediately after detection.

Figure 1: Schematic of the Channel Estimator

Considering the uncoded channel estimator mode first, assume that an initial estimate of the channel is already established (for example, using a training sequence). The received OFDM block of symbols at the output of the FFT (written in vector notation), $\tilde{R}$, is equalised using this initial channel estimate and de-mapped. Then, as well as sending a copy of the de-mapped data to the de-interleaver, a copy is fed-back to the channel estimator. Here, the data is re-mapped to reconstruct the estimate of the transmitted symbols within the OFDM block, $\hat{X}$. An initial noisy estimate of the channel, $\hat{H}$, is then obtained from $\hat{X}$ and $\tilde{R}$ as shown in (1).

$$\hat{H} = \left(\frac{\tilde{R}}{\hat{X}}\right) = \left(\frac{X \cdot H + N}{\hat{X}}\right) \tag{1}$$

In (2), η is the error between the refined channel estimate and the actual channel transfer function and * is the complex conjugate operation.

For the coded mode, the data is de-interleaved and decoded in order to correct any possible errors in the received block. It is then re-encoded, re-interleaved and re-mapped in order to reconstruct the originally transmitted symbols. These are then passed to the channel estimator. This mode provides different estimates for $\hat{X}$ and hence:

$$Z_i = \tilde{R}_i \cdot \hat{H}_{i-1}^*$$
$$= \left(X_i \cdot H_i \cdot (H_{i-1} + \eta)^* + N_i \cdot (H_{i-1} + \eta)^*\right)$$

(2)

II.   MSE CALCULATION

In this section we derive the mean square error of the coefficients of the channel transfer function estimate. In this analysis, we assume that there are no errors in the data estimates (e.g. the system is operated at high E_b/N_o) so that $\hat{X} = X$. First we assume a static channel and estimate the impact of the noise. We then remove the noise and estimate the mean

square error between consecutive blocks due to the time variation of the channel.

The mean square error of the channel estimator, before filtering, is defined [9] as,

$$MSE(\hat{H}) = E\left\{\left(\hat{H} - H\right)^2\right\} \tag{3}$$

where $\hat{H}$ and H, are given by:

$$\hat{H} = \frac{\tilde{R}}{X} \quad \& \quad H = \frac{R}{X} \tag{4}$$

Here, R is the block of noise-free symbols, but with ICI. By combining equations (3) and (4), the MSE may be written as:

$$MSE(\hat{H}) = E\left\{\left(\left(\frac{X \cdot H}{X} + \frac{N}{X}\right) - \frac{X \cdot H}{X}\right)^2\right\} = E\left\{\left(\frac{N}{X}\right)^2\right\}$$
$$= 2\sigma^2 \cdot \alpha$$

(5)

where $2\sigma^2 = E\{N^2\}$ is the noise power, assuming zero mean AWGN, and $\alpha = E\{X\}^{-2}$ is the modulation noise enhancement factor [6].

The impact of using the FFT based filter on the MSE is a reduction in the additive noise power by a factor, L/M, where L is the cut-off frequency of the filter and F is the number of OFDM symbols in the block. Thus the mean square error becomes:

$$MSE^*(\hat{H}'') = \frac{L}{F} \cdot 2\sigma^2 \cdot \alpha \tag{6}$$

The impact of the time-varying channel due to Doppler can be assessed as follows. The channel coefficients for the kth block are related to the channel coefficients for the $(k-1)^{th}$ block if there is no differential Doppler by [10]:

$$H_t = H_{t-1} \cdot \exp(-j2\pi f_D T_L) \qquad (7)$$

where f_D is the Doppler frequency shift, and T_L is the duration of the *OFDM* block. Assuming that $E\{|H|^2\} = 1$, it can be shown that the mean square error due to the time variation can be given by:

$$MSE^{or}(\tilde{H}_t) = E \leq \{(H_{t-1} - H_t)\}^2$$
$$= E\{(1 - \exp(2\pi f_D T_L))^2\}$$
$$\approx (2\pi f_D T_L)^2$$

$$(8)$$

and thus the total mean square error, MSE^{tot}, is given by:

$$MSE^{r}(\hat{H}) = \frac{L}{N} \cdot (\alpha \cdot 2\sigma^2 + (2\pi f_D T_L)^2) \qquad (9)$$

III. BER CALCULATION

Assuming that a large number of sub-carriers are used, the frequency selective fading on the individual sub-carriers becomes flat fading [11]. This implies that the nth sub-carrier of the kth OFDM block will be multiplied by a complex value, $h_{k,n}$, that on the average has a Rayleigh distributed envelope. Using an estimate of the channel coefficients to equalise the signal, the probability of bit error rate for a coherent QPSK detector using the decision variable given by (10) may be calculated.

$$Z = \tilde{R} \cdot \hat{H}^* \qquad (10)$$

The *BER* analysis for this detector is based on appendix C of [11], which results in:

$$P_{BER} = \frac{1}{2} \cdot \left(1 - \frac{\mu}{\sqrt{2 - \mu^2}}\right)$$

$$(11)$$

Where $\mu = \dfrac{\bar{\gamma}}{1 + \bar{\gamma}}$ is the cross-correlation coefficient and $\bar{\gamma}$ is the average *SNR*.

IV. SYSTEM DESCRIPTION

In the previous section, we estimated the error due to a simple feedback method of channel estimation. In order to improve the channel

estimate, in this section we apply a prediction algorithm that is based on the time-domain correlation vector between the estimated samples. Since the intention here is to reduce the mismatch between the estimated and actual channel response, the results are shown in terms of *MSE* which is defined as the time averaged error energy per OFDM symbol between the estimated channel transfer function and the actual channel transfer function.

Linear prediction is based upon the concept of estimating the value of the Mth sample of a signal from the previous $M-1$ samples. Thus, given a set of data h_{t-1}, $h_{t-2}...h_{t-M}$, for a predictor of order M, the predicted value of h_t is given by:

$$\hat{h}_t = \sum_{k=1}^{M} -a_k \cdot h_{t-k} \qquad (12)$$

The prediction error, ε, is defined as the difference between the predicted and actual values, given by:

$$\varepsilon_t = h_t - \hat{h}_t = h_t - \sum_{k=1}^{M} -a_k \cdot h_{t-k}$$
$$= \sum_{k=0}^{M} a_k \cdot h_{t-k} \qquad a_0 = 1$$

$$(13)$$

To obtain the predictor coefficients that minimise the mean square prediction error, $E(\varepsilon)^2$, we differentiate (13), and equate the partial derivatives to zero. It can then be shown that the best coefficients, in the minimum mean square sense, are obtained by solving the following set of linear equation [13]:

$$\begin{bmatrix} \phi_0 & \phi_1 & \cdots & \phi_{M-2} & \phi_{M-1} \\ \phi_1 & \phi_0 & \cdots & \phi_{M-3} & \phi_{M-2} \\ \vdots & \vdots & \vdots & \vdots & \vdots \\ \phi_{M-2} & \phi_{M-3} & \cdots & \phi_2 & \phi_1 \\ \phi_{M-1} & \phi_{M-2} & \cdots & \phi_1 & \phi_0 \end{bmatrix} \cdot \begin{bmatrix} a_1 \\ a_2 \\ \vdots \\ a_{M-1} \\ a_M \end{bmatrix} = - \begin{bmatrix} \phi_1 \\ \phi_2 \\ \vdots \\ \phi_{M-1} \\ \phi_M \end{bmatrix}$$

(14)

where $\phi_j = E[h_t \cdot h_{t+j}]$ is the auto-correlation vector of the time domain signal samples. It is well known that the performance of the predictor is very sensitive to the method used to estimate the auto-correlation vector [30]. Two of the most popular algorithms used to estimate the predictor coefficients are the Levinson-Durbin and Burg algorithms [15],[16]. The Burg algorithm is in fact a development of the Levinson-Durbin algorithm. It is based on minimising the backward and forward prediction errors simultaneously, calcul-ating the predictor coefficients using a recursive procedure. This procedure exploits the Toeplitz symmetry of the autocorrelation matrix to proceed recursively beginning with a predictor of order one coefficient and to increase the order recursively using the low order solutions to obtain the solutions to the next higher order. This method has been proved to be generally a more accurate method than the Levison-Durbin algorithm.

In order to reduce the number of calculations, the prediction is applied on the time domain samples. Assuming that the number of samples involved for each predicted value is M, then $M \cdot L$ samples are stored in a matrix, A, as shown below. The predic-tion is performed on a row by row basis to produce the time-domain samples of the channel estimate. These are then passed onto the F bin (F-L zero padded) FFT to produce the full channel response.

$$A = \begin{bmatrix} h_0^0 & h_0^1 & \cdots & h_0^{M-2} & h_0^{M-1} \\ h_1^0 & h_1^1 & \cdots & h_1^{M-2} & h_1^{M-1} \\ \vdots & \vdots & \vdots & \vdots & \vdots \\ h_{L-1}^0 & h_{L-1}^1 & \cdots & h_{L-1}^{M-2} & h_{L-1}^{M-1} \\ h_L^0 & h_L^1 & \cdots & h_L^{M-2} & h_L^{M-1} \end{bmatrix}$$

(15)

V.   SIMULATIONS AND RESULTS

The results presented here examine the *MSE* performance of the coded and uncoded estimators, with and without the inclusion of

the time-domain predictor under a variety of different conditions. To get an insight into the behaviour of the estimators, the *MSE* was averaged over 10,000 OFDM blocks. Unless otherwise stated, the parameters used are summarised in Table 2. The data was assumed to be transmitted in frames of *K OFDM* blocks with each frame carrying a single block of pilot tones. Initial channel estimation is carried out by the pilot tones, but for the remaining (*K*-1) blocks channel estimation is *via* the decision directed algorithm. In addition, the channel is assumed to be static during each OFDM block. The channel model is the 6 tap COST 207 'urban' model. The Doppler conditions are provided in Table 1.

Number of Subcarriers	512	Pilot to Data Ratio (*1/K*)	2%
Transmission Rate	25Mbps	Cyclic Prefix	5 μsec
Doppler Frequency	100Hz	Modulation Scheme	QPSK
Prediction Length	100 Samples	Prediction Order	4
Maximum Delay Spread	5 μsec	Coding Rate	½ Rate Convolutional

Table 2: Simulation Parameters

Figures 2 and 3 show the impact of the predictor on the system's MSE performance for two OFDM block lengths for the uncoded and coded modes respectively. The two block lengths are 512 and 2048 symbols. It can be seen, especially for the case of the uncoded mode with a block length of 2048, that prediction allows almost a 20dB reduction in SNR to achieve an MSE of −10dB. The reason why the longer block lengths sometimes have a worse performance than the shorter block lengths was discussed in [8]. The other conclusion that can be drawn from these two figures is the fact that the performance of both the coded and uncoded modes become almost identical at *SNR*>15dB when prediction is used.
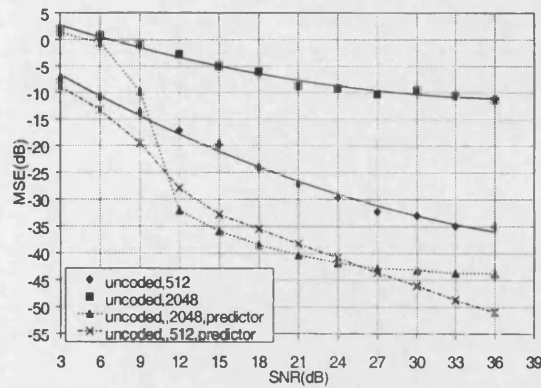
Figure 2: Performance Comparison on the Uncoded Mode with Respect to Block length
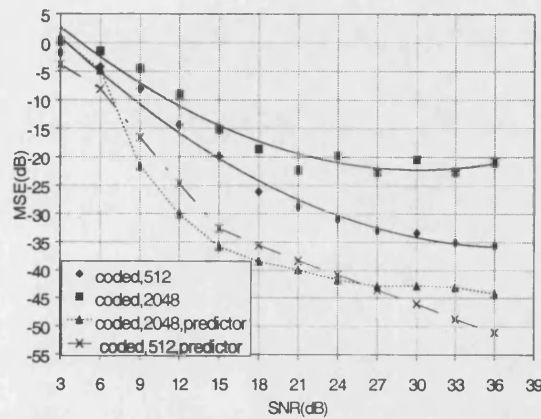

Figure 3: Performance Comparison of the Coded Mode with Respect to the Block length

Similarly, Figures 4 and 5 show the significant improvement achieved by using a predictor in the presence of very high Doppler frequencies. It can also be seen that both estimator modes have a very good performance even at Doppler frequencies as high as 320Hz.
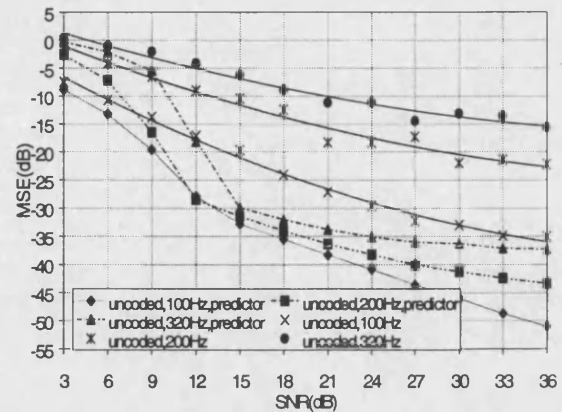

Figure 4: Performance Comparison of the Uncoded Mode with Respect to Doppler

These two figures also confirm that the performance of both estimator modes become almost identical at *SNR*>15dB with prediction.
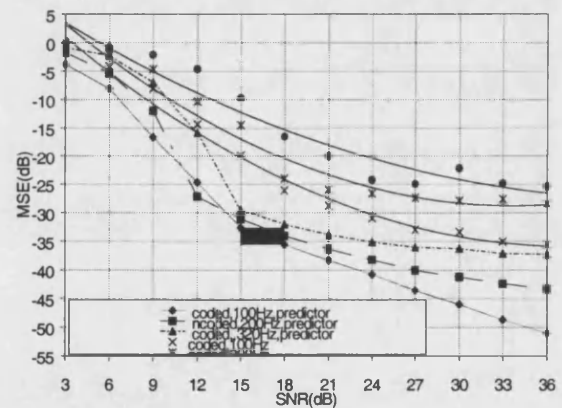

Figure 5: Performance Comparison of the Coded Mode with Respect to Doppler

It was found that the improvement obtained by increasing the number of prediction samples becomes much less significant after a certain length. This is illustrated in figure 6, which shows that when the prediction length exceeds 100 samples there is very little improvement in MSE performance.

A similar test was carried out to investigate the effect of increasing the order of the predictor. The results are shown in figure 7. It can be seen that at low signal to noise ratios there is a performance improvement achieved by increasing the order from two to four, however by increasing the order beyond four

16

the improvement achieved is much less significant. In fact, at high SNR (>14dB) about 1–2 dB performance <u>degradation</u> is inflicted by increasing the order from four to twelve.
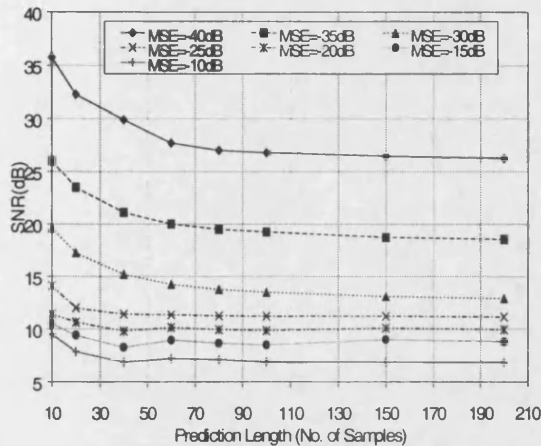

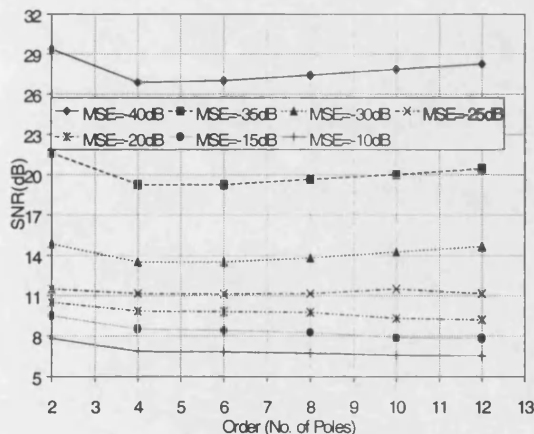**Figure 6: Effect of Increasing the Prediction Length**

Figure 7: Effect of Increasing the Prediction Filter's Order

Figure 8 shows the relationship between the *MSE* and the average *BER* of the system and it can be seen that using a predictor makes it possible to achieve a *BER* of less than 10^{-5} even under very harsh channel conditions.
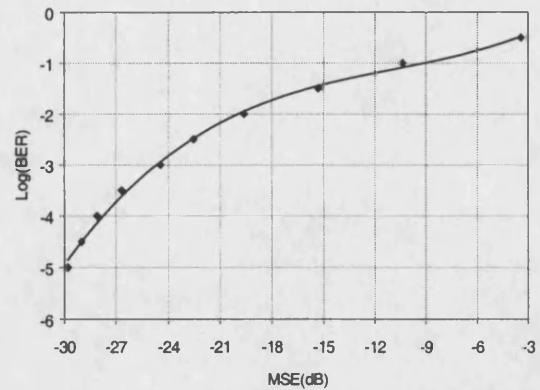

Figure 8: Relation of Average BER to the MSE

VI.   CONCLUSIONS

In this paper we have investigated the use of a time- domain-based predictor with the aim of improving the performance of decision directed feedback channel estimation based methods. It was shown that significant improvements are achieved by exploiting the time-domain characteristics as well as the frequency-domain characteristics of the channel. It was shown that the performance of both the coded and uncoded channel estimator modes behave in a similar manner at SNR>15dB when a predictor is used. It was also shown that the predictor's performance almost saturates when the predictor's length is increased beyond 100 samples.

VII.   REFERENCES

[1] R.W. Chang and R.A. Gibby, "*A theoretical study of performance of an orthogonal multiplexing data /transmission scheme*", IEEE Trans. on Comms., Vol. COM-16, No. 4, 529-541, 1968.

[2] S.B. Weinstein and P.M. Ebert, "*Data trans-mission by frequency division multiplexing using the discrete Fourier transform,*" IEEE Trans. on Comms., Vol. COM-19, No. 5, pp.628-634, 1971.

[3] M. Alard and R. Lasalle, "*Principle of modulation and channel coding for digital broadcasting for mobile receivers*", EBU Technical Review, no. 224, pp. 168-190. Aug. 1987.

[4] A. Ruiz and J.M. Cioffi, *"Discrete multiple tone modulation with coset coding for the spectrally shaped channel"*, IEEE Trans. on Comms, vol. COM-40, No. 6, pp. 1012-1029, 1992

[5] V. Mignone and A. Morello, *"CD3-OFDM: A novel demodulation scheme for fixed and mobile receivers"*, IEEE Trans. on Comms., Vol. 44, No 9, pp.1144-1151, 1996.

[6] A. Chini, Y. Wu, M. El-Tanany and S. Mahmoud *"Filtered decision feedback channel estimation for OFDM-based DTV terrestrial broadcasting system"*, IEEE Trans. on Broadcasting, Vol. 44, No.1, pp. 2-11, 1998.

[7] Y. Li, L.J. Cimini and N.R. Sollenberger, *"Robust channel estimation for OFDM systems with rapid dispersive fading channels"*, IEEE Trans. on Comms., Vol. 46, No. 7, pp. 902-915, 1998.

[8] R.F. Ormondroyd and E. Al-Susa, *"A high efficiency channel estimation and equalisation strategy for a broadband COFDM system"*, ISSSE'98, pp.471-475.

[9] S.M. Kay, *"Fundamentals of Statistical Signal Processing"*, Prentice Hall, Chap. 2, p. 19.

[10] A. Chini, *"Multi-carrier modulation in frequency selective fading channels"*, Ph.D. dissertation, Carleton University, Canada, 1994.

[11] P. Frenger and A. Svensson, *"Decision directed coherent detector for OFDM"*, Proceedings of the IEEE VTC'96, Vol. 3, pp. 1584-1593, 1996.

[12] J.G. Proakis, *"Digital Communications"*, Prentice Hall, 3rd ed., 1995.

[13] B. Porat, *"A Course in Digital Signal Processing"*, John Wiley and Sons, Inc. 1997.

[14] W.H. Press, S.A. Teukolsky, W.T. Vetterling and B.P. Flannery, *"Numerical Recipes in ,C"*, 2nd ed., Cambridge Press.

[15] G.B. Ribicki, *"Computers in Physics"*, Vol. 3, no. 2, pp. 85-87, 1989

[16] R. Shiavi, *"Introduction to Applied Statistical Signal Analysis"*, Aksen Associates Incorporated Publishers, 1991, Chap. 8.

The following paper was submitted to the IEEE Transactions on Vehicular Technology,1999

Improved Channel Estimation and Equalisation for a Broadband COFDM System in a Time Varying Frequency Selective Fading Channel

E Al-Susa

Department of Electronic and Electrical Engineering,
University of Bath, Bath BA2 7AY,UK.
Email: e.alsusa@bath.ac.uk, Fax: +441225 826 305

R F Ormondroyd

Communications and Wireless Networks Group, Cranfield University,
RMCS, Shrivenham, Swindon, SN6 8LA, UK
Email: r.f.ormondroyd@rmcs.cranfield.ac.uk, Fax: +441793 785260

Abstract: This paper investigates the performance of a coherent COFDM system in the presence of a time-varying frequency-selective fading channel using a predictor-based channel estimator. The channel estimation method is based on a decision-directed adaptive technique that uses decisions at the output of either the detector (uncoded mode) or the decoder (coded mode). The main aim is to investigate the effect of using a time-domain predictor on the performance of the channel estimator and to compare its impact on both the coded and uncoded estimator modes. It is found that the predictor significantly improves the estimator's performance, especially when the channel changes rapidly between consecutive OFDM symbols. It is also found that the performance of both the coded and uncoded estimator modes converge for SNR>15dB.

VIII. Introduction

Coded orthogonal frequency division multiplexing (COFDM) is an alternative approach to the design of a bandwidth efficient communication system in the presence of time-varying frequency-selective fading. It is based on the principle of transmitting a high-rate bit stream of data simultaneously on a number of parallel low-rate bit streams by sub-dividing the available bandwidth into many sub-channels. For maximum spectral efficiency, the sub-carriers are orthogonally spaced in frequency [1][18][3]. Forward error correction (FEC) coding and interleaving of the data bits

provides frequency diversity. Since the data is now transmitted at a much lower rate, the impact of the inter-symbol interference (ISI) is significantly reduced. However, the ISI causes loss of orthog-onality between OFDM blocks. This may be main-tained by the use of a cyclic prefix of a duration equal to the maximum delay spread of the channel [4]. Although the use of the cyclic prefix eliminates ISI, the impact of inter-channel interference (ICI) remains and may need to be compensated by the use of channel equalisation, depending on whether coherent or non-coherent modulation is used. The penalty of using a non-coherent scheme, such as differential modulation, is the loss of about 3–4 dB in SNR to achieve a given bit error probability.

For a coherent modulation scheme, the use of decis-ion-directed feedback adaptive channel estimation for the purpose of equalisation has been investigated by a number of researchers [5][6][7]. The estimation of the channel may be obtained by using data-bit decisions at the output of the detector, prior to decoding (*uncoded mode*), or at the output of the decoder (*coded mode*), which, depending on the SNR, takes advantage of the FEC code.

In this paper, using mainly computer simulations we begin by evaluating the sensitivity of the feedback channel estimator to significant channel variation resulting from long block duration and high Doppler frequencies. Then, we investigate the impact

of using a prediction algorithm based on the time-domain autocorrelation function of samples of the previous estimates of the channel response. We also compare the performance of both the *uncoded* and *coded* channel estimator modes with and without the inclusion of the predictor.

This paper is organised as follows. In section two, an expression of the OFDM baseband received signal is presented. This is followed by a description of both the *uncoded* and *coded* channel estimator modes. In sections four and five, we derive equations for the mean square error of the channel transfer function coefficients and bit error rate, respectively. A description of the proposed prediction scheme and the simulation results are presented in sections six and seven. Finally, the conclusion is presented in section eight.

IX. Received OFDM Signal Structure

Since the OFDM technique stretches the duration of the transmitted symbols in time, the analysis presented here assumes that the ISI occurs between pairs of OFDM symbols only. In other words, the impulse response dispersion does not exceed more than one consecutive symbol at a time. In frequency selective fading channels, the impulse response, *h(t)*, may be represented as a vector of samples as shown below:

$$h(t) = [h_0, h_1, \cdots, h_{N-1}]$$

Where it is assumed that the *h(t)* is causal and sampled at a Nyquest sampling rate over a period equal to the OFDM symbol duration. In addition, the individual samples of the channel impulse response are assumed to be uncorrelated Gaussian random variables. Using this definition of the impulse response, the received signal at the input of the receiver's FFT may be given as:

$$r_{j,i} = \sum_{k=0}^{i} x_{j,k} \cdot h_{j,i-k} + \sum_{k=i+1}^{N-1} x_{j-1,k} \cdot h_{j,N+i-k}$$

$$+ n_{j,i}$$

$$i = 0,1 \cdots, N-1$$

$$k = 0,1, \cdots, L-1$$

$$j = 0,1, \cdots, \infty$$

$$15$$

The above equation can be broken further into a more descriptive form as shown below:

$$r_{i,k} = \underbrace{x_{i,k} \cdot h_{i,0}}_{\substack{desired \\ sample}} + \underbrace{\sum_{m=0}^{k-1} x_{i,m} \cdot h_{i,k-m}}_{} + \underbrace{\sum_{m=k+1}^{N-1} x_{i-1,m} \cdot h_{i,N+k-m}}_{ISI} + \underbrace{n_{i,k}}_{\substack{additive \\ noise}}$$

$$16$$

Since the transmitted signal vector, x, can be represented in a matrix form as $x = CDFT^{-1} \cdot X$ where $CDFT^{-1}$ is an *NXN* matrix representing the complex inverse Fourier transform and X is a vector of the complex symbols to be transmitted, equation 15 can be rewritten as:

$$r_j = \overset{m1}{h_j} \cdot CDFT^{-1} \cdot X_j +$$

$$\overset{m2}{h_j} \cdot CDFT^{-1} \cdot X_{j-1} + n_j$$

$$17$$

Where, $\overset{m1}{h}, \overset{m2}{h}$ and $CDTF^{-1}$ are three *NXN* matrices defined as given below:

$$\overset{m1}{h} = \begin{bmatrix} h_0 & 0 & 0 & \cdots \\ h_1 & h_0 & 0 & \cdots \\ \cdot & \cdot & \cdot & \cdot \\ h_{n-1} & h_{N-2} & \cdots & h_0 \end{bmatrix}$$

$$\overset{m2}{h} = \begin{bmatrix} 0 & h_{N-1} & h_{N-2} & \cdots & h_1 \\ 0 & 0 & h_{N-1} & \cdots & h_2 \\ \cdot & \cdot & \cdot & \cdot & \cdot \\ 0 & 0 & 0 & \cdots & 0 \end{bmatrix}$$

and

$$CDFT^1 = \begin{bmatrix} D_N^{00} & D_N^{10} & D_N^{20} & \cdots & D_N^{(N-1)0} \\ D_N^{01} & D_N^{11} & D_N^{21} & \cdots & D_N^{(N-1)1} \\ D_N^{02} & D_N^{12} & D_N^{22} & \cdots & D_N^{(N-1)2} \\ \vdots & \vdots & \vdots & \vdots & \vdots \\ D_N^{0(N-1)} & D_N^{1(N-1)} & D_N^{2(N-1)} & \cdots & D_N^{(N-1)(N-1)} \end{bmatrix}$$

where

$$D_N = \frac{1}{\sqrt{N}} \cdot e^{2i\pi/N}$$

Using these matrix and vector notations, the received signal at the output of the FFT may be given by:

$$R_i = CDFT(r_i) = CDF\left(\overset{m1}{h_i} \cdot CDFT^1 \cdot X_i + \overset{m2}{h_i} \cdot CDFT^1 \cdot X_{i-1} + \right.$$

$$= (CDFT \overset{m1}{h_i} \cdot CDFT^1) \cdot X_i + (CDFT \overset{m2}{h_i} \cdot CDFT^1) \cdot X_{i-1} + CDFT n_i$$

$$= \underbrace{W_i \cdot X_i}_{\substack{desired \\ samples \\ + \\ ICI}} + \underbrace{V_i \cdot X_{i-1}}_{ISI} + \underbrace{N_i}_{AWGN}$$

18

where

$$W_j = CDFT \cdot \overset{m1}{h_j} \cdot CDFT^{-1} \quad (N \times N \text{ matrix})$$

$$V_j = CDFT \cdot \overset{m2}{h_j} \cdot CDFT^{-1} \quad (N \times N \text{ matrix})$$

and

$$N_j = CDFT \cdot n_j \qquad (N \times 1 \text{ matrix})$$

In the rest of the of the paper, it is assumed that the ISI term is fully absorbed by the inserted cyclic prefix and thus the detected signal is only corrupted by ICI and AWGN. Therefore, the received OFDM signal may be given as:

$$\tilde{R}_j = H_j \cdot X_j + N_j$$

19

Where **H**, is a vector representing the channel transfer function.

X. Operation of Uncoded and Coded Channel Estimator Modes

The feedback channel estimator is shown in Figure . Both the *coded* and *uncoded* modes are based on the same principle, except that in the case of the coded mode the decisions for estimating the channel's response is taken after decoding the received symbols whereas for the uncoded mode they are taken immediately after detection.
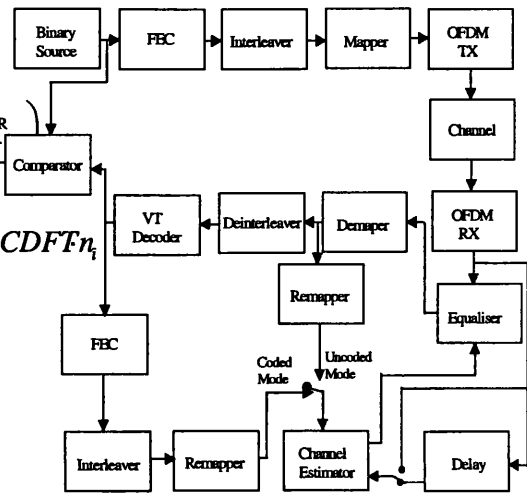

Figure 6 : Schematic of the Channel Estimator

Considering the uncoded channel estimator mode first, assume that an initial estimate of the channel is already established (for example, using a training sequence). The received OFDM block of symbols at the output of the FFT (written in vector notation), $\tilde{R}$, is equalised using this initial channel estimate and de-mapped. Then, as well as sending a copy of the de-mapped data to the de-interleaver, a copy is fed-back to the channel estimator. Here, the data is re-mapped in order to reconstruct the estimate, $\hat{X}$, of the transmitted symbols within the OFDM block. An initial noisy estimate of the channel, $\hat{H}$, is then obtained from $\hat{X}$ and $\tilde{R}$ as shown in equation 1.

$$\hat{H} = \left(\frac{\tilde{R}}{\hat{X}}\right) = \left(\frac{X \cdot H + N}{\hat{X}}\right) \qquad 20$$

where H is the actual channel response vector, X is the vector of transmitted symbols within the OFDM block and N is the additive white Gaussian noise vector.

The noisy estimate of the channel is then refined using a frequency-domain low-pass filter [8], which has a cut-off frequency of the order of the reciprocal of the maximum channel delay-spread. This reduces the error in the channel. This refined channel estimate is denoted $\hat{H}'$.

Assuming that the modulation is QPSK, the symbols of the kth OFDM block, $\tilde{R}_k$, can be phase equalised using the $(k\text{-}1)^{th}$ refined channel estimate, $\hat{H}'_{k-1}$, giving a decision vector, Z_k.

$$Z_k = \tilde{R}_k \cdot \hat{H}_{k-1}^*$$
$$= \left(X_k \cdot H_k \cdot \left(H_{k-1} + \eta\right)^* + N_k \cdot \left(H_{k-1} + \eta\right)^*\right)$$

$$21$$

In equation 2, η is the error between the refined channel estimate and the actual channel transfer function and $*$ is the complex conjugate operation.

For the coded mode, the data is de-interleaved and decoded in order to correct any possible errors in the received block. It is then re-encoded, re-interleaved and re-mapped in order to reconstruct the originally transmitted symbols. These are then passed to the channel estimator. This mode provides different estimates for $\hat{X}$ and hence η.

XI. MSE Calculation

In this section we derive the mean square error of the coefficients of the channel transfer function estimate. In this analysis, we assume

that there are no errors in the data estimates (e.g. operation at high E_b/N_0) so that $\hat{X} = X$. First we assume a static channel and estimate the impact of the noise. Then we remove the noise and estimate the mean square error between consecutive blocks due to the time variation of the channel.

The mean square error of the channel estimator, before filtering, is defined as [9],

$$MSE(\hat{H}) = E\left\{\left(\hat{H} - H\right)^2\right\} \qquad 22$$

where $\hat{H}$ and H, are given by:

$$\hat{H} = \frac{\tilde{R}}{X} \quad \& \quad H = \frac{R}{X} \qquad 23$$

Here, R is the block of noise-free symbols, but with ICI. By combining equations 3 and 4, the MSE may be written as:

$$MSE(\hat{H}) = E\left\{\left(\left(\frac{X \cdot H}{X} + \frac{N}{X}\right) - \frac{X \cdot H}{X}\right)^2\right\} = E\left\{\left(\frac{N}{X}\right)^2\right\}$$
$$= 2\sigma^2 \cdot \alpha$$

$$24$$

Where $2\sigma^2 = E\{N^2\}$ is the noise power, assuming zero mean AWGN, and $\alpha = E\{X\}^{-2}$ is the modulation noise enhancement factor [6].

The impact of using the FFT based filter on the MSE is a reduction in the additive noise power by a factor, L/M, where L is the cut-off frequency of the filter and F is the number of OFDM symbols in the block. Thus the mean square error becomes:

$$MSE^n(\hat{H}'') = \frac{L}{F} \cdot 2\sigma^2 \cdot \alpha \qquad 25$$

The impact of the time-varying channel due to Doppler can be assessed as follows. The channel coefficients for the kth block are

related to the channel coefficients for the (k-1)[th] block by [10] if there is no differential Doppler:

$$H_k = H_{k-1} \cdot \exp(-j2\pi f_D T_L) \qquad 26$$

where f_D is the Doppler frequency shift, and T_L is the duration of the *OFDM* block. Assuming that $E\{H^2\}=1$, it can be shown that the mean square error due to the time variation can be given by:

$$MSE^{DT}(\breve{H}_k) = E \leq \{(H_{k-1} - H_k)\}^2$$
$$= E\{(1-\exp(j2\pi f_D T_L))^2\}$$
$$\approx (2\pi f_D T_L)^2$$

$$27$$

and thus the total mean square error, MSE^{tot}, is:

$$MSE^{ot}(\hat{H}') = \frac{L}{N} \cdot \left(\alpha \cdot 2\sigma^2 + (2\pi f_D T_L)^2\right)$$

$$28$$

In Figure 7 a comparison between the theoretical and simulated estimators performance is presented. Since the theoretical analysis represents an upper bound of the estimator's performance, the simulated and theoretical curves tend to agree more at higher SNRs. In addition when the ratio of the pilot to data is increased from 0.1% to 1% the difference between the theoretical and simulated curves has become smaller. This is a direct result of breaking up the propagation of the inherent feedback errors which the theoretical analysis does not take account of.
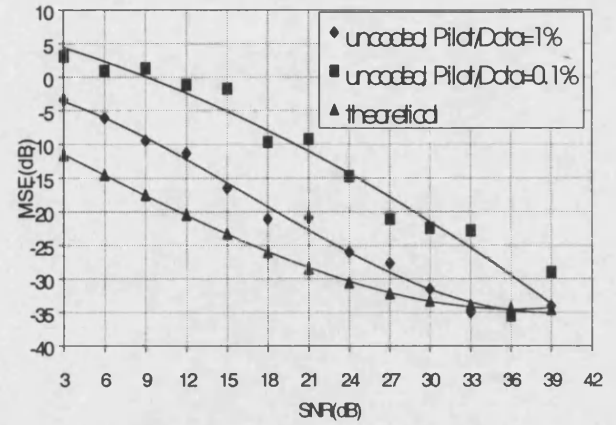

Figure 7 : Comparison between Theoretical and Simulated MSE Estimator's Perfromance

XII.   BER Calculation

Assuming that a large number of subcarriers are used, the impact of the frequency selective fading on the individual subcarriers becomes flat fading [11]. This implies that the nth sub-carrier of the kth OFDM block will be multiplied by a complex value, $h_{k,n}$, that on the average has a Rayleigh distributed envelope. Using an estimate of the channel coefficients to equalise the signal, the probability of bit error rate for a coherent QPSK detector using the decision variable given by equation 10, may be calculated.

$$Z = \tilde{R} \cdot \hat{H}'^* \qquad 29$$

The *BER* analysis for this detector is based on appendix *C* of [11], which results in:

$$P_{BER} = \frac{1}{2} \cdot \left(1 - \frac{\mu}{\sqrt{2-\mu^2}}\right)$$
30

Where $\mu = \dfrac{\overline{\gamma}}{1+\gamma}$ is the cross-correlation coefficient and $\overline{\gamma}$ is the average *SNR*.

In Figure 8 a comparison between the simulated and theoretical BER performance of the uncoded estimator is presented. Similar to the MSE case, better agreement between the

theoretical and simulated curves is obtained at higher SNRs and pilot to data ratios.
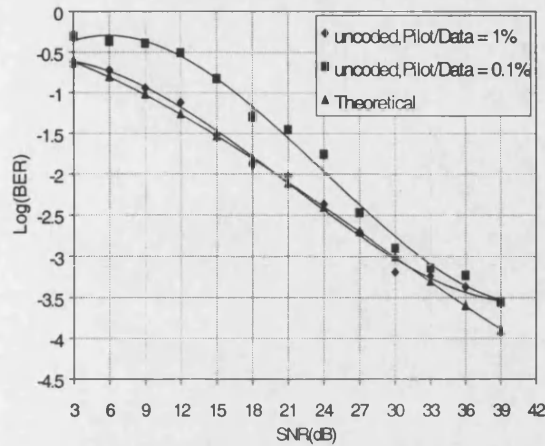

Figure 8 :Comparison Between Theoretical and Simulated BER Performance

XIII. Impact Of Block length and Doppler Spread

In this section the impact of increasing the Doppler frequency and the OFDM block length on the estimator's performance is analysed using computer simulations. Theoretically, the performance of an OFDM based system should improve as the block duration is increased, provided that the subcarriers remain sufficiently apart such that the Doppler effect on the individual subcarriers is negligible. This is due to the resulting increase in the inherent diversity of the OFDM system, which increases in proportion to the increase in the number of subcarriers used. However, in the case of a coherent OFDM system that uses a decision directed feedback channel estimation technique the increase of the OFDM block duration beyond a certain length may result in degradation in the overall system performance. This is due to the fact that the conventional feedback method provides the channel equaliser with a "one block length" delayed estimate of the actual channel transfer function. The difference between the actual channel transfer function and the delayed estimated one increases as the duration of the

OFDM block is made longer. This because the OFDM signal would then take longer in space, allowing the channel to change more, before completely being detected at the receiver.

A similar drawback of the feedback channel estimation method arises due to the presence of high Doppler frequencies which increases the rate at which the channel changes characteristics.

In Figure 9 and Figure 10 the impact of using long block duration and high Doppler frequencies is presented, respectively. It can be seen from Figure 9 that the increase in the number of subcarriers used per OFDM block ceases to improve the system performance after a block duration of 1024 subcarriers. Clearly, this indicates that delay imposed by the block duration begins to impact strongly on the estimate of the channel transfer function. In Figure 10, it can be seen that increasing the Doppler frequency from 40Hz to 320Hz results in about 6dB SNR loss.
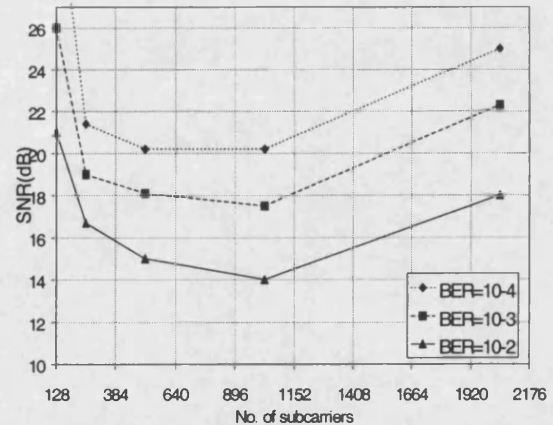

Figure 9 : Impact of the OFDM Block Duration on the Coded Estimator Mode
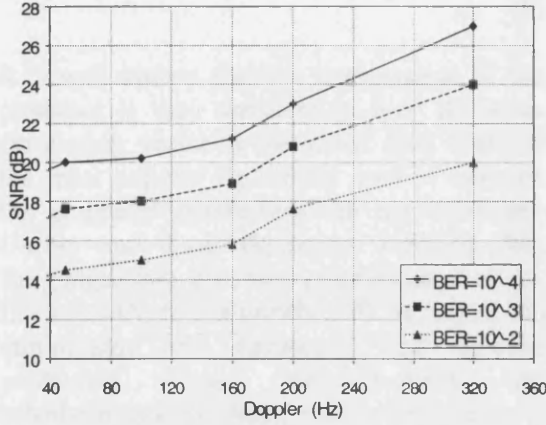
Figure 10 : Impact of the Doppler Frequency on the Coded Estimator Mode

XIV. System Description

In the previous section, we have estimated the error due to a simple feedback method of channel estimation. In order to improve the channel estimate, in this section we apply a prediction algorithm that is based on the time-domain correlation vector between the estimated samples. Since the intention here is to reduce the mismatch between the estimated and actual channel response, the results are shown in terms of *MSE* which is defined as the time averaged error energy per OFDM symbol between the estimated channel transfer function and the actual channel transfer function.

Linear prediction is based upon the concept of estimating the value of the Mth sample of a signal from the previous *M-1* samples. Thus, given a set of data h_{t-1}, $h_{t-2}...h_{t-M}$, for a predictor of order *M*, the predicted value of h_t is given by:

$$\hat{h}_t = \sum_{k=1}^{M} -a_k \cdot h_{t-k} \qquad 31$$

The prediction error, ε, is defined as the difference between the predicted and actual values, given by:

$$\varepsilon_t = h_t - \hat{h}_t = h_t - \sum_{k=1}^{M} -a_k \cdot h_{t-k}$$

$$= \sum_{k=0}^{M} a_k \cdot h_{t-k} \qquad a_0 = 1$$

$$32$$

To obtain the predictor coefficients that minimise the mean square prediction error, $E(\varepsilon)^2$, which is defined by 33, we differentiate with respect to the desired coefficients and equate the partial derivatives to zero. As shown below:

$$E\{\varepsilon_t\}^2 = E\left\{ \sum_{k=0}^{M} a_k \cdot h_{t-k} \right\}^2$$

33

After differentiation, the result is:

$$\frac{\partial E(\varepsilon_t)^2}{\partial a_j} = 2E\left(\frac{\partial \varepsilon_t}{\partial a_j} \cdot \varepsilon_t \right)$$

$$= 2E\left(h_{t-j} \cdot \sum_{k=0}^{M} a_k \cdot h_{t-k} \right)$$

$$= 2\sum_{k=0}^{M} a_k E\left(h_{t-j} \cdot h_{t-k} \right)$$

$$= 2\sum_{k=0}^{M} a_k \cdot \phi_{t-k} = 0, \qquad 1 \le t \le M$$

34

Using the fact that $a_0 = 1$ and the even property of the autocorrelation vector, $\phi_j = E[h_t \cdot h_{t+j}]$, equation 34 can be written in a matrix form as shown in equation 35 which when solved produces the best predictor's coefficients, in the minimum mean square sense:

$$\begin{bmatrix} \phi_0 & \phi_1 & \cdots & \phi_{M-2} & \phi_{M-1} \\ \phi_1 & \phi_0 & \cdots & \phi_{M-3} & \phi_{M-2} \\ \vdots & \vdots & \vdots & \vdots & \vdots \\ \phi_{M-2} & \phi_{M-3} & \cdots & \phi_2 & \phi_1 \\ \phi_{M-1} & \phi_{M-2} & \cdots & \phi_1 & \phi_0 \end{bmatrix} \begin{bmatrix} a_1 \\ a_2 \\ \vdots \\ a_{M-1} \\ a_M \end{bmatrix} = - \begin{bmatrix} \phi_0 \\ \phi_1 \\ \vdots \\ \phi_{M-1} \\ \phi_M \end{bmatrix}$$

It is well known that the performance of the predictor is very sensitive to how the auto-correlation vector is estimated [30]. Two of the most popular algorithms used to estimate the predictor coefficients are the Levinson-Durbin and Burg algorithms [15][16]. The Burg algorithm is in fact a development of the Levinson-Durbin algorithm. It is based on minim-ising the backward and forward prediction errors simultaneously for calculating the predictor coeffic-ients using a recursive procedure. This procedure exploits the Toeplitz symmetry of the autocorrel-ation matrix to proceed recursively beginning with a predictor of order one coefficient and to increase the order recursively using the low order solutions to obtain the solutions to the next higher order. This method has been proved to be generally a more accurate method than the Levison-Durbin algorithm.

In order to reduce the number of calculations, the prediction was applied on the time domain samples. Assuming that the number of samples involved for each predicted value is M, then $M \cdot L$ samples were stored in a matrix, A, as shown below. The predic-tion is performed on a row by row basis to produce the time-domain samples of the channel estimate. These are then passed onto the F bin ($F-L$ zero padded) FFT to produce the full channel response.

$$A = \begin{bmatrix} h_0^0 & h_0^1 & \cdots & h_0^{M-2} & h_0^{M-1} \\ h_1^0 & h_1^1 & \cdots & h_1^{M-2} & h_1^{M-1} \\ \vdots & \vdots & \vdots & \vdots & \vdots \\ h_{L-1}^0 & h_{L-1}^1 & \cdots & h_{L-1}^{M-2} & h_{L-1}^{M-1} \\ h_L^0 & h_L^1 & \cdots & h_L^{M-2} & h_L^{M-1} \end{bmatrix}$$

XV. Simulations and Results

The results presented here examine the *MSE* performance of the coded and uncoded estimators, with and without the inclusion of the time-domain predictor under a variety of different conditions. To get an insight into the

behaviour of the estimators, the *MSE* was averaged over 10000 OFDM blocks. Unless otherwise stated, the parameters used are summarised in Table 2. The data was assumed to be transmitted in frames of K OFDM blocks with each frame carrying a single block of pilot tones as shown in Figure 11. This type of frame structure allows two uses of the pilot tones. One use is for frame synchronisation and the other is to provide an initial estimate of the channel transfer function. Only the initial channel estimation is carried out by the pilot tones, and for the remaining (K-1) blocks channel estimation is *via* the decision directed algorithm. In addition, the channel is assumed to be static during each OFDM block. The channel model is the 6 tap COST 207 'urban' model. The Doppler conditions are provided in Table 1.
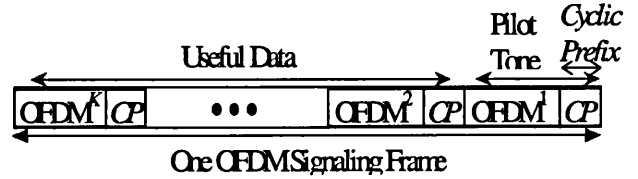
Figure 11 : Schematic of an OFDM Signalling Frame

Number of Subcarriers	512	Pilot to Data Ratio ($1/K$)	2%
Transmission Rate	25Mbps	Cyclic Prefix	5 μsec
Doppler Frequency	100Hz	Modulation Scheme	QPSK
Prediction Length	100 Samples	Prediction Order	4
Maximum Delay Spread	5 μsec	Coding Rate	½ Rate Convolutional

Table 3: Simulation Parameters

Figure and **Figure** show the impact of the predictor on the system's MSE performance for two OFDM block lengths for the uncoded and coded modes. The two block lengths are 512 and 2048 symbols, respectively. It can be seen, especially for the case of the *uncoded* mode with a block length of 2048, that prediction allows almost a 20dB reduction in SNR to achieve an MSE of −10dB. The reason why the longer block lengths sometimes have a worse performance than the shorter block

lengths was discussed in [8]. The other conclusion that can be drawn from these two figures is the fact that the performance of both the *coded* and *uncoded* modes become almost identical at *SNR*>15dB when prediction is used.
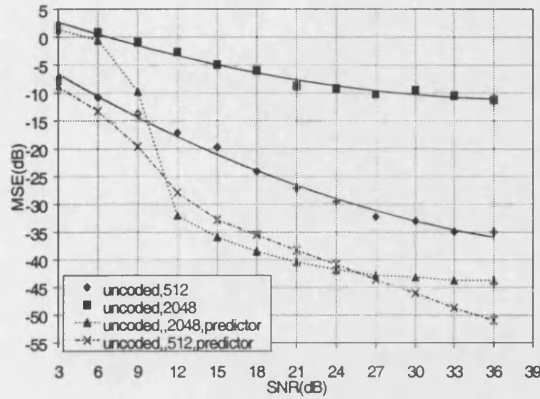

Figure 12: Performance Comparison on the Uncoded Mode with Respect to Block length
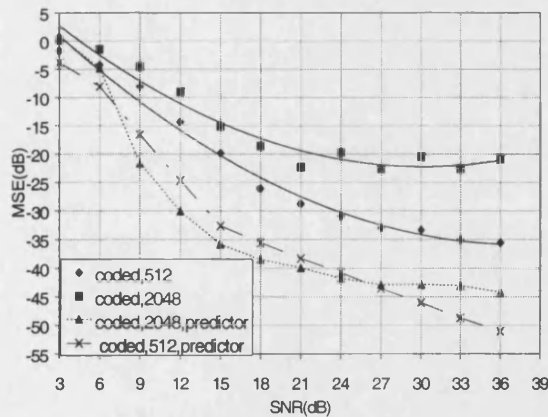

Figure 13: Performance Comparison of the Coded Mode with Respect to the Block length

Similarly, Figure and Figure show the significant improvement achieved by using a predictor in the presence of very high Doppler frequencies. It can also be seen that both estimator modes have a very good performance even at Doppler frequencies as high as 320Hz. These two figures also confirm that the performance of both estimator modes become almost identical at *SNR*>15dB with prediction.
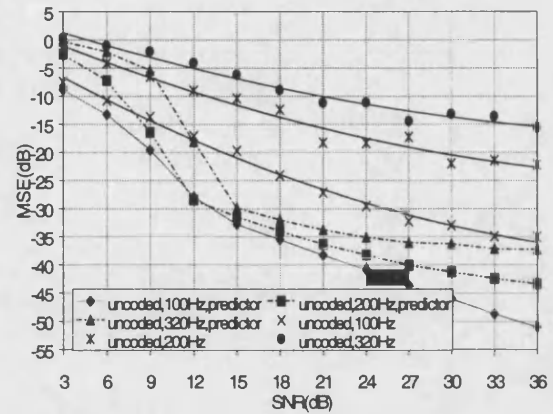
Figure 14: Performance Comparison of the Uncoded Mode with Respect to Doppler
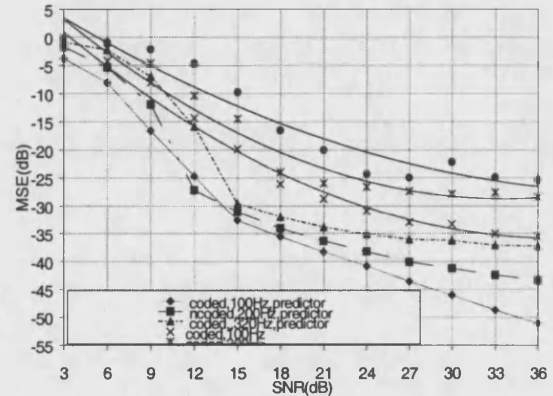
Figure 15: Performance Comparison of the Coded Mode with Respect to Doppler

It was found that the improvement obtained by increasing the number of prediction samples becomes much less significant after a certain length. As can be seen from

Figure, the improvement achieved by increasing the number of samples decreases exponentially.

A similar test was carried out to investigate the effect of increasing the order of the predictor. The results are shown in **Figure**. It can be seen that at low signal to noise ratio there is a performance improvement achieved by increasing the order from two to four, however by increasing the order beyond four the improvement achieved is much less

significant. In fact, at high SNR (>14dB) about 1–2 dB performance degradation is inflicted by increasing the order from four to twelve.

Figure 16: Effect of Increasing the Prediction Length

Figure 17: Effect of Increasing the Prediction Filter's Order

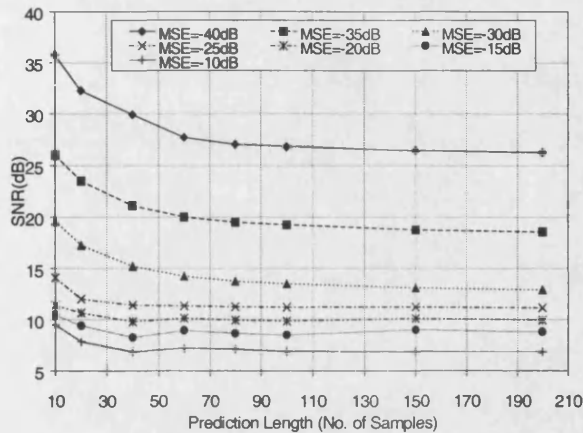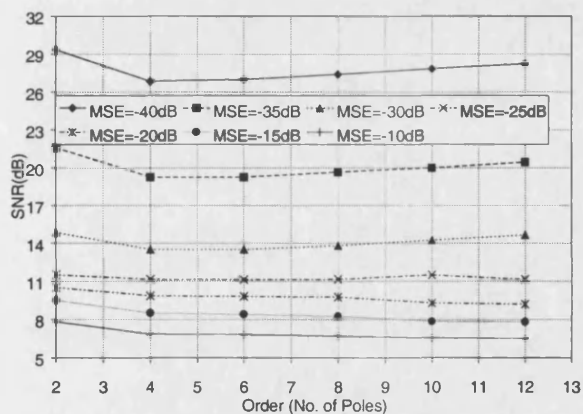Figure shows the relation-ship between the *MSE* and the average *BER* of the system and it can be seen that using a predictor makes it possible to achieve a *BER* of less than 10^{-5} even under very harsh channel conditions.
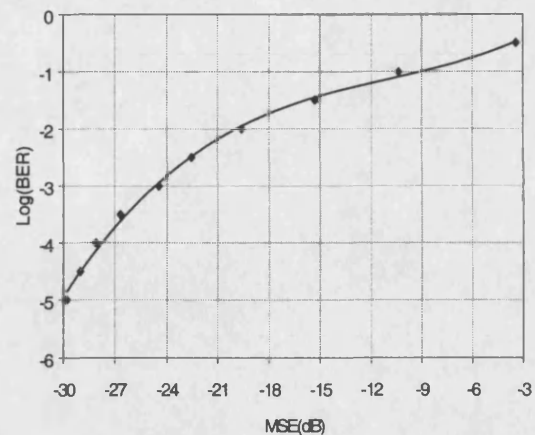
Figure 18: Relation of Average BER to the MSE

XVI. Conclusions

In this paper we have investigated the use of a time- domain-based predictor with the aim of improving the performance of decision directed feedback channel estimation based methods. It was shown that significant improvements are achieved by exploiting the time-domain characteristics as well as the frequency-domain characteristics of the channel. It was shown that the performance of both the coded and uncoded channel estimator modes behave in a similar manner at SNR>15dB when a predictor is used. It was also shown that the predictor's performance almost saturates when the predictor's length is increased beyond 100 samples.

XVII. References

[17] R. W. Chang and R. A. Gibby, "*A theoretical study of performance of an orthogonal multiplexing data /transmission scheme*", IEEE Trans. on Comms., Vol. COM-16, No. 4 1968.

[18] S. B. Weinstein and P. M. Ebert, "*Data transmission by frequency division multiplexing using the discrete Fourier transform,*" IEEE Trans. on Comms., Vol. COM-19, No. 5, pp.628-634, 1971.

[19] M. Alard and R. Lasalle, "*Principle of modulation and channel coding for digital broadcasting for mobile receivers*", EBU

Technical Review, no. 224, pp. 168-190. Aug. 1987.

[20] A. Ruiz and J. M. Cioffi, *"Discrete multiple tone modulation with Coset coding for the spectrally shaped channel"*, IEEE Trans. on Comms, vol. 40, no. 6, June 1992

[21] V. Mignone and A. Morello, *"CD3-OFDM: A novel demodulation scheme for fixed and mobile receivers"*, *"*, IEEE Trans. on Comms. Tech., Vol. 44, No 9, Sept. 1996.

[22] A. Chini, Y. Wu, M. El-Tanany and S. Mahmoud *"Filtered decision feedback channel estimation for OFDM-based DTV terrestrial broadcasting system"*, IEEE Trans.on broadcasting, Vol. 44, No.1, March 1998, pp. 2-11.

[23] Y. Li, L. J. Cimini and N. r. Sollenberger, *"Robust Channel estimation for OFDM Systems with Rapid Dispersive Fading Channels "*, IEEE Trans.on Comms., Vol. 46, No. 7, July 1998, pp. 902-915.

[24] R.F. Ormondroyd and E. Al-Susa, *"A High Efficiency Channel Estimation and Equalisation Strategy for a broadband COFDM System"*, ISSSE'98, pp.471-475.

[25] Steven M. Kay, *"Fundamentals of statistical signal processing"*, PTR Prentice Hall, Chap. 2, pp. 19.

[26] A. Chini, *"Multi-carrier modulation in frequency selective fading channels "*, Ph.D. dissertation, Carleton University, Canada, 1994.

[27] P. Frenger and A. Svensson, *"A decision directed coherent detector for OFDM"*, Proceedings of the IEEE VTC'96, Vol. 3, pp. 1584-1593.

[28] John G. Proakis, *"Digital communications"*, third edition, 1995.

[29] B. Porat, *"A Course in Digital Signal Processing"*, John Wiley and Sons, INC. 1997.

[30] W. H. Press, S. A. Teukolsky, W. T. Vetterling and B. P. Flannery, *"Numerical recipes in C"*, 2nd edition, Cambridge.

[31] G. B. Ribicki, G. B 1989, *"Computers in Physics"*, Vol. 3, no. 2, pp. 85-87.

[32] R. Shiavi, *"Introduction to Applied Statistical Signal Analysis"*, Aksen Associates Incorporated Publishers, 1991, Chap. 8.

The following paper was published in the proceedings of the
IEEE ISSE'98, Sept. 1998

A High Efficiency Channel Estimation and Equalisation Strategy for a Broadband COFDM System

R F Ormondroyd and E A Al-Susa[+]
Cranfield University, Communications and Wireless Networks Research Group,
RMCS Shrivenham, Swindon, SN6 8LA, UK.

+ University of Bath, Department of Electronic and Electrical Engineering,
Bath, BA2 7AY, UK,

5.1 ABSTRACT

COFDM is a channel coding and modulation scheme that mitigates the adverse effects of time-varying, frequency-selective fading by using multi-carrier modulation combined with time- and frequency-domain interleaving and forward error correcting coding (FEC). COFDM effectively transforms the time-domain equalisation problem of conventional single carrier systems into the frequency domain. This paper examines the performance of an efficient feedback channel estimation and equalisation algorithm for a 25Mb/s COFDM-QAM system in a frequency-selective multipath channel. In particular, the effect of the COFDM block length relative to the coherence time of the channel is discussed.

1. INTRODUCTION

Orthogonal frequency division multiplexing (OFDM) is a multi-carrier modulation technique in which the data is transmitted as many bit streams in parallel on sub-carriers rather than as a single high-rate stream. The bit stream on each sub-carrier has a much lower bit rate than for the single carrier case and the sub-carriers can overlap [1], which gives OFDM its high spectral efficiency. Although the sub-carriers overlap, by ensuring that certain orthogonality constraints are satisfied, the sub-carriers can be independently separated at the receiver [2]. The usual method of generating OFDM time-domain waveforms is *via* the Fourier transform [3,4]. The data-rate of conventional serial transmission methods is limited by inter-symbol interference due to the time-dispersion of the

multipath channel. This can extend over several data symbol periods and requires complicated time-domain equalization techniques to mitigate this effect. In contrast, several results [5-8] have showed that a well designed coded OFDM system (COFDM) is much less sensitive to time dispersion and it can improve the bit error rate significantly. At high data rates, COFDM does not eliminate the need for equalization, but the frequency domain approach employed by OFDM systems is considered to be much simpler to implement in DSP-based receivers than time-domain equalisers. Equalisation for the case of coherent demodulation of the received OFDM blocks has been addressed by Sari *et al* [9], amongst others.

In order to equalize and compensate for the degradation imposed by the channel, a good estimate of the channel response is required continuously. This fundamental and important issue of channel estimation has been the subject of many researchers [10-14]. One of the problems of some of these methods is the high percentage of data bits that are lost to the channel sounding process needed to obtain the channel estimate. In this paper, we study the performance of a practical feedback channel estimation algorithm that is extremely efficient and simulation results showing the strengths and weaknesses of this method are presented. The paper is arranged as follows. Section two contains a brief description of the mathematical representation of the OFDM system and its behavior in the multipath channel. A description of the feedback channel estimation method is given in section three whilst section four discusses the simulation

results showing the performance of such system at 25Mb/s.

2. OFDM SYSTEM DESCRIPTION

In this parallel data transmission scheme, the data (represented by complex-valued symbol mappings appropriate to the modulation scheme being adopted, eg. QAM) is transmitted simultaneously over N orthogonal sub-carriers, equally spaced within the desired transmission bandwidth, W. The base-band continuous-time signal, $x(t)$, of the OFDM system may be generated using a set of orthogonal basis functions $\Phi_{j,k}(t)$ which are defined as:

$$\Phi_{j,k}(t) = rect(t - jT) \cdot e^{2i\pi kt/T}$$

(1)

where:

$$rect(t) = \begin{cases} \dfrac{1}{\sqrt{T}} & if & \dfrac{-T}{2} \le t < \dfrac{T}{2} \\ 0 & otherwise \end{cases},$$

and $T=N/W$, is the symbol duration. The transmitted base-band signal, $x(t)$, can therefore be written in the following form for an infinite stream of symbols:

$$x(t) = \sum_{j=-\infty}^{+\infty} \sum_{k=0}^{N-1} X_{j,k} \cdot \Phi_{j,k}(t)$$

(2)

or equivalently:

$$x(t) = \sum_{j=-\infty}^{+\infty} \left\{ rect(t - jT) \cdot \sum_{k=0}^{N-1} X_{j,k} \cdot e^{2i\pi kt/T} \right\} \quad (3)$$

The demodulation of this signal at the receiver is achieved using a set of basis functions that are matched to those used in the transmitter. Thus, the demodulation process can be expressed as [15]:

$$X_{j,k} = \int_{-\infty}^{+\infty} x(t) \cdot \Phi_{j,k}^{*}(t)dt$$

(4)

where * stands for the complex conjugate operation. In the digitally implemented OFDM system, the modulation of the OFDM signal is usually by means of the inverse discrete Fourier transform, preferably the IFFT [2], which is relatively straightforward using DSP. Demodul-ation is by the corresponding DFT or, more commonly, through the FFT algorithm. Therefore, the transmitted base-band signal, $x_j(t)$, of the jth OFDM symbol and its counterpart demodulated signal, X_j, at the receiver may be written as follows:

$$x_j(n) = \frac{1}{\sqrt{N}} \cdot \sum_{k=0}^{N-1} X_{j,k} \cdot e^{2i\pi kn/N}$$

and

$$X_j(n) = \frac{1}{\sqrt{N}} \cdot \sum_{k=0}^{N-1} x(n) \cdot e^{-2i\pi kn/N}$$

(5)

Considering a multipath channel with an impulse response $h(t)$ given by [17]:

$$h(t) = \left(\sum_{i=0}^{M-1} h_i e^{j(2\pi f_{Di}(t)t + \theta_i)} \delta(t - \tau_i) \right) + n$$

(6)

where M is the number of paths, h_i is the path attenuation of the ith path, $f_{Di}(t)$ is the Doppler frequency at time t of the ith path, θ_i and τ_i are the initial phase and time delay of the ith path, respectively, the received signal r, assuming that the delay spread of the channel is limited to only one consecutive OFDM block, can be expressed as:

$$r_{j,k} = \sum_{j=-\infty}^{j=+\infty} \sum_{n=0}^{k} \left\{ \underbrace{h_{j,k-n} \cdot x_{j,n}}_{(1)} + \underbrace{\sum_{n=k+1}^{N-1} h_{j,N+k-n} \cdot x_{j-1,n}}_{(2)} \right\} + \underbrace{n_{j,k}}_{(3)}$$

(7)

where term (1) is the convolution of the OFDM signal with the impulse response of

the channel, term (2) is the convolution of a delayed version of the previous OFDM signal with the impulse response of the channel and term (3) represents the additive white Gaussian noise, (AWGN).

The effect of the delay spread causes the OFDM blocks to lose orthogonality, resulting in severe degradation in the receiver performance. In practice, orthogonality is maintained by ensuring that the OFDM blocks remain independent by appending a *cyclic-prefix* to each block of the serial data stream after the IFFT in the transmitter. The cyclic prefix is a copy of p OFDM symbols from the rear of the OFDM block that are appended to the front of the block [18]. Assuming that the impulse response of the channel is completely absorbed by the cyclic prefix, the rec-eived signal can be expressed in a vector form as:

$$R = H \cdot X + N \qquad (8)$$

The multipath channel used in the following simulation was modelled as a six tap delay line with six complex number multipliers (representing the random path loss) according to [19]. The complex numbers are generated independently and produce a Rayleigh distributed signal envelope [16]. At the receiver, Gaussian noise is added to the distorted signal, in the usual way. Equation (6) assumes a different Doppler frequency for each path, but in the following simulations a common Doppler frequency was used for all the paths.The parameters describing the channel used here (COST 207, urban model) are summarised in table 1, below.

Path Number	1	2	3	4	5	6
Delay (μs)	0	0.2	0.6	1.6	2.4	5
Attenuation (dB)	8.4	2.4	6.4	14.4	18.4	22.4

Table 1. Parameters of the channel model

3. DECISION FEEDBACK CHANNEL ESTIMATION

In an OFDM system, equalisation is usually carried out in the frequency domain. This is possible if the data on each sub-carrier is transmit-ted at a sufficiently low symbol rate that equalis-ation can be carried out by phase

and amplitude correction of each sub-carrier. Channel estimation is required obtain the frequency response of the channel at each sub-carrier frequency. The most common way of channel estimation for OFDM systems operating in time-varying, frequency-selective channels is to use pilot tones [2,10] scattered amongst the transmitted data symbols. These pilot tones provide samples of the frequency response of the channel, which are then fed to an interpolating filter to generate the full channel frequency response from which the equaliser's coefficients are then established. In [11], the use of the LMS algorithm for channel equalisation was examined and some of the problems associated with this technique were discussed. References [13] and [4] proposed a feedback channel estimation method utilising an FEC decoder in addition to the use of scattered pilot tones.

In this paper, we investigate the performance of a simpler decision feedback channel estimation method which could be implemented practically in DSP. This method is based on a (OFDM) symbol by symbol detection technique. Initially, the channel response is estimated in the usual way by sending a comb of pilot tones. However, instead of updating the channel estimate by sending more pilot tones (which is a very inefficient process), the channel frequency response is estimated from the previous equalised OFDM block using a decision feedback algorithm. The block diagram depicting this method is shown in figure 1, below.

As can be seen from the above block diagram, the received OFDM block is fed to the equalizer whose coefficients are already established (from the initial channel sounding process). The equalised block of data is then demapped and a copy of the demapped data is fed back to the channel estimator section where the data is remapped again to reconstruct the original symbols that had been transmitted.
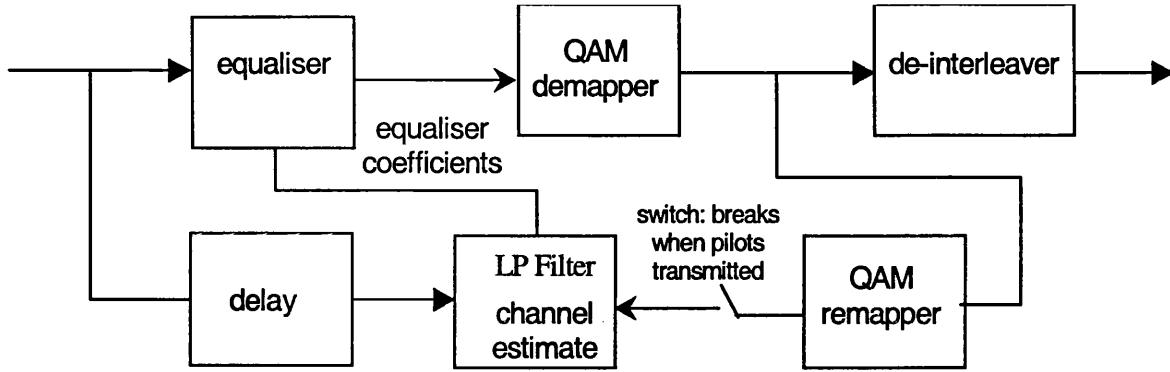
Figure 1: Schematic of the channel estimator and equaliser structure

The reason for the process of demapping and remapping is to reduce the effect of the noise on the reconstructed version of the transmitted symbols. The channel estimate is then established by utilising the relationship between the unequalized version of the OFDM block and its corresponding reconstructed version. This estimate is very noisy and must be low-pass filtered before it can be fed-back to the equaliser in order to equalise the next OFDM block. As will be readily appreciate, the channel estimate fed to the equaliser is delayed by one OFDM block. Thus, this type of channel estimation can only be used if the coherence time of the channel is much longer than the duration of the OFDM block. Simulation results showing the effect of the ratio of the coherence time of the channel to the block duration on the BER performance of the system will be shown in the next section. The estimation of the channel parameters can be obtained using either the zero-forcing (ZF) or the minimum mean square error (MMSE) criterion as given by equations (9) and (10) below.

$$\hat{H}_{n-1}^{ZF} = \frac{\tilde{X}_{n-1} + \eta}{\dot{X}_{n-1}}$$ (9)

$$\hat{H}_{n-1}^{MMSE} = \frac{(\tilde{X}_{n-1} + \eta) \cdot \dot{X}_{n-1}^{*}}{(\dot{X}_{n-1} \cdot \dot{X}_{n-1}^{*}) + \frac{\sigma_{n-1}^{noise}}{\sigma_{n-1}^{signal}}}$$

(10)
where:

$\hat{H}_{n-1}$ is the noisy channel estimate ,

$\tilde{X}_{n-1}$ is the $(n\text{-}1)^{th}$ OFDM block prior to equalisation,

$\dot{X}_{n-1}$ is the $(n\text{-}1)^{th}$ OFDM block after equalisation (reconstructed version),

$\dot{X}_{n-1}^{*}$ is the complex conjugate of $\dot{X}_{n-1}$,

η is the additive white Gaussian noise,

σ_{n-1}^{noise} & σ_{n-1}^{signal} are the instantanuous noise and signal power respectively.

This noisy channel estimate needs to be further improved by passing it through a low-pass filter with a cutoff frequency equal to the coherence bandwidth of the channel. The low-pass filter implemented here is a zero-padding FFT-based filter in which the channel estmate (which corresponds to the channel frequency response) is passed through an IFFT. Then, all the components that fall in the time slots that are longer than the longest expected channel delay are padded to zero before taking the signal back to its original form using the FFT. By doing so, all the high frequency components that belong to the additive noise are eliminated. The graph shown in figure 2 shows the effect of the technique on the channel estimate.
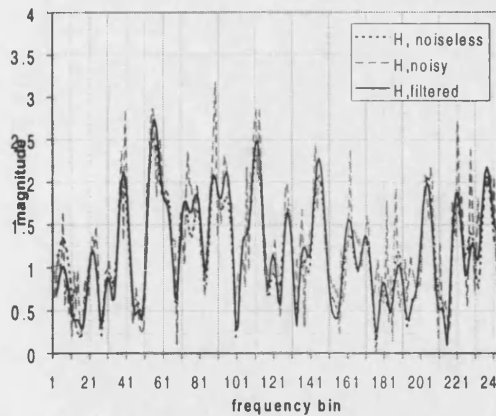
Figure 2: Effect of low-pass filtering on the channel estimate (SNR = 5dB)

Modulation type	4QAM
No. of subcarriers	512
Data rate	25Mbps
Symbol rate	12.5Msps
Symbol duration	41 μ sec
Max. delay	5 μ sec
cyclic prefix	5 μ sec
Doppler. frequency	80Hz
Vehicle speed	70mh
Coding rate	½ convolutional
Constant length	7
Subcarrier spacing	24.4kHz
Interleaving depth	0.32msec

Table 2: Table of principal parameters

In a noisy, multipath faded, channel, data errors are inevitable. In a data feedback equaliser, this can lead to error propagation. To prevent this from happening to a significant extent, the channel is periodically re-sounded using pilot tones. When this happens, the data feedback path is temporarily disconnected, as shown in figure 1. The effect of the period over which the data feedback estimator is connected is investigated in section 4.

4. SIMULATION RESULTS

Computer simulations were used to assess the performance of this feedback channel estimation and equalisation method for a COFDM-4QAM system transmitting at 25Mb/s using bit error rate (BER) as the metric for comparison. To simplify the simulations, only one level of convolutional channel coding was used. Viterbi decoding and time- and frequency-interleaving were implemen-ted. The parameters of the system under test are summarised in Table 2.

The following were assumed throughout:
(i) delay spread is completely absorbed by the cyclic prefix,
(ii) perfect synchronisation and brick-wall filtering is used,
(iii) the effect of phase noise in the receiver's local oscillator is not considered,
(iv) non-linearities in the transmitter and receiver are not considered.

Figure 3 shows the performance of the COFDM-4QAM system using the channel estimation scheme, described above, which employs a low-pass filter. The different graphs in the figure show the effect of re-estimating the channel using the comb of pilot tones at different intervals. In this figure, the re-estimation interval is expressed as the number of data blocks that are transmitted before the next comb of pilot tones. It can be seen that the degradation incurred by re-estimating the channel once every 800 blocks (32msec) instead of once every 8 blocks is about 3dB at a BER of 10^{-3}. It can also be seen from this figure that the need to re-estimate the channel becomes less important as the BER decreases (which corresponds to a required increase in the SNR). From the same figure it can be seen that sampling the channel every 3.84ms produces an average performance loss of about 0.5dB between BER = 10^{-3} and 10^{-5}, whereas the loss in bandwidth efficiency due to the loss of data bits to channel sounding is about 1%. This sampling frequency seems to be the best trade off between bandwidth efficiency and system performance.

In the above simulations, the initial estimate of the channel is assumed to be ideal, (i.e. the received pilots were noise-free). In a practical system, this might be because the pilot tones are transmitted at a higher power than the data

36

bits. Two separate tests were conducted to assess the degradation in bit error rate that ocured when the pilot tones were subjected to AWGN and when the channel estimate was not low-pass filtered. Figure 4 shows the results of these simulations. It can be seen that when the estimated channel frequency response was not low-pass filtered, the perfomance of the system becomes:
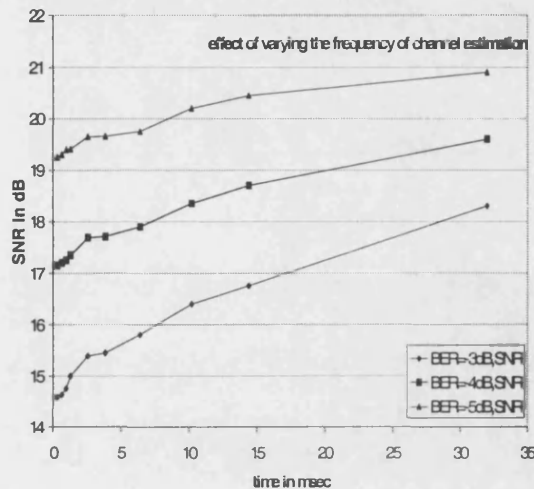

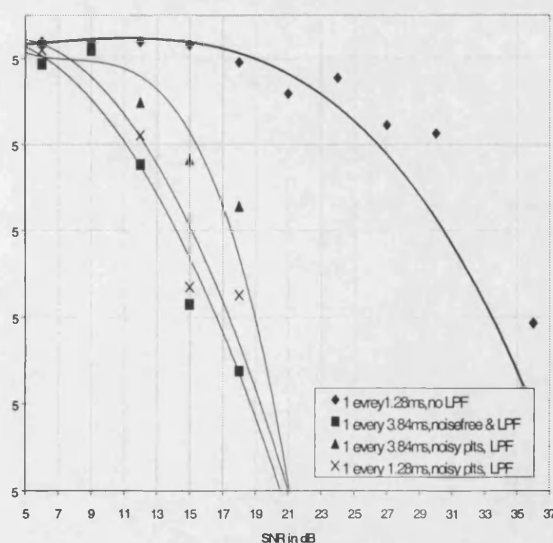Figure 3: Effect channel re-estimation interval on bit error rate

Figure 4: Effect of low-pass filtering and perfect pilot detection on bit error rate

unacceptable even at high SNR since the inherent error propagation becomes dominant. The performance loss due to noisy pilot tone

estimation, however, is less serious but it is still significant. A degradation of about 1.5dB is found at a BER of 10^{-3}. This degradation reduces to almost 0dB at very high SNRs of 20dB or more. Further reduction of the performance loss can be acheived at a cost of a moderate reduction in data throughput by allocating more bandwidth to the pilot tones. Simulations show that a moderate reduction of an additional 2% of the data throughput reduces the performance loss to about 0.5dB at BER of 10^{-3}.

The weakness of this channel estimation method is the insertion of a delay of one OFDM block length. This is a common problem with this kind of equaliser structure. Because of the relative simplicity of our scheme, this delay is kept to an absolute minimum. Using the simulations, we have found the sensitivity of the bit error rate with respect to this delay increases in proportion to the ratio of the channel coherence time to the OFDM block duration, ρ. In addition, the higher the modulation order is the more sensitive the system is to this delay. Figure 5 shows how the BER performance of the system is affected as ρ is varied. This is a key result in the optimisation of the block length parameter of a COFDM system in multipath fading.

It can be seen from figure 5 that as the ratio of the coherence time to the OFDM block duration decreases the performance of the system is initially very poor, with very high error rates, even at high input SNRs, but then improves. For these cases, the block sizes, and hence the delay between channel estimates, are small but the performance is poor because of the very limited frequency diversity provided by the relatively few sub-carriers. When ρ is approximately 0.156, the BER performance is at its best. As ρ continues to decrease due to an increase in the OFDM block size the BER performance worsens again.   This is directly attributable to the increased delay and the fact that the channel characteristics are able to deviate further from

the original estimated value before the channel is re-estimated. It is worthy of note that when the channel is perfectly estimated, the bit error rate performance improves steadily with increase in block size, subject to the limiting effects of Doppler frequency offset and oscillator phase noise which limits the sub-carrier frequency spacing.

5. CONCLUSIONS

This paper has examined the performance of a feedback channel estimation method for a COFDM-4QAM system when transmitting at 25Mb/s over an urban time-varying multipath faded channel. The results show that the system performs well providing that effect of the delay imposed by the method is taken into account. The results show that the performance of the system using such method is within about 2dB of the case which assume an ideal estimate of the channel. The importance of reducing
the effect of noise on the estimated frequency response using low-pass filtering has been found to be vital for good overall system performance. In addition, the effect of the OFDM block length relative to the coherence time of the channel has been found to play an extremely important part in optimising the BER performance of the system when perfect channel estimates cannot be assumed.
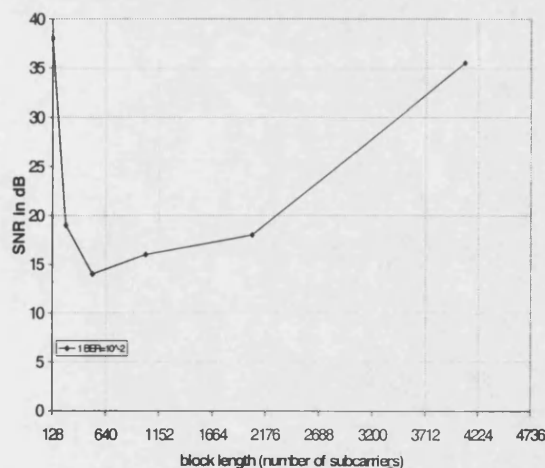

Figure 5: Effect of ρ on system performance

6. REFERENCES

[1] R. W. Chang and R. A. Gibby, *"A theoretical study of performance of an orthogonal multiplex-ing data transmission scheme"*, IEEE Trans. on Comms. Tech., Vol. COM-16, No. 4, August 1968

[2] L. J. Cimini, *"Analysis and simulations of a digital mobile channel using orthogonal frequency division multiplexing"*, IEEE Trans. on Comms., Vol. COM-33, No. 7, July 1985.

[3] S. B. Weinstein and P. M. Ebert, *"Data transmis-sion by frequency division multiplexing using the discrete Fourier transform"* , IEEE Trans. on Comms. Tech., Vol. COM-19, No. 5, pp.628-634, Oct. 1971.

[4] B. Hirosaki, *"An Orthogonal multiplexing QAM system using the discrete Fourier transform "*, IEEE Trans. on Comms. Tech., Vol. COM. 29, No. 7, pp. 982-898, July 1981.

[5] L. Thibault and M. Thien Le, "Performance eval-uation of COFDM for digital audio broadcasting Part I: Parametric study", IEEE Trans. on Broadcasting, Vol. 43, No. 1, March 1997.

[6] Y. Wu, W. Y. Zou, *"Performance simulation of COFDM for TV broadcast application"*, SMPTE Journal, May, 1995.

[7] F. Poegel, S. Zeisberg and A. Finger, *"Compar-ison of different coding schemes for high bit rate OFDM in a 60 GHz environment"*, IEEE Conf. Proc. ISSSTA'96, Vol. 1, pp. 122-125, 1996.

[8] W. Y. Zou and Y. Wu. *"COFDM: an overview"*, 44th IEEE Broadcast Symp., Sept. 1994.

[9] H. Sari, G. Karam and I. Jeanclude, " *Transmiss-ion technique for digital terrestrial TV broad-casting"*, IEEE Communication Magazine, Vol. 33, No. 2, pp. 100-109, Feb. 1995.

[10] J-J van de Beek, O. Edfords, M Sandells, S. K. Wilson, P. O. Borjesson, *"On channel estimation in OFDM systems,"* IEEE Conf. Proc. VTC'95, pp. 815-819, 1995.

[11] J. Rinne and M. Renfors, _"Equalization of orthogonal frequency division multiplexing signals"_, Proc. GLOBCOM'94 pp. 415-419, 1994.

[12] S. Cacopardi, F. Frescura, F. Gatti and G. Reali, _"Channel estimation and tracking of an indoor orthogonal multicarrier DS-CDMA system using measured channel delay profiles"_, Proc. GLOBCOM'96, pp. 415-419,1996.

[13] V. Mignone and A. Morello, _"CD3-OFDM: A novel demodulation scheme for fixed and mobile receivers"_, ", IEEE Trans. on Comms. Tech., Vol. 44, No 9, September 1996.

[14] A. Chini, Y. Wu, M. El-Tanany and S. Mahmoud, _"Filtered decsion feedback channel estimation for OFDM based DTV terrestrial broadcasting system"_, IEEE Trans. on Broadcasting, Vol. 44, No. 1, March 1998.

[15] M. Alard and R. Lassalle, _"Principles of modul-ation and channel coding for digital broadcasting for mobile receivers"_, EBU Technical Review, No. 224, pp. 168-190, Aug. 1987.

[16] R. Steele, _"Mobile radio communications"_, 3rd edition, IEEE Press.

[17] E. Viterbo and K. Fazel, _"How to combat long echoes in OFDM transmission schemes: sub-channel equalization or more powerful channel coding,"_ IEEE Conf. Proc. IEEE GLOBECOM'95, Vol. 3, pp. 2069-2074, 1995.

[18] A. Ruiz and J. M. Cioffi, _"Discrete multiple tone modulation with Coset coding for the spectrally shaped channel"_, IEEE Trans. on Comms. Tech., vol. 40, no. 6, June 1992

[19] Commission of European Communities. _"Digital land mobile radio communications- COST-207,"_ Office for official publications of the European communities, Luxembourg, 1989, Final Report, 14 March, 1984-13 Sept. 1988.

The following paper was published in the proceedings of the
IEEE MILCOM'98, Sept. 1998

Impact of Multipath Fading and Partial-Band Interference on the Performance of a - COFDM/CDMA Modulation Scheme for Robust Wireless Communications

R F Ormondroyd

Communications and Wireless Networks Group, Cranfield University,
RMCS, Shrivenham, Swindon, SN6 8LA, UK

E Al-Susa

School of Electronic and Electrical Engineering
University of Bath, Bath BA2 7AY,UK

ABSTRACT

The performance of a COFDM/CDMA radio communication system in the presence of partial-band jamming is presented where the effects of multipath and additive noise are included. The importance of interleaving and coding is emphasised and their impact on the bit error-rate performance is evaluated. In the first part of the paper, the effect of jamming on a COFDM system is obtained under worst-case conditions. For single tone jamming, the results show that the effect of the jamming signal on the bit error rate is acceptable, even at signal to jamming power ratios as low as −15dB, when interleaving and convolutional coding is used. For the case where 20% of the transmission spectrum is corrupted by partial band jamming, it is necessary for the signal to jamming power ratio to be 5dB or more to achieve an acceptable bit error rate. To provide additional resilience, the case of an OFDM/CDMA scheme is examined where the spread-spectrum process gain is used to provide additional protection against jamming.

INTRODUCTION

Due to its inherent frequency diversity and flexibility, MFSK modulation has long been considered as a highly robust modulation scheme in the presence of tone jamming, particularly when used in conjunction with spread-spectrum modulation [1-4]. In [1], for example, the anti-jamming performance of M-ary non-coherent FSK with fast frequency hopping was evaluated and a method for analysing the performance of M-ary operation with any combination of signal tone distribution, jamming distribution, jamming form and receiver system noise was presented. In [2], the performance degradation resulting from the multi-tone interference of orthogonal non-coherent FH/MFSK, where the effect of thermal noise is not negligible was investigated for both Rayleigh and Rician frequency selective fading channels. In [4], the effect of partial-band noise jamming on fast frequency-hopping spread-spectrum (FFHSS) using binary frequency shift keyed (BFSK) non-coherent receivers was examined for Rician channels. However, non-orthogonal modulation schemes require frequency guard bands and this reduces their spectral efficiency.

Orthogonal frequency division multiplexing (OFDM) is a variant of MFSK that has attracted considerable attention recently for mobile applications because of its very high spectral efficiency [5-6]. In particular, the modulation scheme is capable of operating at extremely high data transmission rates, relative to the delay-spread of the multipath channel, using a combination of

cyclic extension time guard-band to combat ISI and frequency-domain equalisation (when coherent demodulation is used) to minimise the effects of fading. Frequency-domain equalisation can be much easier to implement than time-domain equalisation.

The basic concept of OFDM is to transmit high-speed serial data at a much lower rate in parallel on N sub-carriers that are orthogonally spaced. Consequently, a single broadband data-stream is represented by many narrowband data-streams. Orthogonality of the sub-carriers allows the frequency guard-band, required for MFSK, to be removed. In the presence of highly frequency-selective fading, the channel has a narrow coherence bandwidth due to multipath echoes and this modulation scheme provides frequency diversity in these circumstances. In effect, the frequency selective fade for the single carrier system has been replaced by uncorrelated flat fades for the OFDM system. This, in itself, is not an advantage but by using forward error-correction (FEC) coding and interleaving in the time- and frequency-domains, advantage can be taken of the uncorrelated fades to improve the bit error rate (BER).

In some respects, the generation of errors due to tone jamming and highly frequency selective fading are similar. Consequently, this paper examines the performance of a COFDM system in both single-tone and partial-band (multi-tone) jamming using a Monte-Carlo simulation method. For illustration, a simple non-coherent receiver, with no frequency domain equalisation but with coding and interleaving, was used. The jamming signal bandwidth has been chosen to contain spectral components of equal power that fall within the bandwidth of the COFDM signal. The wanted signal is subjected to time-varying multipath Rayleigh fading, which is much more extreme than Rician fading, and the effect of the thermal noise is also included. In all the simulations, it is assumed that perfect synchronisation between the transmitter and the receiver has been achieved. The paper shows that this type of coded OFDM system (COFDM) is extremely robust in mobile radio channels containing both multipath fading and partial-band jamming signals.

Recently, Kondo and Milstein [7] have proposed a multi-carrier CDMA spread-spectrum system and Rowitch and Milstein [8] have examined the partial-band jamming performance of this system. In this paper, we consider the partial-band jamming performance of a different multi-carrier CDMA configuration in which the data is spread by the CDMA spreading sequence prior to OFDM modulation. This configuration is called OFDM/CDMA.

OFDM SYSTEM AND CHANNEL MODEL

In this parallel data transmission scheme, the data (represented by complex-valued symbol mappings appropriate to the modulation scheme being adopted, eg. m'PSK or QAM) is transmitted simultaneously over N orthogonal sub-carriers, equally spaced within the desired transmission bandwidth, W. The base-band continuous-time signal, $x(t)$, of the OFDM system may be generated using a set of orthogonal basis functions $\Phi_{j,k}(t)$ which are defined as:

$$\Phi_{j,k}(t) = rect(t - jT) \cdot e^{2j\pi kt/T} \qquad (1)$$

where:

$$rect(t) = \begin{cases} \dfrac{1}{\sqrt{T}} & if & \dfrac{-T}{2} \le t < \dfrac{T}{2} \\ 0 & otherwise \end{cases},$$

and $T=N/W$, is the symbol duration. The transmitted base-band signal, $x(t)$, for an infinite stream of symbols, can be written as:

$$x(t) = \sum_{j=-\infty}^{+\infty} \sum_{k=0}^{N-1} X_{j,k} \cdot \Phi_{j,k}(t) \qquad (2)$$

or equivalently:

$$x(t) = \sum_{j=-\infty}^{+\infty} \left\{ rect(t - jT) \cdot \sum_{k=0}^{N-1} X_{j,k} \cdot e^{2j\pi kt/T} \right\} \qquad (3)$$

The demodulation of this signal at the receiver is achieved using a set of basis functions matched to those used in the transmitter. The demodulation process can be expressed as [5]:

$$X_{j,k} = \int_{-\infty}^{+\infty} x(t) \cdot \Phi_{j,k}^*(t) dt \qquad (4)$$

where * is the complex conjugate operation. In the digitally implemented OFDM system, the modulation of the OFDM signal is usually by means of the inverse discrete Fourier transform, preferably the IFFT [5]. Demodulation is by the corresponding DFT or FFT. Therefore, the transmitted base-band signal, $x_j(t)$, of the jth OFDM symbol and its counterpart demodulated signal, X_j, at the receiver may be written as:

$$x_j(n) = \frac{1}{\sqrt{N}} \cdot \sum_{k=0}^{N-1} X_{j,k} \cdot e^{2j\pi kn/N}$$

and $\qquad (5)$

$$X_j(n) = \frac{1}{\sqrt{N}} \cdot \sum_{k=0}^{N-1} x(n) \cdot e^{-2j\pi kn/N}$$

A frequency selective fading channel is assumed with an impulse response $h(t)$, which is defined as:

$$h(t) = \sum_{i=0}^{M-1} h_i e^{j(2\pi f_{Di}(t)t+\theta_i)} \delta(t - \tau_i) \qquad (6)$$

where M is the number of paths, h_i is the path attenuation of the ith path, $f_{Di}(t)$ is the Doppler frequency at time t of the ith path, θ_i and τ_i are the initial phase and time delay of the ith path, respectively. h_i is assumed to be Rayleigh distributed. Limiting the delay spread of the channel to only one consecutive symbol, the received signal contains a number of components and can then be expressed as:

$$r_{j,k} = \sum_{j=-\infty}^{j=+\infty} \left(\underbrace{\sum_{n=0}^{k} \underbrace{h_{j,k-n} \cdot x_{j,n}}_{(1)} + \underbrace{\sum_{n=k+1}^{N-1} h_{j,N+k-n} \cdot x_{j-1,n}}_{(2)}}_{} + \underbrace{n_{j,k}}_{(3)} + \underbrace{\eta_{j,k}}_{(4)} \right)$$

$$(7)$$

In this expression, term (1) is the convolution of the OFDM signal with the impulse response of the channel, term (2) is the convolution of a delayed version of the previous OFDM signal with the impulse response of the channel, term (3) represents the additive white Guassian noise (AWGN) and term (4) corresponds to the effect of the jamming signal.

The effect of the delay spread is to cause the OFDM blocks to lose orthogonality and receiver performance is reduced. In practice, orthogonality is maintained by ensuring that the OFDM blocks remain independent by appending a *cyclic-prefix* to each block of the serial data stream after the IFFT in the transmitter. The cyclic prefix is a copy of p OFDM symbols from the rear of the OFDM block which are appended to the front of the block [6]. This can be viewed as making the transmitted OFDM signal with ISI appear to be periodic. The number, p, of appended symbols is chosen to create a cyclic extension period that exceeds the most significant delay components of the multipath echoes. The receiver uses only the samples within the useful symbol duration. This means that there is a loss of useful signal energy per bit and a corresponding loss of spectral efficiency.

RECEIVER PERFORMANCE IN THE PRESENCE OF PARTIAL-BAND INTERFERENCE

In this section, the bit error probability of an OFDM system is obtained for both BPSK and DBPSK when partial band interference is present. In the analysis, it is assumed that all symbols are equally likely and the received energy of each symbol is E_b. The probabilities of a bit error for BPSK and DPSK in additive white Gaussian channel are given as [9]:

$$P_{BPSK} = Q\left(\sqrt{\frac{2E_b}{N_o}} \right) \qquad (8)$$

$$P_{DBPSK} = \frac{1}{2} \exp\left(\frac{-E_b}{N_o} \right) \qquad (9)$$

where N_o is the one-sided noise spectral density. If the jamming signal is assumed to be noise with power $J = N_j/\rho$, where N_j is the power of the jamming waveform and ρ is the fraction of the jammed bandwidth, defined by:

$$\rho = \frac{w_j}{w_{sig}} \qquad (10)$$

where: w_j is the bandwidth of the jamming signal and w_{sig} is the bandwidth of the OFDM signal. If the jamming signal bandwidth falls completely within that of the OFDM signal, the probability of ρ of the OFDM frame (after the FFT) being affected by the

jamming signal is 50%. Therefore, the average bit error probability for BPSK and DPSK can be written as:

$$P_{DBPSK} = \frac{\rho}{4} \cdot \exp\left(\frac{-E_b}{N_o + N_j}\right) + \left(\frac{2-\rho}{4}\right) \cdot \exp\left(\frac{-E_b}{N_o}\right) \quad (11)$$

$$P_{BPSK} = \frac{\rho}{2} \cdot Q\left(\sqrt{\frac{2E_b}{N_o + N_j}}\right) + (1 - \frac{\rho}{2}) \cdot Q\left(\sqrt{\frac{2E_b}{N_o}}\right) \quad (12)$$

The impact of jamming on the bit error rate of both BPSK and DPSK is shown in figures 1a and 1b, respectively, for the OFDM system in the absence of multipath fading for signal to jamming ratios (SJR) in the range -5dB to +10dB where ρ =20%.
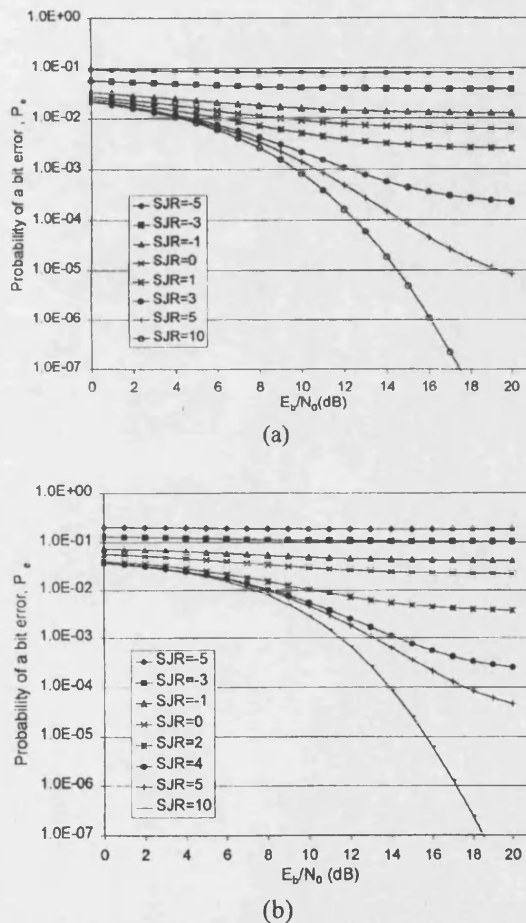

(a)

(b)

Figure 1: Effect of 20% partial-band jamming on the probability of a bit error for an OFDM system using: (a) BPSK and (b) DBPSK modulation

SIMULATION RESULTS

The performance of an OFDM system for both coherent and non-coherent modulation is investigated for two different types of jamming. The first is single-tone jamming and the second is partial-band jamming. For single-tone jamming, the frequency of the jamming tone was made to change slowly in time so that its

effect on the wanted signal was 'randomised'. Similarly, for the case of partial-band jamming, the frequency band of the jamming signal was slowly shifted in time to cover the entire signal bandwidth.

The partial-band jamming was actually represented in the simulation as equal amplitude multi-tones, but with random phase. The frequencies of the simulated jamming signals (both single tone and partial-band multi-tones) were chosen to fall midway between adjacent sub-channel tones of the OFDM signal so that the impact of the jamming was maximised. The reason for this is that when the frequency of the jamming signal is perfectly aligned with one of the sub-channel frequencies of the transmitted signal only data on that carrier is affected by the jamming signal when the received signal is processed using the DFT or FFT algorithm. Furthermore, once the jamming power significantly exceeds the power of the wanted signal, the probability of an error on that sub-carrier saturates. However, when the frequency of the jamming signal lies midway between two sub-channel frequencies, spectral leakage in the spectrum of the jamming signal when the received signal is processed using the FFT algorithm impacts on other frequency components of the received signal. In this case, the jamming power has a significant effect on the average bit error rate as more wanted signal components become affected by the increased magnitude of the spectral leakage components of the jamming signal.

In addition to the intentional jamming, the signal was subjected to time-varying Rayleigh-distributed frequency-selective fading and additive white Guassian noise (AWGN). The frequency-selective fading was simulated using a tapped delay line channel model. The tap coefficients were time-variant Rayleigh-distributed complex numbers whose speed of variation is determined by the Doppler frequency, implemented in this model using a Doppler filter [10]. The tap parameters that were used corresponded to the COST 207 model for the bad urban channel. The main parameters used in the simulations are summarised in the table below.

No of sub-carriers	512	Data rate	2.048Mbps
No of channel paths	6	Jamming bandwidth	0.4096MHz
Max delay spread	5µs	Signal's bandwidth	2.048MHz
Symbol duration	250µs	Coding rate	rate ½ , K=7 convolutional hard decision
Cyclic extension	5µs	Interleaving depth	8msec
Doppler frequency	40Hz	FFT length	1024

Table 1. List of Main Parameters used in Simulation

COFDM System with BPSK Modulation Subject to Partial-band Interference

Figure 2 shows the effect of 20% partial-band jamming only on the BER performance of an OFDM system using BPSK modulation and rate=1/2, K=7 convolutional coding. The other parameters are listed in Table 1. It can be seen that for SJR~3dB, the effect of the jamming signal is severe when there is no interleaving and the system performance is unacceptable for data transmission and marginally acceptable for voice transmission. However, there is a significant performance improvement obtained by interleaving the data. This arises because the

COFDM data is effectively being transmitted in the frequency domain where the jamming tones effectively cause burst errors. The interleaving/de-interleaving process redistributes the burst errors so that the convolutional coding used in this simulation is more effective.
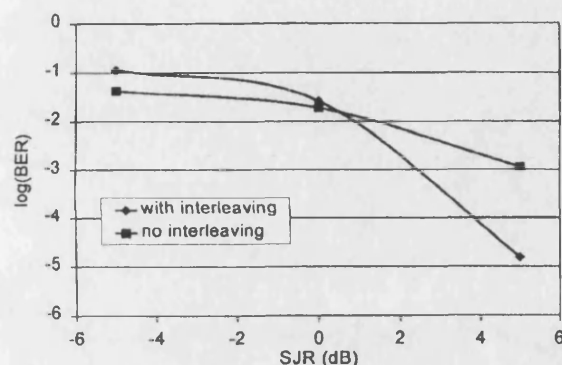

Figure 2: Impact of the signal to jamming power ratio (SJR) of 20% partial band jamming on the average bit error rate for a BPSK COFDM system, with and without interleaving

COFDM System with BPSK Modulation Subject to Partial-band Interference and AWGN

This section further highlights the importance of an adequate interleave depth in combating 20% partial-band jamming. In this set of results, shown in figure 3, the effect of input SNR on the average bit error rate is shown for two cases: one with an interleaving depth of 16ms and the other with no interleaving. This figure shows that there is more than 3dB improvement in performance by using interleaving of this depth, depending on the SJR. It is clear that the effect of the jamming signal at high SJR causes the error floor of the system to saturate at a rate of approximately 10^{-7} for SNRs greater than 13dB. It is also obvious that acceptable bit error rates can be obtained at input signal to noise ratios as low 13dB at an SJR of 0dB
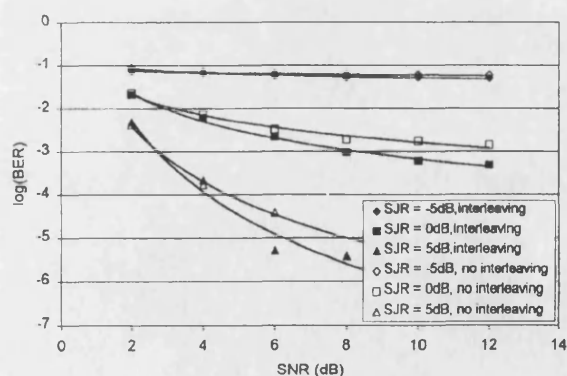

Figure 3: Effect of 20% partial-band jamming on the performance of a BPSK COFDM system in AWGN, with and without interleaving

COFDM System Subject to Single-Tone Interference and AWGN in a Multipath Channel using Differential Demodulation

In this simulation, the effect of single-tone jamming on the performance of a COFDM system using differential binary phase shift keying (DBPSK) is evaluated for the case of a mobile radio channel which is suffering from 6 path Rayleigh fading at a Doppler frequency of 40Hz. This corresponds to a vehicle speed of 50km/h at the carrier frequency of 1.5GHz. The use of differential keying and non-coherent reception solves the problem of equalising the received signal in the time-varying, frequency selective, but the penalty is a worsened detector performance in noise compared with the coherent detector. The system performance, shown in figure 4, can be seen to be adequate in the presence of single tone jamming even at very low SJR of –10dB. It can be seen that by positioning the jamming tone mid-way between the sub-carriers, as the jamming power is increased there is an increase in average BER as more sub-carriers become jammed.
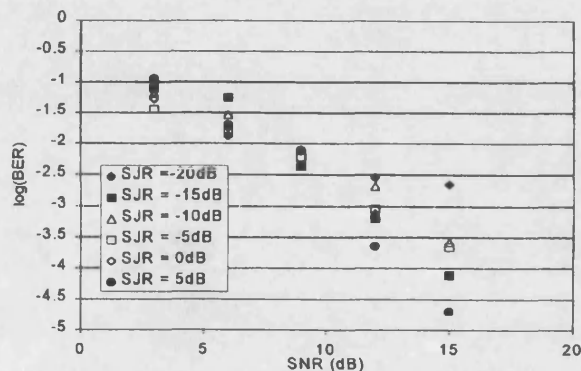

Figure 4: Effect of single tone jamming and AWGN on the BER of a DBPSK COFDM system in multipath fading (with coding and interleaving)

COFDM System subject to Partial-Band Interference and AWGN in a Multipath-Channel Using Differential Demodulation
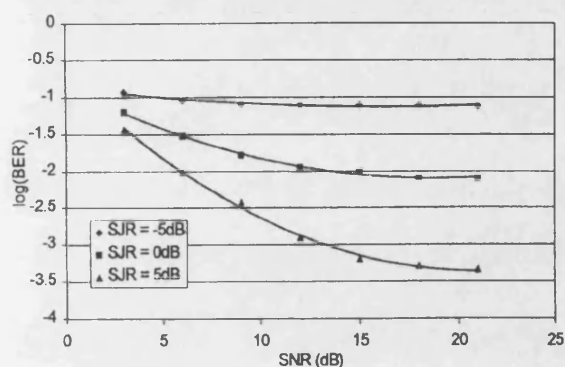
In this simulation, the effect of 20% partial-band jamming on the performance of a COFDM system using DBPSK modulation is evaluated. Comparison of figure 5a with 5b (overleaf) shows that varying the speed of the mobile unit from 0 to 50kph per hour results in little performance degradation, indicating that jamming is the dominant degradation mechanism in the absence of interleaving. Comparison of figure 5b with 5c shows the significant improve-ment in the performance of the system through the use of interleaving, depending on the SJR.
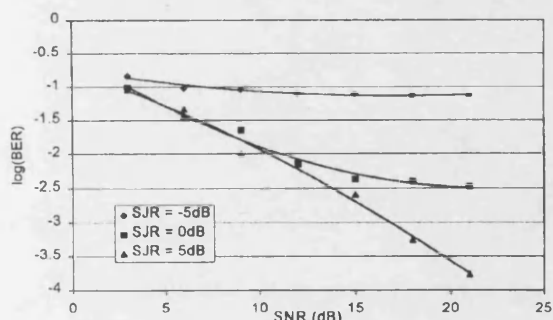
OFDM/CDMA System

In addition to the basic COFDM system, an OFDM/CDMA system was simulated. The block diagram of the system is shown in figure 6, overleaf. It will be seen that the data is first convolutionally coded and then the data is spread. The spread-data is then OFDM modulated. The CDMA spreading parameters used were 511 chips per data bit. In order to maintain the same transmission bandwidth as the cases described above,

the data rate was reduced in proportion to the spreading rate. This data was transmitted on a 512 carrier COFDM system. The performance of this system in 20% partial band jamming, AWGN and multipath fading is presented in figure 7 for a vehicle travelling at 50km/h at SJR of –25dB, -20dB and –15dB.
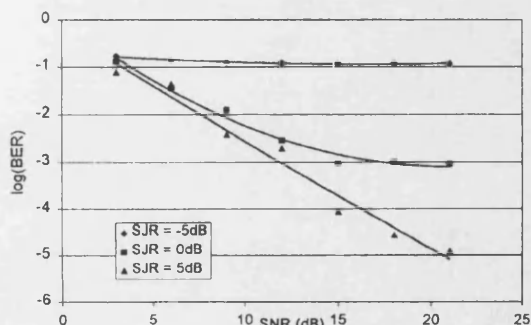
As can be seen, this particular configuration is extremely robust to partial band jamming, multipath and AWGN, but this is at the expense of a lower data transmission rate. However, if some of this jamming performance can be sacrificed, multi-access capability under these harsh conditions is possible.

Figure 6: Schematic diagram of the OFDM/CDMA system

(a)

Figure 7: Effect of partial band jamming on the BER performance of an OFDM/CDMA system

CONCLUSIONS

In this paper, the performance of a COFDM system in the presence of AWGN, multipath frequency selective fading and intentional jamming was examined and shown to be satisfactory at moderate SJR and SNR. It was observed that the effect of partial-band jamming becomes insignificant for many applications at SJR equal or greater than 5dB whereas for single-tone jamming the effect is insignificant from as low SJR as – 15dB when interleaving is included. The effect of subjecting the jamming signal to fading was also examined and it was shown that whether if the jamming signal was subjected to fading or not the net result is the same at low SJR (<5dB) whereas at higher SJR the effect is more significant. In this simulation it was assumed that the jamming signal is subjected to the same fading as that of the OFDM signal. Finally, a direct-sequence CDMA coding strategy was applied to the OFDM signal and it was found that there were substantial improvements in the BER (at the expense of data rate).

(b)

(c)

Figure 5. Effect of 20% partial band jamming combined with multipath fading and AWGN on the performance of a DBPSK COFDM system:
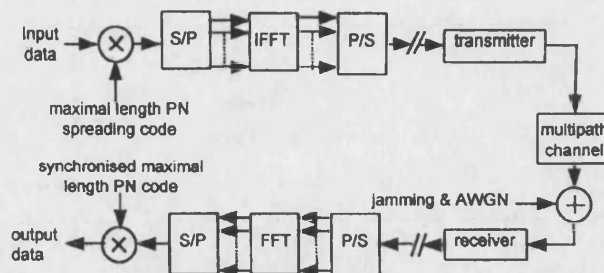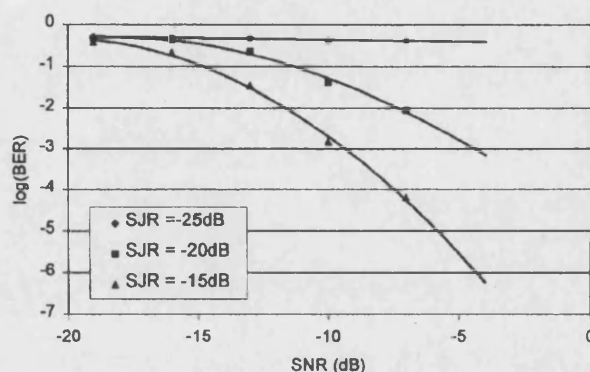(a) 0Hz Doppler and no interleaving, (b) 40Hz Doppler and no interleaving (c) 40Hz Doppler and interleaving

REFERENCES

[1] J S. Bird and E. B Felstead, *"Antijam performance of fast frequency-hopped M-ary NCFSK-an overview"*, IEEE transactions on Selected Areas in Communications,vol.,sac-4,No. 2, March 1986.

[2] R. C Robertson and J Sheltry, *"Multiple tone interference of frequency-hopped noncoherent MFSK signals transmitted over Ricean fading channels"*, IEEE Milcom 95,vol. 1, pp330-334.

45

[3] A Pouttu, *"Performance studies of slow frequency hopping M-ary FSK with concatenated codes in partial band noise jamming"*, IEEE Milcom 95, vol. 1, pp 335-339.

[4] R. C. Robertson and K. Y. Lee, *"Performance of fast frequency-hopped MFSK receivers with linear and self normalisation combining in a Ricean fading channel with partial band interference"*, IEEE J. Selected Areas in Communications, vol. sac-10,pp731-741, May 1992.

[5] M. Alard and R. Lasalle, *"Principle of modulation and channel coding for digital broadcasting for mobile receivers"*, EBU Technical Review, no. 224, pp. 168-190. Aug. 1987.

[6] A. Ruiz and J. M. Cioffi, *"Discrete multiple tone modulation with Coset coding for the spectrally shaped channel"*, IEEE Transactions on Communications, vol. 40, no. 6, June 1992

[7] S. Kondo and L B Milstein, *"Performance of multicarrier DS CDMA systems"*, IEEE Transactions on Communications, Feb 1996, Vol.44, No.2, pp.238-246

[8] D N. Rowitch and L. B. Milstein, *"Convolutional coding for direct sequence multicarrier CDMA"*, IEEE Milcom 95, vol. 1, pp 55-59.

[9] B Sklar, *"Digital communications fundamentals and applications"*, Prentice Hall International edition.

[10] R. Steele, *"Mobile Radio Communications"*, 3rd Edition, IEEE press.

The following paper was published in the proceedings of the IEE Colloquim '1996, May. 1996

COFDM - AN ALTERNATIVE STRATEGY FOR FUTURE-GENERATION MOBILE COMMUNICATIONS

R F Ormondroyd, J J Maxey and E Alsusa

Introduction

Future generations of mobile radio systems, such as the mobile broadband system (MBS), will be required to provide data rates of 2Mb/s and above and it is the dispersive characteristics of the mobile radio channel that will play a key role in determining the most suitable, cost-effective, radio interface solution. The purpose of this paper is to consider the potential of multi-carrier multiple-access techniques as a means of providing a versatile high data rate radio interface for both terrestrial and satellite mobile PCS. After describing the two main forms of multiple-access multi-carrier systems that have been proposed very recently, the paper will describe a new variant of multi-access multi-carrier system called LROCC-OFDM.

There is considerable debate concerning the relative merits of TDMA and CDMA as the most appropriate choice of multiple access method for future generations of digital mobile cellular radio. Direct-sequence-CDMA seems to provide a higher spectral efficiency in comparison to other conventional multiplexing methods[1-3], although this may be attributable more to the noise-limited cellular structure of these systems rather than to any inherent efficiency of the basic direct-sequence spread-spectrum modulation method. However, DS-CDMA systems are also often attributed with systems' benefits which may be potentially greater than pure spectral efficiency. These include:

- robustness against fading
- low density power spectrum - potential for bandsharing
- interference and jamming rejection
- code re-use rather than frequency re-use - improved frequency planning
- soft capacity
- soft hand-off

Certainly, these benefits are achieved individually but once the process gain has been used to achieve a high user capacity it cannot be re-used for jamming rejection etc., so these benefits cannot be achieved collectively. At high data rates over a severely fading channel, other factors may be of greater significance.

If a traditional TDMA approach is adopted at the high data rates anticipated for MBS, complex time domain equalisers based on either a non-recursive linear equaliser or decision feedback equaliser would have to be used to combat the intersymbol interference (ISI) resulting from the effect of multipath delays in the mobile channel. In addition, interleaving and coding would also have to be used to augment the resilience of the system to the burst errors in the fading environment. The problem is no less severe if a CDMA approach is taken because the transmission bandwidth must be extremely large to provide adequate process gain to achieve the required cell capacity. In this case, the bandwidth of the signal will be considerably wider than the coherence bandwidth of the mobile radio channel and so channel fading is likely to be highly frequency selective. Equivalently, this is represented by a channel impulse response with a broad time delay spread due to multipath propagation and the effects of Doppler spread. Consequently, when the channel impulse response is much longer than the symbol duration, significant intersymbol interference (ISI) occurs and the performance of the system is seriously degraded[4].

One of the advantages of the DS-CDMA system is that it can efficiently implement a RAKE receiver[5-6] which acts as a matched filter for multipath combining and effectively provides path diversity. The RAKE receiver must continuously estimate the relative delay of each path and there is considerable current research on the benefits of maximum ratio combining (MRC) and equal gain combining (EGC). These methods require considerable signal processing within the receiver, particularly if other users' multipath interference has to be

rejected. Also, the technique does not handle significant Doppler spread which may be a major problem for satellite systems.

To combat these effects in two high data rate broadcasting applications which are also subject to severe multipath fading, digital audio broadcasting[7] and terrestrial HDTV[8], coded orthogonal frequency division multiplexing (COFDM) has been proposed.

OFDM/COFDM Techniques

The broad aim of OFDM or COFDM is to sub-divide the available (non-ideal) channel bandwidth into a number of narrowband sub-channels such that the performance of each sub-channel is almost ideal. By making the bandwidth of each sub-channel sufficiently narrow, the effects of ISI become negligible and equalisation is unnecessary[6]. In OFDM systems, the symbol rate of the serial data is reduced by a factor N by multiplexing it into N parallel paths which are then modulated onto N carriers. The key to the spectral efficiency of OFDM lies in the way in which the symbols are modulated onto the N carriers. Normally, it would be necessary to separate the frequency spacing of each carrier with a frequency guard band to prevent upper and lower sidebands of adjacent carriers from overlapping and producing aliasing. In OFDM/COFDM the carriers are all chosen to be orthogonal so that with an appropriate modulation scheme such as QPSK or QAM it is possible for upper and lower 'sidebands' to fully overlap yet still be correctly demodulated. The common method of achieving a large number of orthogonal carriers is to use the Fourier transform method[9]. Figure 1 illustrates a typical OFDM system based on the IFFT/FFT transform pair.
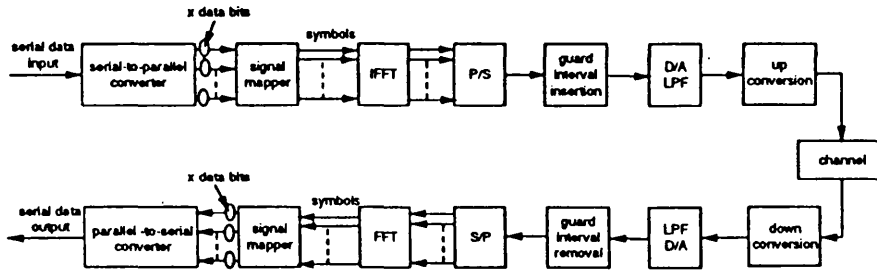

Figure 1   Typical OFDM system based on the IFFT/FFT transforms

Frames of M serial (encoded) data are first converted into $N' = M/x$ parallel groups of x data bits which are mapped into N complex value symbols, X_k, in the modulator corresponding to the signal constellation of the corresponding sub-carrier. Performing the inverse DFT on these N complex values results in N complex valued Fourier coefficients:

$$y_n = \frac{1}{\sqrt{N}} \sum_{k=0}^{N-1} X_k e^{j2\pi nk/N}, \quad n = 0,1,....N-1$$

where $1/\sqrt{N}$ is used for normalisation. These coefficients are then parallel to serial converted into a time sequence of N complex coefficients (or two real value time series representing real and imaginary parts of the complex Fourier coefficients) and these are clocked at the original symbol rate T_s such that the discrete time series $\{y_k\}$ represents samples of $y(t)$ at intervals of $t = nT_s/N$, where $n = 0,1...N-1$, i.e:

$$y(t) = \frac{1}{\sqrt{N}} \sum_{k=0}^{N-1} X_k e^{j2\pi kt/T_s}, \quad 0 \le t \le T_s$$

this signal is then used to modulate the carrier. From this it can be seen that the sub-carrier frequencies are:
$$f_k = k/T_s, \quad k = 0,1,.....N$$

Furthermore, the baseband sub-carriers are all orthogonal in that:
$$\int_0^{T_s} \cos(2\pi f_i t + \theta_i) \cdot \cos(2\pi f_j t + \theta_j) dt = 0, \quad \text{for } i \ne j$$

It is also obvious from the above that the discrete DFT can be used in the receiver to recover the samples, X_k. By increasing the period of each frame of data, i.e. the period at which the IDFT is carried out, so that it is many times longer than the channel impulse response, it has been argued that the effects of ISI due to multipath propagation effects can be significantly reduced This can be achieved by increasing the size of the IDFT at the cost of computation complexity and the delay through the system is also increased. However, as the size of the DFT is increased, the sensitivity of the receiver to timing errors and phase jitter increases. Normally[10] Doppler spread sets the limit on the closeness to which the sub-carriers are spaced and this effectively places an upper limit on N and there may still be some ISI due to long echoes. To counter this, it has been suggested in a number of papers[10] that a time guard band is required at the end of each IDFT conversion, which may be as large as 25% of the symbol duration. This guard period, or cyclic extension is represented by a zero padding of the Fourier coefficients which lasts for T_g seconds beyond the normal frame period. Although this adds little complexity to the receiver, it means that the efficiency of data transmission is significantly degraded, however this period can also be used to obtain correct timing to mark the start of each Fourier transformation, which is very critical in maximising the system performance.

Viewed in the frequency domain, because the channel exhibits frequency selective fading not all N data symbols being transmitted in parallel will be corrupted simultaneously and the data on the degraded carriers can be corrected relatively easily with appropriate use of error correcting codes and interleaving. A number of different coding strategies have been considered, including: block codes, convolutional codes, Reed-Solomon codes and Turbo codes.

Clearly, to gain significant benefits from the use of COFDM, frequency selective fading is required. In fact, Sari et al[11] have pointed out, that except for PSK signals, OFDM does not solve the channel equalisation problem but simply shifts it from the time domain to the frequency domain. It has been argued, however, that this is a much easier problem to solve using the time guard band and a simple LMS algorithm one-tap equaliser after the DFT to provide frequency equalisation against co-channel interference. Most OFDM implementations use this structure, despite the obvious loss in capacity, but more complex multi-tap equaliser structures have been proposed recently[12-14] to reduce or remove the guard period and hence recover the capacity. However, these multi-tap equaliser systems can be optimised by the use of combining to form a RAKE structure[15] where it will be seen immediately that the use of a RAKE system after the DFT in the OFDM receiver will be very robust against Doppler spread. If Doppler spread is a problem, as it may be for satellite based broadband systems, the OFDM/COFDM approach is very powerful.
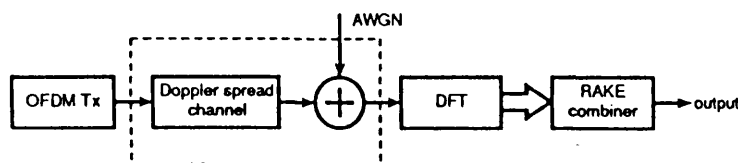

Figure 2   Simplified schematic showing how a RAKE combiner can be
used with an OFDM receiver to combat multipath[15]

Multiple Access Systems Based on Multi-Carrier Techniques

Because of the success of COFDM in providing a high bit rate service in severe frequency selective fading and following the paper of Cimini[16], who proposed this form of signalling for digital mobile radio, there have been a number of recent proposals[17,18] for this and broadly similar multi-carrier [19,20](MC) techniques to be applied to multiple-access radio schemes.

In the systems proposed to date, multiple access-capability is gained using conventional CDMA techniques and each user is given a unique PN code in the usual way. However, transmission of the users' data is achieved in one of two ways.

CDMA-OFDM   In the first method, the data modulated spreading sequence is serial-to-parallel converted and each chip modulates a different carrier frequency via the IDFT routine. This implies that the number of carriers is equal to the processing gain and each carrier conveys a relatively narrowband waveform **50**

rather than a direct-sequence waveform. Effectively, the FFT has given the resulting signal a PN coded structure in the frequency domain. This technique is referred to as CDMA-OFDM, or similar. A typical CDMA-OFDM base-station system is shown in figure 3. Other variants are possible.
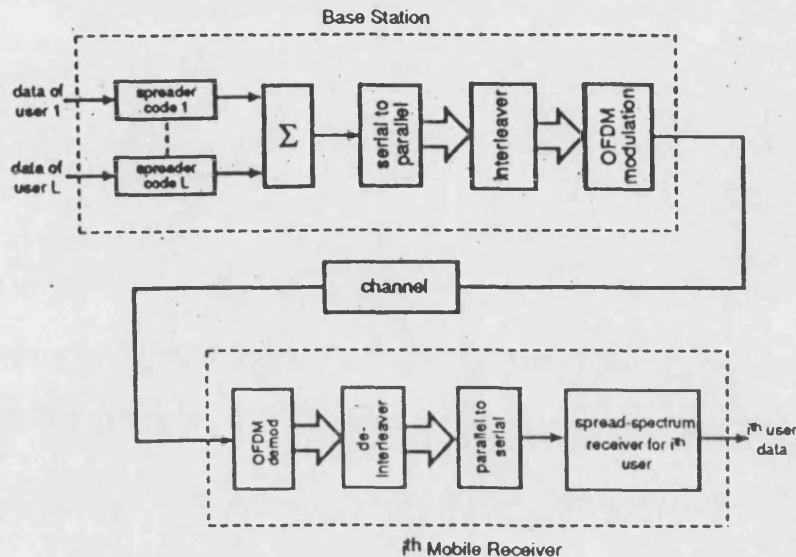

Figure 3 Simplified structure of the down-link of a CDMA-OFDM multiple access scheme

Here, each user's data is spread, in the usual way and the data modulated chips from each user are arithmetically summed (chip synchronously). The resulting non binary values are serial to parallel converted and interleaved before being transformed by the IDFT and modulated onto the carrier in the usual way. In the receiver, OFDM demodulation is accomplished by the DFT. The output of the parallel to serial converter is represented as a composite multi-user spread-spectrum signal from which any particular user can be demodulated in the usual way using a correlator, digital matched filter or maximum likelihood detector. In t above, steps to add and remove time guard bands, or the use of a RAKE receiver to reduce ISI and Doppler i assumed. As with other orthogonal systems, synchronisation of the symbols is essential and implicit on botl the down-link (which is straightforward to arrange) and also on the up-link (which is not so straightforward!

Multicarrier DS-CDMA   In the other method, the total available frequency spectrum of the CDMA system is divided into M equi-width frequency bands, where M is the number of carriers, typically much le: than the process gain and each frequency band is used to transmit a 'narrowband' DS-CDMA signal[20]. The response to frequency selective fading is similar in both cases, but it is claimed that this method is easier to implement. Figure 4 shows a typical implementation of a multi-carrier DS-CDMA system[20].
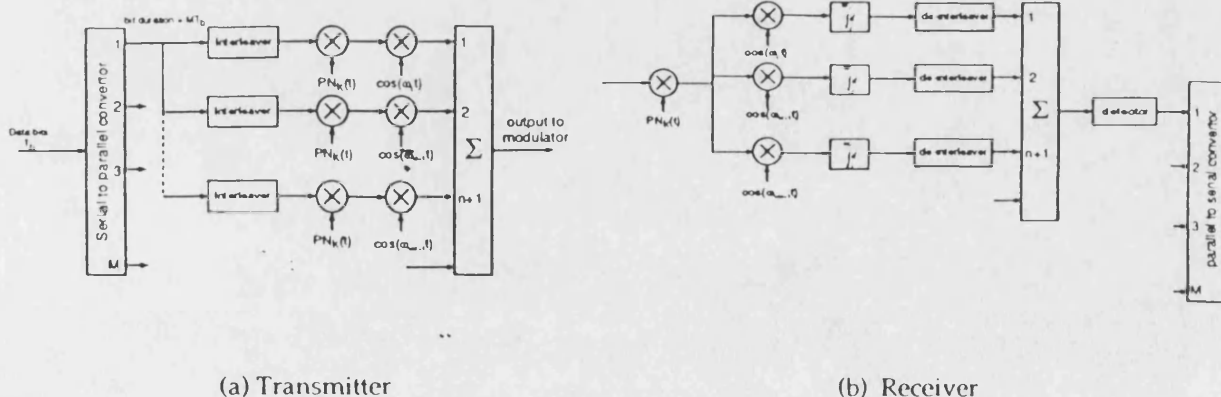
(a) Transmitter   (b) Receiver
Figure 4   Simplified schematic of a multicarrier DS-CDMA system

In this system, the data is split into M parallel streams. Each of these streams is split S ways and spread by the same PN sequence and modulated onto S orthogonal carriers, i.e. the same data bit is transmitted on S carriers. The total number of carriers in this arrangement is thus M x S.

LROCC-OFDM

A new method of providing multi-access operation of an OFDM system which promises to have higher ultimate capacity than the CDMA-OFDM method is to use LROCC-OFDM. The technique replaces the conventional pseudo-noise spreading sequences of the CDMA part of the system by low-rate orthogonal convolutional codes (LROCC)[21]. The LROCC system combines the spreading function with powerful coding by the use of a low rate convolutiona code of rate 1/N, which is used to spread the data by N times. By using orthogonal codes based on the Hadamard matrix[22,23], large numbers of convolutional codes can be obtained, and isolation of users in a multi-access CDMA scenario is obtained, particularly if additional non-spreading PN randomisation is used[24]. The LROCC-OFDM transmitter, shown in figure 5, is similar to the CDMA-OFDM system of figure 2. A feature of the system is that since the convolutional codes are based on radix 2, rather than $2^n - 1$ of the PN spreading codes, the DFT can be performed using the FFT.
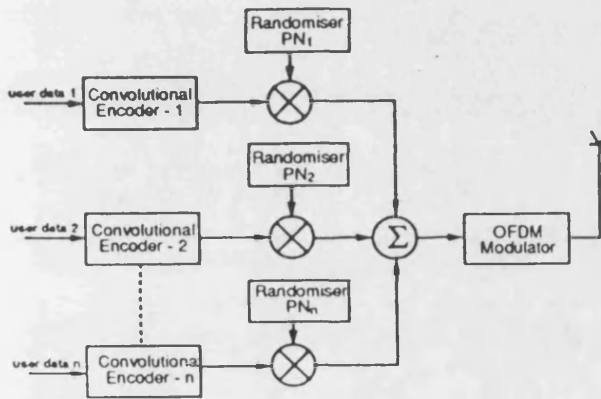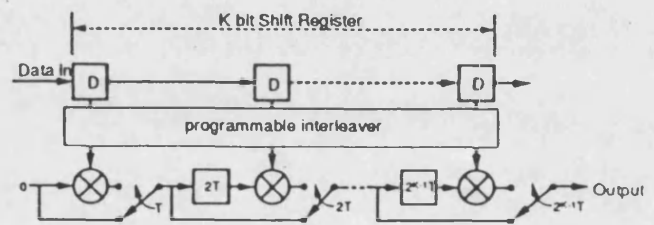

| Figure 5a   LROCC-OFDM Transmitter | Figure 5b   LROCC Encoder |

In the receiver, the normal CDMA demodulator is replaced by modified form of Viterbi soft decision decoder which provide a maximum likelihood decision on the decoding of the ith user[24]. Clearly, the performance of the LROCC-OFDM system is very much dependent upon the performance of the basic LROCC-CDMA system. Figure 6 provides a comparison of a conventional DS CDMA system and the LROCC system for the case of a system in which other-user noise is dominant and there are no channel imperfections.
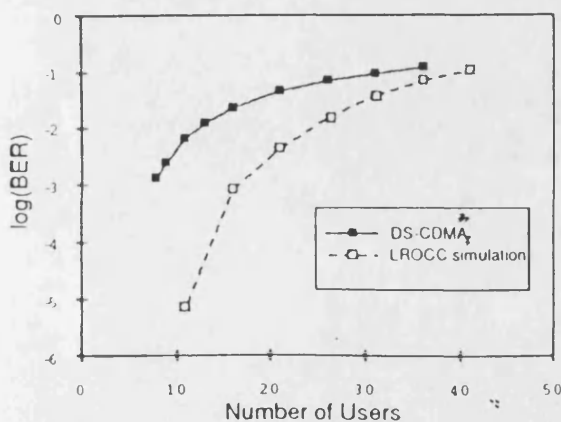

Figure 6a Comparison of DS-CDMA and LROCC
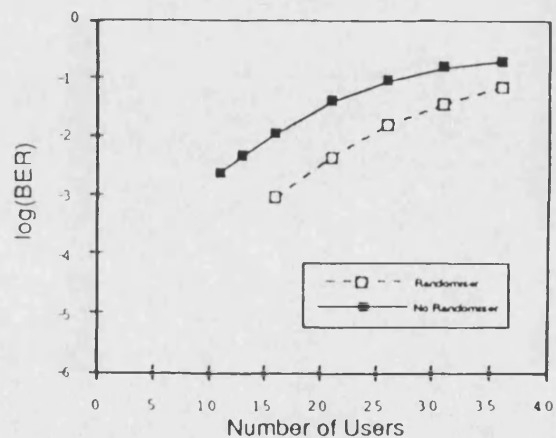system performance

Figure 6b Effect of the randomiser on LROCC
performance

In figure 6a the DS-CDMA system has a spreading sequence of 63 chips whilst the LROCC system uses a 64 chip Hadamard sequence. Channel imperfections are expected to be handled by the OFDM part of the system in a similar way to DS-CDMA-OFDM[20]. Clearly, LROCC outperforms the comparable DS-CDMA system, and so it is expected that the LROCC-OFDM system will provide similar performance improvements over CDMA-OFDM.

Acknowledgements

References
1. Gilhausen K S, Jacobs I M, Padovani R and Weaver, L A: "Increased capacity using CDMA for mobile satellite communications", IEEE J. Sel. Areas in Comms., Vol. SAC-8, pp 503-514, 1990.

2. Pickholtz, R L, Milstein, L B and Schilling, D L: "Spread-spectrum for mobile communications", IEEE Trans. Veh. Tech., Vol. VT-40, pp313-321, 1991.

3. Omura, J K, and Yang, P T: "Spread-spectrum S-CDMA for personal communications services", Proc. IEEE Milcom'92, pp 269-273, 1992.

4. Pursley, M B: "Effects of specular multipath fading on spread-spectrum communications ", New concepts in multi-user communications, J Skwirzynski, ed. NATO Adv. Study Inst., Sijthoff and Noordhoff, pp 481-505, 1981.

5. Turin, G L: "Introduction to spread-spectrum antimultipath techniques and their application to urban digital radio", Proc. IEEE, Vol. 68, pp 328-353, 1980.

6. Proakis, J G: "Digital Communications", McGraw Hill, New York, 1989.

7. For example: Alard, M and Lassalle, R: "Principles of modulation and channel coding for digital broadcasting for mobile receivers", EBU Review, pp47-69, August 1987.

8. Frazel, K, Kaiser, S, Robertson, P and Ruf, M J:" A concept of a reconfigurable digital-TV/HDTV transmission scheme with flexible channel coding & modulation for terestrial broadcasting", Proc Int. Workshop on HDTV, October 1994.

9. for example: Webb, W T and Hanzo, L:"Modern Quadrature Amplitude Modulation", Pentech Press/IEEE Press, 1994.

10. Zou, W Y and Wu, Y: "COFDM: an overview", IEEE Trans. on Broadcasting, Vol. 41, 1-8, 1995.

11. Sari, H, Karam, G and JeanClaude, I: "Channel equalisation and carrier synchronization in OFDM systems", Tirrenia Int Workshop on Digital Communications, Italy, 1993.

12. Sari, H, Karam, G and Jeanclaude, I: "An analysis of orthogonal frequency division multiplexing for mobile radio applications", IEEE Proc. 44th Vehicular Technology Conf., pp1635-1639, 1994.

13. Casas, E F and Leung, C: "OFDM for data communication over mobile radio FM channels - part 1", IEEE Trans on Comms, Vol. 39, pp. 783-793, 1991.

14. Vahlin, A and Holte, N: "Use of a guard interval in OFDM on multipath channels", Electronics Letters, Vol. 30 pp. 2015-2016, 1994

15. Fettweis, G, Bahai, A S and Anvari, K: "On multicarrier code division multiple access (MC-CDMA) modem design", IEEE Proc. 44th Vehicular Technology Conf, pp 1670 - 1674, 1994.

16. Cimini, L C: "Analysis and simulation of a digital mobile channel using orthogonal frequency division multiplexing", IEEE Trans. on Comms., Vol. COM-33, pp665-675, 1985.

17. Fazel, K and Papke, L: On the performance of convolutionally-coded CDMA/OFDM for mobile communicatior system", Proc. PIMRC'93, Yokohama, D3.2.1-5, 1993.

18. Kaiser, S: "OFDM-CDMA vs DS-CDMA: preformance evaluation in fading channels", IEEE Proc., ICC'95, p; 1722-1726, 1995.

19. Sourour, E A and Nakagawa, M: "Performance of orthogonal multicarrier CDMA in a multipath fading channel" IEEE Trans. on Comms., Vol COM-44, pp 356-367, 1996.

20. Kondo, S and Milstein, LB: "Performance of multicarrier DS-CDMA Systems", IEEE Trans on Comms., Vol. COM-44, pp 238-246, 1996

21. Viterbi, A J: "Very low-rate convolutional codes for maximum theoretical performance of spread-spectrum multiple-access channels", IEEE Journal on SAC, Vol. 8, No.4, 1990

22. Monogioudis, P, Edmonds, R, Tafazolli, R and Evans, B G: "Multirate 3rd generation CDMA systems", IEEE International Conference on Communications, ICC'93, pp. 151-155, 1993

23. Ormondroyd, R F and Maxey, J J: "A high performance CDMA cellular radio system based on orthogonal low-rate convolutional coding", IEE International Conference on Radio Receivers and Associated Systems, Conference Proc. Vol. 414, pp. 17-21, 1995